



Universitat de Lleida

Design, development and characterisation of a Combined Solar Thermal Collection and Radiative Cooling System for heat and cold production

Sergi Vall Aubets

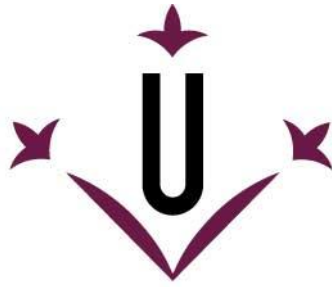
<http://hdl.handle.net/10803/675491>



Design, development and characterisation of a Combined Solar Thermal Collection and Radiative Cooling System for heat and cold production està subjecte a una llicència de [Reconeixement-NoComercial-CompartirIgual 4.0 No adaptada de Creative Commons](https://creativecommons.org/licenses/by-nc-sa/4.0/)

Les publicacions incloses en la tesi no estan subjectes a aquesta llicència i es mantenen sota les condicions originals.

(c) 2021, Sergi Vall Aubets



Universitat de Lleida

TESI DOCTORAL

**Design, development and characterisation of a
Combined Solar Thermal Collection and
Radiative Cooling System for heat and cold
production**

Sergi Vall Aubets

Memòria presentada per optar al grau de Doctor per la Universitat de Lleida
Programa de Doctorat en Enginyeria i Tecnologies de la Informació

Director
Dr. Albert Castell Casol (Universitat de Lleida, Spain)

2021



This page intentionally left blank

Acknowledgements

In the first place, I would like to thank my PhD thesis supervisor, Dr Albert Castell, not only for giving me the opportunity to widen my knowledge and to rediscover myself, but also for the time we shared, his kind support, his wise guidance and advise, and the encouragement received during this long journey.

I would like to wish my gratitude to Dr Kéryn Johannes and Dr Etienne Vergnault for their advice and guidance during my research stay in the Centre for Energy and Thermal Sciences of Lyon (CETHIL).

I would also like to thank my colleagues from SEMB research group for their kind welcome from the beginning, their willingness to help, the dedication they have transmitted me, and the time spent.

Thanks to my family and friends, the old and the new, with whom I shared time and experiences.

Last but not least, I would like to express my sincere gratitude to my parents, my sister, my life partner, Clara, and my daughter, for being always by my side, their comprehension, and all the affection and love received.

Institutional acknowledgements

The candidate would like to thank all the funding received to carry out this PhD thesis. To the Secretaria d'Universitats i Recerca del Departament d'Economia i Coneixement de la Generalitat de Catalunya for the PhD fellowship received (2015FI_B_00456, 2016FI_B1_00002, 2017FI_B2_00132). To the Societat Econòmica d'Amics del País (SEBAP) for the mobility grant awarded to promote research in research centres and abroad universities, allowing the candidate to do a research stay at the Centre for Energy and Thermal Sciences of the University of Lyon. The candidate would also like to thank the funding institutions Oficina de Desenvolupament i Cooperació from Universitat de Lleida, Agència de Gestió d'Ajuts Universitaris i de Recerca of the Catalan government (2017 SGR 659), and Ministerio de Ciencia, Innovación y Universidades from the Spanish government (RTI2018-097669-A-I00).



AMICS DEL PAÍS

SOCIETAT ECONÒMICA BARCELONESA
D'AMICS DEL PAÍS -1822-



Resum

La concepció d'un món millor per a les generacions futures passa pel compromís de mitigar o revertir el canvi climàtic. L'origen del canvi climàtic és ben conegut: l'emissió de gasos d'efecte hivernacle relacionats amb l'ésser humà, bàsicament per la dependència dels combustibles fòssils. És necessari canviar aquest paradigma; és per això que les energies renovables juguen un paper fonamental: ajuden a reduir la dependència energètica dels combustibles fòssils, augmenten la diversificació energètica i són tecnologies de producció d'energia in situ.

La present tesi doctoral té com a objectiu contribuir al desenvolupament d'una innovadora tecnologia d'energia renovable per a la producció de calor i fred. La tesi doctoral s'ocupa inicialment de l'estudi i revisió bibliogràfica de la tecnologia anomenada *Radiative Cooling*, o Refredament Radiatiu, una tecnologia renovable per a la producció de fred mitjançant l'aprofitament del fred disponible a l'espai exterior. Aquesta tecnologia va ser objecte d'investigació en el passat i, gràcies a desenvolupaments recents, està recuperant interès entre les altres tecnologies renovables per a la producció de fred.

Els descobriments de l'estudi inicial condueixen la tesi doctoral a enfocar-se en una innovadora combinació de Refredament Radiatiu amb Captació Solar Tèrmica, una tecnologia consolidada, amb fins de rendibilitat i operacionals. Aquesta combinació de tecnologies renovables en un dispositiu físic s'anomenarà Col·lector i Emissor Radiatiu (RCE, sigles en anglès de *Radiative Collector and Emitter*), basant-se en la importància de la radiació electromagnètica en el balanç de calor en aquesta tecnologia/dispositiu.

Després de detectar les condicions climàtiques desitjades per a facilitar l'àmplia implementació de RCE en edificis, la tesi doctoral segueix amb el disseny, desenvolupament i caracterització d'un dispositiu RCE mitjançant modelatge numèric i proves experimentals. Els resultats demostren la capacitat i idoneïtat de RCE per escalfament i refredament, i presenten els paràmetres més influents de les aplicacions RCE.

Resumen

La concepción de un mundo mejor para las generaciones futuras pasa por el compromiso de mitigar o revertir el cambio climático. El origen del cambio climático es bien conocido: la emisión de gases de efecto invernadero relacionados con el ser humano, básicamente por la dependencia de los combustibles fósiles. Es necesario cambiar este paradigma; es por eso que las energías renovables juegan un papel fundamental: ayudan a reducir la dependencia energética de los combustibles fósiles, aumentan la diversificación energética y son tecnologías de producción de energía in situ.

La presente tesis doctoral tiene como objetivo contribuir al desarrollo de una innovadora tecnología de energía renovable para la producción de calor y frío. La tesis doctoral se ocupa inicialmente del estudio y revisión bibliográfica de la tecnología llamada *Radiative Cooling*, o Enfriamiento Radiativo, una tecnología renovable para la producción de frío mediante el aprovechamiento del frío disponible en el espacio exterior. Esta tecnología fue objeto de investigación en el pasado y, gracias a desarrollos recientes, vuelve a ganar interés entre las demás tecnologías renovables para la producción de frío.

Los descubrimientos del estudio inicial conducen la tesis doctoral a enfocarse en una innovadora combinación de Enfriamiento Radiativo con Captación Solar Térmica, una tecnología consolidada, con fines de rentabilidad y operacionales. Esta combinación de tecnologías renovables en un dispositivo físico se mencionará Colector y Emisor Radiativo (RCE, siglas en inglés de *Radiative Collector and Emitter*), basándose en la importancia de la radiación electromagnética en el balance de calor en esta tecnología/dispositivo.

Después de detectar las condiciones climáticas deseadas para facilitar la amplia implementación de RCE en edificios, la tesis doctoral sigue con el diseño, desarrollo y caracterización de un dispositivo RCE mediante modelado numérico y pruebas experimentales. Los resultados demuestran la capacidad y la idoneidad de RCE para calentamiento y enfriamiento, y presentan los parámetros más influyentes de las aplicaciones RCE.

Summary

The conception of a better world for future generations passes through the commitment to mitigate or reverse climate change. The origin of climate change is well-known: the human-related emission of greenhouse gases, basically from fossil fuel burning dependency. There is a need to change this paradigm; therefore, renewable energies play an essential role: they help reduce energy dependency on fossil fuels, increase energy diversification and are on-site energy production technologies.

The present PhD thesis aims to contribute to the development of a novel renewable energy technology for heat and cold production. The PhD thesis initially deals with the study and review of Radiative Cooling technology, a renewable technology for cold production by harvesting the coldness of the outer space. This technology was investigated in the past and, thanks to recent developments, it is regaining interest among the renewable technologies for cold production.

The findings from the initial study lead the present PhD thesis to focus on a novel combination of Radiative Cooling with Solar Thermal Collection, a well-established technology, for profitability and operational purposes. This combination of renewable technologies in a physical device is onwards named Radiative Collector and Emitter (RCE), based on the importance of electromagnetic radiation in the heat balance in this technology/device.

After the spotting of the desired climatic conditions to ease the broadwise implementation of RCE in buildings, the PhD thesis follows to the design, development and characterisation of an RCE device by numerical modelling and experimental testing. The results demonstrate RCE ability and suitability for heating and cooling, and present the most influencing parameters of RCE applications.



This page intentionally left blank

Table of contents

List of figures	xii
List of tables	xiii
Nomenclature	xiv
Chapter 1. Introduction	1
1.1. Background	1
1.2. Energy consumption in buildings.....	1
1.3. Solar thermal energy	4
1.4. Radiative cooling concept	6
1.5. Radiative cooling technology	8
1.5.1. Radiative cooling technology background	8
1.5.2. Technology readiness level	11
1.5.3. Radiative Cooling and Solar Thermal Collection technology combination/integration: Radiative Collector and Emitter	12
Chapter 2. Objectives	13
Chapter 3. Methodology and PhD thesis structure	14
Chapter 4. Radiative cooling as low-grade energy source: A literature review ..	17
4.1. Introduction	17
4.2. Contribution to the state-of-the-art	17



4.3.	Contribution to the objectives of the PhD thesis	19
4.4.	Journal paper.....	19
4.5.	Review update.....	38
4.5.1.	Selective day-time radiative cooling	38
4.5.1.1.	Polymer foils on metal surfaces.....	38
4.5.1.2.	Multilayer materials and Photonics structures/designs.....	39
4.5.1.3.	Single-material surface	41
4.5.1.4.	Selective screen and convection shield.....	41
4.5.1.5.	Directional selectivity	42
4.5.2.	Theoretical approach and numerical simulation	42
4.5.3.	Radiative cooling prototypes.....	42
4.5.4.	Radiative cooling combination.....	43
Chapter 5. Energy Savings Potential of a Novel Radiative Cooling and Solar Thermal Collection Concept in Buildings for Various World Climates		
48		
5.1.	Introduction	48
5.2.	Contribution to the state-of-the-art	49
5.3.	Contribution to the objectives of the PhD thesis	52
5.4.	Journal Paper.....	52
Chapter 6. A new flat-plate radiative cooling and solar collector numerical model: Evaluation and metamodeling		
63		
6.1.	Introduction	63
6.2.	Contribution to the state-of-the-art	64
6.3.	Contribution to the objectives of the PhD thesis	67
6.4.	Journal Paper.....	68

Chapter 7. Combined Radiative Cooling and Solar Thermal Collection:	
Experimental Proof of Concept.....	85
7.1. Introduction	85
7.2. Contribution to the state-of-the-art	86
7.3. Contribution to the objectives of the PhD thesis	89
7.4. Journal Paper.....	89
Chapter 8. Conclusions	103
8.1. Conclusions	103
8.2. Recommendations for future work	107
8.2.1. Numerical modelling future work	107
8.2.2. Experimental testing future work.....	108
Scientific foreign exchange	109
References.....	110

List of figures

Figure 1 – Final energy consumption by sector, World 1990-2018 [3]	2
Figure 2 - Buildings sector energy use by service, World 2017 [7]	2
Figure 3 – Global Horizontal Irradiation (GHI) map (up). Direct Normal Irradiation (DNI) map (down) [15]	5
Figure 4 - Earth’s energy budget [14]	7
Figure 5 - Heat transfer balance on a radiative cooling surface	8
Figure 6 - PhD thesis structure	14
Figure 7 - RCE operational diagram	49
Figure 8 – Conceptual radiation diagram flow for RCE day-time and night-time operation modes.	50
Figure 9 - RCE device 3D representation.....	50
Figure 10 - 1D resistance-capacitance thermal model.....	65
Figure 11 – Radiation model	66
Figure 12 – Solar thermal collector plate (left); radiative cooling plate (right)	66
Figure 13 – Experimental setup sketch.....	87

List of tables

Table 1 - Detailed characteristics of newly developed materials for day-time radiative cooling (since 2017)	45
Table 2 - Radiative cooling experimental appliances and combination of technologies (since 2017)	47

Nomenclature

STE	Solar Thermal Energy
STC	Solar Thermal Collection
RC	Radiative Cooling
RCE	Radiative Collector and Emitter
HVAC	Heating Ventilation and Air Conditioning
DHW	Domestic Hot Water
TRL	Technology Readiness Level
FPC	Flat Plate Collector
PV	Photovoltaic
PVT	Photovoltaic Thermal Collectors
GHI	Global Horizontal Irradiance
KPI	Key Performance Indicator

Chapter 1. Introduction

1.1. Background

Climate change is a reality that humanity must face in the coming decades. The effects of climate change are becoming more evident, dangerous and destructive [1]. There is scientific consensus in what are the causes of climate change: the emission of greenhouse gases from human activities such as fossil fuels consumption and farming livestock, and the destruction of the rainforest [2]. The leading cause is fossil fuel consumption which is a consequence of an increase of global energy consumption by more than 58% during the last three decades [3].

To mitigate or reverse climate change effects, international institutions are setting long-term global goals [4,5]. One of these ambitious goals is a set of policy initiatives by the European Commission named the European Green Deal aiming to make the European Union climate neutral (greenhouse gases emissions neutral), as well as setting economic (decoupling economic growth from resource consumption) and social (not excluding any person nor place) objectives by 2050 [5]. Some of the actions stated in the plan are: to decarbonise the energy sector, to ensure more efficient buildings, and to invest in environmental-friendly technologies.

1.2. Energy consumption in buildings

Buildings are critical to a sustainable future because their design, construction, operation, and use are significant contributors to energy-related sustainability challenges. The direct energy consumption in buildings is responsible for approximately 32% of global final energy consumption, around 2.900 Mtoe (34 PWh) [3] (see Figure 1). Buildings also represent nearly 40% of total global direct (10%) and indirect (30%) energy-related CO₂ emissions, and almost 50% of global electricity final consumption. Global building-related CO₂ emissions have continued to rise by nearly 1% per year since 2010 [3,6].

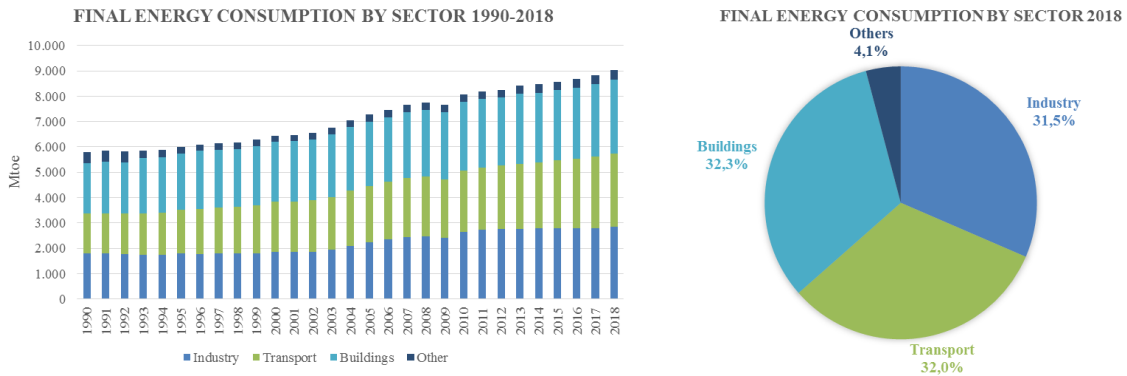


Figure 1 – Final energy consumption by sector, World 1990-2018 [3]

The energy consumed in buildings is related to various services: space heating, domestic hot water (DHW), space cooling, lighting, cooking, household appliances and others (see Figure 2). This energy consumption has increased by more than 20% between 2000 and 2018, approximately 1.2% yearly average growth rate.

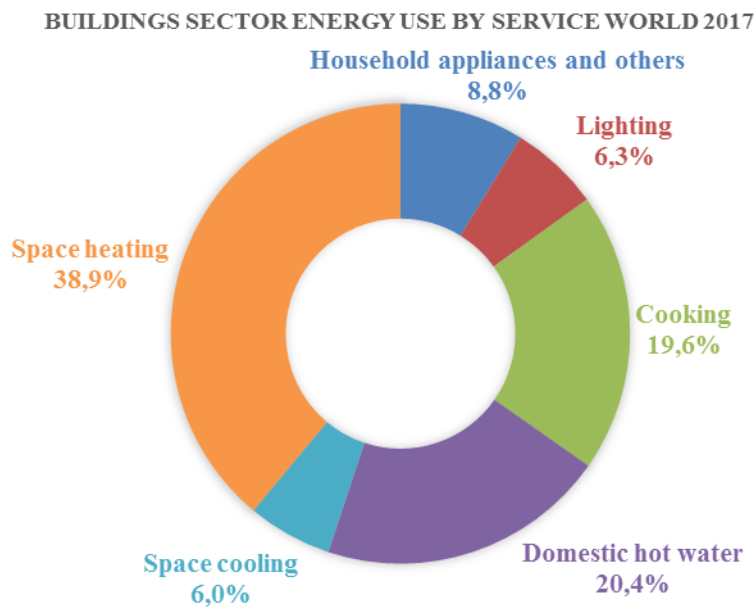


Figure 2 - Buildings sector energy use by service, World 2017 [7]

Space heating is the largest energy end-use in the building sector, representing almost 39% of it. The introduction, enforcement, and revision of building energy codes, along with policies to improve equipment performance, have helped keep energy use for space heating relatively constant since 2000 while increasing thermal comfort in buildings. However, low-efficient heating technologies, including coal, oil, and natural gas boilers as well as electric resistance heating technologies, still dominate heat production in most buildings [7].

Domestic hot water represents 20% of energy end-use in the building sector, being its production dominated by fossil fuel and low-efficiency electrical technologies. Sales of solar thermal technologies and energy-efficient heat pump water heaters have progressively been taken up since 2010. Still, they were not enough to offset the rapidly rising energy service demand [7].

Space cooling accounts for 6% of energy end-use in the building sector; however, it is by far the fastest-growing energy end-use worldwide [7]. Energy demand for space cooling has more than tripled since 1990, responsible for nearly 8.5% of the total final electricity consumption in 2019. Rising demand for space cooling is already putting enormous strain on electricity distribution systems in many countries, as well as driving up CO₂ emissions. Rising living standards, population growth, and more frequent and extreme heatwaves are expected to stimulate an unprecedented cooling demand in the next decade [8].

Other energy end-use services are cooking, which accounts for almost as much energy as DHW (19.6%), and electricity consumption services such as lighting (8.8%) and household appliances (6.3%), with an average growth rate of 2.2%, almost doubling the energy consumption rate of the building sector (1.2%) [3,7].

Among these services, the higher energy consumptions are space heating and cooling, and DHW generation. For that reason, there is a general interest to reverse this energy consumption trend by deploying integral solutions.

For space heating and space cooling, active and passive strategies can be applied to reduce energy consumption. However, energy consumption cannot be reduced to zero if thermal comfort conditions are to be preserved [9]. Similarly occurs for domestic hot water; energy demand cannot be reduced to zero. It is at this point when renewable sources should emerge to cover these energy needs.

When talking about space heating and DHW, solar thermal collection is a well-known technology to meet these heating demands [10]. However, for cooling, there is still no simple renewable alternative with such potential and development. Sustainable approaches to achieve cooling involve environmental heat sinks. These environmental heat sinks include (i) ambient air, heat transfer by convection and evaporation; (ii) ground (or large masses), heat transfer by conduction or convection; and (iii) sky, heat transfer by thermal radiation [11].

Ambient air (or atmosphere) is the primary means to reject heat. In general, this heat rejection is by convection, but it is also possible by evaporation as latent heat rejection. Heat rejected by convection of a body to the ambient air is the most cost-effective cooling solution whenever temperature difference allows it. Evaporation is also an excellent solution when the ambient air is dry enough, and water is not a scarce resource. Current active applications of this natural heat sink are cooling towers and evaporative cooling towers [11].

The ground has a very stable temperature and is increasingly becoming an option as a heat sink. The temperature is not only constant during the day, but annually very stable depending on the depth. The heat is transferred by conduction to the ground, thus requiring large exchange surfaces. Other large masses, such as rivers, lakes or seas, are also very temperature stable. In this case, convection favours the heat exchange. Ground source and water source heat pumps are examples of active applications of this natural heat sink [11].

Finally, the sky (or outer space) is the least studied and exploited heat sink. The heat rejection is based on the fact that every object above 0K emits electromagnetic radiation and, according to outer space low effective temperature ($\sim 3\text{K}$ [12]), it has the highest potential among the heat sinks. Radiative cooling devices take advantage of this low temperature to achieve below ambient air temperature [11] with minor energy consumption, in active systems, proven as one of the cooling strategies that can displace the use of heat pumps [13]. However, its difficult accessibility (physical limitation based on Stefan–Boltzmann law, the need for favourable climatological conditions, material choice, energy management), results in limited applicability.

1.3. Solar thermal energy

One of the most studied renewable energies is solar energy. The Sun is also the origin of other renewable energies (wind, hydro, biomass, tidal). Two main groups of energies are harnessed from the Sun: thermal energy, using solar thermal collection, and electrical energy, using photovoltaic.

One key topic of this PhD thesis is Solar Thermal Energy (STE) or solar thermal collection. STE is the energy and a technology for harvesting incoming solar energy to generate thermal energy for residential, commercial and industrial sectors.

Solar energy has enormous potential; Earth receives 174 PW of incoming solar radiation at the upper side of its atmosphere, where part of this energy is absorbed or reflected by clouds and atmosphere, arriving 96 PW at the Earth's surface (840.960 PWh/year) [14] whereas around the world is consumed 116 PWh of primary energy per year [3]. This number is an average, and the reality is that harvestable solar energy differs a lot from site to site, because of different factors such as geography and climatology, limiting the amount of available solar energy (3).

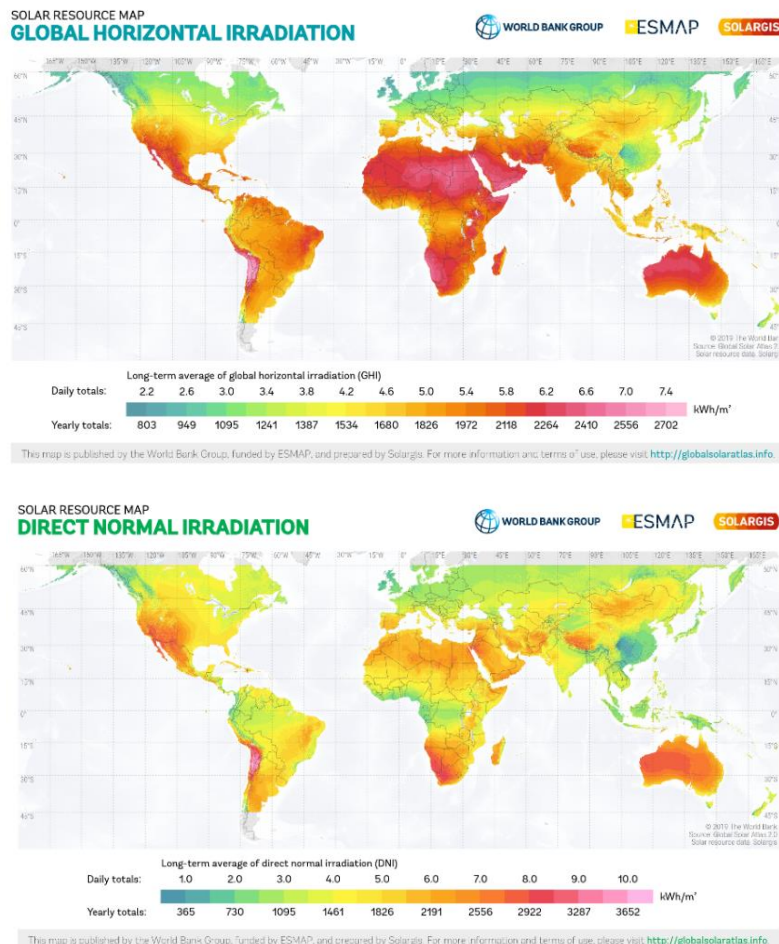


Figure 3 – Global Horizontal Irradiation (GHI) map (up). Direct Normal Irradiation (DNI) map (down) [15]

Solar technologies are classified as passive or active, depending on how they capture or convert the sunlight and distribute this energy. Active solar technologies convert sunlight

into a useful energy source. Passive solar techniques are the selection of materials with favourable thermal properties for a specific application and the design of buildings or any element taking into account the Sun.

STE active technologies can be used for different applications and can be classified according to their operating temperature:

- Low-temperature ($< 50^{\circ}\text{C}$) collectors. Generally, unglazed collectors, or similar, using air or water as heat transfer fluid. Applications: heat swimming pools, space heating.
- Medium-temperature ($50\text{-}200^{\circ}\text{C}$) collectors. Usually flat-plate collectors (FPC) and evacuated tube collectors, for DHW, space heating for residential and commercial buildings, and industrial processes (solar absorption heat pumps).
- High-temperature ($> 200^{\circ}\text{C}$) collectors. These technologies concentrate sunlight to achieve high temperatures, using mirrors (linear Fresnel reflectors (LFR), compound parabolic collectors (CPC), parabolic trough collectors (PTC), parabolic dish reflectors (PDR), heliostat field collectors (HFC)) or lenses. This high temperature is used for hot water or steam generation in industries and electric power production.

STE technologies have the potential to cover the heating and cooling demand in the residential sector and contribute significantly to meet the heating and cooling demand of the commercial and industrial sector. Active STE technologies for heat supply can reduce the fuel demand for domestic hot water from 50%-70% and 40-60% for space heating. The potential for STE technologies will dramatically increase when suitable devices to store thermal heat for the mid-long term (seasonal storage) are available [16].

1.4. Radiative cooling concept

In general, radiative cooling is the thermal process by which a body losses heat by emitting electromagnetic radiation to the environment. When a body surface presents a net cooling balance between the emitted and the absorbed radiation (in case of inexistent or negligible heat gains by thermal conduction and convection from surroundings), it results in a surface temperature decrease, namely radiative cooling.

The principles of radiative cooling play an essential role in the Earth's energy budget. The Earth's energy budget refers to the net balance between the energy the Earth receives from outside, basically from the Sun, and the energy the Earth radiates back into outer space (Figure 4).

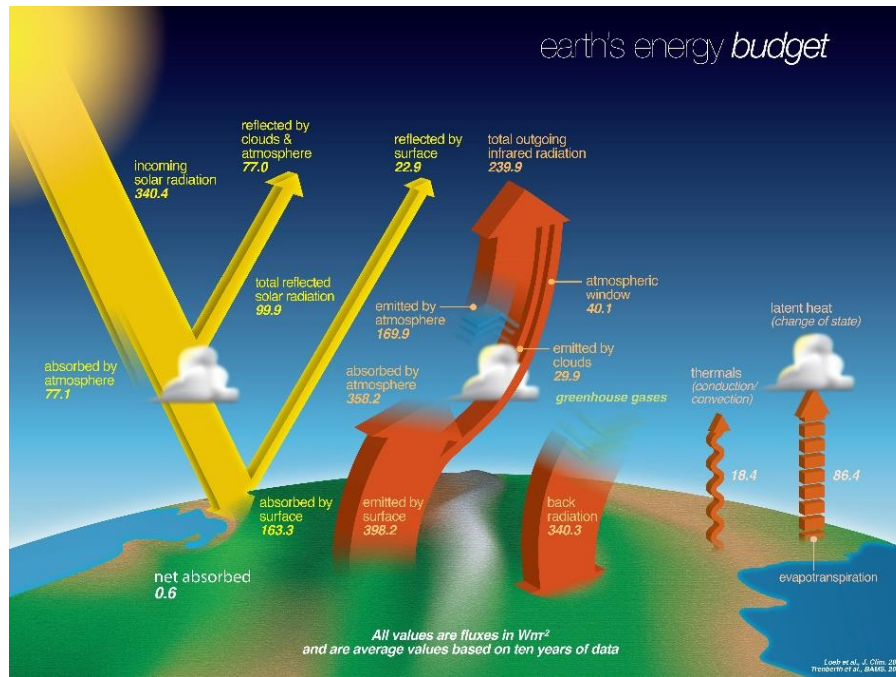


Figure 4 - Earth's energy budget [14]

Three natural heat sinks are part of this process: the outer space, the atmosphere and the Earth. However, when mentioning the term “radiative cooling” in scientific literature, it mainly refers to use the outer space/sky as a heat sink. This natural process is the foundation of radiative cooling applicability.

Referring to any surface located on Earth's surface facing the sky, the effective outgoing infrared radiation is the difference between the infrared radiation emitted by this surface and the infrared radiation coming from the atmosphere absorbed by this surface. The radiation emitted by the Earth's atmosphere is similar to blackbody radiation but with a “gap” between wavelengths 7–14 μm , known as “infrared atmospheric window” [17]. The thermal radiation emitted between these wavelengths going to sky passes mostly directly to outer space, and no counter radiation is received. This singularity results in an effective outgoing infrared radiation that allows the achievement of temperatures below ambient.

Radiative cooling holds great promise as the next generation cooling technology thanks to its operation with little energy consumption and the non-emission of environmental pollution.

1.5. Radiative cooling technology

1.5.1. Radiative cooling technology background

Since ancient times, long before the understanding of this natural phenomenon, night radiative cooling had been used by humanity to keep buildings cool, for ice production, and for fog dew water harvesting. Under clear sky nights, with low wind, some realised that surfaces get colder than ambient temperature. This observation was the foundation for future research.

Before applying this natural phenomenon to any specific application, it must be understood and technically studied. The net cooling power of a radiative cooling surface is defined based on the heat transfer balance that considers all the heat exchange processes involved with this surface (Figure 5).

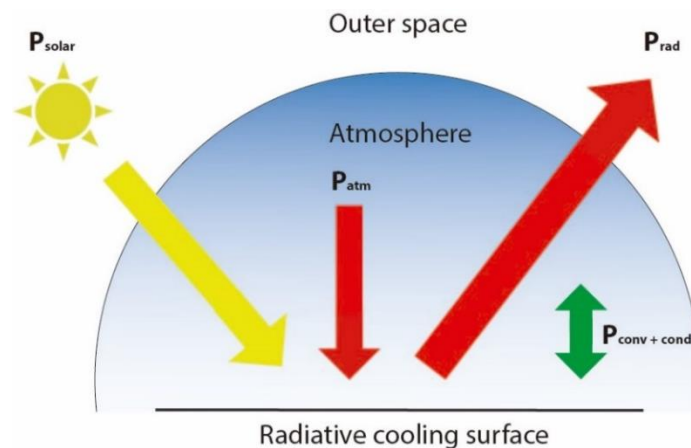


Figure 5 - Heat transfer balance on a radiative cooling surface

From the radiative balance (Eq. 1), three fluxes are depicted: solar radiation (P_{solar}), incoming radiation from the atmosphere (P_{atm}) and outgoing radiation emitted by the surface (P_{rad}). Among these three fluxes, atmospheric radiation is the lesser-studied and, probably, as necessary to be understood as the others fluxes.

$$\text{Eq. 1} \quad P_{\text{net}}^{\text{rad}} = P_{\text{rad}} - \alpha_{\text{solar}} \cdot P_{\text{solar}} - \alpha_{\text{IR}} \cdot P_{\text{atm}}$$

Where:

α_{solar} Radiative cooling surface absorptivity in the solar band [-].

α_{IR} Radiative cooling surface emissivity in the infrared band [-].

Atmospheric radiation originates from some gases that compose the atmosphere, also known as “greenhouse gases”. The main gases involved in infrared atmospheric radiation at ground level are water vapour and carbon dioxide, being water vapour the major contributor [18].

Also, the presence of clouds increases the incoming infrared atmospheric radiation compared to clear sky conditions. Clouds act like a blackbody emitter, supplementing the waveband where the atmospheric emission lacks, and its radiative effect is to “close” the infrared atmospheric window.

Some of these factors (water vapour content, humidity and cloudiness) can be related to climate, thus pointing out regions with higher radiative cooling availability.

For engineering purposes, there is an interest in measuring and predicting the atmosphere infrared radiation. Although this radiation can be measured with specific equipment (Pyrgeometer), the dynamic properties of the Earth atmosphere make it difficult to predict its behaviour. Nevertheless, as already stated, incoming infrared radiation can be related to climatological parameters and geographical places to predict its value in the future, using, for instance, empirical correlations.

There are two extended methods to express empirical correlations in an understandable and straightforward form, using Stefan-Boltzmann law:

1. To assume the sky acting as a blackbody emitter at an effective sky temperature (T_{sky}):

$$\text{Eq. 2} \quad R_{\downarrow} = \varepsilon \cdot \sigma \cdot T_{sky}^4$$

2. To assume the sky having the ambient dry bulb temperature (T_a) with an effective sky emissivity (ε_{sky}):

$$\text{Eq. 3} \quad R_{\downarrow} = \varepsilon_{sky} \cdot \sigma \cdot T_a^4$$

Where:

- R_{\downarrow} incoming infrared atmosphere radiation (P_{atm} in Eq. 1)
- ε blackbody emissivity
- σ Stefan–Boltzmann constant
- T_{sky} effective sky temperature
- ε_{sky} effective sky emissivity
- T_a Ambient temperature

There is extended bibliography of these measurements and correlations, which are summarised and analysed as part of this PhD thesis in Chapter 2.

Once atmospheric radiation becomes tangible, radiative cooling applications can be studied, simulated, and evaluated.

The main purposes of radiative cooling applications are to emit/reject heat to a heat sink and achieve low temperatures for specific applications. The best strategy to increase heat emission is to increase the temperature of the emitting surface, therefore increasing thermal radiation emitted according to Planck's law.

The radiative cooling equilibrium temperature is around 5-10°C below ambient. This natural equilibrium can be enhanced to achieve lower temperatures using selective materials with specific optical properties, to emit in the infrared atmospheric window. These optical properties are: to be a perfect emitter in the infrared atmospheric window wavelength band (8–13 μm) and a perfect reflector anywhere else. With these properties, surface temperatures around 50°C below ambient temperature could be reached [19].

Selective materials have been studied, searched, and manufactured since long ago. However, for the last three decades, there have been many studies on the development and analysis of materials and devices for potential use in nocturnal cooling. Most of the studies aim to develop appropriate materials with high emissivity in the infrared atmospheric window wavelength range. As part of this PhD thesis, an extensive review of radiative cooling materials has been done and is presented in Chapter 2.

Until recent developments, radiative cooling was only available and harvestable during night-time. However, with the development of new selective materials, this barrier was

overcome, and nowadays, it is also possible during day-time [20]. Therefore, radiative cooling applications can be classified according to its two operating periods, namely night-time and day-time.

Moreover, depending on how radiative cooling is produced and distributed, it is categorised as:

- Passive radiative cooling: when the radiator is the building surface or object envelope which radiates towards the sky or environment to keep it cool or to cool it down.
- Active radiative cooling: when the radiator is a plate or similar which radiates towards the sky and gets cool. This coolness is then transferred to a fluid to be used in another system.

Passive radiative cooling is not as attractive as active because the applicability is limited to the buildings envelope to reduce cooling loads [21]. On the other hand, active radiative cooling has more potential and applicability, being HVAC systems the main end-users of the cold produced by radiative cooling devices [22].

1.5.2. Technology readiness level

The technology readiness level (TRL) of radiative cooling is little past halfway to reach the final user (general research is in steps 5-6 over 9, at the step of technology validated and demonstrated in relevant environments with some pioneering research on steps 7-8 [23,24]). An extensive State-of-the-art review of radiative cooling technology is part of this PhD thesis and is presented in Chapter 2. Nevertheless, some insights are presented below.

Much radiative cooling research has focused on the development of prototypes and numerical models, as well as on testing of empirical devices. The knowledge of radiative cooling technology is high regarding the current TRL because radiative cooling lies on general thermal properties, with particular consideration of radiation, and a similar conceptualisation to solar thermal collectors. However, no commercial device has reached the market due to its low available power density (between 20 and 80 W/m² [25]). Recently, a commercial product for day-time radiative cooling can be found in the market

[24], but only for demonstration projects. Technology deployment is still waiting for the development of new selective meta-materials, aiming to increase energy production and reduce device cost, and the implementation of new strategies to integrate radiative cooling with other technologies.

1.5.3. Radiative Cooling and Solar Thermal Collection technology combination/integration: Radiative Collector and Emitter

Radiative cooling is a renewable cooling technique which dissipates heat to outer space. As technology, radiative cooling has low power density, compared to other renewable technologies such as solar thermal collection or PV, and has encountered challenges on day-time operating ability. The low power density could be a problem to achieve sufficient energy production to cover manufacturing and operation costs. As already mentioned, integrating radiative cooling with other technologies (solar photovoltaic/thermal collectors), that do not operate at night, could provide this affordability.

As the main topic of this PhD thesis, it is proposed to integrate radiative cooling with solar thermal collection, from now on named Radiative Collector and Emitter (RCE). Considering the similitude in the device end-design and the capability to operate in solar thermal collection mode during day-time and radiative cooling mode during night-time, it becomes a potential technological integration.

Apart from technological aptitudes, the integration of RCE with the vast majority of buildings is possible and of great interest, not only because of the ease of physical installation but because the different demanded services of heat and cold by buildings can be partially or totally covered with a single system.

Chapter 2. Objectives

This PhD thesis aims to develop, analyse, and implement a system to collect solar thermal energy and nocturnal radiative cooling in a single device for heat and cold production for thermal energy supply.

The general objective is divided into several specific objectives detailed next:

- I. To review radiative cooling, both principles and technology, from the first studies to the state-of-the-art research, to make a helpful document to foster and sustain the present PhD thesis and future research.
- II. To review the existing and new materials, and study the radiation properties suitable for both technologies separately and together: radiative cooling and solar thermal collection.
- III. To analyse the technical feasibility of RCE worldwide implementation by comparing its energy production to the energy consumption of different building typologies.
- IV. To develop a numerical model of an RCE device to simulate its behaviour based on its dimensional parameters and external/climatological parameters.
- V. To experimentally test an RCE device with real working conditions to evaluate the system's operation and to validate the numerical model with data.
- VI. To study and optimise an RCE device using the numerical model to determine the most influencing parameters and extract relevant conclusions of the system.

Chapter 3. Methodology and PhD thesis structure

The present PhD thesis bases its structure on four scientific papers, which have already been published in Journal Citation Reports journals. The PhD thesis structure is the framework that guides the reader through it and intends to follow the natural process of discovering new technology. Figure 6 presents the PhD thesis structure:

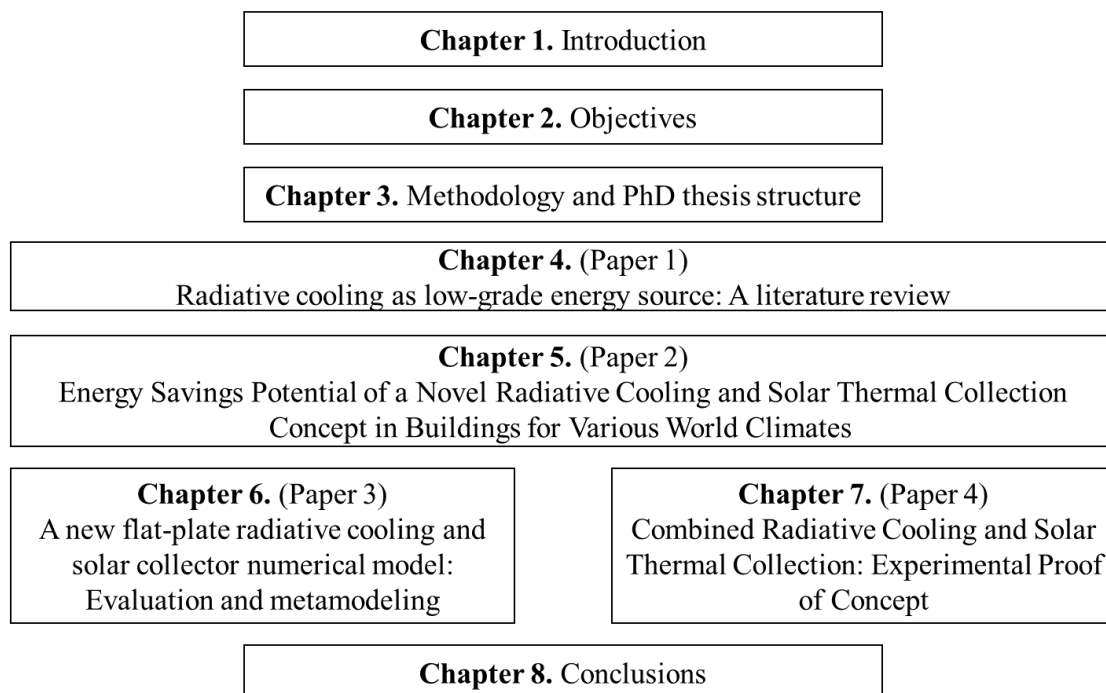


Figure 6 - PhD thesis structure

- Chapter 1 introduces the reader to the PhD thesis topic, from global sustainability problems to specific renewable energy-savings technology.
- Chapter 2 presents the objectives defined for this PhD thesis going from general to more detailed and specific objectives.
- Chapter 3 presents the methodology and the structure followed in the present PhD thesis.

The four scientific papers are an essential part of the thesis, and the methodology of each is described inside it. The following chapters introduce, present, and acknowledge the contributions of these four papers.

- Chapter 4 presents a complete literature review of radiative cooling. It reviews radiative cooling technology from the oldest available to state-of-the-art research. Part of this task is in the following review paper, which is included in this chapter:

- S. Vall and A. Castell, “Radiative cooling as low-grade energy source: A literature review,” *Renewable and Sustainable Energy Reviews*, vol. 77, pp. 803–820, 2017. DOI:10.1016/j.rser.2017.04.010.

This review paper introduces the reader to the topic by presenting radiative cooling basics, then poses particular attention to selective radiative cooling materials and strategies, theoretical and numerical radiative cooling modelling research and finally experimental radiative cooling research.

Chapter 4 also includes a summary of newly disclosed research from continuous literature surveillance since the review paper publication to complement this chapter. The reviewed literature focused on day-time radiative cooling, and radiative cooling technology combined with other renewable technologies.

- Chapter 5 presents the potential energy savings of the combination of radiative cooling with solar thermal collection, a novel concept named Radiative Collector and Emitter, based on energy demands of different buildings typologies and for worldwide climatology. This chapter comprises the following journal paper:

- S. Vall, A. Castell, and M. Medrano, “Energy Savings Potential of a Novel Radiative Cooling and Solar Thermal Collection Concept in Buildings for Various World Climates,” *Energy Technology*, vol. 6, no. 11, pp. 2200–2209, 2018. DOI:10.1002/ente.201800164.

The research fundamentals the assessment in the coverage ratio between the energy demands for space cooling and DHW of different building typologies and the energy production of the studied technology combination, for different locations worldwide.

As presented in Figure 6, the development of journal papers 3 and 4 (Chapter 6 and Chapter 7) was in parallel. The reason is that paper 3 needed empirical data for validation from an experimental setup, and this experimental setup is analysed in paper 4.

- Chapter 6 presents a numerical modelling of an RCE to improve existing research by giving more strength and precision to the radiation functionalities. The model was validated with data from an RCE experimental setup; then it was used to determine and optimise the relevant radiative cooling parameters. This chapter comprises the following journal paper:
 - S. Vall, K. Johannes, D. David, and A. Castell, “A new flat-plate radiative cooling and solar collector numerical model: Evaluation and metamodeling,” *Energy*, vol. 202, art. 117750, 2020. DOI:10.1016/j.energy.2020.117750.

The conception and development of the numerical RCE modelling presented in this chapter were done during the four-month PhD candidate research stay at the Centre for Energy and Thermal Sciences of Lyon (CETHIL) at the University of Lyon.

- Chapter 7 presents the experimental results of an RCE experimental setup used for concept validation. The experimental setup consisted of two adapted solar thermal collectors, one used for solar thermal collection and the other for radiative cooling. The results were presented in the following journal paper, included in this chapter:
 - S. Vall, M. Medrano, C. Solé, and A. Castell, “Combined Radiative Cooling and Solar Thermal Collection: Experimental Proof of Concept,” *Energies*, vol. 13, no. 4, p. 893, 2020. DOI:10.3390/en13040893.
- Chapter 8 presents the conclusions of the PhD thesis and future work. This chapter discusses and summarises all research breakthroughs at the end of this PhD thesis and presents possible next steps on this topic.

Chapter 4. Radiative cooling as low-grade energy source: A literature review

4.1. Introduction

Chapter 4 aims to compile and structure all available information scattered in the literature on radiative cooling for whoever wants to catch up on this topic, or for researchers on this topic who need a foundation to lay its research.

Paper 1 presents a complete literature review of radiative cooling considering all different radiative cooling aspects, such as the environmental conditions affecting the phenomena, the selection and development of materials, the analytical and numerical methods, and the experimental prototypes until 2016. Radiative cooling has been studied since the early 20th century, but in recent years, great interest has been aroused around this topic due to the exploration of renewable cooling techniques. Because of this, the authors performed a literature review update to analyse the newly disclosed research.

4.2. Contribution to the state-of-the-art

Before the publication of the review paper (paper 1), all radiative cooling related research was scattered in the literature, becoming an arduous work to identify new research opportunities. Paper 1 presents this research in a structured review. Apart from generating a complete compendium of radiative cooling research, paper 1 made other contributions.

First of all, the paper included general but precise information on the radiative cooling physical phenomenon. The first technical approaches for incoming infrared radiation estimation were empirical correlations. The authors made a particular effort to compile a complete list of empirical correlations for clear and cloudy sky conditions. From this task, the authors detected that the precision of empirical correlation is bare and do not depict the physical phenomenon: an average approximate overall value instead of real-time data

and uniform spectrum instead of real sky radiation. However, they can be used as a good approximation only if adapted or chosen to a specific location.

The review also spotted the lack of research on radiative cooling harvesting potential (locations, climates, power density, etc.). Radiative cooling requires a world climate analysis to evidence which climates are of interest to implement this technology.

Further, the authors reviewed and discussed available selective radiative cooling applications research, classifying them according to their specific position in the application, the selective material technology, and other selective strategies. Recently, new selective materials have opened a new field of research with high potential.

The paper also reviewed and compared analytical and numerical simulations of radiative cooling research, orientated to flat plate design. The review classifies the research depending on how they deal with the sky, the ambient, or the internal fluid. The results pointed out the desirability of windscreen usage, fluid as internal thermal-carrier usage, and heat storage usage.

Moreover, the paper reviewed experimental active radiative cooling devices. The results showed the applicability of this technology for some climates and pointed out to add new aspects or functionalities in new prototypes to improve its performance, applicability, and profitability.

From this radiative cooling literature review, the authors detected a feasible potential of radiative cooling for cold production. The authors also spotted the interest in selective material usage, the need to improve optical properties in simulations, and the interest in combining radiative cooling with other energy production technologies, as proposed in this PhD thesis with solar thermal collection.

Also, the literature extension identified two main research interest. First, the development of selective materials for day-time radiative cooling, which is preferred instead of nocturnal because cooling peak demand happens during the day-time period. Second, the development of experimental prototypes combining radiative cooling with other generation technologies. This combination of technologies complements radiative cooling by producing other types of energy, thus making it more profitable. Some promising combinations are with solar thermal collection and photovoltaic.

Moreover, the comprehensive review reveals the difficulties of comparing/benchmarking new devices and materials due to the lack of standardised key performance indicators (KPI).

4.3. Contribution to the objectives of the PhD thesis

Chapter 4 contributes to accomplishing objectives I and II (partially), both related to the reviewing and detection process.

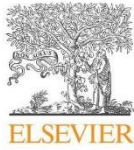
In the present chapter, a complete review of all available radiative cooling literature is performed and presented in a review paper (paper 1) and extended with the latest research in the field, therefore, accomplishing objective I. The review paper has an easy-to-follow structure, dividing the research into different topics. The literature review extension has focused on the new trends and similarly followed the structure of the review paper.

Additionally, as part of the same process, the review of existing and new materials suitable for radiative cooling is performed. So, objective II has partially been accomplished in the present chapter and completed in Chapter 6.

4.4. Journal paper

Reference:

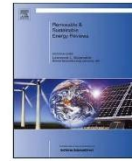
S. Vall and A. Castell, “Radiative cooling as low-grade energy source : A literature review,” *Renewable and Sustainable Energy Reviews*, vol. 77, pp. 803–820, 2017. DOI:10.1016/j.rser.2017.04.010.



Contents lists available at ScienceDirect

Renewable and Sustainable Energy Reviews

journal homepage: www.elsevier.com/locate/rser



Radiative cooling as low-grade energy source: A literature review



Sergi Vall, Albert Castell*

Department of Computer Science and Industrial Engineering, University of Lleida, Edifici CREA, Pere de Cabrera s/n, 25001 Lleida, Spain

ARTICLE INFO

Keywords:

Radiative cooling
Renewable cooling
Night sky radiation
Low-grade cooling

ABSTRACT

Radiative cooling is a technology intended to provide cooling using the sky as a heat sink. This technology has been widely studied since 20th century but its research is scattered all over the literature, requiring of a review to gather all information and a state-of-the-art. In the present article, the research has been classified in: (1) radiative cooling background, (2) selective radiative cooling, (3) theoretical approach and numerical simulations, and (4) radiative cooling prototypes. Even though this is a low-grade technology it can dramatically reduce the energy consumption, since it is renewable and requires low energy for its operation. However, new functionalities of the device, apart from radiative cooling, are required for profitable reasons. Some recommendations extracted from the literature to improve the efficiency of radiative cooling are: to use a cover to achieve low temperatures, to use water instead of air as heat-carrier fluid, and to couple the device with heat storage. Finally, further research should be focused in the development of new materials with improved radiative properties, the measurement of incoming infrared atmospheric radiation and/or new technics to predict it, and the evaluation of new device concepts.

1. Introduction

The environmental awareness is growing fast nowadays with special attention to the energy consumption and environment preservation. Regarding to energy consumption, the building sector can contribute in a remarkable way in achieving the transition to a less energy intensive system. There is huge potential in reducing energy consumption with profitable measures that reduce the economic and environmental costs. The energy consumption of buildings represents 40% of total energy consumption in the European Union [1], where space conditioning of buildings represents almost half of the building energy consumption.

For space conditioning, especially in hot climate countries, most of the buildings use reversible heat pumps which consume a large amount of electrical energy. New legislations consider electrically driven heat pumps as a renewable source of energy when they achieve seasonal average efficiencies higher than $SCOP_{NET} \geq 2.5$ [2,3], since they take advantage of the air temperature to reduce electrical consumption. However, there are other renewable sources that further reduce the use of non-renewable energy, since they can achieve the required temperature level with no or very low electrical use. Solar energy is one of the most widely studied sources; however, its use for cooling is limited by the implementation of absorption heat pumps.

Another technology that has been studied in order to provide cooling and displace the use of heat pumps is radiative cooling. This technique is based on emitting long-wave thermal radiation from a terrestrial body toward space through the infrared atmospheric window

between 8 and 13 μm wavelengths. The atmosphere infrared window is the dynamic behaviour of earth's atmosphere that allows some infrared radiation pass through the atmosphere without being absorbed and, thus without heating the atmosphere.

It is known that a body emits electromagnetic radiation in a wavelength range depending on its temperature. At ambient temperature most of the radiation is emitted in the infrared spectrum. Radiative cooling technique uses these properties to generate a cooling net balance between the emitted thermal radiation from the terrestrial surface and the received from the atmosphere.

Using this technology for cooling purposes will dramatically reduce the energy consumption; depending on the case, the energy consumption can be zero or just the energy consumed by a small pump running on the operating hours. The performance of the radiative cooling technology is affected by the physical properties of the device and also by the surrounding conditions. Therefore, special attention must be paid to materials and environmental conditions.

From early 20th century, several authors have worked on the field of radiative cooling. However, in the present all the information is scattered in the literature, making it difficult to identify new research opportunities. Although Lu et al. developed a practical review of radiative cooling [4], they focused in passive radiative cooling in buildings, and they did not include detailed information about the phenomenon and the studied materials for radiative cooling as well as the radiative cooling devices and models. Therefore, there is a clear need to compile and structure all this information. For that reason, this

* Corresponding author.

<http://dx.doi.org/10.1016/j.rser.2017.04.010>

Received 3 August 2016; Received in revised form 24 January 2017; Accepted 10 April 2017

Available online 05 May 2017

1364-0321/ © 2017 Elsevier Ltd. All rights reserved.

Nomenclature	
Symbol	Description Equation where appears Variable adapted
Δt	maximum day length (h) 24
$\Delta \epsilon$	correction factor to take into account the day-night and seasonal variation (-) 24
$\Delta \epsilon_e$	pressure correction factor (-) 19, 20
$\Delta \epsilon_h$	diurnal correction factor (-) 17, 18, 19 $\Delta \epsilon$ in [23].
A	factor that takes into account the variation of the emissivity 24
clf	cloud fraction term (-) (see [38]) 41
C_p	specific heat of the fluid ($J \cdot kg^{-1} \cdot K^{-1}$) (see [115]) 52
e_0	partial pressure of water vapour (mbar). 4, 5, 6, 9, 10, 11, 12, 25, 26, 29, 30, 31, 32, 33, 40, 41, 42, 44, 45 e in [5,9–12,29,38,42,43], e_d in [39].
$\bar{\epsilon}_s^H$, $\bar{\epsilon}_{s,2}^H$ and η^H	parameters to compare radiative cooling selective materials (see [45]) (-) 49, 50, 51
f	factor that takes into account the delay of the emissivity cycle in relation to the solar cycle (-) 24
$f_{s,i}$	fraction of black body radiation emitted through the infrared window by layer “i” (-) 37
F	collector efficiency factor (-)(see [115]) 52 F’ in [115].
H	relative humidity (%), 14
$I_{b,\lambda}$	spectral radiance of a blackbody ($W \cdot m^{-2}$) 49, 50 W in [45].
k	empirical coefficient depending on the cloud type, to be defined in the original paper (-) 34
$K(t), L(t)$	correction factors (see values in [25]) 23 $K(H)$, $L(H)$ in [25].
K_0	daily clearness index (-) (see [37]) 40
\dot{m}	mass flow rate ($kg \cdot s^{-1}$) (see [115]) 52
n	number of parallel tubes (-)(see [115]) 52
P_0	atmospheric pressure (mbar) 20 P in [24].
R	effective outgoing infrared radiation from a surface on earth ($W \cdot m^{-2}$) 1, 34 I in [5], R_W in [33].
R_{\uparrow}	infrared radiation emitted by a surface on earth ($W \cdot m^{-2}$) normally calculated using Stefan-Boltzmann law 1 I_1 in [5].
R_{\downarrow}	infrared radiation from atmosphere, absorbed by a surface on earth ($W \cdot m^{-2}$). 1, 35, 37 R_{\downarrow} in [35], $R_{\downarrow,ic}$ in [36], LW_d in [38], I_1 in [5].
$R_{\downarrow,0}$	infrared radiation from atmosphere under clear sky conditions ($W \cdot m^{-2}$) 7, 35, 37, 45 $I_{1,0}$ in [5], E_a in [9,10,33], R in [11,14,15], R_A in [18], F_1 in [29], $F_{LW,cl}$ in [27], R_{LD} in [19], F in [31], R_a in [35], $R_{d,i}$ in [36], LW_n in [39].
R_0	effective outgoing infrared radiation under clear-sky conditions ($W \cdot m^{-2}$) 34, 43 R in [33].
s	ratio between the measured solar irradiance to the clear-sky irradiance (-) 41
S	absorbed solar radiation per unit area ($W \cdot m^{-2}$) (see [115]) 52
$SCOP_{NET}$	estimated average seasonal performance factor of electrically driven heat pumps (-)
t	time of the day (hour) 18
t’	approximate hour of sunrise in solar time (hour) 24
$[t(\lambda)/t_{av}]$ and b	empirical parameters (see [46]) (-) 48
T_a	ambient dry bulb temperature (K). 3, 7, 8, 9, 10, 11, 12, 23, 30, 31, 32, 33, 40, 41, 42, 52 T in [5,11,14,15,31,38,39,43], T_A in [18], T_0 in [19,20,27,29,30].
$T_{a,corrected}$	corrected ambient dry bulb temperature (K) 23
$T_{c,i}$	cloud temperature of layer “i” (K) 37 T_i in [35].
T_{dp}	dew point temperature ($^{\circ}C$) 15, 16, 21, 22, 23, 27, 28 t_d in [25].
T_s	surface temperature (K) 49, 50
T_f	temperature of the fluid at the desired point (normally the outlet fluid temperature) (K) (see [115]) 52
T_{fi}	inlet fluid temperature (K) (see [115]) 52
T_{sky}	effective sky temperature (K) 2, 40, 45 T_s in [37].
u, v	empirical parameters with different values depending on the different cloud types (-) (see [36]) 39
U_L	collector overall heat loss coefficient ($W \cdot m^{-2} \cdot K^{-1}$) (see [115]) 52
w	distance between parallel tubes (m) (see [115]) 52 W in [115].
W	fractional area of sky covered by clouds (-) 34, 35, 36, 38, 39 A/A_i in [34,35], N in [22], n in [24], m_c in [36].
y	tubes length (m) (see [115]) 52
Z	altitude above sea level (km) 14
$\alpha, \beta, \gamma, a, b$	empirical coefficients, to be defined in the original paper (-) 4, 5, 45
γ	parameter to take into account humidity (see [42]) 43, 44
Γ	factor depending on the cloud base temperature (-) (see [24]) 38
ϵ_{sky}	effective sky emissivity (-) 3, 35, 36, 38, 39, 41, 42, 47, 48 ϵ in [22,24,38].
$\epsilon_{sky,0}$	effective sky emissivity under clear sky conditions (-) 4, 5, 6, 7, 8, 9, 12, 14, 15, 16, 17, 19, 21, 22, 25, 26, 27, 28, 29, 30, 31, 32, 33, 35, 36, 38, 39, 48 ϵ_a in [7,20,29], ϵ_0 in [22,24], ϵ_{sky} in [8,28], ϵ in [5,23,25], $\epsilon_{a,0}$ in [19], ϵ_c in [38], ϵ_a in [45], ϵ_s in [46].
$\epsilon_{10.5-12.5,0}$ and $\epsilon_{8-13,0}$	effective sky emissivity for the wavelength range showed, under clear sky conditions (-) 10, 11 $\epsilon_{10.5-12.5}$ and $\epsilon_{8-13,0}$ in [20].
$\epsilon_{cloud,i}$	emissivity of cloud layer “i” (-) 37 ϵ_c in [35], ϵ_c in [24].
$\epsilon_{cloudy sky}$	equivalent sky emissivity with entirely cloudy sky 36 A in [22].
θ	zenith angle (rad) 43, 45, 46, 47, 48 z in [5,42,43].
λ	wavelength (μm) 46, 47, 48
ξ	parameter to take into account humidity and ambient temperature (see [30]) ($g \cdot cm^{-2}$) 31
σ	Stefan-Boltzmann’s constant: $5.6704 \cdot 10^{-8} (W \cdot m^{-2} \cdot K^{-4})$ 2, 3, 33, 37, 45
ρ	reflectivity (-) 49, 50 R in [45].
τ	parameter to take into account humidity and ambient temperature (see [31]) 32
τ_8	transmittance of the atmosphere in the infrared window (-) 37

paper reviews all different aspects of radiative cooling, such as the environmental conditions affecting the phenomena, the selection and development of materials, the analytical and numerical methods, and the experimental prototypes.

2. Radiative cooling background

Radiative cooling is the thermal process by which a body loses heat by emitting long-wave radiation to another body at lower temperature.

Referred to buildings, radiative cooling is a passive cooling technique which uses thermal radiation properties to cool a body or part of a building facing a colder surface such as the sky. This cooling process occurs when a surface presents a cooling net balance between the emitted and the absorbed radiation, considering also convection and conduction between the surface and the surroundings. With this technique, temperatures below ambient temperature can be achieved. The effective outgoing infrared radiation from a surface on earth (R) is defined as the difference between the infrared radiation emitted by this

surface (R_1) and the infrared radiation from the atmosphere absorbed by this surface (R_1) (Eq. (1)) [5]:

$$R = R_1 - R_1 \quad (1)$$

The spectral distribution of the radiation emitted by the clear sky atmosphere is similar to a blackbody's one at ambient dry bulb temperature but with a gap in the spectral region between wavelengths 8–13 μm . This gap is known as “infrared atmospheric window”.

Research has been conducted in order to determine and analyse the infrared atmospheric window while analysing the atmospheric infrared radiation [6]. The spectral location of the infrared atmospheric window corresponds to the spectrum where most of the terrestrial surfaces emit with its maximum intensity.

2.1. Infrared atmospheric radiation

Atmospheric radiation originates from gases that compose the atmosphere such as water vapour, carbon dioxide, ozone, and other asymmetrical molecules. 90% of the total infrared atmospheric radiation received at ground level comes from the first 800–1600 m above the surface [5]. The main gases involved in infrared atmospheric radiation at ground level are water vapour and carbon dioxide, being water vapour the major contributor [7]. Analysing the radiative properties of these gases can be seen that the atmosphere spectrum in the 8–13 μm band (infrared atmospheric window) is very transparent under clear sky conditions [8].

These dynamic properties of earth's atmosphere make the atmosphere an interesting heat sink to eliminate heat excess. As the atmosphere does not act like a blackbody emitter, it is difficult to predict its behaviour although the physical phenomenon can be physically described as it was presented in [4]. Therefore, for engineering purposes, it would be interesting to measure and/or predict the incoming infrared radiation from the atmosphere on a surface facing the sky.

This data can be measured with specific equipment or predicted with some empirical correlations. When the incoming infrared radiation from the atmosphere is known, there are two methods to express it in an understandable and simple form:

1. To assume the sky acting as a blackbody emitter (effective sky emissivity $\epsilon_{sky}=1$) at an effective sky temperature (T_{sky}) which equals the incoming infrared radiation from the atmosphere based on the Stefan-Boltzmann law (Eq. (2)):

$$R_1 = \sigma \cdot T_{sky}^4 \rightarrow T_{sky} = \left(\frac{R_1}{\sigma} \right)^{1/4} \quad (2)$$

2. To assume the sky having the ambient dry bulb temperature (T_a) with an effective sky emissivity (ϵ_{sky}) which equals the radiation coming from the atmosphere based on the Stefan-Boltzmann law (Eq. (3)):

$$R_1 = \epsilon_{sky} \cdot \sigma \cdot T_a^4 \rightarrow \epsilon_{sky} = \frac{R_1}{\sigma \cdot T_a^4} \quad (3)$$

These two methods simplify the way the incoming infrared radiation from the atmosphere is quantified for engineering calculations. However, the incoming infrared atmospheric radiation is not commonly measured in meteorological stations; therefore, correlations must be elaborated to connect measured simple meteorological parameters to the infrared atmospheric radiation.

There are two types of methods to estimate the incoming infrared radiation from atmosphere under clear sky conditions [8]. The first type is based on direct measurements of the atmosphere radiation spectrum or sky irradiance. These empirical methods use measurements of the incoming infrared atmospheric radiation to generated suitable correlations. The second type consists on analysing the profiles

of atmospheric constituents to calculate their spectral atmospheric radiation based on radiative properties of the gases. Although more rigorous, this second type is more complex, and detailed information on the state of the atmosphere is needed, such as pressure, temperature and density variation with altitude, concentration profiles and spectral absorption coefficients of the gases.

2.1.1. Clear sky correlations

Making a proper estimation of the incoming infrared atmospheric radiation is important for modelling and engineering purposes. Although estimations never adapt perfectly to the reality, neither clear sky is the most common condition depending on the weather; however they can be enough accurate as a first approach. In this section, different correlations for clear sky conditions are presented and reviewed, distinguishing between empirical and detailed correlations.

2.1.1.1. Empirical correlations. Empirical correlations are based on total atmospheric radiation measurements made with a pyrgeometer. A pyrgeometer is a device that measures downward atmospheric long wave radiation. In some measurements a spectral radiometer was also used to calibrate the pyrgeometer and also to detect the presence of clouds.

However, these measurements do not provide any spectral information of the incoming infrared atmospheric radiation. This is a simple way to estimate the incoming infrared atmospheric radiation but it cannot be enough accurate for some calculations, especially when spectral information is required.

First works providing a correlation were presented by Ångström [9,10] and Brunt [11], relating sky emissivity to the partial pressure of water vapour (Eqs. (4) and (5)). Both correlations are based in clear-sky atmospheric radiation values measured in specific locations (Algeria and California).

$$\epsilon_{sky,0} = a - \beta \cdot 10^{-\tau^{e_0}} \rightarrow (\text{Ångström}) \quad (4)$$

$$\epsilon_{sky,0} = a + b \cdot \sqrt{e_0} \rightarrow (\text{Brunt}) \quad (5)$$

These expressions require the calculation of some empirical coefficients ($a, b, \alpha, \beta, \gamma$) which are somewhat variable and depend on the geographical region. Later works calculated empirical coefficients for Ångström's and Brunt's equations considering different meteorological and geographical conditions. A compilation of these coefficients can be found in Elsasser [12] and Kondratyev [13], where significant discrepancies can be seen in the coefficients found for different locations.

Later on, Elsasser concluded that the sky emissivity has a logarithmic relation with the partial pressure of water vapour [12], developing a new correlation (Eq. (6)).

$$\epsilon_{sky,0} = 0.21 + 0.22 \cdot \ln(e_0) \quad (6)$$

While the previous correlations to estimate the incoming infrared atmospheric radiation depend on the partial pressure of water vapour, later works use ambient temperature as the main parameter.

Swinbank [14] conducted a reassessment of previous work published in [9–11] on the attempt to avoid local specificity of the correlation coefficients (as demonstrated in [12]) and proposed alternatively a correlation that only depends on ambient temperature, showing the low influence of humidity at low level stations (Eq. (7)).

$$R_{1,0} = 5.31 \cdot 10^{-14} \cdot T_a^6 \rightarrow \epsilon_{sky,0} = 9.35 \cdot 10^{-6} \cdot T_a^2 \quad (7)$$

From original equation it is readapted to have it in function of $\epsilon_{sky,0}$. Swinbank's correlation [14] attempted to be general. However, Idso and Jackson [15] stated that, based on new findings, Swinbank's correlations were not general. Therefore, they attempted to relate atmospheric radiation to ambient temperature to a universally applicable correlation which should be valid for any air temperature reached on earth and for any latitude (Eq. (8)). However, in a following work

S. Vall, A. Castell

Renewable and Sustainable Energy Reviews 77 (2017) 803–820

[16], Aase and Idso concluded that below 273 K this correlation overestimates the total effective emissivity.

$$\epsilon_{sky,0} = 1 - (0.261 \cdot e^{-7.77 \cdot 10^{-4} \cdot (273.15 - T_a)^2}) \quad (8)$$

In 1983, Hatfield et al. [17] concluded that correlations models which only use ambient temperature [14,15] do not estimate properly the effective emissivity over wide geographical areas. They concluded that these models are too specific for a location because they assume a relationship between ambient temperature and partial pressure of water vapour in their empirical constants. From here on, authors developed correlations which depend on both ambient temperature and partial pressure of water vapour.

Satterlund [18], based on experimental measurements from literature, proposed a new correlation to take into account both ambient temperature and vapour pressure (Eq. (9)). This correlation presents improvements on estimating the incoming infrared atmospheric radiation over a wide range of temperatures, particularly at low temperatures where most of the formulas perform poorly for air temperatures below freezing. This model has also probed to perform better when compared to two other models [15,19] (see Detailed Method section).

$$\epsilon_{sky,0} = 1.08 \cdot (1 - e^{T_a/2016}) \quad (9)$$

Idso [20] performed an experiment at Phoenix, Arizona (USA) to obtain measurements of the total incoming infrared atmospheric radiation and proposed two correlations for different wavelengths (10.5–12.5 μm in Eqs. (10) and (8)–(13) μm in Eq. (11)) and another one for the whole range (Eq. (12)). The three correlations depend on the temperature and the partial pressure of water vapour.

$$\epsilon_{10.5-12.5,0} = 0.1 + 3.53 \cdot 10^{-8} \cdot e_0^2 \cdot e^{3000/T_a} \quad (10)$$

$$\epsilon_{8-13,0} = 0.24 + 2.98 \cdot 10^{-8} \cdot e_0^2 \cdot e^{3000/T_a} \quad (11)$$

$$\epsilon_{sky,0} = 0.7 + 5.95 \cdot 10^{-5} \cdot e_0 \cdot e^{1500/T_a} \quad (12)$$

Andreas and Ackley [21] proposed a modification of Eq. (12) to be used at the Arctic and the Antarctic where the concentration of aerosols in these remote areas is lower.

$$\epsilon_{sky,0} = 0.601 + 5.95 \cdot 10^{-5} \cdot e_0 \cdot e^{1500/T_a} \quad (13)$$

From here on, authors started to use other parameters such as altitude, dew point temperature, relative humidity, and ambient pressure in their correlations, trying to predict in a better way the incoming infrared atmospheric radiation.

Centeno [22] proposed a clear sky emissivity correlation based on measurements from the literature and his own measurements at Venezuela. This correlation takes into account the altitude, the ambient temperature and the relative humidity (Eq. (14)). To develop this correlation the author forced the correlation to be constituted by the product of three functions, each dependant of a parameter.

$$\epsilon_{sky,0} = [5.7723 + 0.9555 \cdot 0.6017Z] \cdot T_a^{1.893} \cdot H^{0.0665} \cdot 10^{-14} \quad (14)$$

Berdahl and Fromberg [8], based on their own measurements at three USA cities (Tucson, Arizona; Gaithersburg, Maryland; and St. Louis, Missouri), proposed two different correlations to estimate the sky emissivity: one for night-time (Eq. (15)) and one for day-time (Eq. (16)). These correlations only depend on the dew point temperature.

$$\epsilon_{sky,0} = 0.741 + 0.0062 \cdot T_{dp}(\text{night}) \quad (15)$$

$$\epsilon_{sky,0} = 0.727 + 0.0060 \cdot T_{dp}(\text{day}) \quad (16)$$

Later on, Berdahl and Martin [23] corrected a previous work [8] by using more measurements (also in USA: San Antonio, Texas; West Palm Beach, Florida; and Boulder City, Nevada) and proposed a new correlation (Eq. (17)) with a diurnal correction factor (Eq. (18)). Finally, Martin and Berdahl [24] further extended their correlation by adding a pressure correction factor (Eqs. (19) and (20)).

$$\epsilon_{sky,0} = 0.711 + 0.56 \left(\frac{T_{dp}}{100} \right) + 0.73 \left(\frac{T_{dp}}{100} \right)^2 + \Delta \epsilon_h \quad (17)$$

$$\Delta \epsilon_h = 0.013 \cdot \cos \left(\frac{2\pi t}{24} \right) \quad (18)$$

$$\epsilon_{sky,0} = 0.711 + 0.56 \left(\frac{T_{dp}}{100} \right) + 0.73 \left(\frac{T_{dp}}{100} \right)^2 + \Delta \epsilon_h + \Delta \epsilon_e \quad (19)$$

$$\Delta \epsilon_e = 0.00012 \cdot (P_0 - 1000) \quad (20)$$

Berger et al. [25] based on measurements at Carpentras, France proposed a night-time correlation that depends on the dew point temperature (Eq. (21)). Moreover, they also proposed a correlation for the whole day (Eq. (22)), where the ambient temperature must be corrected (Eq. (23)) in order to include annual and diurnal effects.

$$\epsilon_{sky,0} = 0.770 + 0.0038 \cdot T_{dp}(\text{night}) \quad (21)$$

$$\epsilon_{sky,0} = 0.752 + 0.0048 \cdot T_{dp}(\text{allday}) \quad (22)$$

$$T_{a,corrected} = T_a + K(t) + L(t) \cdot (T_{dp} - T_a) \quad (23)$$

Alados-Arboledas and Jimenez [26] proposed a deviation correction factor (Eq. (24)) to take into account the day-night and seasonal variation of the effective emissivity based on measurements in Granada, Spain. This correction factor was tested in Eqs. (12) and (5), being Eq. (12) the one with better results.

$$\Delta \epsilon = A \cdot \sin \pi \left[\frac{t - t'}{\Delta t} - \left(\frac{f}{\Delta t} \right) \right] t' + f \leq t \leq t' + \Delta t \quad (24)$$

The parameters in Eq. (24) should be calculated according to the region and the season.

Niemelä et al. [27], based on measurements at Sodankylä, Finland, proposed two correlations (Eqs. (25) and (26)) for cold and dry weather conditions which only depend on the partial water vapour pressure.

$$(e_0 \geq 2) \rightarrow \epsilon_{sky,0} = 0.72 + 0.009 \cdot (e_0 - 2) \quad (25)$$

$$(e_0 < 2) \rightarrow \epsilon_{sky,0} = 0.72 - 0.076 \cdot (e_0 - 2) \quad (26)$$

Tang et al. [28], based on measurements at Negev Highlands, Israel, proposed a correlation (Eq. (27)) for warm and dry weather conditions which only depend on the dew point temperature.

$$\epsilon_{sky,0} = 0.754 + 0.0044 \cdot T_{dp} \quad (27)$$

Empirical correlations are designed to make estimations of the incoming infrared atmospheric radiation from the atmosphere in an easy way. A tendency to use the simplest atmospheric parameters that allow a proper estimation is observed. However, there is no agreement in which parameters are better. From the literature, the importance of the atmospheric humidity and the ambient temperature is demonstrated to provide a good regression. Nevertheless, using just one or two parameters does not allow the correlation to be applicable at any location. Therefore, most of the correlations above are valid for specific locations and their empirical coefficients should be recalculated for new locations. Last tendencies are to provide correlations easy to use and location dependant.

It is also important to highlight that the difference in the correlations which use the same parameters is on the mathematical model that the authors choose to adapt the physical phenomena. Some of them are based on physical properties while others are based in a statistical approach.

2.1.1.2. Detailed method. Detailed methods are based on radiative properties of the gases that compound the atmosphere and on their concentration. They can provide a rigorous estimation of the incoming infrared atmospheric radiation, although they need detailed information. There are three methods: using the gas transmittance to

S. Vall, A. Castell

Renewable and Sustainable Energy Reviews 77 (2017) 803–820

estimate the atmospheric emissivity; using an accurate radiative-transfer models/modelization (LOWTRAN, MODTRAN, SBDART); and using a flux emissivity model.

Based on theoretical concepts of gas emissivity and empirical correlations for gas properties, Bliss [7] obtained sky emissivity values with the only dependence of dew point temperature (Eq. (28) created from data in [7]):

$$\varepsilon_{sky,0} = 0.8004 + 0.00396 \cdot T_{dp} \quad (28)$$

Staley and Jurica [29] proposed a correlation (Eq. (29)) based on the analysis of the radiation properties of water vapour, carbon dioxide and ozone.

$$\varepsilon_{sky,0} = 0.67 \cdot e_0^{0.08} \quad (29)$$

Brutsaert [19], based on analytical correlations of atmosphere parameters, proposed a sky emissivity correlation (Eq. (30)) which depends on the vapour pressure and the ambient temperature. Below 273 K this correlation underestimates the total effective emissivity [16].

$$\varepsilon_{sky,0} = 1.24 \cdot (e_0/T_a)^{1/7} \quad (30)$$

Prata [30], based on an emissivity model, proposed a correlation

(Eq. (31)) which depends on ambient temperature and partial pressure of water vapour. This model has been tested with experimental measurements from several locations and has also been assessed by using radiosonde profiles and an accurate radiative-transfer model (LOWTRAN-7) to find the coefficients. The model has also been compared to five previous models [14,15,18–20] showing a better performance.

$$\varepsilon_{sky,0} = 1 - (1 - \xi) \cdot e^{-\sqrt{1.2+3\xi}} \quad \xi = 46.5 \cdot \left(\frac{e_0}{T_a}\right) \quad (31)$$

Dilley and O'Brien [31], based on parameterization of physical processes and using a computer software model (LOWTRAN), proposed two correlations (Eqs. (32) and (33)) which depend on ambient temperature and partial pressure of water vapour.

$$\varepsilon_{sky,0} = 1 - e^{(-1.66\tau)} \quad \tau = 2.232 - 1.875 \left(\frac{T_a}{273.15}\right) + 0.7356 \sqrt{18.6 \left(\frac{e_0}{T_a}\right)} \quad (32)$$

$$\varepsilon_{sky,0} = \frac{1}{\sigma \cdot T_a^4} \left[59.38 + 113.7 \cdot \left(\frac{T_a}{273.15}\right)^6 + 96.96 \sqrt{18.6 \left(\frac{e_0}{T_a}\right)} \right] \quad (33)$$

The detailed method can provide good estimations of the incoming

Table 1
Summary of clear-sky correlations.

Authors	Clear-sky correlations	Equation
Ångström [9,10]	$\varepsilon_{sky,0} = \alpha - \beta \cdot 10^{-\tau \cdot e_0}$	4
Brunt [11]	$\varepsilon_{sky,0} = a + b \cdot \sqrt{e_0}$	5
Elsasser [12]	$\varepsilon_{sky,0} = 0.21 + 0.22 \ln(e_0)$	6
Bliss [7]	$\varepsilon_{sky,0} = 0.8004 + 0.00396 T_{dp}$	28
Swinkbank [14]	$\varepsilon_{sky,0} = 9.35 \cdot 10^{-6} \cdot T_a^2$	7
Idso and Jackson [15]	$\varepsilon_{sky,0} = 1 - (0.261 \cdot e^{-7.77 \cdot 10^{-4} (273.15 - T_a)^2})$	8
Staley and Jurica [29]	$\varepsilon_{sky,0} = 0.67 \cdot e_0^{0.08}$	29
Brutsaert [19]	$\varepsilon_{sky,0} = 1.24 \cdot (e_0/T_a)^{1/7}$	30
Satterlund [18]	$\varepsilon_{sky,0} = 1.08 \left(1 - e^{\sigma_0 T_a^{2016}}\right)$	9
Idso [20]	$\varepsilon_{sky,0} = 0.7 + 5.95 \cdot 10^{-5} \cdot e_0 \cdot e^{(1500/T_a)}$	12
Andreas and Ackley [21]	$\varepsilon_{sky,0} = 0.601 + 5.95 \cdot 10^{-5} \cdot e_0 \cdot e^{1500/T_a}$	13
Centeno [22]	$\varepsilon_{sky,0} = [5.7723 + 0.9555 \cdot (0.6017)^2] \cdot T_a^{1.893} \cdot H^{0.0665} \cdot 10^{-14}$	14
Berdahl and Fromberg [8]	$\varepsilon_{sky,0} = 0.741 + 0.0062 T_{dp} \text{ (night)}$ $\varepsilon_{sky,0} = 0.727 + 0.0060 T_{dp} \text{ (day)}$	15, 16
Berdahl and Martin [23]	$\varepsilon_{sky,0} = 0.711 + 0.56 \left(\frac{T_{dp}}{100}\right) + 0.73 \left(\frac{T_{dp}}{100}\right)^2 + \Delta \varepsilon_h$ $\Delta \varepsilon_h = 0.013 \cos\left(\frac{2\pi t}{24}\right)$	17, 18
Martin and Berdahl [24]	$\varepsilon_{sky,0} = 0.711 + 0.56 \left(\frac{T_{dp}}{100}\right) + 0.73 \left(\frac{T_{dp}}{100}\right)^2 + \Delta \varepsilon_h + \Delta \varepsilon_e$ $\Delta \varepsilon_e = 0.00012 (P_0 - 1000)$	19, 20
Berger et al. [25]	$\varepsilon_{sky,0} = 0.770 + 0.0038 T_{dp} \text{ (night)}$ $\varepsilon_{sky,0} = 0.752 + 0.0048 T_{dp} \text{ (all day)}$	21, 22
Alados-Arboledas and Jimenez [26]	$\Delta \varepsilon = A \sin \pi \left[\frac{(t-t')}{\Delta t} - \frac{f}{\Delta t} \right]$	24
Prata [30]	$\varepsilon_{sky,0} = 1 - (1 - \xi) \cdot e^{-\sqrt{1.2+3\xi}} \quad \xi = 46.5 \cdot \left(\frac{e_0}{T_a}\right)$	31
Dilley and O'Brien [31]	$\varepsilon_{sky,0} = 1 - e^{(-1.66\tau)} \quad \tau = 2.232 - 1.875 \left(\frac{T_a}{273.15}\right) + 0.7356 \sqrt{18.6 \left(\frac{e_0}{T_a}\right)}$ $\varepsilon_{sky,0} = \frac{1}{\sigma \cdot T_a^4} \left[59.38 + 113.7 \cdot \left(\frac{T_a}{273.15}\right)^6 + 96.96 \sqrt{18.6 \left(\frac{e_0}{T_a}\right)} \right]$	32, 33
Niemelä et al. [27]	$(e_0 \geq 2) \rightarrow \varepsilon_{sky,0} = 0.72 + 0.009 \cdot (e_0 - 2)$ $(e_0 < 2) \rightarrow \varepsilon_{sky,0} = 0.72 - 0.076 \cdot (e_0 - 2)$	25, 26
Tang et al. [28]	$\varepsilon_{sky,0} = 0.754 + 0.0044 \cdot T_{dp}$	27

infrared atmospheric radiation. However, this method requires detailed information about atmosphere composition. It has been confirmed that radiative transfer modelling produces better results than previously published simple parameterizations based only on surface measurements [32].

There is a lack of comparisons between different correlations in the literature. There just exist few articles comparing correlations [18,30].

It is also important to highlight that measurements are sporadically made and not very regular in time and location. So this means that it is difficult to get available data that fits a specific climate.

Clear-sky correlations are a first approach, although they do not represent the common scenario. Moreover, most of the correlations do not provide real-time values but average values. Table 1 presents a summary of the correlations found in the literature for clear-sky conditions.

2.1.2. Cloudy sky relations

Clear sky conditions do not happen all the time. The presence of clouds increases the incoming infrared atmospheric radiation compared to clear sky conditions. This is because clouds act like a blackbody emitter supplementing the waveband the atmospheric emission lacks of. Any cloud which is visually opaque can be considered as a blackbody emitter at the temperature of the cloud base [7] and its radiative effect is to close the infrared atmospheric window. Thus, clear sky correlations must be modified to adjust the cloudiness.

According to its own observations, Ångström [33] proposed a relation to take into account the cloudiness (Eq. (34)).

$$R = R_0 \cdot (1 - kW) \tag{34}$$

Eq. (34) is a cloud correction relation which is being applied to the emitted radiation from the earth surface, and also to the incoming infrared atmospheric radiation. A more logical relation has been proposed by Bolz [34]. This relation (Eq. (35)) takes into account the cloudiness of the sky only on the incoming infrared atmospheric radiation.

$$R_1 = R_{1,0} \cdot (1 + kW^2) \rightarrow \epsilon_{sky} = \epsilon_{sky,0} (1 + kW^2) \tag{35}$$

Centeno [22] proposed a correlation to estimate the clear-sky emissivity (Eq. (14)) and also a relation to get the effective sky emissivity bearing in mind the cloudiness (Eq. (36)).

$$\epsilon_{sky} = \epsilon_{sky,0} + W \cdot (\epsilon_{cloudy sky} - \epsilon_{sky,0}) \tag{36}$$

Kimball et al. [35] developed a method that assumes that the cloud radiation is transmitted through the air only at the infrared atmospheric window. The model (Eq. (37)) takes into account the information obtained from every cloud layer.

$$R_1 = R_{1,0} + \sum_i^N \tau_8 W_i \epsilon_{cloud,i} f_{8,i} \sigma T_{c,i}^4 \tag{37}$$

The authors also proposed a series of correlations to calculate these parameters.

Martin and Berdahl [24] proposed a relation that takes into account the cloud emissivity and the cloud-base temperature (Eq. (38)).

$$\epsilon_{sky} = \epsilon_{sky,0} + (1 - \epsilon_{sky,0}) \cdot W \cdot \epsilon_{cloud} \Gamma \tag{38}$$

Sugita and Brutsaert [36] proposed new and more accurate values (Eq. (39)) for parameters of a previous correlation (Eq. (35)).

$$R_1 = R_{1,0} \cdot (1 + u \cdot W^v) \rightarrow \epsilon_{sky} = \epsilon_{sky,0} \cdot (1 + u \cdot W^v) \tag{39}$$

Aubinet [37] proposed a correlation to estimate the effective sky temperature that takes into account the clearness index (Eq. (40)).

$$T_{sky} = 94 + 12.6 \cdot \ln(e_0) - 13 \cdot K_0 + 0.341 \cdot T_a \tag{40}$$

Crawford and Duchon [38] improved a previous correlation [19] (Eq. (30)) to take into account the annual variation between dry and wet season and also proposed a relation for estimating the effect of cloudiness (Eq. (41)).

$$\epsilon_{sky} = clf + (1 - clf) \cdot \left(1.22 + 0.06 \cdot \sin \left((month + 2) \cdot \frac{\pi}{6} \right) \right) \left(\frac{e_0}{T_a} \right)^{\frac{1}{7}} \tag{41}$$

$$clf = 1 - s$$

Sridhar et al. [39] modified a correlation from previous work [19] (Eq. (30)) by calibrating it for different sites representing different climatic and geographical conditions to make it valid for all sky conditions (day and night; clear and cloudy) (Eq. (42)).

$$\epsilon_{sky} = 1.31 \cdot \left(\frac{e_0}{T_a} \right)^{1/7} \tag{42}$$

Note that in Eq. (42) e_0 must be used in mbar, in contrast to the original reference, where it is used in kPa (introducing a conversion factor in the equation).

Also, with overcast sky can be used previous presented radiative-transfer models/modelization (LOWTRAN, MODTRAN, SBDART), showing good agreement with pyrgeometer measurements [40]. Also, this work shows that cloud base height should be measured and taken into account.

All the relations that consider cloudy-sky just take into account the long-wave radiation. Under cloudy conditions short-wave radiation is reduced; however long-wave radiation is increased. Therefore, previous equations are not suitable when short-wave radiation needs to be calculated.

As proposed at the beginning of this section, some works conclude

Table 2
Summary of cloudy-sky correlations.

Authors	Cloudy-sky correlations	Equation
Ångström [33]	$R = R_0 \cdot (1 - kW)$	34
Bolz [34]	$\epsilon_{sky} = \epsilon_{sky,0} \cdot (1 + kW^2)$	35
Centeno [22]	$\epsilon_{sky} = \epsilon_{sky,0} + W \cdot (\epsilon_{cloudy sky} - \epsilon_{sky,0})$	36
Kimball et al. [35]	$R_1 = R_{1,0} + \sum_i^N \tau_8 W_i \epsilon_{cloud,i} f_{8,i} \sigma T_{c,i}^4$	37
Martin and Berdahl [24]	$\epsilon_{sky} = \epsilon_{sky,0} + (1 - \epsilon_{sky,0}) \cdot W \cdot \epsilon_{cloud} \Gamma$	38
Sugita and Brutsaert [36]	$\epsilon_{sky} = \epsilon_{sky,0} \cdot (1 + u \cdot W^v)$	39
Aubinet [37]	$T_{sky} = 94 + 12.6 \cdot \ln(e_0) - 13 \cdot K_0 + 0.341 \cdot T_a$	40
Crawford and Duchon [38]	$\epsilon_{sky} = clf + (1 - clf) \cdot \left[1.22 + 0.06 \cdot \sin \left((month + 2) \cdot \frac{\pi}{6} \right) \right] \left(\frac{e_0}{T_a} \right)^{1/7}$	41
Sridhar et al. [39]	$\epsilon_{sky} = 1.31 \cdot \left(\frac{e_0}{T_a} \right)^{1/7}$	42

S. Vall, A. Castell

Renewable and Sustainable Energy Reviews 77 (2017) 803–820

that clear-sky correlations underestimate the incoming infrared atmospheric radiation under cloudy conditions [36,38,41]. Also, in Table 2 is presented a summary of the correlations found in the literature for cloudy-sky conditions.

2.1.3. Influence of the zenith angle/tilted surfaces/sky view factor

To maximise the effective outgoing infrared radiation, the radiator should be placed horizontally, facing the sky. However, sometimes it is desirable to install the radiator with an inclination, as for example to allow drainage or because it is the inclination of the roof where it is placed. The inclination of the radiator increases the incoming infrared radiation at radiator surface. This increase in the incoming radiation is mainly caused by the reduction of the sky view factor from the radiator surface (therefore, the surface is facing the ground which acts more likely to a blackbody), and also because the radiator's surface is more exposed to the "warmer" regions of the sky near the horizon (due to the less "visual thickness" of the atmosphere in the zenith direction [6] than in other directions).

As the effect produced by the variation of the view factor is easier to estimate than the effect of being exposed to "warmer" zones of the sky, research was mainly focused on finding simple expressions of the effect of having the radiator surface exposed to "warmer" regions of the sky, rather than the analytical expression of the phenomenon as presented in [4].

Some of the authors tried to establish correlations to relate the incoming infrared radiation or the effective outgoing infrared radiation to the inclination angle or the zenith angle. To express the variation of the net outgoing infrared radiation in relation with the zenith angle Linke [42] found an expression (Eq. (43)) that adapts adequately to measurements from literature.

$$R_0(\theta) = R_0(0)\cos^{\gamma}\theta \quad (43)$$

$$\gamma = 0.11 + 0.0255 \cdot e_0 \quad (44)$$

In a similar way, Strong [43], based on its own measurements of the angular dependence of clear-sky infrared radiation from the atmosphere, readapted a previous formula (Eq. (5)) to take into account the zenith angle (Eq. (45)).

$$R_{1,0}(\theta) = (a+b\sqrt{e_0 \cdot \sec\theta})\sigma T_a^4 \quad (45)$$

Based on Eqs. (43) and (45), and from experimental measurements from the literature [5,42,43], it can be drawn that for angles smaller than 45° the effect of the deviation from the zenith angle is not significant (about 4–6% error [44]).

Other authors made some effort on searching good expressions that allow calculating the effect of inclination on the equivalent sky emissivity.

Granqvist and Hjortsberg [45] proposed an expression to relate the sky emissivity to the zenith angle (Eq. (46)), considering the atmospheric transmittance proportional to the pathlength, which depends on wavelength and zenith angle.

$$\varepsilon_{sky,0}(\theta, \lambda) = 1 - [1 - \varepsilon_{sky,0}(0^\circ, \lambda)]^{1/\cos\theta} \quad (46)$$

Eq. (46) relates the sky emissivity at zenith angle to any sky emissivity at any angle from the zenith, showing good agreement in the atmospheric window range when compared to LOWTRAN data (Fig. 1).

As Eq. (46) performs well in the infrared atmospheric window, the "box model" was proposed [45], which consists of dividing the infrared range in three parts where each part has an emissivity according to Eq. (47).

$$\varepsilon_{sky,0}(\theta, \lambda) = \begin{cases} \varepsilon_{sky,0}(\theta)=1 & 3 < \lambda < 8 \mu\text{m} \\ \varepsilon_{sky,0}(\theta) = 1 - [1 - \varepsilon_{sky,0}(0)]^{1/\cos\theta} & 8 < \lambda < 13 \mu\text{m} \\ \varepsilon_{sky,0}(\theta)=1 & 13 < \lambda < 50 \mu\text{m} \end{cases} \quad (47)$$

In a similar way, Martin and Berdahl [46] measured and studied the spectral and angular dependence of the sky radiation. Considering the atmospheric transmittance proportional to the pathlength and also making some approximations, they proposed a correlation (Eq. (48)) that relates the equivalent sky emissivity with the zenith angle and the wavelength.

$$\varepsilon_{sky,0}(\theta, \lambda) = 1 - (1 - \varepsilon_{sky,0})[t(\lambda)/t_{at}]e^{b(1.7-1/\cos\theta)} \quad (48)$$

Due to the low influence of zenith angle for small angles and the difficulty to calculate accurate correlations, no extended research had been conducted in this issue.

2.2. Radiative cooling potential (resource)

Radiative cooling as a technology is considered new and little tested. Before evaluating any device, the energetic and economic potential of the technology should be analysed. The main factors that determine whether to use this technology are the weather (meaning by weather the atmospheric conditions), and the cooling requirements of the building in the particular location. All work done until date is limited to taking into account the weather, but omitting the cooling requirements.

In the early research, Atwater and Ball [47] computed values of infrared atmospheric radiation from 11 USA meteorological stations (continental/subtropical climates) to create a model to estimate the average sky temperature. They also created some contour maps with the areal distribution of the sky temperature and the temperature depression (difference between ambient temperature and sky temperature) for each season, showing temperature depression maps, percentage maps (showing sky temperature below 16°C) and temperature depression histograms to characterise the radiative cooling resource. These results show up some climates to be more suitable to use radiative cooling than others, as for example Fresno's (California) climate.

The radiative cooling potential of a tropical country as Thailand, has also been analysed. Exell [48] used two methods to determine the potential in Thailand. The first method uses empirical correlations previously shown (Eqs. (8) and (34)), while the second method uses a theoretical equation of radiative transfer for atmospheric radiation [13]. Results show effective sky temperatures about 8°C below minimum daily temperature, demonstrating the potential of radiative

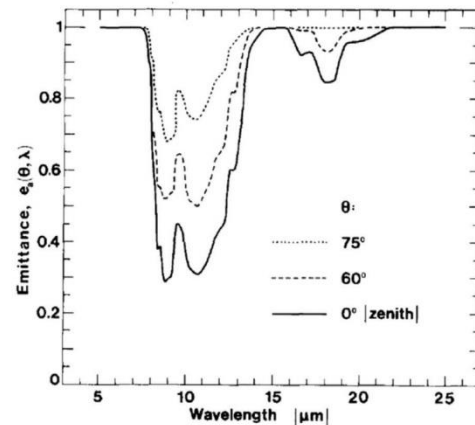


Fig. 1. Spectral emissance of the atmosphere for three zenith angles as obtained from the radiance data computed from a LOWTRAN model [45].

cooling to provide some of the cooling demands. Moreover, Hanif et al. [49] performed an analysis of the radiative cooling potential for Malaysia. They attempted to get a correlation to relate the radiative cooling power and the temperature depression by using climate data from 10 different locations. The study found that the potential savings in Malaysia due to radiative cooling are up to 11% of cooling energy consumption.

Exploring another typology of climate, Pissimanis and Notaridou [50] calculated the radiative cooling potential in Athens (Subtropical/Mediterranean) during summer using the model proposed by Atwater and Ball [47]. Their results were corroborated with 7 years of measurements and 2 empirical correlations (Eqs. 5 and 8). In the same way, Argiriou et al. [51] calculated the radiative cooling potential also in Athens, using 12 years of hourly weather measurements. Argiriou et al. (1994) used Berdahl and Martin [23] model to calculate the sky emissivity. They presented sky-temperature depression histograms, cumulative frequency distribution of the stagnation temperature graphs, and cumulative frequency distribution of the outlet temperature with or without wind screen graphs, concluding that the location is suitable to apply radiative cooling techniques.

After initial research in assessing radiative cooling potential, Burch et al. [52] presented a new insight by taking into account the energy demand coverage of a standard building when assessing radiative cooling potential in a specific location. It was used a model to predict the energy production and energy demand coverage, space heating and cooling and domestic hot water, for a building located in Albuquerque, Madison and Miami (USA). Overall results of energy demand coverage and money savings were presented for each city.

Very little is done in evaluating the potential of the technology and also very few climates had been evaluated. More research is needed to evidence which climates are meaningful to implement this technology according not just to the weather conditions but also to the cooling requirements.

In conclusion, a world climate analysis should be performed in order to determine where this technology may be implemented and how well can it perform. However, as radiative cooling is a new technology, some parameters should be standardized.

3. Selective radiative cooling

The net thermal balance between a terrestrial surface and its surroundings determines the surface temperature. Radiative cooling takes into account radiative properties of the atmosphere to generate a net cooling thermal balance. To take advantage of the infrared atmospheric window,

some authors proposed the use of selective materials with specific optical properties, in order to achieve lower surface temperatures by emitting mainly in the infrared atmospheric window [53–56]. These optical properties should ideally be those of a perfect emitter in the infrared atmospheric window (8–13 μm) and a perfect reflector elsewhere. In this case the cooling power is on the order of 100W/m² at ambient temperature, and temperatures around 50°C below ambient temperature could be reached (considering radiation balance only) [57].

A perfect material for radiative cooling applications does not exist, but some research has been conducted in order to determine the optical properties of existing materials and also to create new materials with better properties.

Selective properties can be achieved by using a selective surface, but they can also be achieved by using a selective screen, which can at the same time block the convection heat transfer between the cold surface and the ambient air, as well as reflect some unwanted radiation. A combination of a selective surface and a selective screen can also be a solution. If a cover screen is used, there is also the possibility to replace the air between the radiator surface and the cover screen with another gas with more desirable radiative properties or create vacuum. Moreover, the use of mirrors to focus the radiation of a specific zone from the sky is also seen as a potential improvement.

In this section, research and advances in selective materials for radiative cooling are reviewed, classified and discussed. The main classifications for the materials, bearing in mind their specific position in the device, are: surface of the radiator, cover for the radiator, gas between cover and surface, and auxiliary systems (as mirrors).

3.1. Selective surface

Some research has been conducted on this topic trying to find a suitable material or coating to enhance radiative cooling. The aim is to develop an ideal material with high emissivity in the infrared atmospheric window wave range (8–13 μm) and high reflection in the remaining wavelengths.

To optimise and compare selective surfaces for radiative cooling applications, some parameters are defined [45] in order to represent the potential of the selective surface. This parameters are: the average emissivity for different wavelengths ranges ($\bar{\epsilon}_s^H$ and $\bar{\epsilon}_{s,2}^H$) (Eqs. (49) and (50)) and a new comparative parameter (η^H) (and Eq. (51)):

$$\bar{\epsilon}_s^H = \int_0^\infty I_{b,\lambda}(\lambda, T_s) [1 - \rho(\lambda)] d\lambda / \int_0^\infty I_{b,\lambda}(\lambda, T_s) d\lambda \quad (49)$$

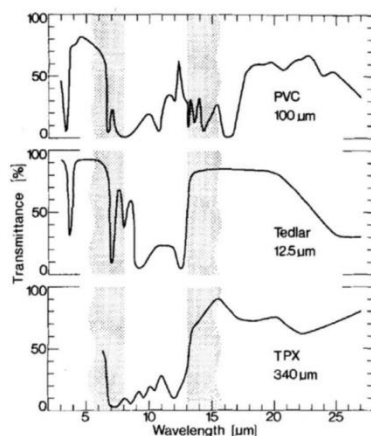


Fig. 2. Left: Transmittance spectra for three different plastic films. Right: Table of cooling parameters estimated for plastic films backed by aluminium [45].

S. Vall, A. Castell

Renewable and Sustainable Energy Reviews 77 (2017) 803–820

$$\bar{\epsilon}_{s,2}^H = \int_{8\mu\text{m}}^{13\mu\text{m}} I_{b,\lambda}(\lambda, T_s) [1 - \rho(\lambda)] d\lambda / \int_{8\mu\text{m}}^{13\mu\text{m}} I_{b,\lambda}(\lambda, T_s) d\lambda \quad (50)$$

$$\eta^H = \bar{\epsilon}_{s,2}^H / \bar{\epsilon}_s^H \quad (51)$$

Eq. (49) is the average emissivity of the material, Eq. (50) is the average emissivity of the material between 8 – 13 μm wavelengths and indicates the maximum achievable cooling power, and Eq. (51) is a comparison parameter between the previous two parameters and indicates the maximum achievable temperature drop. Therefore, high values of $\bar{\epsilon}_{s,2}^H$ and η^H are desired. These parameters appear in some of the works presented below to discuss and analyse the feasibility of the selective surfaces.

These selective surfaces can be obtained by means of Polymer foils on metal surfaces, Silicon-based coatings on metal surfaces, Ceramic oxide layers, Paints and New Materials (multilayers).

3.1.1. Polymer foils on metal surfaces

In the search of a selective surface for radiative cooling applications, polymer foils on metal surfaces (highly reflective) have been tested, mainly on aluminium. Three different polymers were analysed (polyvinyl-chloride (PVC) [58], polyvinyl-fluoride (PVF-TEDLAR) [53–55] and poly 4-methyl-1-pentene (TPX) [59]), and had been also compared to each other [45]. Results of the comparison between the three polymers can be seen in Fig. 2.

These results show that the three polymer foils present a low reflectivity in the infrared atmospheric window (consequently high emissivity) but do not show such a good performance outside it. When compared with *SiO* films, the polymer foils show a better performance in the infrared atmospheric window but worse reflectivity outside the window, therefore, polymer foils show worse overall performance [45].

Polyvinyl-difluoride (PVDF) was also proposed as selective material for radiative cooling applications but only when used also in solar collection [60]. Even though the radiative performance was not as good as other selective materials, it performed better than non-selective surfaces.

In a recent work [61], where solar heating and radiative cooling were required, polyethylene terephthalate (PET) coated with titanium (Ti) was studied (called TPET by the authors), showing selective properties in the infrared window and also in the solar band, as shown in Fig. 3.

3.1.2. Silicon-based coatings on metal surfaces

Several authors have studied the use of thin silicon-based coatings. The idea was to coat highly reflective metals, as aluminium, with silicon coatings which selectively emit in the infrared atmospheric window.

Silicon monoxide (*SiO*) is a coating that shows good performance. The reflectance and transmittance of *Si* on transparent *KRS* – 5 and the reflectance of *SiO* films on aluminium substrates were studied by Hjortsberg and Granqvist [62] (Fig. 4). The purpose of their research was to provide accurate knowledge of the optical properties over the whole thermal infrared range. They conclude that their measurements are similar to what is found in the literature, so they endorsed results pointed out in previous works.

Also, Granqvist et al. [57] tested *SiO* films on aluminium for different thicknesses (Fig. 5 Left). In this research was compared a *SiO* film on aluminium to a black painted plate. The selective surface reached 14°C below ambient whereas the black plate reached slightly lower temperatures. The reason for this small difference between the selective surface and the black plate lied in an unfavourable low value of $\bar{\epsilon}_{s,2}^H$ for the *SiO* coating and an insufficient thermal insulation of the test box.

Moreover, Granqvist et al. [57] also studied *Si₃N₄* films on aluminium (Fig. 5 Right), showing better performance than *SiO* coatings according to the greater infrared atmospheric window range covered.

Another coating, *SiO_{0.6}N_{0.2}*, was tested by Eriksson and Granqvist

[63] and by Eriksson et al. [64], showing better performance than *SiO* but worse than *Si₃N₄*. Nevertheless, it showed suitable properties for radiative cooling (Fig. 6).

A bilayer coating of *SiO_{2.0}/SiO_{0.25}N_{1.52}* on *Al* was also analysed by Eriksson et al. [65], showing a worse performance regard to *SiO_{0.6}N_{0.2}* coating (Fig. 7).

The performance of a multilayer coating of *SiO_xN_y* using different concentrations of oxygen and nitrogen was measured by Diatezua et al. [66] (Fig. 8). The authors pointed out that the performances of the analysed multi-layered samples are far from the perfect selective material. Moreover, their results are even worse than other single layer materials [53,65].

Another configuration using a *SiO* film as outer layer consisting of vanadium dioxide (doped with tungsten or not) (*V_{1-x}W_xO₂*), a thermochromic film, as intermediate layer, and a blackbody surface as base, was numerically studied by Tazawa and Tanemura [67] and Tazawa et al. [68].

Transition metal oxide thermochromic films, like *V_{1-x}W_xO₂*, show optical switching behaviour corresponding to the phase transition from metallic to semiconductor at a certain temperature. Thermochromic materials have a high reflectance in the high temperature phase and low reflectance in the low temperature phase. Due to the fact that spectral selectivity only appears at higher temperatures, as seen in Fig. 9 (left), it provides an automated temperature control of the surface.

Vanadium dioxide films (doped with tungsten or not) are candidate materials because the transition temperature of Vanadium dioxide (around 68°C) can be reduced down below room set point temperature by adjusting the doping level. These works [67,68] present results of radiative cooling power and temperature stability of sky radiators for different doping level of tungsten.

Although these configurations do not show better performance than *SiO/Al* configurations, as can be seen in Fig. 9 (centre), they present higher temperature control and stability as can be seen in Fig. 9 (right) [68].

3.1.3. Ceramic oxide layers

Another possibility to achieve radiative cooling to low temperatures is to use materials with high values of reflectivity at high wavelengths ($\lambda > 13\mu\text{m}$) instead of using high reflective materials all over the spectrum and coat it with high emissive materials at the infrared atmospheric window.

Magnesium oxide (*MgO*) ceramic samples have been studied [69] (Fig. 10) and their behaviour has been compared to white painted surfaces, showing the first ones a better performance. *MgO* can reach lower temperatures than selective surfaces based on polyvinyl-fluoride (PVF), and has a high solar reflectivity which may allow radiative cooling with daylight.

Lithium fluoride (*LiF*) is also considered a good material for

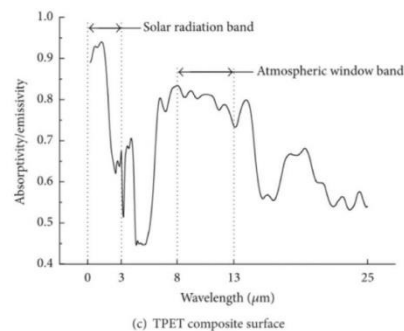


Fig. 3. Spectral absorptivity (emissivity) of TPET composite surface [61].

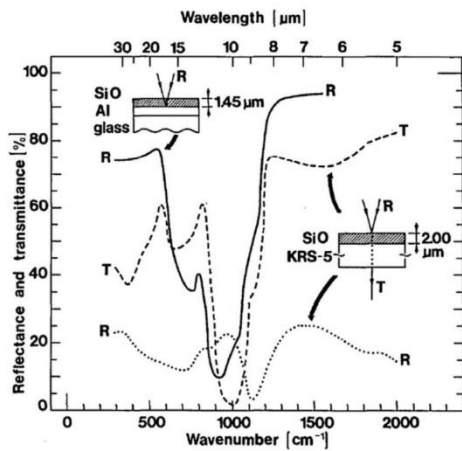


Fig. 4. Spectral infrared reflectance and transmittance for evaporated SiO films [62].

radiative cooling due to the similar optical properties at the infrared region as MgO [69] (Fig. 10). Furthermore, it has also been suggested to manufacture selective radiators with LiF/MgO mixtures.

3.1.4. Paints

In hot regions, white paints are commonly used when painting buildings in order to reflect solar radiation. Furthermore, the use of additives to enhance painting performance has been tested in order to provide high emissivity at the infrared atmospheric window. Therefore, the combination of white paints with these additives provides both high emissivity at the infrared atmospheric window and high reflectivity of solar radiation. White paints with some concentration of TiO_2 were tested (on aluminium plate) by Harrison and Walton [70] showing that high concentrations of TiO_2 (35%) can cool down $15^\circ C$ below ambient temperature in Calgary, Canada.

In the same way, Awanou [71] developed a diode roof system that had a pebbled roof with white paint with TiO_2 in order to reduce absorption of solar radiation and to emit radiation during the night. The results were not as good as expected but better results are foreseen for hot and dry climates with long nights ($> 8h$).

Two other white pigmented paints based on $TiO_2/BaSO_4$ and TiO_2/ZnS were analysed by Orel et al. [72] showing that the addition of $BaSO_4$ improves the performance of radiative cooling.

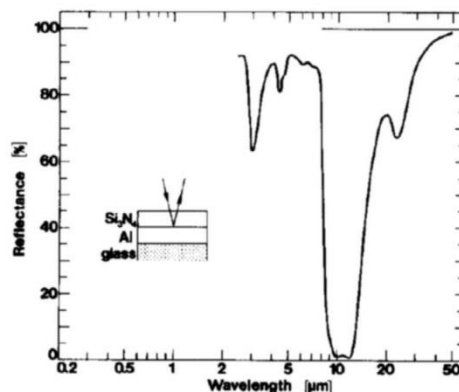
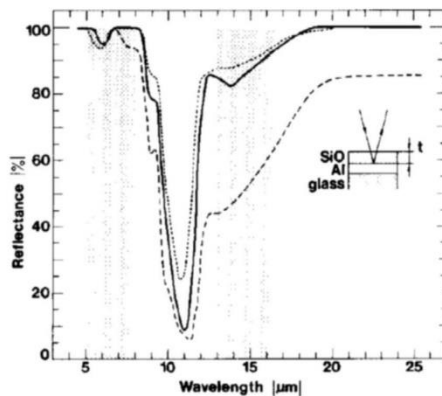


Fig. 5. Left: measured spectral reflectance for SiO/Al films on glass with three SiO film thicknesses [57]. Right: measured spectral reflectance for an Si_3N_4/Al film on glass [57].

3.1.5. New materials (multilayers)

Recently, new manufacturing techniques allowing the development of new materials have been developed. These new materials are nanoscale multilayer combinations of materials, optimized to have better optical properties for radiative cooling.

Two new multilayer combinations of materials have been tested. The first one made of several layers of titanium dioxide TiO_2 and magnesium fluoride MgF_2 on silver cover with silicon carbide SiC and quartz [73], and the other consisting of alternating layers of silicon dioxide (SiO_2) and hafnium dioxide (HfO_2) on top of silver and silicon [74]. Both of them showed a good performance even under sunlight due to its high reflectivity of solar radiation and high emissivity in the infrared atmospheric window, as can be seen in Fig. 11.

3.2. Selective screen and convection shield

Due to the difficulty of achieving a material with perfect properties for radiative cooling and also reduce convection heat gains, the use of selective screens is proposed.

3.2.1. Polyethylene (PE)

First attempts in using convection shields [53–55,57,64,69,70] were conducted with polyethylene (PE) foils due to their good transmittance almost all over the spectrum (Fig. 12). Due to its high transmittance at the infrared atmospheric window (85% [75]) it could be complementary to a selective surface radiator.

Different configurations were analysed instead of flat screens, as for example a V-corrugate screen design of high-density polyethylene (HDPE) foils (Fig. 13, [75]). A better performance than a flat screen was observed when analysing its transmittance and thermal insulation as a convection shield.

For a better understanding of polyethylene performance as a convection shield and selective screen, Ali et al. [76] studied the effects of aging, thickness, and colour on both the radiative properties of polyethylene films and the performance of the radiative cooling system, highlighting the poor aging of polyethylene foils. The authors also concluded that thinner films present a better performance in terms of night sky radiation, but worse mechanical properties. Moreover, the colour of the film does not significantly affect its optical properties. In a recent research a polymeric mesh has been proposed as a solution for structural weakness of PE [77]. However, although the authors (Gentle et al.) state that this configuration could extend the PE film life span to more than five years, they do not provide any data to support this statement, and do not analyse any potential optical properties degradation.

In order to reduce solar gains and increase the longevity of

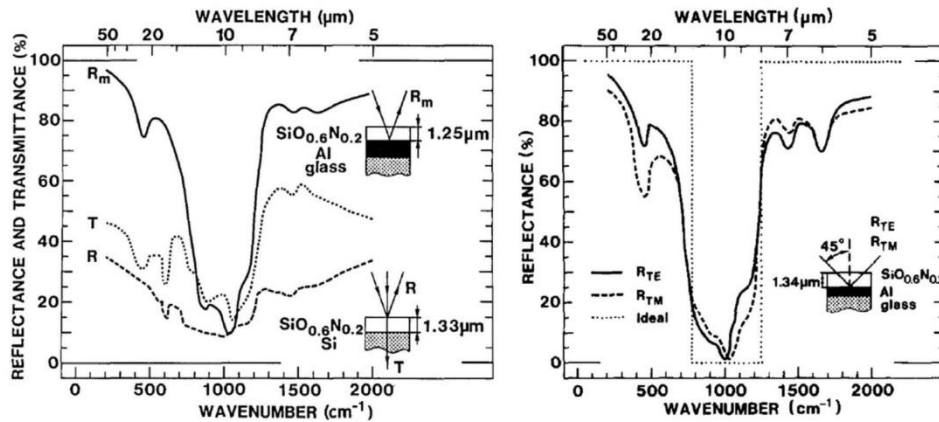


Fig. 6. Left: Spectral reflectance and transmittance of evaporated $SiO_{0.6}N_{0.2}$ films on two different substrates [63]. Right: Spectral reflectance for a film of $SiO_{0.6}N_{0.2}$ deposited onto Al [64].

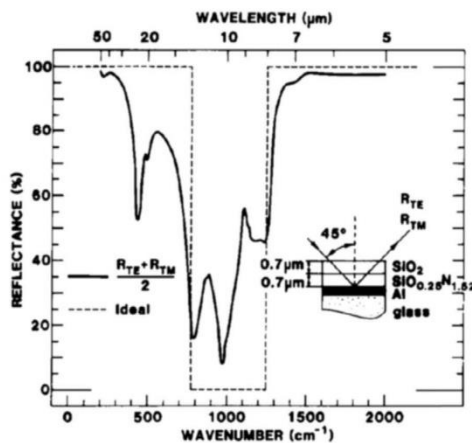


Fig. 7. Computed spectral reflectance of $SiO_{2.0}/SiO_{0.25}N_{1.52}$ coating on Al [65].

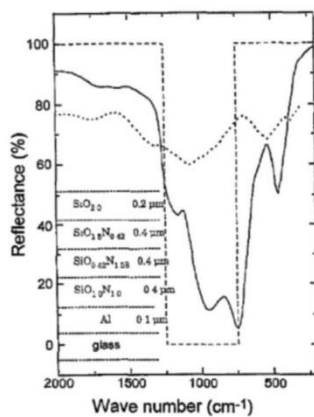


Fig. 8. Reflectance measured for the sample represented on the figure [66].

polyethylene foils several researches have been conducted, analysing different types of coatings. Nilsson et al. [78] studied zinc sulphide (ZnS) coating on low-density polyethylene (LDPE), showing a good solar reflectance and also a good transmittance in the infrared atmospheric window. This coating enables radiative cooling during the night and reduces heating under direct sunlight. Later on, Nilsson and Niklasson [79] described the optimization of optical properties and simulations of thermal performance during the day for pigmented polyethylene foils. The simulated pigment materials were ZnS , $ZnSe$, TiO_2 , ZrO_2 , and ZnO . Simulations showed that ZnS is the best of the pigmented materials tested for a cover foil.

Similarly, Mastai et al. [80] studied the optical properties of a coating of TiO_2 on polyethylene for different thicknesses, showing favourable optical characteristics, high reflectance in the solar band, and high transmittance in the atmospheric window band.

Low band gap semiconductors (Te , PbS , and $PbSe$), are expected to block solar radiation, while being transparent in the infrared region. Engelhard et al. [81] studied semiconductors of Te on polyethylene foils, exhibiting suitable characteristics for radiative cooling, high transmission in the mid-IR region, and high solar blocking. In the same way, Dobson et al. [82] studied the performance of semiconductor coatings of PbS and $PbSe$ on polyethylene foils, showing that combined with pigmented polyethylene foils of ZnS and ZnO they can provide optical and radiative cooling properties.

3.2.2. Other convection covers

Benlattar et al. [83] described the use of thin film $CdTe$ onto Silicon substrate by measuring its optical properties. $CdTe$ thin film is suitable for radiative cooling due to its low reflectance and high transmittance in the atmospheric infrared window. Moreover, Benlattar et al. [84] also described the use as selective cover of CdS , showing good optical properties for radiative cooling.

Mouhib et al. [85] studied stainless steel deposited on a tin coating layer and on a float glass sheet, as a selective screen over a blackbody emitter. This screen has negligible transmittance so it has a different behaviour in each side. The overall behaviour is that the upper face prevents the transmission of the greatest part of radiation coming from the sky, and allows the lower face to evacuate most of the thermal radiation emitted by an underlying material. The energy balance indicates that this configuration would be suitable for radiative cooling device based on spectral selectivity. Direct measurements confirmed this conclusion.

Bathgate and Bosi [86] analysed and tested experimentally the use of polyethylene and zinc sulphide as selective covers. They concluded

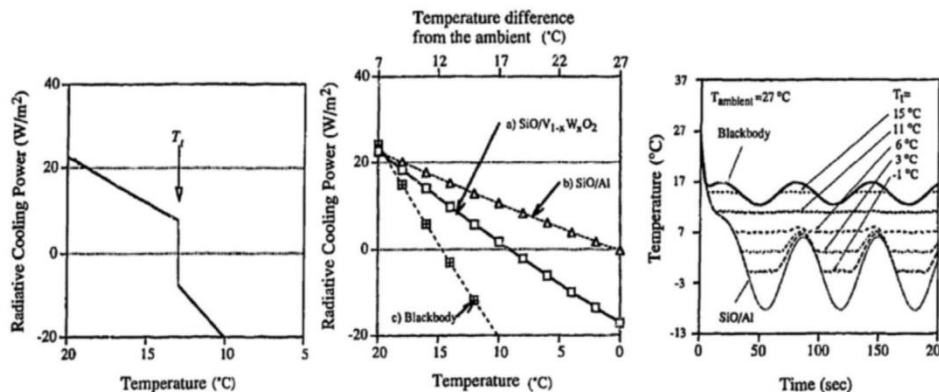


Fig. 9. Left: Radiative cooling power of the sky radiator with respect to the phase transition of the thermochromic film [67]. Centre: calculated radiative cooling power of the three different sky radiators [67]. Right: Temperature changes of the spectral selective radiating material [68].

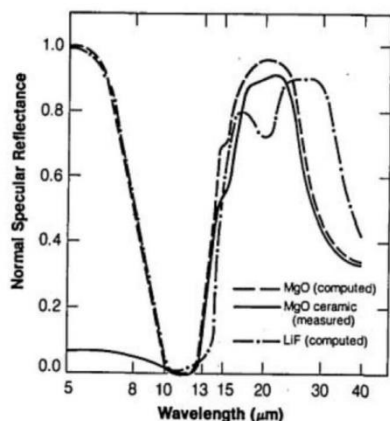


Fig. 10. Computed normal specular reflectance for layers of MgO and LiF backed with a reflecting layer, and normal specular reflectance of a polished MgO ceramic sample [69].

that both covers perform similarly in thermal aspects, such as heat loss and radiative power, but mechanical/structural properties and durability of ZnS are much better, making it a more suitable material. Finally, they also mentioned the high price of ZnS glass and suggested that a much cheaper way to manufacture zinc sulphide screens should be developed to make it affordable to be used as cover.

3.3. Gas slab

Another point to take into account is the air gap between the cover and the radiator plate. Little research has been conducted in the study of optical properties of certain gases to emit through the infrared atmospheric window. These gases should emit/absorb mainly in the infrared atmospheric window but transmit elsewhere.

The main gases studied for this purpose are ethylene(C_2H_4) [64,87–89], ethylene oxide(C_2H_4O) [64,88,89] and ammonia(NH_3) [64,88–90].

Lushiku and Granqvist [89] presented a concise summary of the research conducted in this topic, identifying ethylene(C_2H_4), ethylene oxide(C_2H_4O) and ammonia(NH_3) as proper gases for radiative cooling. They measured the optical properties of these gases for different thicknesses and also computed and analysed the cooling capacity of the three gases as well as for mixtures of ethylene and ethylene oxide. Finally, they tested ethylene and ammonia as infrared selective gases in

a simple radiative cooling device. The experiment showed the cooling effect but did not demonstrate its full potential. They concluded that ammonia was preferred when larger cooling power is required at near-ambient temperature, whereas mixtures of ethylene and ethylene oxide allow cooling to lower temperatures.

3.4. Directional selectivity

Part of the research in this topic has been conducted in analyse the behaviour of the radiator when using parabolic mirrors or in analyse how to control the direction of the incident/outgoing radiation. Such approaches are based on perfect reflector materials acting as mirrors; therefore, the system and not the material is analysed.

Du Marchie van Voorthuysena and Roes [91] proposed the use of parabolic mirrors to produce radiative cooling effect, even in daytime, by focusing the mirrors to a low effective temperature part of the sky. This concept is based on the adaptation of a parabolic solar collector for this purpose, so these collectors could produce both effects. The purpose of the research was to find out if radiative cooling and wind cooling have enough power to cool down large parabolic trough solar power stations. They conclude that there exists such potential to be used but occasionally supported by additional cooling.

Another research [92,93] proposed the use of Compound Parabolic Concentrator (CPC) technology to improve the radiative cooling effect focusing the radiator to the lowest effective temperature part of the sky. CPCs allow absorbing radiation coming from just a specific part of sky, reject all emitted radiation from other parts of sky and also reject all radiation emitted by the radiator. This technology could provide up to $135W/m^2$ at $10^\circ C$ below the ambient [93].

4. Theoretical approach and numerical simulation

Some authors have conducted their research in theoretical approaches of radiative cooling phenomenon and in simulating them. Also, numerical simulations are suitable tools for the design and evaluation of radiative cooling systems. Moreover, several authors have focused their research in the development of numerical models capable to accurately simulate radiative cooling systems. In this section, these models are reviewed and compared in order to identify research needs for improvement.

When analysing radiative cooling devices, the radiator plate is the main part of the device. Most authors modelled the radiator plate in a similar way as a solar flat-plate collector that, instead of gaining heat from the Sun, loses heat toward sky.

Most solar collectors have a cover to reduce the heat losses.

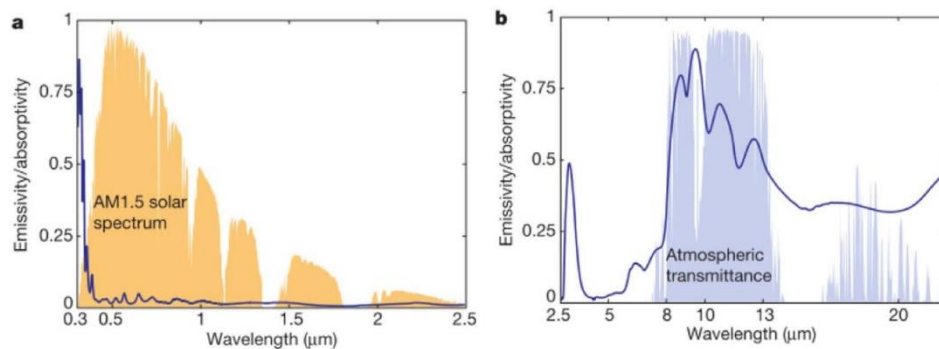
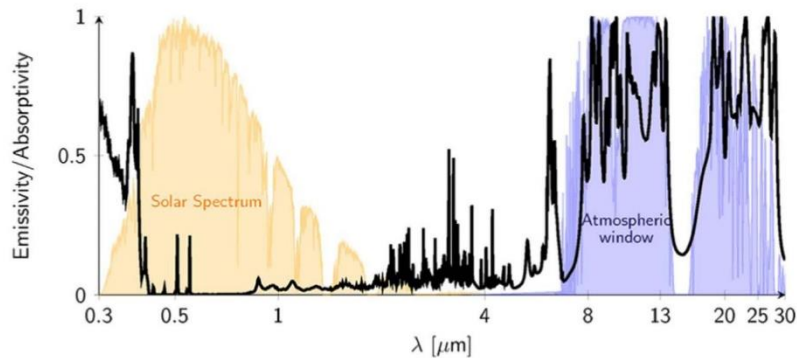


Fig. 11. Up: Emissivity of the optimized daytime radiative cooler [73]. Down: Measured emissivity of the photonic radiative cooler [74].

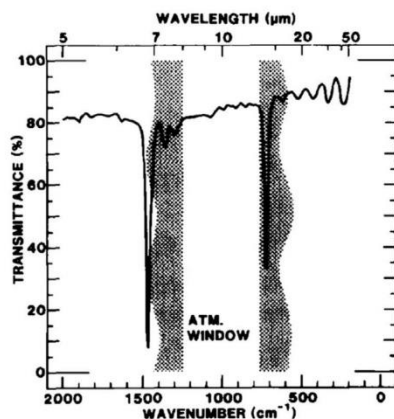


Fig. 12. Normal spectral transmittance of a 30 μm thick foil of high-density polyethylene [75].

However, in radiative cooling devices, losses are beneficial, therefore, for particular weather conditions, the cover is not desired. For instance, if ambient temperature is lower than the radiator one, using cover is a disadvantage. Otherwise, using a cover when ambient temperature is higher than the radiator temperature avoids undesired heat gains.

The thermal behaviour of the radiator is influenced by the heat transfer between the radiator and the surrounding media (sky, ambient, and internal fluid). Most of the authors consider at least the sky and the ambient when performing simulations to assess the

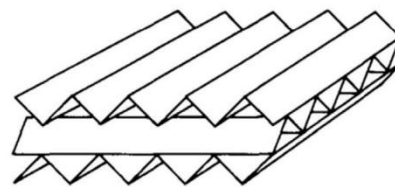


Fig. 13. Sketch of the material with high infrared transmittance and low non-radiative heat exchange [75].

potential of the device.

The most challenging effect to model is the influence of the sky, especially when the radiator is covered with a screen. Nevertheless, first attempts [94–99] considered the use of a screen. They presented analytical approaches combined with optical transmittance profiles of the screen and the sky.

Most recent works [73,74,100–114] on simulation either did not consider a cover or omit its influence. In these works the sky influence is treated in two ways: having it an effective temperature determined with empirical correlations [100–114] or considering the sky to have a wavelength dependant emittance and treat it analytically [73,74].

Not using a cover on the radiator plate simplifies the model of the radiative cooling device. However, if low temperatures are required, the use of a cover is necessary to reduce heat transfer from the ambient.

Another effect is the influence with ambient which is mainly by convection. When analysing convection between the device and the ambient is more difficult when there is a cover. This is due to the additional phenomena involving the air between the radiator surface and the cover that must be taken into account. Even that, it is difficult to determine the convection heat transfer coefficient in both cases. So,

to deal with it, some authors [73,74,95] used parametric analysis with different convection heat transfer coefficients, in order to avoid to calculate for every condition, and to provide enough information to present some conclusions.

Finally the influence of the internal fluid with the radiator temperature for some authors it is considered in different ways: function of the accumulation tank temperature or conditioned space temperature [101–104,108,109,111–113], simulated with CFD [105], or not used (just calculated the maximum reachable temperature) [73,74,95,96].

There exists a formula (Eq. (52)) that gathers the overall of the effects and gives the fluid temperature at any point of a solar collector when operating at steady state [115]:

$$\frac{T_f - T_a - S/U_L}{T_{fi} - T_a - S/U_L} = e^{(-U_L n w F y / m C_p)} \quad (52)$$

where T_f is the temperature of the fluid at the desired point (normally the outlet fluid temperature), T_{fi} is the inlet fluid temperature, T_a is the ambient temperature, S is the radiation absorbed by the solar collector, U_L is the overall heat loss coefficient, n is the number of parallel tubes, w is the distance between parallel tubes, F is the collector efficiency factor, y is the tubes length, m is the mass flow rate and C_p is the specific heat of the fluid. This equation is for solar collectors. Readapting it for a radiator plate by replacing the solar heat gain for the net radiative heat loss was used by some authors [100–103,106–108,110,114] to predict the outlet fluid temperature.

The research conducted in this topic has now been introduced according to its influence to surroundings. From here on, conclusions from their authors are presented.

First approaches of radiative cooling devices showed that this technology could be used to provide part of the cooling demand of a building (50% cooling demand [94]), achieving promising values of net cooling power and reaching temperatures far below ambient ($65W/m^2 - \Delta T \geq 10K$ [95] and $60W/m^2 - \Delta T = 14K$ [96]). Also, some of this research has been conducted in hot and arid areas (Jordan) [98] modelling a radiative cooling device and validating it with empirical data showing good correlation and also good results (reducing the temperature of a 120L tank to 15°C in a night, 13MJ/m²-night). Later on, the same authors used this device to improve a previous nocturnal cold storage [99], presenting some conclusions about its dynamic thermal behaviour.

Recent research [73,74] computed selective materials with photonic design optimization, showing that this new combination of materials can produce cooling (up to 100W/m² [73]). They also demonstrated that cooling can be achieved even under daylight conditions, reaching experimental values of 40W/m² of cooling power [74].

The coupling between radiative cooling and photovoltaic solar collection [109] was also studied. After validating the model with empirical data, it was used to perform an analysis of its performance in two cities, Madrid and Shanghai. The cooling annual potential calculated is of 51 and 55kWh/m²year for each location.

Some research [101–103] studied multistep refrigeration systems combining radiative cooling with evaporative cooling for climate conditions in Iran. Their model has been validated with the results from [116]. The potential of the radiative cooling device was investigated for four cities showing that can be provided air up to 16K below ambient temperature and when combined with evaporative cooling up to 24K below ambient temperature, entailing savings up to 80% of the total cooling demand.

A research combining radiative cooling with microencapsulated phase change material [104], was simulated in five typical cities across China also showing great performance with savings up to 77% of the total cooling demand.

The one using CFD to simulate radiative cooling devices do not show good results if only is considered the thermal radiation (up to

20W/m² [105]). Maybe, this is because the thermal radiation is calculated in a chosen steady state by the author that may not represent the reality.

An air-based system tested in a building in Greece [108], using an aluminium painted tube set to work as a nocturnal metallic plate radiator, was used to validate an analytical model showing good agreement.

A model using water as inner fluid and using general heat transfer equations was proposed [110]. The model was validated with experimental data with statistical methodology of analysis. The model showed uncertainty less than 5% when validated with data under experimental conditions showing experimental average powers of 60W/m².

The combination of solar heating and radiative cooling, as passive system, has been simulated to condition the interior temperature of a building [111]. Savings up to 54% of heating and 53% of cooling can be achieved.

Some of the numerical simulations, validated with experimental data, were used to determine the effects of different parameters on the performance of the radiative cooling device, such as fin efficiency factor, flow rate, and overall heat transfer coefficient in [106,107,114], area/volume tank ratio, flow ratio, tank volume, and radiators surface in [116], and flow rate in [112,113]. In [107] are presented some different required characteristics between radiative cooling radiators and solar flat plate collectors used for solar heating. The authors concluded that fins used in flat plate solar collectors are less efficient for cooling applications, and an appropriate solution is radiators consisting entirely of pipes. Moreover, previous experimental data [114] was also used to validate a research [112] which also assess the influence of the flow rate in the model performance.

After analysing all research done in theoretical approach and numerical simulations of radiative cooling devices it can be seen that great effort has been done since the first attempts in testing new aspects that improve its performance and applicability.

5. Radiative cooling prototypes

Part of the research has been conducted in testing experimental radiative cooling devices under certain circumstances. Most of this research has been done in order to provide experimental data to validate numerical models and to experimentally analyse the thermal behaviour of the prototypes. Most of the prototypes have the same shape as a solar collector, a flat plate as radiator.

First attempts [71,117] aimed at providing a roof which could produce some cooling during night and reflect the incident solar radiation during day. Air based systems were used to cool down the temperature of huts where were tested. In [117] 2 different covers were compared, galvanised steel painted white and aluminium coated with Tedlar. Both cases provided low cooling powers (22W/m²), showing better performance the painted one, which reached lower temperatures (6°C below ambient temperature during night). In [71] a new concept called diode roof was tested. Although this concept allows reaching lower temperatures than ambient during night, the main purpose was to avoid the heat to go inside the building.

Another type of air-based system was tested in a building in Greece [108], using an aluminium painted tube set to work as a nocturnal metallic plate radiator. This study was performed in two different offices, one office using a radiative cooling and the other one with no cooling device. The system operation is to pass interior air through the tube to be cooled down before reintroduce it inside the room during night hours. Experimental results showed that the office using radiative cooling achieved temperatures between 2.5 – 4°C below the one with no cooling device. Two different paints were tested, demonstrating the importance of a high emissivity of the radiator to achieve lower temperatures. Moreover, a numerical model was developed and experimentally validated.

Later research focussed in the use of high heat capacity transfer fluids, as water, because water-based systems can be better controlled and operated. Water-based systems can either be open or closed. Open water-based systems combine evaporative cooling, radiative cooling and convective cooling. However, water is in contact with ambient, therefore it can evaporate and the system may need refilling. One of the first open water-based systems was developed by Dan and Chinnappa [118]. They used a solar collector where water was trickled over the cover glass during the night and 400 L of heated water were cooled down almost to the diurnal minimum temperature. Another purpose of open water-based systems is to use water to clean and remove the dust from the collector cover.

To avoid losing water and catching dust in the water, the majority of water-based systems are closed systems. A closed water-based system was used by Matsuta et al. [60] who were some of the first authors to combine and evaluate solar heating and radiative cooling using a solar collector. They showed that, even this combination does not perform as well as they do separately, it could provide a good heating and cooling power (up to 610W/m^2 – 51W/m^2 respectively).

In a similar way, Ezekwe [119] tested a radiative cooling device to cool down a small refrigerator to store food and other perishable goods in developing countries and in remote areas. The system provided an average cooling capacity of $628\text{kJ/m}^2\text{night}$ and reached temperatures 7°C below ambient.

Bearing in mind that the thermal demand of cooling is required during day time and the cooling is obtained during night; the use of thermal storage is needed. Ito and Miura [120] started using sensible thermal storage in combination with radiative cooling. An experimental and theoretical investigation of an uncovered radiative cooling radiator was performed. Results showed cooling powers of $40 - 60\text{W/m}^2$ in clear summer nights and $60 - 80\text{W/m}^2$ in winter, with thermal storage temperatures $2 - 5^\circ\text{C}$ below ambient temperature.

Later on, a Erell and Etzion did a series of experiments in Israel about how radiative cooling performs in this hot and arid weather [106,107,121–123]. First experiment was set to determine the effect of the thermal storage mass in radiative cooling plate [121]. Four test boxes including an internal concrete slab at different locations were tested, trying to show the influence of this slab with the heat transfer by natural convection. The authors stated that the thermal storage mass has the role of being a heat sink and also of preventing the radiator to have lower temperatures than the design temperature of the cooled space. The authors concluded that the existence of a thermal storage mass is a very important part of a cooling system but even more important is the location of the thermal mass and the coupling between it and the radiating surface.

Later on, the same authors set an experiment using water as heat exchange medium [122]. The experiment was performed using a test box similar to those used in [121] which was adapted to a solar collector (without glass) by adding a roof pond and a pumping system. The effect of the water flow rate was tested, showing that it affects the temperature difference between radiators inlet and outlet temperature. So, in this sense, the emerged hypothesis that a higher flowing rate increases the cooling rate was not supported by the data. The authors concluded that this is a self-regulated system, in the sense that higher daytime heat loads results in higher night-time cooling rates. Moreover, the amount of water in the pond is an important parameter; it can be used to regulate the radiator temperature in order to achieve a suitable temperature for cooling purposes when needed as well as an acceptable cooling rate during night. Finally, they found that the coupling of the radiator with the thermal mass of the building results in higher temperatures than ambient air, making it possible to take advantage of convective cooling. This feature of the system obviates the need for wind screens, which previous research demonstrated that are essential for achieving low radiator temperatures. For this prototype, the cooling potential, taking into account convective and radiative cooling, was up to 90W/m^2 .

Additionally, Erell and Etzion used this previous radiative cooling device to test it as a solar heating collector [123], resulting in a considerable heating output (mean daily heating rate $94\text{kWh/m}^2\text{day}$), although it was not designed for such use. Finally, the authors proposed an analytical formulation to simulate a radiative cooling device based on a solar collector analysis [106,107,114]. The model was experimentally validated, showing good agreement.

In a similar approach, Meir et al. [116] tested an unglazed radiator, using water as a heat transfer fluid, coupled to a large storage tank in Norway. An analytical model was developed and validated with experimental data, and then it was used to optimise some parameters. Although the device performed well for clear and low humidity nights, the authors recommended analysing the performance of the system in climates with significant cooling demands, with outdoors nocturnal temperature not suitable to meet the comfort temperatures, to corroborate their simulation results.

Similarly to preceding research, Hosseinzadeh and Taherian [113] tested an unglazed radiator with storage in Iran. The experimental results were also used to validate an analytical model. The prototype showed an average net cooling power of 45W/m^2 and capability of lowering 8°C a 130 L water tank.

Also using a closed water-based system, Ferrer Tevar et al. [110] tested 3 different radiators with different infrared emissivities (0.02, 0.5 and 0.9) in Almeria, Spain. The one with low emissivity material was used to isolate the effect of convection from the others. The experimental results showed averaged powers of 60W/m^2 . They conclude that the use of this technology could lower the cooling demands of buildings and also that is interesting to integrate it in buildings, specially combined with inertial elements.

Lately, Ahmadi et al. [124] tested a prototype, using a plastic sheet as cover and with a storage tank, in Iran. The radiator surface reached temperatures 20°C below ambient temperature. It was also tested the influence of the numbers of plastic layers as cover showing that the best performance was achieved when there was a single layer.

Apart from research in testing specific devices, development and testing of new materials was also addressed. Bathgate and Bosi [86] used two different covers, Polyethylene (PE) and Zinc Sulphide (ZnS), to analyse its potential and to justify the use of ZnS instead of PE, based on the similar behaviour of both covers and the higher durability of ZnS. The study showed a good performance of both PE and ZnS covers, reaching 6°C below ambient and a total net heat radiation loss up to $580\text{Wh/m}^2\text{night}$ for PE and $470\text{Wh/m}^2\text{night}$ for ZnS.

Recent research have been conducted in order to find new ways to enhance radiative cooling or combine it with other technologies that could benefit its economical profit/overall performance [61,74,109,125].

Eicker and Dalibard [109] tested and developed a combination of radiative cooling with photovoltaic solar collector to produce cooling and electricity. This device was tested in Madrid, showing cooling powers of $60 - 65\text{W/m}^2$ when coupled to the heat sink storage tank (depending on the temperature the tank was used to cool a radiant floor or for heat rejection from a chiller), and $40 - 45\text{W/m}^2$ when directly used to cool down a ceiling containing phase change material (PCM). For this research, a numerical model was developed and validated.

Selective materials could improve the performance of radiative cooling in such a way that it can even work during daytime. Raman et al. [74] used the so called photonics design optimization to develop a material which can reflect 97% of the sunlight and also strongly emit in the infrared window. This improvement allows producing cooling during the whole day rather than only during the night. Empirical results showed a radiator temperature 5°C below ambient temperature and a 40W/m^2 cooling power during exposition at direct sunlight conditions.

Finally, some research has been conducted in combining radiative cooling and solar heating [61,125,126] in the same device, showing a

great potential. In [125] the systems was a vertical wall with a coated aluminium plate. This research showed perfect integration between the building and the heating/cooling system. Further on this concept, Hu et al. [61] developed and tested a selective material that performs well on both heating and cooling. Results showed a performance of 76.8% in heating and 75% in cooling compared to that of conventional systems. Afterwards, Hu et al. [126] used this material in a prototype whose performance was compared to a traditional flat-plate solar collector. In diurnal testing mode it showed a thermal efficiency of 86.4% compared to the traditional solar collector, whereas in cooling mode, it presented a cooling power density of $50\text{W}/\text{m}^2$ when the radiator surface was at ambient temperature, as well as a capability of reaching 7.2°C below ambient temperature.

Research tendencies from the development of the first prototype have gone to the use of selective materials and the combination of radiative cooling with other technologies. The main goals are to reduce the payback time and to be able to provide different energy demands (e.g. cooling, heating, electricity).

6. Conclusions

In the present paper, research in the topic of radiative cooling is reviewed and classified, presenting the main results and conclusions. The articles are classified in four different sections: radiative cooling background, selective radiative cooling, theoretical approach and numerical simulation for radiative cooling, and radiative cooling prototypes.

Radiative cooling has been long, but not widely, analysed as a physical phenomenon in order to determine its influence in superficial heat balances, showing that, due to its low energy density, even minor heat fluxes are significant for the system performance. This phenomenon is fitted by straightforward correlations which are explained and summarized in the present work. These correlations depend on meteorological parameters, meaning that somehow they are very location dependant. As this phenomenon is not usually measured, the implementation potential for cooling purposes was barely analysed. Although correlations do not depict radiative cooling phenomenon better than real data, they can be used as a good approach, if adapted to the specific location. It is also important to mention that the radiation coming from the sky is not uniform through the spectrum as explained before; therefore the optical properties in the specific wave range (atmospheric window) may be important and should be accurately measured.

Given the low cooling power reached by this technology, different improvements have been analysed and studied. Materials with appropriate properties were fully analysed in the literature, from optical to thermal properties. General tendency leads to two possibilities: to develop/use materials that improve the cooling capacity of the system, or to develop/use materials that provide other benefits to the system (such as solar collection, PV, structural strength, etc.). Currently the design of these materials has entered to a microscopically level of precision.

Despite radiative cooling is a novel technology, analytical approaches and numerical simulations are spread all over the literature. The research done is mainly orientated to flat plate design. This design presents similarities to a solar collector, since both designs have similar shape, both can adapt to the building envelope and both should face upward to the sky.

In the present review, the research about numerical simulations and prototypes has been classified bearing in mind the influencing parameters of the sky, the ambient, and the internal fluid. From this research, some interesting conclusions are extracted: (1) the use of cover is recommended to achieve low temperatures, (2) the use of water instead of air as a heat-carrier fluid is also recommended to control the system, and (3) heat storage is recommend to reach high cooling power densities.

Experimental analysis of this technology has also been widely performed in order to prove the concept and it has also been used to validate numerical models. Results show that the applicability of this technology is possible in some climates. These results lead new prototypes to provide new functionalities apart from radiative cooling for profitable reasons, such as generate heating using solar collection or electricity using PV.

Even though this is a low-grade technology and may not be enough for some particular requirements, the use of this technology for cooling purposes, actively or passively, can dramatically reduce the energy consumption, since it requires low energy for its operation and it comes from a renewable source.

Nevertheless, there exist some issues to be taken into account that limit the implementation of this technology. For instance, the use of a material with appropriate properties is an issue to be solved. Also, referring to simulations, some optical phenomena are omitted, when developing the model, related to electromagnetic optics or to photonics. This omission is a simplification of such complex effects. Finally, mention that this technology has a low energetic density for cooling purposes, so significant improvements are expected.

Thus, further research is warranted in order to determine the real potential of such technology, to develop new concepts and systems, and to overcome the main limitations existing at the moment.

Acknowledgements

Sergi Vall would like to thank the Secretaria d'Universitats i Recerca del Departament d'Economia i Coneixement de la Generalitat de Catalunya for his research fellowship.

References

- [1] European Parliament . Directive 2010/31/EU of the European Parliament and of the Council of 19 May 2010 on the energy performance of buildings. *J Eur Union* 2010;153:13–35.
- [2] European Parliament . Directive 2009/28/EC of the European Parliament and of the Council of 23 April 2009 on the promotion of the use of energy from renewable sources and amending and subsequently repealing Directives 2001/77/EC and 2003/30/EC. *J Eur Union* 2009;140:16–62. http://dx.doi.org/10.3000/17252555.L_2009.140.eng.
- [3] European Commission . Decision of 1 March 2013 (2013/114/EU) establishing the guidelines for Member States on calculating renewable energy from heat pumps from different heat pump technologies pursuant to Article 5 of Directive 2009/28/EC of the European Parliament and of the. *J Eur Union* 2013;62:27–35.
- [4] Lu X, Xu P, Wang H, Yang T, Hou J. Cooling potential and applications prospects of passive radiative cooling in buildings: the current state-of-the-art. *Renew Sustain Energy Rev* 2016;65:1079–97. <http://dx.doi.org/10.1016/j.rser.2016.07.058>.
- [5] Sellers WD. *Physical climatology*. Chicago London: University of Chicago; 1965.
- [6] Bell E, Eisner L, Young J, Oetjen R. Spectral-radiance of sky and terrain at wavelengths between 1 and 20 microns. II. Sky measurements. *J Opt Soc Am* 1960;50:1313–20. <http://dx.doi.org/10.1364/JOSA.50.001313>.
- [7] Bliss RW. Atmospheric radiation near the surface of the ground: a summary for engineers. *Sol Energy* 1961;5:103–20. [http://dx.doi.org/10.1016/0038-092X\(61\)90053-6](http://dx.doi.org/10.1016/0038-092X(61)90053-6).
- [8] Berdahl P, Fromberg R. The thermal radiance of clear skies. *Sol Energy* 1982;29:299–314. [http://dx.doi.org/10.1016/0038-092X\(82\)90245-6](http://dx.doi.org/10.1016/0038-092X(82)90245-6).
- [9] Ångström AK. A study of the radiation of the atmosphere. *Smithson Inst Misc Collect* 1915;65:159.
- [10] Ångström AK. Effective radiation during the second international polar year. *Medde Stat Met Hydrogr Anst* 1936:6.
- [11] Brunt D. Notes on radiation in the atmosphere. I. *Q J R Meteorol Soc* 1932;58:389–420. <http://dx.doi.org/10.1002/qj.49705824704>.
- [12] Elsasser WM. Heat transfer by infrared radiation in the atmosphere. Harvard University Press; 1942.
- [13] Kondratyev KY. Radiation in the atmosphere. New York: Academic Press; 1969.
- [14] Swinbank WC. Long-wave radiation from clear skies. *Q J R Meteorol Soc* 1963;89:339–48. <http://dx.doi.org/10.1002/qj.49708938105>.
- [15] Idso SB, Jackson RD. Thermal radiation from the atmosphere. *J Geophys Res* 1969;74:5397–403.
- [16] Aase JK, Idso SB. A comparison of two formula types for calculating long-wave radiation from the atmosphere. *Water Resour Res* 1978;14:623–5. <http://dx.doi.org/10.1029/WR014i004p00623>.
- [17] Hatfield JL, Reginato RJ, Idso SB. Comparison of long-wave radiation calculation methods over the United States. *Water Resour Res* 1983;19:285. <http://dx.doi.org/10.1029/WR019i001p00285>.

- [18] Satterlund DR. An improved equation for estimating long-wave radiation from the atmosphere. *Water Resour Res* 1979;15:1649. <http://dx.doi.org/10.1029/WR015i006p01649>.
- [19] Brutsaert W. On a derivable formula for long-wave radiation from clear skies. *Water Resour Res* 1975;11:742–4. <http://dx.doi.org/10.1029/WR011i005p00742>.
- [20] Idso SB. A set of equations for full spectrum and 8- to 14 micron and 10.5- to 12.5 micron thermal radiation from cloudless skies. *Water Resour Res* 1981;17:295–304. <http://dx.doi.org/10.1029/WR017i002p00295>.
- [21] Andreas EL, Ackley SF. On the differences in ablation seasons of Arctic and Antarctic Sea Ice. *J Atmos Sci* 1982;39:440–7. [http://dx.doi.org/10.1175/1520-0469\(1982\)039<0440:OTDIAS>2.0.CO;2](http://dx.doi.org/10.1175/1520-0469(1982)039<0440:OTDIAS>2.0.CO;2).
- [22] Centeno VM. New formulae for the equivalent night sky emissivity. *Sol Energy* 1982;28:489–98. [http://dx.doi.org/10.1016/0038-092X\(82\)90320-6](http://dx.doi.org/10.1016/0038-092X(82)90320-6).
- [23] Berdahl P, Martin M. Emissivity of clear skies. *Sol Energy* 1984;32:663–4. [http://dx.doi.org/10.1016/0038-092X\(84\)90144-0](http://dx.doi.org/10.1016/0038-092X(84)90144-0).
- [24] Martin M, Berdahl P. Characteristics of infrared sky radiation in the United States. *Sol Energy* 1984;33:321–36. [http://dx.doi.org/10.1016/0038-092X\(84\)90162-2](http://dx.doi.org/10.1016/0038-092X(84)90162-2).
- [25] Berger X, Buriot D, Garnier F. About the equivalent radiative temperature for clear skies. *Sol Energy* 1984;32:725–33. [http://dx.doi.org/10.1016/0038-092X\(84\)90247-0](http://dx.doi.org/10.1016/0038-092X(84)90247-0).
- [26] Alados-Arboledas L, Jimenez JI. Day-night differences in the effective emissivity from clear skies. *Bound-Layer Meteorol* 1988;45:93–101. <http://dx.doi.org/10.1007/BF00120817>.
- [27] Niemelä S, Räisänen P, Savijärvi H. Comparison of surface radiative flux parameterizations part I: longwave radiation. *Atmos Res* 2001;58:1–18. [http://dx.doi.org/10.1016/S0169-8095\(01\)00084-9](http://dx.doi.org/10.1016/S0169-8095(01)00084-9).
- [28] Tang R, Etzion Y, Meir IA. Estimates of clear night sky emissivity in the Negev Highlands, Israel. *Energy Convers Manag* 2004;45:1831–43. <http://dx.doi.org/10.1016/j.enconman.2003.09.033>.
- [29] Staley DO, Jurica GM. Effective atmospheric emissivity under clear skies. *J Appl Meteorol Climatol* 1972;11:349–56. [http://dx.doi.org/10.1175/1520-0450\(1972\)011<0349:EAUFUC>2.0.CO;2](http://dx.doi.org/10.1175/1520-0450(1972)011<0349:EAUFUC>2.0.CO;2).
- [30] Prata AJ. A new long-wave formula for estimating downward clear-sky radiation at the surface. *Q J R Meteorol Soc* 1996;122:1127–51.
- [31] Dilley AC, O'Brien DM. Estimating downward clear sky long-wave irradiance at the surface from screen temperature and precipitable water. *Q J R Meteorol Soc* 1998;124:1391–401.
- [32] Viúdez-Mora A, Calbó J, González JA, Jiménez MA. Modeling atmospheric longwave radiation at the surface under cloudless skies. *J Geophys Res Atmos* 2009;114:1–12. <http://dx.doi.org/10.1029/2009JD011885>.
- [33] Ångström AK. Radiation and the Temperature of snow and convection of the air at its surface. *Akt För Mat Astron Och Fys* 1919;13:1–18.
- [34] Bolz HM. Die Abhängigkeit der infraroten Gegenstrahlung von der Bevölkerung. *Meteorol Z* 1949;3:201–3.
- [35] Kimball B, Idso SB, Aase JK. A model of thermal radiation from partly cloudy and overcast skies. *Water Resour Res* 1982;18:931. <http://dx.doi.org/10.1029/WR018i004p00931>.
- [36] Sugita M, Brutsaert W. Cloud effect in the estimation of instantaneous downward longwave radiation. *Water Resour Res* 1993;29:599–605. <http://dx.doi.org/10.1029/92WR02352>.
- [37] Aubinet M. Longwave sky radiation parameterizations. *Sol Energy* 1994;53:147–54. [http://dx.doi.org/10.1016/0038-092X\(94\)90475-8](http://dx.doi.org/10.1016/0038-092X(94)90475-8).
- [38] Crawford TM, Duchon CE. An improved parameterization for estimating effective atmospheric emissivity for use in calculating daytime downwelling longwave radiation. *J Appl Meteorol* 1999;38:474–80. [http://dx.doi.org/10.1175/1520-0450\(1999\)038<0474:AIPFEE>2.0.CO;2](http://dx.doi.org/10.1175/1520-0450(1999)038<0474:AIPFEE>2.0.CO;2).
- [39] Sridhar V, Elliott RL. On the development of a simple downwelling longwave radiation scheme. *Agric Meteorol* 2002;112:237–43. [http://dx.doi.org/10.1016/S0168-1923\(02\)00129-6](http://dx.doi.org/10.1016/S0168-1923(02)00129-6).
- [40] Viúdez-Mora A, Costa-Surós M, Calbó J, González JA. Journal of geophysical research : atmospheres. *J Geophys Res Atmos* 2014;120:199–214. <http://dx.doi.org/10.1002/2014JD022310>. Received.
- [41] Malek E. Evaluation of effective atmospheric emissivity and parameterization of cloud at local scale. *Atmos Res* 1997;45:41–54. [http://dx.doi.org/10.1016/S0169-8095\(97\)00020-3](http://dx.doi.org/10.1016/S0169-8095(97)00020-3).
- [42] Linke F. Die Nächtliche effektive Ausstrahlung unter verschiedenen Zenitdistanzen. *Meteorol Z* 1931;48:25–31.
- [43] Strong J. Study of atmospheric absorption and emission in the infrared spectrum. *J Frankl Inst* 1941;232:22.
- [44] Cook J. *Radiative cooling Passiv. cool.* Cambridge and London: MIT Press; 2000. p. 606.
- [45] Granqvist CG, Hjortsberg A. Radiative cooling to low temperatures: general considerations and application to selectively emitting SiO films. *J Appl Phys* 1981;52:4205–20. <http://dx.doi.org/10.1063/1.329270>.
- [46] Martin M, Berdahl P. Summary of results from the spectral and angular sky radiation measurement program. *Sol Energy* 1984;33:241–52. [http://dx.doi.org/10.1016/0038-092X\(84\)90155-5](http://dx.doi.org/10.1016/0038-092X(84)90155-5).
- [47] Atwater MA, Ball JT. Computation of IR sky temperature and comparison with surface temperature. *Sol Energy* 1978;21:211–6. [http://dx.doi.org/10.1016/0038-092X\(78\)90023-3](http://dx.doi.org/10.1016/0038-092X(78)90023-3).
- [48] Exell RHB. The atmospheric radiation climate of Thailand. *Sol Energy* 1978;21:73–9. [http://dx.doi.org/10.1016/0038-092X\(78\)90032-4](http://dx.doi.org/10.1016/0038-092X(78)90032-4).
- [49] Hanif M, Mahlia TMI, Zare A, Salsahdan TJ, Metselaar HSC. Potential energy savings by radiative cooling system for a building in tropical climate. *Renew Sustain Energy Rev* 2014;32:642–50. <http://dx.doi.org/10.1016/j.rser.2014.01.053>.
- [50] Pissimanis DK, Notaridou VA. The atmospheric radiation in Athens during the summer. *Sol Energy* 1981;26:525–8. [http://dx.doi.org/10.1016/0038-092X\(81\)90164-X](http://dx.doi.org/10.1016/0038-092X(81)90164-X).
- [51] Argiriou A, Santamouris M, Assimakopoulos DN. Assessment of the radiative cooling potential of a collector using hourly weather data. *Energy* 1994;19:879–88. [http://dx.doi.org/10.1016/0360-5442\(94\)90040-X](http://dx.doi.org/10.1016/0360-5442(94)90040-X).
- [52] Burch J, Christensen C, Salasovich J, Thornton J. Simulation of an unglazed collector system for domestic hot water and space heating and cooling. *Sol Energy* 2004;77:399–406. <http://dx.doi.org/10.1016/j.solener.2003.12.014>.
- [53] Catalanotti S, Cuomo V, Piro G, Ruggi D, Silvestrini V, Troise G. The radiative cooling of selective surfaces. *Sol Energy* 1975;17:83–9. [http://dx.doi.org/10.1016/0038-092X\(75\)90062-6](http://dx.doi.org/10.1016/0038-092X(75)90062-6).
- [54] Bartoli B, Catalanotti S, Coluzzi B, Cuomo V, Silvestrini V, Troise G. Nocturnal and diurnal performances of selective radiators. *Appl Energy* 1977;3:267–86. [http://dx.doi.org/10.1016/0306-2619\(77\)90015-0](http://dx.doi.org/10.1016/0306-2619(77)90015-0).
- [55] Addeo A, Monza E, Peraldo M, Bartoli B, Coluzzi B, Silvestrini V, et al. Selective covers for natural cooling devices. *Nuovo Cim C* 1978;1:419–29. <http://dx.doi.org/10.1007/BF02507668>.
- [56] Granqvist CG. Radiative heating and cooling with spectrally selective surfaces. *Appl Opt* 1981;20:2606–15.
- [57] Granqvist CG, Hjortsberg A, Eriksson TS. Radiative cooling to low temperatures with selectively IR-emitting surfaces. *Thin Solid Films* 1982;90:187–90.
- [58] Trombe F. Perspectives sur l'utilisation des rayonnements solaires et terrestres dans certaines régions du monde. *Rev Générale Therm* 1967;6:1285–314.
- [59] Grenier P. Réfrigération radiative. Effet de serre inverse. *Rev Phys Appliquée* 1979;14:87–90. <http://dx.doi.org/10.1051/rphysap:0197900140108700>.
- [60] Matsuta M, Terada S, Ito H. Solar Heating and radiative cooling using a solar collector-sky radiator with a spectrally selective surface. *Sol Energy* 1987;39:183–6.
- [61] Hu M, Pei G, Li L, Zheng R, Li J, Ji J. Theoretical and Experimental Study of Spectral Selectivity Surface for Both Solar Heating and Radiative Cooling. *International J Photoenergy* 1–9. doi:<http://dx.doi.org/10.1155/2015/807875>; 2015.
- [62] Hjortsberg A, Granqvist CG. Infrared optical properties of silicon monoxide films. *Appl Opt* 1980;19:1694–6.
- [63] Eriksson TS, Granqvist CG. Infrared optical properties of electron-beam evaporated silicon oxynitride films. *Appl Opt* 1983;22:3204–6.
- [64] Eriksson TS, Lushiku EM, Granqvist CG. Materials for radiative cooling to low temperature. *Sol Energy Mater* 1984;11:149–61.
- [65] Eriksson TS, Jiang S-J, Granqvist CG. Surface coatings for radiative cooling applications: silicon dioxide and silicon nitride made by reactive RF-sputtering. *Sol Energy Mater* 1985;12:319–25.
- [66] Diatezua MD, Thiry PA, Caudano R. Characterization of silicon oxynitride multi-layered systems for passive radiative cooling application. *Vacuum* 1995;46:1121–4. [http://dx.doi.org/10.1016/0042-207X\(95\)00120-4](http://dx.doi.org/10.1016/0042-207X(95)00120-4).
- [67] Tazawa M, Jin P, Tanemura S. Thin film used to obtain a constant temperature lower than the ambient. *Thin Solid Films* 1996;281–282:232–4. [http://dx.doi.org/10.1016/0040-6090\(96\)08620-8](http://dx.doi.org/10.1016/0040-6090(96)08620-8).
- [68] Tazawa M, Jin P, Yoshimura K, Miki T, Tanemura S. New material design with V1-xWxO2 film for sky radiator to obtain temperature stability. *Sol Energy* 1998;64:3–7. [http://dx.doi.org/10.1016/S0038-092X\(98\)00057-7](http://dx.doi.org/10.1016/S0038-092X(98)00057-7).
- [69] Berdahl P. Radiative cooling with MgO and/or LiF layers. *Appl Opt* 1984;23:370. <http://dx.doi.org/10.1364/AO.23.000370>.
- [70] Harrison AW, Walton MR. Radiative cooling of TiO2 white paint. *Sol Energy* 1978;20:185–8.
- [71] Awanou CN. Radiative cooling by a diode roof. *Sol Wind Technol* 1986;3:163–72. [http://dx.doi.org/10.1016/0741-983X\(86\)90030-5](http://dx.doi.org/10.1016/0741-983X(86)90030-5).
- [72] Orel B, Klanjšek Gunde M, Krainer A. Radiative cooling efficiency of white pigmented paints. *Sol Energy* 1993;50:477–82.
- [73] Rephaeli E, Raman A, Fan S. Ultrabroadband photonic structures to achieve high-performance daytime radiative cooling. *Nano Lett* 2013;13(A-E). <http://dx.doi.org/10.1021/nl4004283>.
- [74] Raman AP, Anoma MA, Zhu L, Rephaeli E, Fan S. Passive radiative cooling below ambient air temperature under direct sunlight. *Nature* 2014;515:540–4. <http://dx.doi.org/10.1038/nature13883>.
- [75] Nilsson NA, Eriksson TS, Granqvist CG. Infrared-transparent convection shields for radiative cooling: initial results on corrugated polyethylene foils. *Sol Energy Mater* 1985;12:327–33. [http://dx.doi.org/10.1016/0165-1633\(85\)90002-4](http://dx.doi.org/10.1016/0165-1633(85)90002-4).
- [76] Ali AHH, Saito H, Taha IMS, Kishinami K, Ismail IM. Effect of aging, thickness and color on both the radiative properties of polyethylene films and performance of the nocturnal cooling unit. *Energy Convers Manag* 1998;39:87–93. [http://dx.doi.org/10.1016/S0196-8904\(96\)00174-4](http://dx.doi.org/10.1016/S0196-8904(96)00174-4).
- [77] Gentle AR, Dybdal KI, Smith GB. Polymeric mesh for durable infra-red transparent convection shields: applications in cool roofs and sky cooling. *Sol Energy Mater Sol Cells* 2013;115:79–85. <http://dx.doi.org/10.1016/j.solmat.2013.03.001>.
- [78] Nilsson TMJ, Niklasson GA, Granqvist CG. A solar reflecting material for radiative cooling applications: ZnS pigmented polyethylene. *Sol Energy Mater Sol Cells* 1992;28:175–93. [http://dx.doi.org/10.1016/0927-0248\(92\)90010-M](http://dx.doi.org/10.1016/0927-0248(92)90010-M).
- [79] Nilsson TMJ, Niklasson GA. Radiative cooling during the day: simulations and experiments on pigmented polyethylene cover foils. *Sol Energy Mater Sol Cells* 1995;37:93–118. [http://dx.doi.org/10.1016/0927-0248\(94\)00200-2](http://dx.doi.org/10.1016/0927-0248(94)00200-2).
- [80] Mastai Y, Diamant Y, Aruna ST, Zaban A. TiO2 nanocrystalline pigmented polyethylene foils for radiative cooling applications: synthesis and characterization. *Langmuir* 2001;17:7118–23.
- [81] Engelhard T, Jones ED, Viney I, Mastai Y, Hodes G. Deposition of tellurium * lms

- by decomposition of electrochemically-generated H₂Te: application to radiative cooling devices, 370; 2000. p. 101–105.
- [82] Dobson KD, Hodes G, Mastai Y. Thin semiconductor films for radiative cooling applications. *Sol Energy Mater Sol Cells* 2003;80:283–96. <http://dx.doi.org/10.1016/j.solmat.2003.06.007>.
- [83] Benlattar M, Oualim EM, Harmouchi M, Mouhsen A, Belafhal A. Radiative properties of cadmium telluride thin film as radiative cooling materials. *Opt Commun* 2005;256:10–5. <http://dx.doi.org/10.1016/j.optcom.2005.06.033>.
- [84] Benlattar M, Oualim EM, Mouhib T, Harmouchi M, Mouhsen A, Belafhal A. Thin cadmium sulphide film for radiative cooling application. *Opt Commun* 2006;267:65–8. <http://dx.doi.org/10.1016/j.optcom.2006.06.050>.
- [85] Mouhib T, Mouhsen A, Oualim EM, Harmouchi M, Vigneron JP, Defrance P. Stainless steel/tin/glass coating as spectrally selective material for passive radiative cooling applications. *Opt Mater* 2009;31:673–7. <http://dx.doi.org/10.1016/j.optmat.2008.07.010>.
- [86] Bathgate SN, Bosi SG. A robust convection cover material for selective radiative cooling applications. *Sol Energy Mater Sol Cells* 2011;95:2778–85. <http://dx.doi.org/10.1016/j.solmat.2011.05.027>.
- [87] Hjortsberg A, Granqvist CG. Radiative cooling with selectively emitting ethylene gas. *Appl Phys Lett* 1981;39:507–9. <http://dx.doi.org/10.1063/1.92783>.
- [88] Lushiku EM, Eriksson TS, Hjortsberg A, Granqvist CG. Radiative cooling to low temperatures with selectively infrared-emitting gases. *Sol Wind Technol* 1984;1:115–21. [http://dx.doi.org/10.1016/0741-983X\(84\)90013-4](http://dx.doi.org/10.1016/0741-983X(84)90013-4).
- [89] Lushiku EM, Granqvist CG. Radiative cooling with selectively infrared-emitting gases. *Appl Opt* 1984;23:1835–43. <http://dx.doi.org/10.1364/AO.23.001835>.
- [90] Lushiku EM, Granqvist CG. Radiative cooling with selectively infrared-emitting ammonia gas. *J Appl Phys* 1982;53:5526–30. <http://dx.doi.org/10.1364/AO.23.001835>.
- [91] Du Marchie Van Voorthuysen E, Roes R. Blue sky cooling for parabolic trough plants. *Energy Procedia* 2013;49:71–9. <http://dx.doi.org/10.1016/j.egypro.2014.03.008>.
- [92] Hull JR, Schertz WW. Evacuated-tube directional-radiating cooling system. *Sol Energy* 1985;35:429–34. [http://dx.doi.org/10.1016/0038-092X\(85\)90132-X](http://dx.doi.org/10.1016/0038-092X(85)90132-X).
- [93] Smith GB. Amplified radiative cooling via optimised combinations of aperture geometry and spectral emittance profiles of surfaces and the atmosphere. *Sol Energy Mater Sol Cells* 2009;93:1696–701. <http://dx.doi.org/10.1016/j.solmat.2009.05.015>.
- [94] Johnson TE. Radiation cooling of structures with infrared transparent wind screens. *Sol Energy* 1975;17:173–8. [http://dx.doi.org/10.1016/0038-092X\(75\)90056-0](http://dx.doi.org/10.1016/0038-092X(75)90056-0).
- [95] Landro B, McCormick PG. Effect of surface characteristics and atmospheric conditions on radiative heat loss to a clear sky. *Int J Heat Mass Transf* 1980;23:613–20. [http://dx.doi.org/10.1016/0017-9310\(80\)90004-6](http://dx.doi.org/10.1016/0017-9310(80)90004-6).
- [96] Berdahl P, Martin M, Sakkal F. Thermal performance of radiative cooling panels. *Int J Heat Mass Transf* 1983;26:871–80. [http://dx.doi.org/10.1016/S0017-9310\(83\)80111-2](http://dx.doi.org/10.1016/S0017-9310(83)80111-2).
- [97] Hamza H, Ali A, Taha IMS, Ismail IM. Cooling of water flowing through a night sky radiator. *Sol Energy* 1995;55:235–53. [http://dx.doi.org/10.1016/0038-092X\(95\)00030-U](http://dx.doi.org/10.1016/0038-092X(95)00030-U).
- [98] Al-Nimr M, Kodah Z, Nassar B. A theoretical and experimental investigation of a radiative cooling system. *Sol Energy* 1998;63:367–73. [http://dx.doi.org/10.1016/S0038-092X\(98\)00098-X](http://dx.doi.org/10.1016/S0038-092X(98)00098-X).
- [99] Al-Nimr M, Tahat M, Al-Rashdan M. A night cold storage system enhanced by radiative cooling—a modified Australian cooling system. *Appl Therm Eng* 1999;19:1013–26. [http://dx.doi.org/10.1016/S1359-4311\(98\)00103-3](http://dx.doi.org/10.1016/S1359-4311(98)00103-3).
- [100] Mihalakakou G, Ferrante A, Lewis JO. The cooling potential of a metallic nocturnal radiator. *Energy Build* 1998;28:251–6. [http://dx.doi.org/10.1016/S0378-7788\(98\)00006-1](http://dx.doi.org/10.1016/S0378-7788(98)00006-1).
- [101] Farmahini Farahani M, Heidarinejad G, Delfani S. A two-stage system of nocturnal radiative and indirect evaporative cooling for conditions in Tehran. *Energy Build* 2010;42:2131–8. <http://dx.doi.org/10.1016/j.enbuild.2010.07.003>.
- [102] Heidarinejad G, Farmahini Farahani M, Delfani S. Investigation of a hybrid system of nocturnal radiative cooling and direct evaporative cooling. *Build Environ* 2010;45:1521–8. <http://dx.doi.org/10.1016/j.buildenv.2010.01.003>.
- [103] Farmahini-Farahani M, Heidarinejad G. Increasing effectiveness of evaporative cooling by pre-cooling using nocturnally stored water. *Appl Therm Eng* 2012;38:117–23. <http://dx.doi.org/10.1016/j.applthermaleng.2012.01.023>.
- [104] Zhang S, Niu J. Cooling performance of nocturnal radiative cooling combined with microencapsulated phase change material (MPCM) slurry storage. *Energy Build* 2012;54:122–30. <http://dx.doi.org/10.1016/j.enbuild.2012.07.041>.
- [105] Sima J, Sikula O, Kosutova K, Plasek J. Theoretical evaluation of night sky cooling in the Czech Republic. *Energy Procedia* 2014;48:645–53. <http://dx.doi.org/10.1016/j.egypro.2014.02.075>.
- [106] Erell E, Etzion Y. Analysis and experimental verification of an improved cooling radiator. *Renew Energy* 1999;16:700–3.
- [107] Erell E, Etzion Y. Radiative cooling of buildings with flat-plate solar collectors. *Build Environ* 2000;35:297–305. [http://dx.doi.org/10.1016/S0360-1323\(99\)00019-0](http://dx.doi.org/10.1016/S0360-1323(99)00019-0).
- [108] Bagiorgas HS, Mihalakakou G. Experimental and theoretical investigation of a nocturnal radiator for space cooling. *Renew Energy* 2008;33:1220–7. <http://dx.doi.org/10.1016/j.renene.2007.04.015>.
- [109] Eicker U, Dalibard A. Photovoltaic-thermal collectors for night radiative cooling of buildings. *Sol Energy* 2011;85:1322–35. <http://dx.doi.org/10.1016/j.solener.2011.03.015>.
- [110] Ferrer Tevar JA, Castañó S, Garrido Marijuán A, Heras MR, Pistono J. Modelling and experimental analysis of three radiative panels for night cooling. *Energy Build* 2015;107:37–48. <http://dx.doi.org/10.1016/j.enbuild.2015.07.027>.
- [111] Sameti M, Kasaçian A. Numerical simulation of combined solar passive heating and radiative cooling for a building. *Build Simul* 2015;8:239–53. <http://dx.doi.org/10.1007/s12273-015-0215-x>.
- [112] Man Y, Yang H, Qu Y, Fang Z. A novel nocturnal cooling radiator used for supplemental heat sink of active cooling system. *Procedia Eng* 2015;121:300–8. <http://dx.doi.org/10.1016/j.proeng.2015.08.1072>.
- [113] Hosseinzadeh E, Taherian H. An experimental and analytical study of a radiative cooling system with unglazed flat plate collectors. *Int J Green Energy* 2012;9:766–79. <http://dx.doi.org/10.1080/15435075.2011.641189>.
- [114] Etzion Y, Erell E. Low-cost long-wave radiators for passive cooling of buildings. *Archit Sci Rev* 1999;42:79–85. <http://dx.doi.org/10.1080/00038628.1999.9696856>.
- [115] Duffie JA, Beckman WA. *Solar engineering of thermal processes*. Hoboken, NJ, USA: John Wiley & Sons, Inc; 2013. <http://dx.doi.org/10.1002/9781118671603>.
- [116] Meir MG, Rekstad JB, Løvvik OM. A study of a polymer-based radiative cooling system. *Sol Energy* 2002;73:403–17. [http://dx.doi.org/10.1016/S0038-092X\(03\)00019-7](http://dx.doi.org/10.1016/S0038-092X(03)00019-7).
- [117] Michell D, Biggs KL. Radiation cooling of buildings at night. *Appl Energy* 1979;5:263–75.
- [118] Dan PD, Chinnappa JCV. The cooling of water flowing over an inclined surface exposed to the night sky. *Sol Wind Technol* 1989;6:41–50. [http://dx.doi.org/10.1016/0741-983X\(89\)90036-2](http://dx.doi.org/10.1016/0741-983X(89)90036-2).
- [119] Ezekwe CI. Performance of a heat pipe assisted night sky radiative cooler. *Energy Convers Manag* 1990;30:403–8. [http://dx.doi.org/10.1016/0196-8904\(90\)90041-V](http://dx.doi.org/10.1016/0196-8904(90)90041-V).
- [120] Ito S, Miura N. Studies of radiative cooling systems for storing thermal energy. *J Sol Energy Eng* 1989;111:251–6. <http://dx.doi.org/10.1115/1.3268315>.
- [121] Etzion Y, Erell E. Thermal storage mass in radiative cooling systems. *Build Environ* 1991;26:389–94. [http://dx.doi.org/10.1016/0360-1323\(91\)90065-J](http://dx.doi.org/10.1016/0360-1323(91)90065-J).
- [122] Erell E, Etzion Y. A radiative cooling system using water as a heat exchange medium. *Archit Sci Rev* 1992;35:39–49. <http://dx.doi.org/10.1080/00038628.1992.9696712>.
- [123] Erell E, Etzion Y. Heating experiments with a radiative cooling system. *Build Environ* 1996;31:509–17. [http://dx.doi.org/10.1016/0360-1323\(96\)00030-3](http://dx.doi.org/10.1016/0360-1323(96)00030-3).
- [124] Ahmadi A, Karaei MA, Fallah H. Investigation of night (radiative) cooling event and construction of experimental radiator. *Int J Adv Biotechnol Res* 2016;7:1180–4.
- [125] Yong C, Yiping W, Li Z. Performance analysis on a building-integrated solar heating and cooling panel. *Renew Energy* 2015;74:627–32. <http://dx.doi.org/10.1016/j.renene.2014.08.076>.
- [126] Hu M, Pei G, Wang Q, Li J, Wang Y, Ji J. Field test and preliminary analysis of a combined diurnal solar heating and nocturnal radiative cooling system. *Appl Energy* 2016;179:899–908. <http://dx.doi.org/10.1016/j.apenergy.2016.07.066>.

4.5. Review update

Since the publication of this review (paper 1), radiative cooling literature has been expanding. Other radiative cooling reviews [26–29], as well as several cutting edge scientific papers have been published, requiring an update of the published state of the art review.

A brief update of these new papers is summarised in Chapter 4. Special attention is focused on papers of new materials suitable for radiative cooling under sunlight, in experimental active radiative cooling devices for day-time and active radiative cooling combined with other strategies or technologies.

This bibliography extension is structured similarly to the review paper and, for better comprehension, summarised into two tables, one for newly day-time radiative cooling materials (Table 1) and another for new radiative cooling experimental work and radiative cooling combined with other technologies (Table 2).

4.5.1. Selective day-time radiative cooling

Radiative cooling generation is of more utility during the day-time period rather than night-time because cooling peak demand occurs during the day-time period [30]. Selective materials are essential to achieve radiative cooling under sunlight or maximise cooling performance. For day-time radiative cooling, the required optical properties are to reflect maximum incident solar irradiation (0.3-4 μm) whereas emitting in the infrared atmospheric window (7–14 μm).

New reviewed research is classified into the following groups: Polymer foils on metal surfaces, Multilayer materials and Photonics structures/designs, Single-material surface, Selective screen and convection shield, and Directional selectivity.

4.5.1.1. Polymer foils on metal surfaces

Combinations of a highly reflective metal surface with the addition of polymer foils on top of it have been developed and tested because of its high day-time radiative cooling

performances (low solar spectrum absorption, high emission in the infrared band), low cost, large-scalable and straightforward manufacturing process.

Kou et al. [30] developed a polymer-silica-mirror consisting of fused silica (SiO_2) coated with a polydimethylsiloxane (PDMS) top layer and a silver (Ag) back reflector (PDMS/ SiO_2 /Ag), which experimentally demonstrated to achieve passive radiative cooling under direct sunlight. Zhou et al. [31] developed a material with a similar composition, consisting of a PDMS top layer on Ag with good performances, pointing PDMS as a promising coating material for day-time radiative cooling due to its transmissivity in the visible spectrum and high emissivity in the mid-infrared. Meng et al. [32] proposed polyvinyl fluoride (PVF) as polymer coating because of its better durability, anti-staining performance and corrosion protection than other polymer materials, though achieving good radiative cooling performance under direct sunlight.

In contrast to other polymer coatings, Mandal et al. [33] proposed a simple, scalable, and inexpensive polymer: hierarchically porous poly(vinylidene fluoride-co-hexafluoropropylene) ($\text{P(VdF-HFP)}_{\text{HP}}$) coating, which has paint-like applicability and exhibits good day-time radiative cooling performance. Liu et al. [34] also proposed a cost-effective and simple to manufacture day-time radiative cooling material, using bisphenol A (BPA) epoxy resin as a coating of an Ag layer, which also proved good day-time performances.

4.5.1.2. Multilayer materials and Photonics structures/designs

Concepts recently developed in photonic design, nanomaterials, and manufacturing processes have opened a range of possibilities for day-time radiative cooling, allowing exceptional cooling performance levels.

Zhai et al. [35] demonstrated efficient day-time radiative cooling with a randomised glass-polymer hybrid metamaterial, designed and fabricated by encapsulating randomly distributed silicon dioxide (SiO_2) microspheres in the matrix material of polymethylpentene (PMP or trademark TPX). The metamaterial showed good day-time radiative cooling performances and, with the advantages of using TPX, offering potentially long lifetimes for outdoor use and the possibility of cost-effective, scalable

fabrication. Similarly, Fan et al. [36], developed and tested a double-layer structure foil composed of transparent fluorinated polyimide (FPI) with SiO₂ microspheres embedded, on top of an Ag coating (FPI@SiO₂/Ag), prepared by a simple polymerisation process and easily fabricated in large area foils reducing the cost, which also showed good day-time radiative cooling performances.

Zhao et al. [37] experimentally investigated the day-time radiative cooling performance of a SiO₂ mirror emitter, consisting of deposited SiO₂ on an Ag layer on a thin SiO₂ substrate, showing that good performance is possible, but also detecting the strong influence of different climate conditions on the performance.

The wide range of possibilities offered by photonic design leads to the development of materials not only capable of day-time radiative cooling but with aesthetics and functional purposes. Lee et al. [38] present a coloured passive radiative cooler with potential for day-time cooling, displaying primary colours to exhibit the desired appearance.

Based on the suggestion made by Kou et al. [30], that the polymer-silica-mirror (PDMS/SiO₂/Ag) emitter could improve its cooling performance by reducing solar absorption in the ultraviolet region, Zhu et al. [39] experimentally demonstrated this improvement with a multilayer structure (PDMS/TiO₂/MgF₂/SiO₂/Ag).

Ao et al. [40] proposed two different surfaces to achieve day-time radiative cooling: ultra-white glass-plated Ag, and the zinc phosphate sodium (NaZnPO₄) particles on aluminium (Al) substrate. Both materials showed effective day-time radiative cooling under certain conditions being both of low cost.

Jeong et al. [41] developed an optimised multi-layered photonic material for day-time radiative cooling, based on four TiO₂-SiO₂ layers on Ag, estimating promising results. The authors claim a cost drop when compared to other materials and manufacturing processes.

Huang et al. [42] proposed single nanoporous MgHPO₄·1.2H₂O powder as day-time radiative cooling material due to its good optical properties. This simple and low-cost material demonstrated good performances.

Some authors explored the multi-dimensional photonics topic. Jeong et al. [43] present a bio-inspired material with a prismatic structure of PDMS, on SiO₂ and Ag layers, with good day-time radiative cooling performances, though with solar shading.

4.5.1.3. Single-material surface

Li et al. [44] proposed and tested aluminium phosphate (AlPO₄) as day-time radiative cooling material/coating, with promising day-time performances in the form of tridymite-type AlPO₄ (T-APO).

Yang et al. [45] proposed a day-time radiative cooling material consisting of a layer of lithium fluoride (LiF) crystal on silver (Ag), demonstrating good day-time performance due to the good selective emission of LiF (almost perfectly matching the atmospheric window).

Li et al. [46] developed a multifunctional passive radiative cooling material composed of wood presenting good day-time radiative cooling performance and good structural properties. This material is also manufacture-scalable, thus promoting the practical application of radiative cooling into buildings.

4.5.1.4. Selective screen and convection shield

Other materials and functionalities presented in the literature reflect solar irradiation selectively, such as Torgerson & Hellhake [47] proposed: a material that blocks almost all solar irradiation while letting infrared thermal radiation pass through. This material allows different possibilities in the day-time radiative cooling topic with a scalable and low-cost material.

On the other hand, Zimming et al. [48] proposed a selective screen that lets visible light pass through while emitting thermal radiation. This application has several appliances (for instance: PV cells, glass roof, and vehicles), but for day-time active radiative cooling, it must be backed by a solar reflector, in this research a silver-plated Al sheet bladed, with good performance according to the authors.

4.5.1.5. Directional selectivity

Directional selectivity is a strategy of high importance because of its high generation potential, even the difficulty in achieving feasible applications. In that way, Bhatia et al. [49] proposed an approach to benefit from angular confinement of solar irradiation to achieve day-time radiative cooling almost regardless of the reflectivity of the material in the solar wavelength range. This technique achieved good performance, proving that solar radiation input suppression is an important issue, allowing the use of low-cost materials without excellent optical properties.

4.5.2. Theoretical approach and numerical simulation

Theoretical models are essential to evaluate a device/solution in different scenarios. The combination of radiative cooling with other technologies is of great interest, even in theoretical modelling. Hu et al. [50] modelled a trifunctional system with radiative cooling, photovoltaic and photo-thermal (PV-PT-RC). The model was based on an experimental prototype already presented in [51] and validated with real data.

4.5.3. Radiative cooling prototypes

Active radiative cooling systems use a heat transfer fluid to carry the cold produced to a thermal system where it is stored and consumed when needed. In contrast, passive radiative cooling systems directly cool an object surface and are of more simplicity. Active radiative cooling is more efficient than passive because cold produced is managed [52].

This reason turns the development of quasi-real day-time active radiative cooling devices into a research trend. This radiative cooling development of active devices is not only using new metamaterials that demonstrated its effectiveness in the lab, but also with commercially available materials. Goldstein et al. [53] developed and tested a radiative cooling device using an available commercial material as the emitting surface to prove this promising technology. The authors tuned the water flow in the test to see its effect on temperature drop and cooling power.

Zhao et al. [52] and Aili et al. [54] used a metamaterial called RadiCold [35] in quasi-real devices, similar to a thermal collector, to analyse the day-time active radiative cooling performance of this material under real conditions, showing good performance, as summarized in Table 2. Yuan et al. [55] used the metamaterial RadiCold on top of a box with enclosed water to experimentally investigate day-time passive radiative cooling with results proving day-time cooling.

4.5.4. Radiative cooling combination

Radiative cooling can be effectively achieved during night-time with the absence of solar irradiation that mismatches solar thermal collectors/photovoltaic operation time. It is of great interest to combine radiative cooling with these technologies, making the device more profitable.

Hu et al. [56] developed and tested a prototype for night-time radiative cooling and solar thermal collection using black acrylic paint as panel coating, presenting good performances.

Chen et al. [57] tested a prototype, developed by Chen et al. [58], to demonstrate simultaneous heating and cooling harvesting. This device singularity lies in the ability of the solar absorber, placed above the radiative cooler, to be transparent to mid-infrared radiation. This proof-of-principle experiment demonstrates simultaneous generation with potential for large scale deployment. However, the prototype needs a practical thermal management system to conduct generation in the device to any external appliance.

Zhao et al. [59] developed and tested a prototype of hybrid day-time photovoltaic (PV) generation and night-time radiative cooling (RC). The performance of the PV-RC hybrid system was evaluated and proved the suitability of the combination. Additionally, the measured data was used to validate a thermal model for parametric study. Later on, Hu et al. [60] developed and tested a prototype of a hybrid double-covered day-time photo-thermal (PT) collector and night-time radiative cooling (RC) module, showing good combined performance. The device used a double cover, a windscreen, and glazing to enhance PT, whereas glazing acted as an emitter for the RC module. Finally, Hu et al. [50,51] developed a hybrid photovoltaic-photothermic-radiative cooling (PV-PT-RC) collector, which tested outdoors proved good performance for all three technologies.

Liu et al. [61] developed and tested a device coupling radiative cooling and solar thermal collection as passive technologies to control indoor temperature. The device used the two faces for such combination, one for RC and the other for SC. The model demonstrated the ability to work in both modes. According to the authors, it was then modelled and integrated into a building to evaluate its potential as passive and active technology with good results.

Additionally, other options are to combine radiative cooling with other cooling technologies, such as heat pumps, to improve its performance. Goldstein et al. [53], after developing and testing a radiative cooling prototype, modelled the radiative cooling device to be integrated into a heat pump system used as a cold source, showing potential for significant energy savings.

Table 1 - Detailed characteristics of newly developed materials for day-time radiative cooling (since 2017)

Reference/Year	Materials	Infrared emittance	Solar reflectance	Cooling potential/performance
1 Kou et al. (2017) [30]	Polymer-coated fused silica mirror: polydimethylsiloxane (PDMS), fused silica and 120 nm silver.	100 μm (8–13 μm)	> 0.95	Maximum temperature reduction of 8.2 °C under direct sunlight. Average net cooling power around 127 W/m ² .
2 Zhai et al. (2017) [35]	Randomised glass-polymer hybrid metamaterial: 50 μm thick polymethylpentene (TPX) containing 6% of SiO ₂ microspheres by volume, backed with a 200 nm thick silver coating.	> 0.93 (8–13 μm)	~ 0.96	Peak cooling power of about 93 W/m ² under direct solar irradiation of 900 W/m ² at noontime, with an average cooling power of >110 W/m ² .
3 Bhatia et al. (2018) [49]	Copper emitter coated with white/black spray paint	~ 0.9	~ 0.8	Minimum temperature of 6 °C below ambient temperature and maximum cooling power of 45 W/m ² .
4 Mandal et al. (2018) [33]	Hierarchically porous poly(vinylidene fluoride-co-hexafluoropropene) [P(VdF-HFP)] _{HP} . Optimal composition: ~50% porosity and thickness \geq 300 nm	0.97 \pm 0.02	0.96 \pm 0.03	Subambient temperature reduction of 6°C under 890 W/m ² sunlight and cooling powers of 96 W/m ² under 750 W/m ² sunlight.
5 Lee et al. (2018) [38]	Coloured passive radiative cooler (CPRC) based on a thin-film optical resonator: 650 nm SiO ₂ , 910 nm Si ₃ N ₄ , 100 nm Ag on a Si substrate.	> 0.9	~ 0.9	Average temperature of 3.9 °C below ambient air temperature.
6 Ao et al. (2019) [40]	A specular surface consisting of 3mm thick ultra-white glass placed on top of 200nm thick silver (Ag)	0.9	0.94	2.5 °C below ambient temperature under 420 W/m ² solar irradiation.
6' Ao et al. (2019) [40]	A diffuse surface composed of aluminium (Al) substrate sprayed by zinc phosphate sodium (NaZnPO4) particles	0.7	0.93	1.5 °C below ambient temperature under 420 W/m ² solar irradiation.
7 Li et al. (2019) [44]	Tridymite-type AlPO ₄ (TAPO)	0.9 (8–13 μm)	0.97	Temperature drop of ~4.2 °C under solar irradiation.
8 Li et al. (2019) [46]	Radiative cooling structural material: "Cooling wood": composed of cellulose nanofibers partially aligned in tree's growth direction.	> 0.9 (8–13 μm)	0.96	Radiative cooling power of 16 W/m ² and temperature drop > 4°C at midday
9 Zhu et al. (2019) [39]	Multilayer emitter (five layers, from top to bottom): a 100 μm thick PDMS film on top, a 36 nm thick TiO ₂ , a 200 nm thick MgF ₂ , a 500 μm thick silica, and a 120 nm thick Ag film on the back.	> 0.95	> 0.95	Average temperature reduction of about 12.6 °C under solar irradiation.
10 Zhou et al. (2019) [31]	Planar polydimethylsiloxane(PDMS)-coated metal structure: 100 μm PDMS on aluminium.	~0.95 (8–13 μm)	> 0.9	Temperature reductions of 11°C with an average cooling power of ~120 W/m ² .
11 Fan et al. (2019) [36]	Double-layer foil composed of: a top layer with the fluorinated polyimide SiO ₂ microspheres (FPI@SiO ₂) and a 200 nm thick Ag layer on the rear side.	0.94 \pm 0.03 (8–13 μm)	0.93 \pm 0.02	4.6°C temperature reduction under direct solar irradiation.
12 Zhao et al. (2019) [37]	The SiO ₂ mirror emitter consists of a 500- μm -thick SiO ₂ film on top of a 150-nm-thick Ag film, deposited on top of a 50-nm-thick SiO ₂ film	0.79 (8–13 μm)	0.96	5.9 °C below ambient temperature under solar irradiation.

Reference/Year	Materials	Infrared emittance	Solar reflectance	Cooling potential/performance
13 Huang et al. (2020) [42]	Single nanoporous MgHPO ₄ ·1.2H ₂ O on ceramic tile	0.94 (8–13 μm)	0.92	Temperature drop of 4.1 °C below the ambient, average cooling power reaches 78 W/m ² .
14 Jeong et al. (2020) [41]	Photonic multi-layered radiative: four alternating 500 nm TiO ₂ - 500 nm SiO ₂ sub-layers on the top of the 200 nm silver (Ag) coated silicon wafer.	0.84 (8–13 μm)	0.94	Net cooling power of 14.3 W/m ² and temperature reduction of 7.2 °C under solar irradiation.
15 Jeong et al. (2020) [43]	Ultra emissive bio-inspired polymeric surface: A 8 μm top layer of polydimethylsiloxane (PDMS) triangular array, a 525 μm layer of silicon dioxide (SiO ₂) and a 160nm layer of silver (Ag) layer.	0.98 (8–13 μm)	0.95	Net cooling power of 19.7 W/m ² and temperature reduction of 6.2 °C under solar irradiation.
16 Liu et al. (2020) [34]	Clear epoxy resin: a 50 μm thick bisphenol A epoxy resin coating on a 300 nm thick Ag layer.	0.92	0.93	An average temperature drop of about 2.75 °C in the day-time.
17 Meng et al. (2020) [32]	A bilayer film consisting of polyvinyl fluoride (PVF) 200-μm-thick layer and Ag 200-nm-thick coating.	> 0.9	~0.9	2 °C below the ambient temperature under solar irradiation of 950 W/m ² .
18 Torgerson and Hellhake (2020) [47]	Polymer film STATIC (Spectrally Tuned All-Polymer Technology for Inducing Cooling): 250-μm	~0.75 (trans.)	~0.9	Cooling power of 110 W/m ² .
19 Yang et al. (2020) [45]	Lithium fluoride (LiF) on silver (Ag): 1-mm-thick lithium fluoride crystal coated with 200 nm silver backing.	>0.95	> 0.95	Temperature drop of 5 °C below ambient and a net cooling power of 60 W/m ² under horizontal solar irradiation > 900 W/m ² .
20 Zimming et al. (2020) [48]	Blade-coating with resonant polar dielectric SiO ₂ microparticles randomly mixed into an acrylic resin backed silver-plated aluminium sheet bladed with a 70 μm coating.	0.94 (8–13 μm)	0.91 (trans.)	Maximum sub-ambient decrease in temperature of ~8.7 °C and a maximum cooling power of 108 W/m ² .

Table 2 - Radiative cooling experimental appliances and combination of technologies (since 2017)

Reference/Location/Year	System	Strategy	Material	Combination potential
1 Goldstein et al. (2017) [53]	Non-evaporative fluid cooling panel	Active radiative cooling	Visibly-reflective extruded copolymer mirror (3M Vikiuti ESR film) [79]	Panels cool water up to 5 °C below ambient air temperature with power up to 70 W/m ²
2 Zhao et al. (2019) [59]	Hybrid photovoltaic and night-time radiative cooling	PV + active nocturnal radiative cooling	Tedlar-Polyester-Tedlar (TPT) layer	Daily average electricity output of 94W/m ² . Cooling power of 54W/m ² when inlet water temperature equal to ambient temperature, and 73 W/m ² when the panel temperature equals to ambient.
3 Hu et al. (2018) [51] & Hu et al. (2020) [50]	Photovoltaic-photothermic-radiative cooling (PV-PT-RC) collector	PVT + active nocturnal radiative cooling	Windscreen: 6 µm-thick polyethylene film. Multilayer collecting panel: transparent tedlar-polyester-tedlar (TPT) + monocrySTALLINE silicon solar cell + 0.3 mm-thick layer of black TPT + 0.4 mm-thick aluminum plate	Average electrical efficiency up to 10.3%, average thermal efficiency 55.3%. RC reached 72 W/m ² .
4 Hu et al. (2019) [56]	Hybrid photo-thermal and radiative cooling collector	Solar collection + active nocturnal radiative cooling	Black acrylic paint	Radiative cooling power of 55 W/m ² in a clear night. The hybrid system collected 8.6 MJ daily heat in 8 h, and 1 MJ of cooling energy in 11.5 h
5 Zhao et al. (2019) [52] & Aili et al. (2019) [54]	Radiative cooled-cold collection (RadiCold) module.	Active radiative cooling	Randomised glass-polymer metamaterial [35]	Water cooling temperature drop of 5-7 °C. An average net cooling power of around 80 W/m ² .
6 Chen et al. (2019) [57]	A solar absorber placed above a radiative cooler	Passive solar thermal collection + Passive radiative cooling	70-nm-thick silicon nitride (Si ₃ N ₄) layer, 700-nm-thick amorphous silicon (Si) layer, and a 150-nm-thick aluminium (Ag) layer from top to bottom, with a silicon (Si) wafer underneath for mechanical support. [58]	The solar absorber is heated to 24 °C above ambient temperature and the radiative cooler 29 °C below ambient temperature
7 Hu et al. (2020) [60]	Double-covered hybrid photo-thermal and radiative sky cooling module	Solar thermal collection + Active nocturnal radiative cooling	Double cover (6 µm LDPE + 2.8 mm ultra-white glass) + 0.4 mm aluminum plate	Day-time stagnation temperature of 159.8°C and night-time minimum temperature 11°C below ambient
8 Yuan et al. (2020) [55]	Radiative water plate	Passive radiative cooling	Randomised glass-polymer metamaterial-based radiative cooling film [35]	Water temperature between 2-14°C below ambient air temperature and radiative cooling power of 15 - 100 W/m ² during day-time.
9 Liu et al. (2020) [61]	Temperature-regulating module (TRM)	Passive solar thermal collection + Passive radiative cooling	Windshield: 10 µm polyethylene film Emitter: 300 µm porous cooling material [33], 3 mm aluminium conductor and 500 µm solar absorbing material (chromium plating)	Cooling mode: maximum indoor temperature of 27.5 °C. Heating mode: maximum indoor temperature of 25 °C without heat supply.

Chapter 5. Energy Savings Potential of a Novel Radiative Cooling and Solar Thermal Collection Concept in Buildings for Various World Climates

5.1. Introduction

Radiative cooling uses the sky as a heat sink by taking advantage of its lower-than-ambient effective temperature, thus becoming an option to supply buildings cooling demands in hot and dry regions [62]. However, radiative cooling has lower production rates than other renewable technologies such as solar thermal or photovoltaic [25,63]. Therefore, although radiative cooling consumes small amounts of energy compared to other technologies, such as compression heat pumps, it needs new strategies or improvements to become feasible and more appealing for widespread deployment, as confirmed in the reviewed literature in Chapter 4.

A possible technology to combine with radiative cooling is solar thermal collection. These two technologies are operationally compatible because, in general, radiative cooling takes place during night-time and solar thermal collection during day-time, and both technologies present a similar flat-plate design. However, radiative cooling is the antagonist to solar thermal collection because they work with different radiation wavelengths, so they are generally not designed to work together. Chapter 4 presents a more detailed analysis of the differences and similitudes between these two technologies.

Even though the necessity of technical improvements, this combination presents significant benefits, such as generating two energy products in a single device, the reduction of non-renewable energy consumption, and the achievement of a more cost-effective device.

Additionally, from the reviewed literature in Chapter 4, the authors noticed the lack of research on radiative cooling harvesting potential and the need for a world climate analysis to determine which climates or regions the implementation is of real interest.

Chapter 5 aims to demonstrate that radiative cooling technology has the potential to be coupled with solar thermal collection and cover part of the space cooling and DHW demands of different buildings in different climates. First, paper 2 introduces the novel concept, the combination of radiative cooling technology with solar thermal collection, and its characteristics. Then, paper 2 presents the study and results of the potential energy savings of this combination based on the energy coverage between energy generation and energy demand for different locations, climates, and building typologies.

5.2. Contribution to the state-of-the-art

Paper 2 introduces a novel concept named Radiative Cooler and Emitter (RCE), which combines radiative cooling and solar thermal collection in the same device, with two operational modes for cold and heat production (see Figure 7).

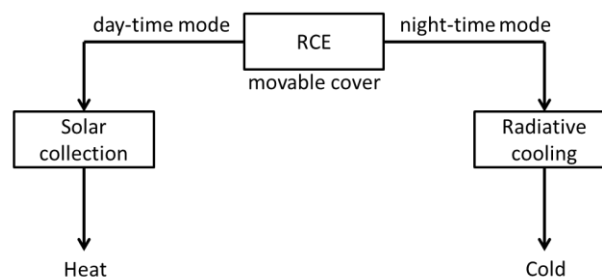


Figure 7 - RCE operational diagram

This novel concept, the RCE, is conceived to take the full potential of both technologies and operational modes, thus requiring the understanding of the present radiations: solar radiation (0.3-4 μm) and thermal radiation (4-50 μm), and how these different radiations affect the device performance.

The idea of achieving full potential for both operation modes leads to the distinguishing feature of RCE against other researches: the use of an adaptable (movable or exchangeable) cover (Figure 8). Paper 2 describes this feature and presents a possible specific application/solution (Figure 9).

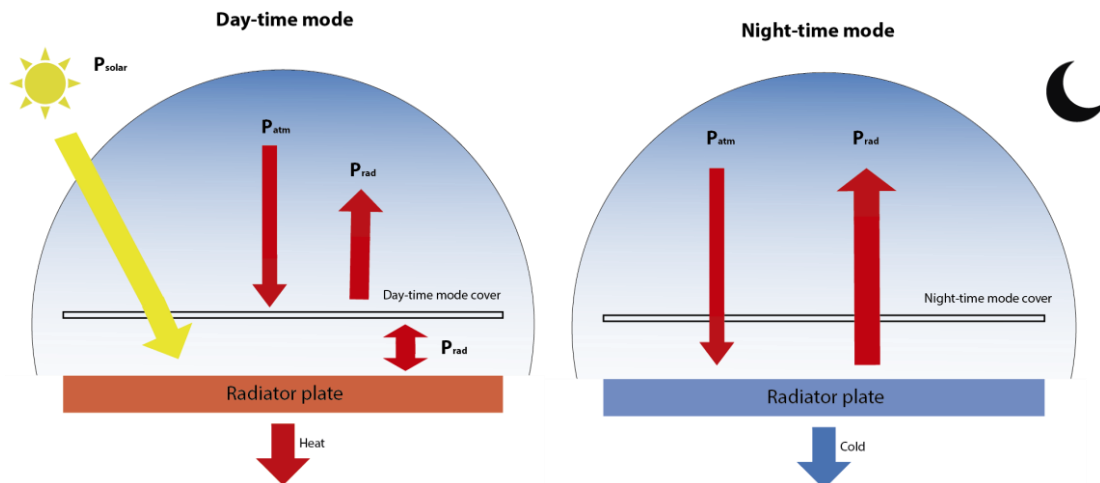


Figure 8 – Conceptual radiation diagram flow for RCE day-time and night-time operation modes.

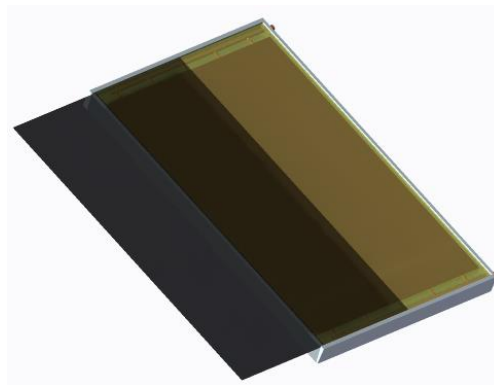


Figure 9 - RCE device 3D representation

Paper 2 presents the analysis of the potential implementation of RCE based on the energy coverage of space cooling and DHW demands of different building typologies under different climatic conditions.

The energy production of the RCE is calculated for each mode separately, with some standard assumptions presented in paper 2. Day-time or solar thermal collection mode uses global horizontal irradiance values and a performance ratio to calculate the energy production in this operational mode. Night-time or radiative cooling mode uses the radiation balance between the RCE surface and the sky. The RCE emitted radiation is calculated considering a surface temperature of 20°C, and the incoming infrared radiation is calculated using different empirical correlations [64–67] depending on the climate and taking into account clear/cloudy sky conditions from weather datasets.

The energy demand was calculated for different building typologies, provided by the USA Department of Energy (two residential buildings: single-family detached house and multi-

family low-rise apartment building; and two commercial buildings: medium office and small hotel), and different climates (sixteen representative cities of most Köppen-Geiger classification climates) by using specific software: EnergyPlus™.

The analysis compares the energy demands of space cooling and DHW with the energy production of RCE for the scenarios mentioned above, for monthly basis. The research detected suitability of RCE in several cities. According to the analysis, climates with warm summers and cool/cold winters are preferred for RCE implementation with appropriate coverage ratios of space cooling higher than 25% and DHW higher than 75%.

According to the results, climates with unbalanced demands, either with too high heating demand or too high cooling demand, are not suitable for RCE. In those climates, mainly one technology (solar thermal collection or radiative cooling) is required, with limited RCE implantation. Therefore, an appropriate ratio between cooling and DHW demand helps to take full potential of RCE. In particular, buildings with constant heat demands, such as DHW in residential buildings and hotels, and low cooling demands, such as residential buildings in climates with warm summers, are spotted to be more appropriate because they present a better energy demand balance for RCE.

The results in paper 2 outlined the potential of RCE implementation in some climates and building typologies. However, the authors proposed further research in developing a more detailed numerical model of RCE to improve the accuracy of the calculations. The authors also highlighted the necessity of experimental testing to analyse RCE technology under real operation conditions.

This paper fills a gap in the literature with little research presenting the potential of radiative cooling technology and none for the combination of radiative cooling with solar thermal collection.

Paper 2 will help to take a step forward on the development of this technology by spotting for which locations or climatological conditions and for which building applications the use of RCE is suitable and profitable in terms of energy savings.

5.3. Contribution to the objectives of the PhD thesis

Chapter 5 contributes to accomplishing objective III by presenting, in paper 2, the worldwide implementation study and results of potential energy savings of RCE. This study based its results on the coverage ratio between RCE energy production and energy demands for different buildings typologies and climates.

This chapter also contributed somehow to the later accomplishment of objective IV, by generating a simple numerical model of RCE to simulate its performance under different climatological conditions. However, with this initial model, it was not possible to study RCE general behaviour under external conditions. This model was not meant to study the device parameters (such as material properties, dimensional properties, operating properties).

5.4. Journal Paper

Reference:

S. Vall, A. Castell, and M. Medrano, “Energy Savings Potential of a Novel Radiative Cooling and Solar Thermal Collection Concept in Buildings for Various World Climates,” *Energy Technology*, vol. 6, no. 11, pp. 2200–2209, 2018. DOI:10.1002/ente.201800164.

Energy Savings Potential of a Novel Radiative Cooling and Solar Thermal Collection Concept in Buildings for Various World Climates

Sergi Vall, Albert Castell,* and Marc Medrano^[a]

A novel radiative cooling and solar collection concept is presented, and the combination of these two technologies and its energy integration in residential and commercial buildings is evaluated. This innovative concept, herein named Radiative Collector and Emitter (RCE), allows for supplying both cooling and Domestic Hot Water (DHW) demands. First, the RCE concept is introduced by presenting its background, with special attention to the overlapping and switching between radiative cooling and solar thermal collection. Then the DHW

and cooling demands for four building typologies, two residential and two commercial, are compared with the energy production of the RCE. The analysis is performed for representative cities of the world climates according to Köppen-Geiger classification. The RCE concept showed suitability in some of the studied cities (San Francisco, Cape Town, Johannesburg, London, and Ottawa) with C (temperate) and D (continental) climates in residential and tertiary buildings.

Introduction

Nowadays, the effect of fossil fuels on climate change has reached scientific consensus. New policies are focused on energy efficiency and on renewable sources to reduce the energy dependency on fossil fuels. In this sense, the building sector is one of the strategic sectors to achieve these new objectives. Residential and commercial buildings represent nearly 40% of total energy consumption in the European Union (EU-28)^[1] (residential buildings 24.9% and commercial buildings 13.6%^[2]). For instance, in the residential buildings energy budget, space conditioning of buildings represents 65% of it while Domestic Hot Water (DHW) 13.8%^[2].

For space conditioning purposes, active and passive strategies can be applied to reduce energy consumption. Despite these strategies, energy consumption cannot be usually reduced to zero if thermal comfort conditions are to be preserved.^[3] It is at this point when renewable sources should emerge to cover these energy needs.

When talking about heating and DHW, solar thermal collectors are well known as an effective system to meet these heat demands.^[4] However, for cooling there is still no simple renewable alternative with such potential and development as solar thermal collection is for heat demands. Two possibilities for cooling are compression heat pumps and absorption heat pumps. On the one hand, compression heat pumps are a non-renewable technology that needs substantial amounts of electricity, although according to some legislations they can be considered as renewable.^[5,6] On the other hand, absorption heat pumps may use solar energy as driving heat, but they are not available for residential applications, have low overall efficiencies, require high operation temperatures, and need large cooling towers.^[7] Moreover, their coupling with suitable solar heat sources is not well researched.

It is at that point where radiative cooling gains strength in providing cooling. This technology uses the sky as a heat sink taking advantage of its effective temperature lower than ambient. Thus, it may be a good option to supply the cooling demands of houses in hot and dry regions.^[8] Lot of research has been conducted in the study of the radiative cooling phenomenon^[9,10] and, more recently, in the development of radiative cooling experimental prototypes and numerical/theoretical models. A comprehensive review of radiative cooling is presented in.^[11] The research conducted in^[12,13] used unglazed solar collectors to test the radiative cooling achievable with a simple modification, showing the capability of cooling production. Recently, the research evolved into the development and testing of more sophisticated materials^[14,15] allowing the radiative cooling effect even under sunlight conditions, and achieving lower temperatures. Though, some other research has been conducted in the development and validation of a robust numerical model with experimental data.^[16] However, despite the efforts done in this field, the few studied systems have not yet reached the market due to its low available cooling rates (between 20–80 W/m²,^[17] with peak values of 120 W/m²^[18]). Therefore, new concepts and improvements are required for radiative cooling to become feasible.

Radiative cooling phenomenon is antagonist to solar thermal collection, mainly due to the different radiation wavelength used (longwave radiation for radiative cooling and shortwave radiation for solar thermal collection) and because solar thermal collection takes place during sunlight

[a] S. Vall, Dr. A. Castell, Prof. Dr. M. Medrano
Department of Computer Science and Industrial Engineering
University of Lleida
Edifici CREA, Pere de Cabrera s/n, 25001 Lleida, Spain
E-mail: acastell@diei.udl.cat

Energy Technology

FULL PAPER

hours while radiative cooling mainly when there is no sunlight. A more detailed analysis of the differences between these two technologies is presented in.^[11]

Since both technologies can be conceived in analogous devices, it comes to mind to combine these technologies to provide heat and cold using a single device. However, these two technologies are not generally prepared to work together when they are designed to work autonomously;^[19] therefore some adjustments have to be done for this purpose.

The combination of solar collection and radiative cooling in a single device would be a qualitative leap forward to renewable suitability for meeting different energy demands. The use of both technologies may substantially reduce the non-renewable primary energy consumption for space conditioning and domestic hot water. Moreover, the extra cooling savings for about the same economic investment will make the investment more cost-effective. This new concept that combines solar thermal collection and radiative cooling in a single device is based on radiation heat transfer, since it collects radiation (solar) from the Sun as a heat source, and emits radiation (thermal) to the sky to provide cooling. Therefore, this concept will be mentioned from here on as Radiative Collector and Emitter (RCE).

Up to now, little research has been conducted in this topic. First attempts were focused in testing a device designed to perform one function (radiative cooling or solar collection) and see if the same device could also perform the other function. This research either used unglazed solar thermal collectors and observed radiative and convective cooling during the night^[12,20] or alternatively observed the production of heating during day by a radiative cooling device.^[21] However, these systems were not designed to perform both functions and, thus, presented such low efficiencies that did not justify its usefulness. More recently, it was developed and tested a suitable material to be used for radiative cooling and solar heating.^[9] Once the material was proved, it was built a prototype to be tested in real conditions, showing good performances.^[22] However, these studies were limited to certain specific conditions, did not assess the potential of combining such technologies under different climatic conditions, and did not consider the heating and cooling demands.

Several energy and economic studies on the potential of a particular energy technology for the integration in different building types and various climates have been published recently. These technologies include solar absorption cooling,^[23] fuel cell micro-CHP^[24] and building-integrated photovoltaics^[25] as well as Smart-grid operation.^[26–27] These studies show the interest of this type of methodologies and allow framing the present work, which is contributing with the above mentioned novel RCE technology to this type of building integration potential studies.

The purpose of this article is to introduce the RCE concept, which comprises two technologies: radiative cooling and solar collection, as well as to investigate and determine the RCE potential to cover cooling and DHW energy demands in residential and commercial buildings in different

climates. For different climates, different building typologies were evaluated to determine the most suitable application. This worldwide climate suitability study has never been performed neither for radiative cooling nor for the novel RCE concept.

The RCE Concept

The RCE concept presented in this paper is conceived as a device capable of producing heat and cold for any existing demand, in the present case for space conditioning and DHW demands. This concept produces heat and cold in the same manner as two separated devices would do. Similar devices already tested in the literature were designed to produce either heat or cold and, without any modification of the original device, the other service was studied.^[11,20,21] The RCE concept is conceived since the beginning to produce both. This commitment entails the use of some strategies in the design of it to allow the generation of such different energy products.

The RCE device was conceived to have a similar architecture to a flat plate solar thermal collector, namely, it has an absorber/emitter surface and a cover on top of it. Additionally to that, it was also conceived to be capable of working in two modes: solar collection mode and radiative cooling mode (Figure 1a), producing both heat and cold. To be able to operate under these different modes, the RCE incorporates a movable cover (Figure 1b). This cover is composed of two different sections (one for each operation mode) made of different materials. The main drawback of this system is the movable element in the cover that did not exist before, therefore presenting a potential increase in maintenance needs.

The section of the cover used for the solar collection mode lets solar radiation pass through and blocks mid and far infrared radiation. On the contrary, the section used for radiative cooling lets thermal radiation pass through. The two different sections of the cover are exchanged for each operation mode via a sliding cover system. The absorber/emitter surface is assumed to have blackbody properties. These considerations were taken into account when evaluating the energy production of the RCE device.

The operation and control of the two sections of the cover should be done considering both the presence of solar radiation and the time of the day. When there is solar radiation the device is operated in the solar collection mode; on the other hand, when there is no solar radiation and the time is between dusk and dawn the device is operated in the radiative cooling mode.

The RCE device needs to be connected with the HVAC and DHW installation (cold and hot tanks) of the building, providing such systems with heat and cold. In terms of HVAC, any distribution system can be used to deliver the cold to the different spaces to condition. Thus, systems such as radiant ceilings that require lower temperature differences between the circulating water and the ambient set-point can

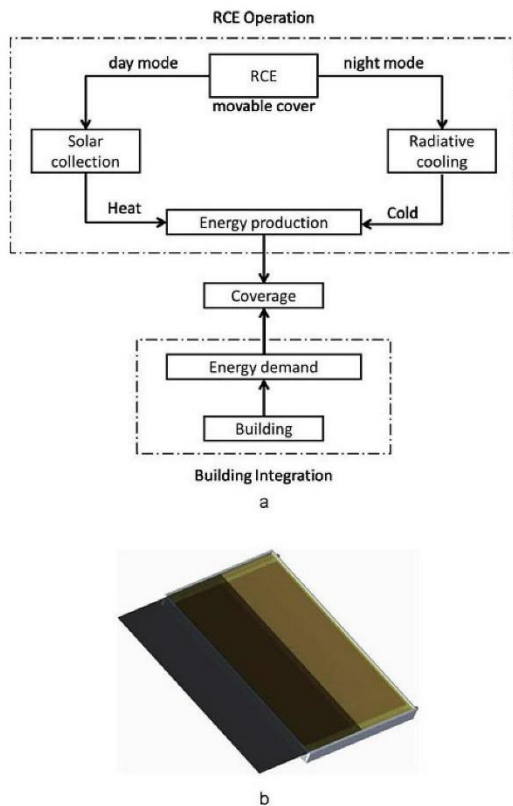


Figure 1. a) Block diagram for Radiative Collector and Emitter concept and its building integration. b) 3D representation of a Radiative Collector and Emitter device.

be used. These systems could provide better thermal comfort [28–29] but also need additional systems to cope with the latent heat. The distribution system is not the goal of this research and it is therefore not considered in the analysis.

Methods

To evaluate the coverage of the cooling and DHW demands by the RCE under different climatic conditions, the energy production of the RCE and the energy demand of the different building typologies were determined as shown in this section (Figure 1a).

Energy Production

The RCE total energy production was calculated for each mode separately (Figure 1a) having each mode its own calculations and procedures. However, some considerations are made for both modes.

A steady-state model is developed to determine the energy production potential under different climates, thus helping to identify and highlight most interesting applications and world climates for such new technology.

Conductive and convective losses are assumed to be negligible in the RCE device, since the RCE is considered to incorporate strong thermal insulation and an evacuated space between the absorber/emitter surface and the cover.

The tilt angle, which is a relevant parameter for the RCE, is selected to achieve the best results under radiative cooling operation, because this is the technology with lower production rate. Since the best tilt angle for radiative cooling is horizontal,^[30] the RCE is considered to have an inclination angle of 0°. This may result in a decrease of the solar collection efficiency since the angle is not optimum for solar collection.

The optical properties of the different covers used are (Table 1): for the solar collection mode perfect transmission

	Transmissivity in the solar spectrum	Transmissivity in the thermal spectrum
Solar collection mode	1	0
Radiative cooling mode	1	1

in the solar spectrum and blocking of thermal radiation (similar to glass), for the radiative cooling mode perfect transmission in the whole spectrum (similar to low-density polyethylene). These optical properties are not the exact ones of real materials (for instance glass or polyethylene). However, the aim of this paper is to assess the potential of such technology, therefore the assumption of such values is considered to be valid.

Solar Thermal Collector Mode

For solar collection the RCE energy production potential was evaluated considering the Global Horizontal Irradiance (GHI) and a system performance ratio (Eq. 1). The system performance ratio is a common methodology used in other research^[31] and takes into account in a single parameter all the inefficiencies of the system (solar collector efficiency, losses due to inclination and shadows, etc.). Based on previous works,^[31] a similar performance ratio of 0.6 was used for the solar collection calculations.

$$P_{\text{solar,net}} [\text{W}/\text{m}^2] = \text{GHI} \cdot \eta_{\text{sc}} \quad (1)$$

The energy production was monthly evaluated to be compared to the DHW demands (Eq. 2).

$$E_{\text{solar,month}} [\text{Wh}/(\text{m}^2 \cdot \text{month})] = \sum_{\text{month}} (P_{\text{solar,net}} \cdot \Delta t) \quad (2)$$

Energy Technology

FULL PAPER

Radiative Cooling Mode

Radiative cooling potential has not been widely studied^[32] and there are no world potential maps available. Therefore, some assumptions were considered to standardize the results and to present its potential in a similar way as solar thermal collection.

Apart from the assumptions already presented for the RCE concept, the absorber/emitter surface temperature also needs to be considered. The surface is assumed to be at a constant temperature of 20°C for the periods where cooling is required. This absorber average surface temperature along the night is considered a good trade-off between an acceptable upper limit for achieving internal fluid temperatures low enough to be used in HVAC systems, and a reasonable lower limit for good radiative cooling performances.

Given these assumptions, the radiation balance between the sky and the radiator is presented in Eq. 3. The monthly energy production was determined considering only the time when there is no solar radiation (Eq. 4). The clear sky emissivity was calculated using empirical correlations (Eq. 5, Eq. 6, Eq. 7) bearing in mind the climate for which they were proposed^[33–35] (Table 3). The opaque fraction of the sky was also considered to evaluate the effective sky emissivity. In that sense, Eq. 8 was used to modify the clear sky emissivity based on empirical correlations^[36] and data from EnergyPlus weather data.

$$P_{\text{radiator,net}} [\text{W}/\text{m}^2] = \varepsilon_{\text{radiator}} \cdot \sigma \cdot (T_{\text{radiator}})^4 - \varepsilon_{\text{sky}} \cdot \sigma \cdot (T_{\text{ambient}})^4 \quad (3)$$

$$E_{\text{radiator,month}} [\text{Wh}/(\text{m}^2 \cdot \text{month})] = \sum_{\text{month}} (P_{\text{radiator,net}} \cdot \Delta t) \quad (4)$$

Empirical correlations for clear sky emissivity:

$$\varepsilon_{\text{sky},0} = 0.711 + 0.56 \cdot (T_{\text{dp}}/100) + 0.73 \cdot (T_{\text{dp}}/100)^2 \quad (5)$$

$$\varepsilon_{\text{sky},0} = 0.741 + 0.0062 \cdot T_{\text{dp}} \quad (6)$$

$$\varepsilon_{\text{sky},0} = 0.754 + 0.0044 \cdot T_{\text{dp}} \quad (7)$$

Effective sky emissivity:

$$\varepsilon_{\text{sky}} = \text{clf} + (1-\text{clf}) \cdot \varepsilon_{\text{sky},0} \quad (8)$$

Energy Demands

The DHW and cooling demands of the different buildings considered were determined by numerical simulation using EnergyPlus for the same locations where the energy production was calculated. To standardize the results, four typologies of standard buildings were chosen. These buildings were taken from the USA Department of Energy (DOE), which provides a set of prototype building models to be used in EnergyPlus. These models are either based on the International Energy Conservation Code (IECC) for residential buildings^[37] or the ASHRAE Standard 90.1 for commercial buildings.^[38]

For the present work 2 residential and 2 commercial buildings were chosen to represent a large share of the existing building stock. These 4 buildings are: a single-family (SF) detached house with crawlspace (Figure 2a), a multi-family (MF) low-rise apartment building with crawlspace (Figure 2b), a medium office (Figure 2c), and a small hotel (Figure 2d). The main geometric parameters describing the selected building typologies are presented in Table 2.

Table 2. Geometric parameters of the different buildings analysed and additional passive and active strategies.

	SF building	MF building	Office	Hotel
Wall area (m ²)	221.2	876.2	1978.0	1694.2
Window area (m ²)	33.2	246.9	652.6	184.2
Window-Wall Ratio [%]	15%	28%	33%	11%
Net Conditioned Area (m ²)	223.1	2007.4	4982.2	4013.6
Roof Area (m ²)	116.4	784.9	1660.5	1003.4
Additional passive and active strategies				
Cooling set point temperature (°C)	25	25	25/27 (schedule)	25
Summer night ventilation	20–8 h	20–8 h	–	–
Natural ventilation through occupants controlled windows	–	–	7–22 h	–
Solar protection (Overhangs)	Included	Included	–	–

These standard buildings are fully defined in terms of envelope, schedules, internal loads, DHW consumption, etc.^[37,39] Nevertheless, some additional active and passive strategies not considered by the original models were included to make the models closer to the real behavior and also more efficient (set point temperature schedules, summer night ventilation, overhangs, etc. see Table 2).

For each climate, some of the building characteristics of the standardized models, such as the overall heat transfer coefficient (U-factor) of the building envelope elements (roofs, walls, floors, doors, windows), and the solar heat gain coefficient (SHGC) of the non-opaque envelope elements (windows), change according to the previously mentioned codes (IECC/ASHRAE Standard 90.1). As these codes are ASHRAE standards, the building models are also referred to ASHRAE climate zones. However, in this paper a worldwide climate analysis using the Köppen-Geiger climate classification^[39] is performed, since it is a more general and known climate classification. For this purpose, the model used for a particular climate of the Köppen-Geiger classification was chosen according to its similarity to the ASHRAE climate zone (Table 3).

In the present paper 16 representative cities were studied covering most of the climates of Köppen-Geiger climate classification (Table 3). For some climates two cities were selected since the differences between them were sufficiently significant to consider more than one city. Climates that do not require cooling demands were not considered in this study, since the technology under study aims at providing both DHW and cooling. Once the climates and the building

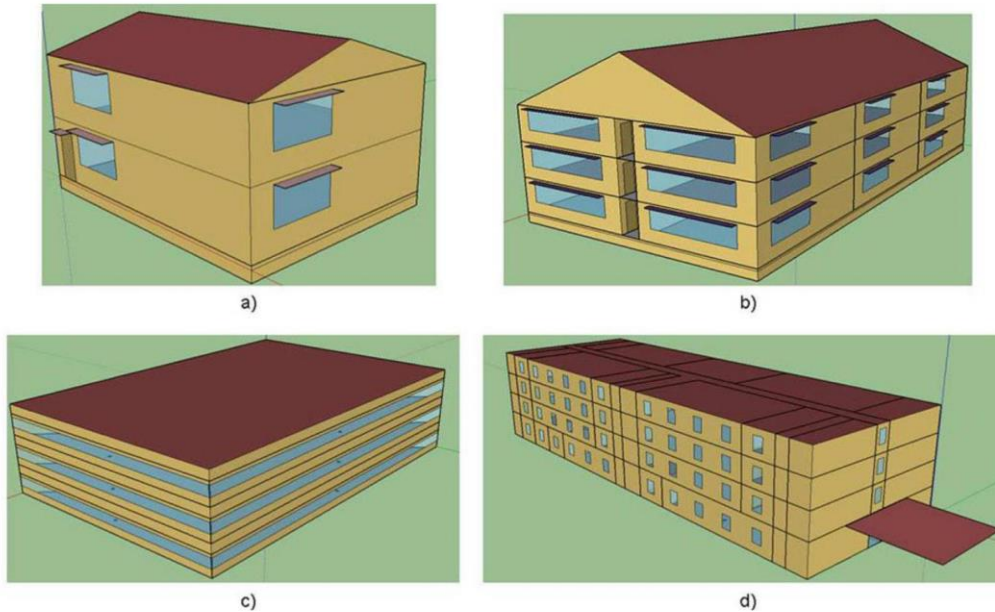


Figure 2. Analysed buildings: a) Single-family detached house; b) Multi-family low-rise apartment building; c) Medium office; d) Small hotel.

Table 3. Representative cities, sky emissivity correlation used and equivalences between Köppen-Geiger classification, USA climate and IECC.

Representative Cities	Sky emissivity correlation		Köppen-Geiger classification ^[a]	ASHRAE climate zone	IECC climate zone model used
	Clear	Cloudy			
Singapore, Caracas	Eq. 5	Eq. 8	Af/Am ^[b] /Aw	1A	1
Riyadh	Eq. 7		BWh/BSH ^[b]	1B/2B	2
Denver, Tehran	Eq. 7		BWk ^[b] /BSk	3B/4B/5B	3
Rome, Perth, San Francisco, Cape Town	Eq. 5		Csa/Csb	2A/3C	2
Brisbane, Tokyo, Johannesburg	Eq. 5		Cfa/Cwa ^[b] /Cwb	2A/3A/4A	3
London	Eq. 5		Cwc ^[c] /Cfb/Cfc ^[c]	4C/5C	5
Pyongyang, Chicago	Eq. 6		Dsa ^[b] /Dwa/Dfa	5A	5
Ottawa	Eq. 6		Dsb ^[b] /Dwb ^[b] /Dfb	6A/6B/7A/7B	6
-	-		Dsc ^[c] /Dsd ^[c] /Dwc ^[c] Dwd ^[c] /Dfc ^[c] /Dfd ^[c] ET ^[c] /EF ^[c]	7A/7B/8	7

[a] Köppen-Geiger climate classification.^[9] [b] Climate not considered or climatic data from a representative city not found. [c] Climate not considered, cold climate or without cooling requirements.

15 min, only monthly demands were considered for coverage purposes.

Coverage Calculations

Once the demand and the production were calculated, the percentage of coverage was also evaluated. The coverage is an important parameter since it can represent the suitability of this technology for a particular combination of climate and building typology. In other words, it means how well the energy production from the new RCE concept can match the energy demands of the building in that specific climate. In any case, the production of renewable heating and cooling with the RCE can contribute to significant energy and money savings, even if its contribution to the total building HVAC demand is small.

The energy coverage was determined as the minimum between the monthly energy demand and the monthly energy production. The heat and cold produced is only used to cover the DHW and the cooling demands. When there is an excess of energy production it is not used.

Since for different cities both the energy demand and production change the coverage for a fixed surface of RCE changes as well. Therefore, a parametric analysis of the DHW coverage was performed to show how changing the surface affects the coverage of the energy requirements.

models were chosen, the energy demands were calculated. Although the time step for the building simulations was of

Energy Technology

FULL PAPER

Results and Discussion

Simulations to calculate the energy demand (DHW and cooling) of different building typologies and the energy production of RCE were performed in 16 cities. The aim of these simulations was to evaluate the RCE suitability in each city and, consequently, each climate. The results to assess that suitability are presented and discussed in this section.

The annual results of all cities for every building typology are shown in Figure 3. This figure includes the energy demand, the energy production and the percentage of coverage per square meter of conditioned surface considering an installed RCE surface of: 5 m² for the single-family house, 30 m² for the multi-family house, 20 m² for the office and 100 m² for the hotel. These surfaces were chosen according to the DHW demand, trying to cover a significant part of it, and also considering that there was enough room on the roof of these buildings (the percentage of covered roof was in the range of 2–6 %).

In Figure 3 it is observed that with an installed surface of 5 m² much of the DHW energy demand of a single-family house can be covered in most of the cities. Also, cooling demands are partially covered. The multi-family building is behaving similarly to the single-family house. In contrast, the office seems to be the most different building typology when evaluating its demands. Its cooling demands are much higher than the DHW ones. This is mainly due to the higher internal loads and the higher requirements of air ventilation in the office. Moreover, the DHW demand of the office is low, and can be covered with 20 m² of RCE. Finally, the hotel typology has a higher DHW demand than the office. This high DHW demand requires a large amount of RCE installed surface (100 m²) to have reasonable coverage, leading to higher cooling coverage than the office. On the other hand, the cooling energy demand is also higher than in the office since the use of natural ventilation in this building typology is not considered.

Analyzing the different building typologies, one can see that for residential buildings the cities with low cooling demands match better with the new RCE concept. Other cities require a lot more RCE installed surface to cover a significant part of the cooling demand.

The office is the less suitable building typology due to its high cooling demand combined with low DHW demand. This scenario requires using the RCE mainly in radiative cooling operation mode, and thus not taking benefit of its use in solar thermal collector operation mode.

Finally, the hotel is an intermediate case between residential buildings and the office because of its high DHW demand. However, for the warmest cities it may be better using the RCE mainly in the radiative cooling operation mode and reducing its use as solar thermal collection to avoid excess heat.

A parametric analysis of the DHW coverage was performed to observe how the different energy coverages change with the installed surface. For the sake of clarity just 3 cities (Ottawa, Cape Town and Tehran) are shown, accord-

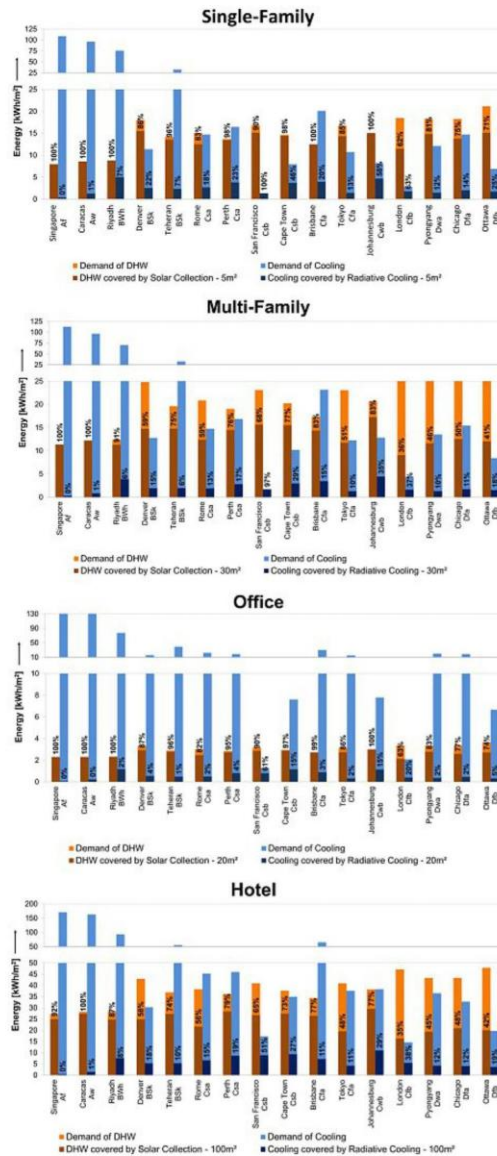


Figure 3. Annual energy demand, production and percentage of coverage for 16 cities and per square meter of conditioned surface considering an installed surface of Radiative Collector and Emitter of: 5 m² for the single-family house; 30 m² for the multi-family house; 20 m² for the office; 100 m² for the hotel.

ing to different weather conditions (cold, mild and warm) (Figure 4).

A constant relation between DHW coverage and installed surface is observed in Figure 4. There is a turning point beyond which the required surface increases drastically. Therefore, the optimal coverage is close to this point which is located approximately between 50–75 % of DHW coverage.

Energy Technology

FULL PAPER

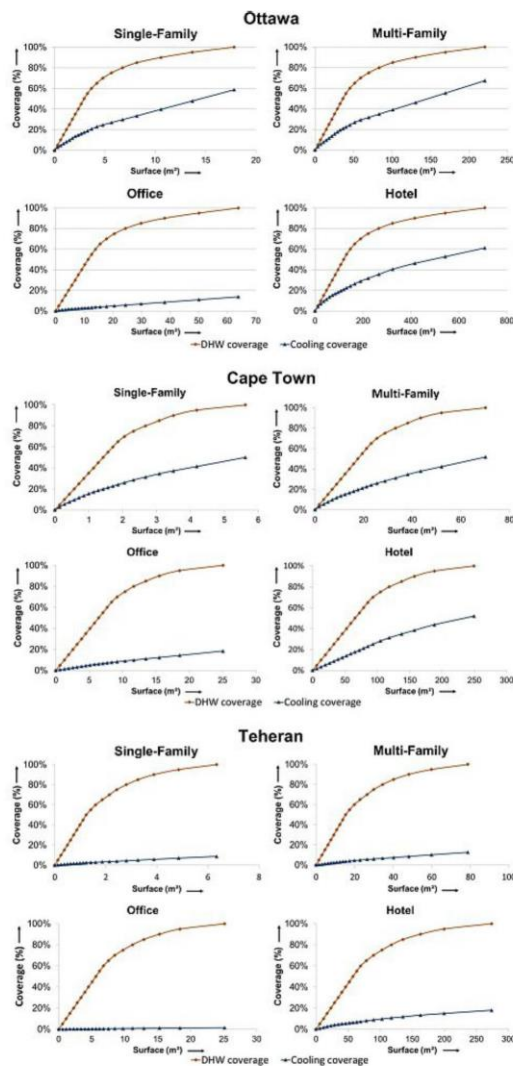


Figure 4. Parametric analysis of Domestic Hot Water and cooling coverage against installed Radiative Collector and Emitter surface for building typology in Ottawa (top), Cap Town (middle) and Teheran (bottom).

This optimal point agrees with some policies of minimum solar coverage of DHW demand in some countries.^[40] Based on this result, the cooling energy savings when an installed surface of RCE covers at least the 75% of DHW demand are presented for all 16 initial studied cities. An indivisible RCE unit of 2 m² of surface is considered. A world map for each building typology with the cooling savings is shown in Figure 5 with the corresponding data presented in Table 4.

From the results shown in Figure 4 and 5 and presented in Table 4, it is observed that there exists a significant potential for RCE technology to cover the DHW and cooling demands.

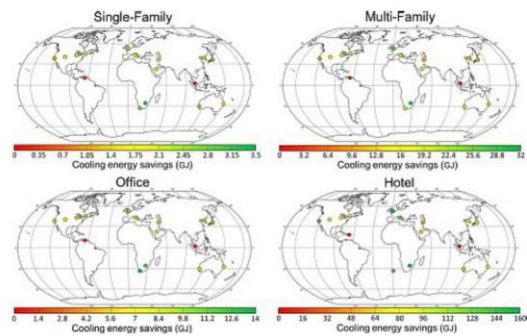


Figure 5. Cooling savings for an installed Radiative Collector and Emitter surface to cover a minimum of 75% of Domestic Hot Water demand for the studied locations (based on Radiative Collector and Emitter units of 2 m² of surface).

Therefore, to determine the cities and building typologies with higher potential for RCE implementation, a common criteria was defined (Table 5). The present study aimed at getting the maximum benefit of the RCE concept, thus using it both as solar thermal collector and radiative cooling. Therefore, a minimum DHW coverage of 75% and a minimum cooling coverage of 25% were defined as common criteria. Other climates or cities may also be suitable for RCE implementation although they may get benefits mainly from either solar thermal collection or radiative cooling, but not both.

Table 5 presents the different cities meeting the criteria, as well as the climate zone where they belong. The results evidence a significant difference between residential and commercial buildings, especially the office which is the most different building typology. Residential buildings show more suitability due to the more balanced demand between heat and cold. Hotel typology presents a similar behavior to residential buildings. On the other hand, office buildings show suitability in relatively cold climates, where cooling demands are low.

The cities presenting most potential in terms of demand coverage are presented in Table 5. Although the extrapolation from cities to climates is not direct, the cities located in climates presented in Table 5 may present a higher potential in terms of demand coverage than the other ones. However, other locations may also present important absolute energy savings with low demand coverages. As an example, the results from Cape Town and San Francisco can better explain the debate. A single-family house in San Francisco presents high cooling demand coverage (100%), whereas in Cape Town it presents a lower coverage (32%). However, Cape Town produces much more cooling energy savings (2.57 GJ vs 1.07 GJ) when both have the same RCE installed surfaces.

Energy Technology

FULL PAPER

Table 4. Domestic Hot Water /Cooling coverage and savings for an installed Radiative Collector and Emitter surface covering a minimum of 75 % of Domestic Hot Water demand for the studied locations (based on Radiative Collector and Emitter units of 2 m² of surface).

	Single-Family Surface (m ²)	DHW savings (GJ) and coverage (%)	Cooling savings (GJ) and coverage (%)	Multi-Family Surface (m ²)	DHW savings (GJ) and coverage (%)	Cooling savings (GJ) and coverage (%)	Office Surface (m ²)	DHW savings (GJ) and coverage (%)	Cooling savings (GJ) and coverage (%)	Hotel Surface (m ²)	DHW savings (GJ) and coverage (%)	Cooling savings (GJ) and coverage (%)
Singapore	2	6.36 100%	0.12 0%	18	64.99 79%	1.11 0%	10	36.24 88%	0.62 0%	82	296.04 75%	5.06 0%
Caracas	2	6.86 99%	0.41 1%	16	68.21 77%	3.30 0%	8	34.24 83%	1.65 0%	72	306.96 75%	14.84 1%
Riyadh	2	5.91 84%	1.91 3%	20	68.06 76%	17.84 4%	8	33.34 80%	8.78 1%	74	309.62 75%	81.12 6%
Denver	4	11.40 79%	1.65 18%	46	135.98 76%	19.78 21%	14	40.52 75%	6.96 2%	150	467.28 75%	96.73 22%
Teheran	4	10.32 91%	1.55 6%	30	106.56 75%	14.60 6%	10	39.48 76%	4.74 1%	104	401.93 76%	79.28 10%
Rome	4	9.18 76%	1.74 15%	50	114.55 76%	22.13 21%	16	40.52 75%	6.96 2%	168	415.86 75%	132.82 20%
Perth	4	10.17 92%	2.49 19%	30	104.52 76%	20.12 17%	12	40.83 80%	8.83 3%	94	395.66 76%	117.22 18%
San Francisco	4	11.40 84%	1.07 100%	38	126.97 76%	12.30 100%	14	45.15 79%	10.08 44%	128	445.23 75%	148.20 60%
Cape Town	4	11.03 88%	2.57 32%	30	112.21 77%	21.37 29%	12	42.91 81%	13.76 10%	106	409.68 75%	143.82 29%
Brisbane	2	7.55 75%	1.51 9%	26	97.06 77%	21.92 13%	10	37.77 77%	8.81 2%	96	372.13 75%	99.85 11%
Tokyo	4	12.78 95%	1.54 18%	48	125.98 76%	13.87 16%	16	43.54 76%	4.69 2%	164	445.57 75%	80.47 15%
Johannesburg	4	11.60 96%	2.43 37%	28	118.65 79%	30.45 33%	10	42.41 79%	12.12 9%	98	417.82 76%	156.04 28%
London	10	11.81 80%	1.94 88%	106	137.94 75%	26.55 84%	34	45.74 76%	10.63 28%	350	510.95 75%	157.65 75%
Pyongyang	6	13.19 90%	1.60 16%	54	138.45 76%	14.25 15%	18	47.60 79%	6.02 2%	174	472.06 75%	87.63 17%
Chicago	6	12.27 84%	1.99 17%	62	137.14 75%	21.43 19%	20	46.30 77%	8.28 2%	198	468.97 75%	97.90 21%
Ottawa	6	13.53 80%	1.53 28%	70	157.30 75%	19.35 32%	22	50.31 77%	6.23 5%	222	519.11 75%	90.27 32%

Table 5. Criteria values and suitable cities and climates.

	Single-Family	Multi-Family	Office	Hotel
Min. Cooling coverage	25 %			
Min. DHW coverage	75 %			
Cities accomplishing criteria values	San Francisco, Cape Town, Johannesburg, London, Ottawa	San Francisco, Cape Town, Johannesburg, London, Ottawa	San Francisco, London	San Francisco, Cape Town, Johannesburg, London, Ottawa
Climates of suitable cities (Köppen-Geiger classification)	Csb, Cwb, Cfb, Dfb	Csb, Cwb, Cfb, Dfb	Csb, Cfb	Csb, Cwb, Cfb, Dfb

Conclusions

In the present work the building integration potential of a new concept, the Radiative Collector and Emitter (RCE), was presented. To determine the heat and cold production a simplified model was used.

The results showed that in several cities located in different Köppen-Geiger climate classification regions the use of the RCE concept in residential and commercial buildings is suitable, and the building demand will take advantage from the combined capacity of the RCE to produce both heat and

cold. For the Single-Family, Multi-Family, and Hotel building typologies, a minimum coverage of 25 % of cooling and 75 % of DHW is achieved in five of the studied cities (San Francisco, Cape Town, Johannesburg, London, and Ottawa), representing four climate zones (Csb, Cwb, Cfb, Dfb). On the other hand, the Office building typology achieves these levels of coverage in only two of the studied cities (San Francisco and London), representing two climate zones (Csb, Cfb).

Other studied cities showed less benefit from the use of RCE, since either heat or cold were the major demand. The conditions were not suitable to make use of the combined

capacity to produce heat and cold because mainly one demand was required.

Therefore, to take full advantage of the RCE concept, an appropriate ratio between cooling and DHW demand is required. This ratio depends on the climate but also on the building typology. Some climates are not adequate because they are either too hot or too cold to meet both requirements. Therefore, only one technology (radiative cooling for hot climates or solar thermal collection for cold climates) is mainly required, being the other less needed or unnecessary. Regarding building typologies, those with a constant demand of heat during the whole year, such as DHW, make RCE more suitable, since both heat and cold production can be used.

The potential presented in this paper outlined a first approach to determine in which combinations of climates and building typologies this novel RCE concept may be implemented. However, further research should be done in the development of a more detailed numerical model of the RCE concept. This model could then be used for economic viability studies in certain locations.

Nomenclature

clf	Opaque fraction of the sky [–]
$E_{\text{radiator,month}}$	Monthly radiative cooling energy $\left[\frac{\text{Wh}}{\text{m}^2 \cdot \text{month}}\right]$
$E_{\text{solar,month}}$	Monthly solar thermal collection energy $\left[\frac{\text{Wh}}{\text{m}^2 \cdot \text{month}}\right]$
GHI	Hourly average global horizontal irradiation $\left[\frac{\text{W}}{\text{m}^2}\right]$
$P_{\text{solar,net}}$	Hourly average solar radiation power $\left[\frac{\text{W}}{\text{m}^2}\right]$
$P_{\text{radiator,net}}$	Hourly average radiative cooling power $\left[\frac{\text{W}}{\text{m}^2}\right]$
T_{ambient}	Ambient temperature [°C]
T_{radiator}	Temperature of the radiator surface [°C]
T_{dp}	Dew point temperature [°C].
Δt	Time step [h]
$\epsilon_{\text{radiator}}$	Emissivity of the radiator (ideally $\epsilon_{\text{radiator}} = 1$) [–]
ϵ_{sky}	Effective sky emissivity [–]
$\epsilon_{\text{sky},0}$	Sky emissivity under clear sky conditions [–]
η_{sc}	solar collector performance ratio [–]
σ	Stefan-Boltzmann constant $\left[\frac{\text{W}}{\text{m}^2 \cdot \text{K}^4}\right]$

Acknowledgements

Sergi Vall would like to thank the Secretaria d'Universitats i Recerca del Departament d'Economia i Coneixement de la Generalitat de Catalunya for his research fellowship. The authors would like to thank Generalitat de Catalunya for the project grant given to their research group (2017 SGR 659).

Conflict of interest

The authors declare no conflict of interest.

Keywords: Radiative cooling · Solar thermal collection · Renewable energy · Low grade energy source · Building integration

- [1] European Parliament. Directive 2010/31/EU of the European Parliament and of the Council of 19 May 2010 on the energy performance of buildings. *Off J Eur Union* **2010**, *153*, 13–35.
- [2] ODYSSEE-MURE project. ODYSSEE and MURE database 2014. www.odyssee-mure.eu (accessed March 15, 2017).
- [3] L. Yang, H. Yan, J. C. Lam, *Appl. Energy* **2014**, *115*, 164–173.
- [4] A. Gautam, S. Chamoli, A. Kumar, S. Singh, *Renewable Sustainable Energy Rev.* **2017**, *68*, 541–562.
- [5] European Parliament. Directive 2009/28/EC of the European Parliament and of the Council of 23 April 2009 on the promotion of the use of energy from renewable sources and amending and subsequently repealing Directives 2001/77/EC and 2003/30/EC. *Off J Eur Union* **2009**, *140*, 16–62.
- [6] European Commission. Decision of 1 March 2013 (2013/114/EU) establishing the guidelines for Member States on calculating renewable energy from heat pumps from different heat pump technologies pursuant to Article 5 of Directive 2009/28/EC of the European Parliament and of the Council. *Off J Eur Union* **2013**, *62*, 27–35.
- [7] H. Z. Hassan, A. A. Mohamad, *Renewable Sustainable Energy Rev.* **2012**, *16*, 5331–5348.
- [8] D. Michell, K. L. Biggs, *Appl. Energy* **1979**, *5*, 263–275.
- [9] R. W. Bliss, *Sol. Energy* **1961**, *5*, 103–120.
- [10] B. Bartoli, S. Catalanotti, B. Coluzzi, V. Cuomo, V. Silvestrini, G. Troise, *Appl. Energy* **1977**, *3*, 267–286.
- [11] S. Vall, A. Castell, *Renewable Sustainable Energy Rev.* **2017**, *77*, 1–18.
- [12] E. Erell, Y. Etzion, *Building Environ.* **2000**, *35*, 297–305.
- [13] E. Hosseinzadeh, H. Taherian, *Int. J. Green Energy* **2012**, *9*, 766–779.
- [14] A. P. Raman, M. A. Anoma, L. Zhu, E. Rephaeli, S. Fan, *Nature* **2014**, *515*, 540–544.
- [15] Z. Chen, L. Zhu, A. Raman, S. Fan, *Nat. Commun.* **2016**, *7*, 1–5.
- [16] J. A. Ferrer Tevar, S. Castaño, A. Garrido Marijuán, M. R. Heras, J. Pistono, *Energy* **2015**, *107*, 37–48.
- [17] R. Cavalius, C. Isaksson, E. Perednis, G. E. F. Read, Passive cooling technologies. Austrian Energy Agency, **2005**.
- [18] U. Eicker, A. Dalibard, *Sol. Energy* **2011**, *85*, 1322–1335.
- [19] M. Hu, G. Pei, L. Li, R. Zheng, J. Li, J. Ji, *Int. J. Photoenergy* **2015**, *2015*, 1–9.
- [20] M. Matsuta, S. Terada, H. Ito, *Sol. Energy* **1987**, *39*, 183–186.
- [21] E. Erell, Y. Etzion, *Building Environ.* **1996**, *31*, 509–517.
- [22] M. Hu, G. Pei, Q. Wang, J. Li, Y. Wang, J. Ji, *Appl. Energy* **2016**, *179*, 899–908.
- [23] T. Mateus, A. C. Oliveira, *Appl. Energy* **2009**, *86*, 949–957.
- [24] A. Adam, E. S. Fraga, D. J. L. Brett, *Appl. Energy* **2015**, *138*, 685–694.
- [25] R. Rüther, P. Braun, *Sol. Energy* **2009**, *83*, 1923–1931.
- [26] P. Kohlhepp, V. Hagenmeyer, *Energy Technol.* **2017**, *5*, 1084–1104.
- [27] S. Weitemeyer, D. Kleinhans, L. Wienholt, T. Vogt, C. Agert, *Energy Technol.* **2016**, *4*, 114–122.
- [28] J. Miriel, L. Serres, A. Trombe, *Appl. Therm. Eng.* **2002**, *22*, 1861–1873.
- [29] S. Oxizidis, A. M. Papadopoulos, *Energy* **2013**, *57*, 199–209.
- [30] M. Martin, P. Berdahl, *Sol. Energy* **1984**, *33*, 241–252.
- [31] E. Zambolin, D. Del Col, *Sol. Energy* **2010**, *84*, 1382–1396.
- [32] J. L. Molina, E. Erell, S. Yannas, *Roof Cooling Techniques: A Design Handbook*. London: Routledge; **2005**.
- [33] P. Berdahl, M. Martin, *Sol. Energy* **1984**, *32*, 663–664.
- [34] P. Berdahl, R. Fromberg, *Sol. Energy* **1982**, *29*, 299–314.
- [35] R. Tang, Y. Etzion, I. A. Meir, *Energy Convers. Manage.* **2004**, *45*, 1831–1843.
- [36] T. M. Crawford, C. E. Duchon, *J. Appl. Meteorol.* **1999**, *38*, 474–480.

Energy Technology

FULL PAPER

- [37] U.S. Department of Energy. Residential Prototype Building Models n.d. https://www.energycodes.gov/development/residential/iecc_models (accessed October 24, 2016).
- [38] U.S. Department of Energy. Commercial Prototype Building Models n.d. https://www.energycodes.gov/development/commercial/90.1_models (accessed October 24, 2016).
- [39] M. C. Peel, B. L. Finlayson, T. A. McMahon, *Meteorol. Z.* **2006**, *15*, 259–263.
- [40] European Solar Thermal Industry Federation (ESTIF). English translation of the solar thermal sections of the Spanish Technical Building Code (Royal Decree 314/2006 of 17 March 2006) n.d. http://www.estif.org/fileadmin/estif/content/policies/downloads/CTE_solar_thermal_sections_ENGLISH.pdf (accessed October 31, 2016).
- Manuscript received: February 28, 2018
Revised manuscript received: May 7, 2018
Version of record online: September 4, 2018
-

Chapter 6. A new flat-plate radiative cooling and solar collector numerical model: Evaluation and metamodeling

6.1. Introduction

The combination of radiative cooling with solar thermal collection in a single device is a possible solution to increase the profitability and widespread implementation of radiative cooling thanks to producing both heat and cold thermal energy.

Chapter 5 presented the RCE, a novel concept that combines radiative cooling and solar thermal collection in a single device, having an adaptable cover as the differentiating and unique feature. This feature allows for different material usage with different optical properties, thus allowing differentiated operational periods (day-night).

Also, Chapter 5 presented promising results of RCE potential implementation for some weathers and buildings typologies. However, it also pointed out the requirement for more accurate calculations or modelling to reaffirm these results.

So, there is a necessity in developing a detailed numerical model to simulate RCE energy production. According to the literature reviewed in Chapter 4, the new model should include specific details to emulate incoming infrared radiation physical phenomenon honestly (real spectrum) and improvements by using a cover and fluid as internal thermal-carrier.

There is no numerical model in the literature capable of simulating both radiative cooling and solar thermal collection, with accurate incoming infrared radiation simulation/calculation, and with adaptable cover capability.

Chapter 6 presents the numerical modelling of a Radiative Collector and Emitter, with several improvements or new features, compared to the reviewed numerical models, and

its validation with experimental data. Once the model was validated, a sensitivity analysis was performed to determine the most influencing parameters to the radiative cooling production. There is no sensitivity analysis for radiative cooling parameters in the literature and, even no sensitivity analysis was found for solar thermal collection, there is extensive experimental research focused on analysing its most influencing parameters [68–71].

Chapter 6 aims to develop a helpful tool for evaluating RCE performance under any climatological circumstance (weather, season) and operational use.

6.2. Contribution to the state-of-the-art

The paper presents an experimentally validated numerical model capable of representing the behaviour of an RCE device under any environmental circumstance. It also presents a sensitivity analysis to determine the most influencing radiative cooling parameters.

Before this paper, no numerical model combining radiative cooling and solar thermal collection existed in the literature. There exist some numerical models for solar thermal collection that integrate radiative cooling phenomenon (presented as “radiative losses”) on the thermal balance. However, these integrations were not conceived for cold generation but to estimate heat losses during operation (day-time). Moreover, these models use simple empirical correlations to estimate the radiative cooling effect instead of real data as in the present research.

The numerical model discretises a flat plate collector: its components (radiator plate, back insulation, air gap, cover, water) and the environment (ambient air, Sun, sky), into some nodes. The model uses 1D relations based on electrical analogy for simplified modelling (resistance-capacitance modelling) and radiation balance (Figure 10). Convection heat transfer coefficients are calculated with empirical Nusselt correlations and conduction heat transfer coefficient with specific FEM software: COMSOL Multiphysics®. The use of 1D modelling against 2D or 3D was based on the ease of implementation and greater flexibility.

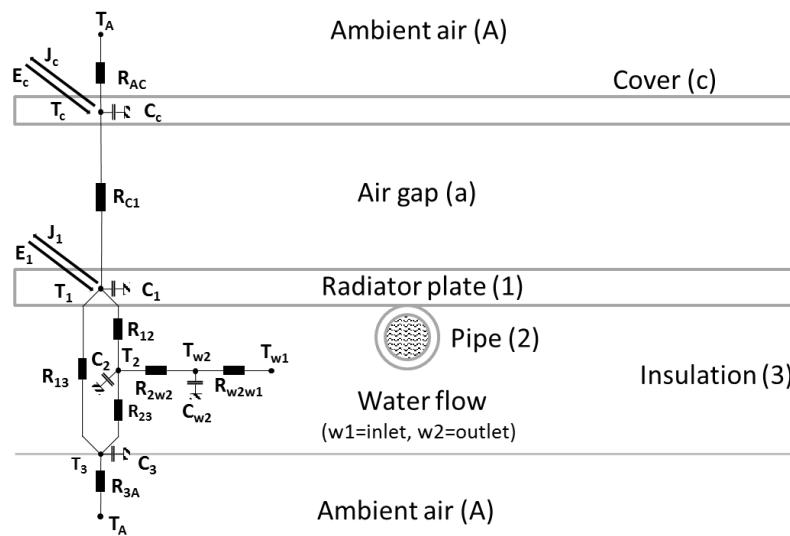


Figure 10 - 1D resistance-capacitance thermal model

Another essential part of the model is the radiation balance modelling. The authors conceived the radiation model in four different wavelengths ranges (0-4 μm , 4-7 μm , 7-14 μm , and >14 μm) to represent better the solar radiation (0.3-4 μm), the infrared radiation (4-50 μm), but especially the infrared atmospheric window range (7-14 μm), as well as the optical properties of the materials involved in the radiation balance which are wavelength dependant. The model also uses real data measurements from a Pyranometer (solar radiation) and a Pyrgeometer (infrared radiation). These two features applied in this model are not present in any other numerical model, giving the model tools to take special care of radiation data.

The radiation balance used the radiosity-irradiation method for calculations where it intervenes the surfaces of two physical elements of the flat plate collector (cover and radiation plate) and the incoming radiations: solar radiation and atmospheric radiation (Figure 11).

The authors chose to integrate the numerical model into TRNSYS software, creating a new TRNSYS type. The reason was the ease of integrating the model coding into a software with a large community of users and an extensive list of utilities (SC/PV systems, building, storage, control and logic, visualisation, etc.).

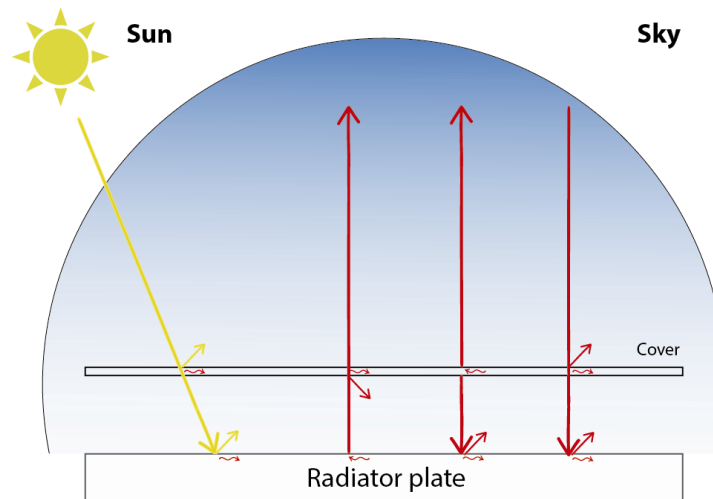


Figure 11 – Radiation model

In parallel to the numerical modelling, an experimental setup was designed and built (Figure 12) for model validation. For the sake of simplicity, the experimental setup used two different flat plates: one emulating an RCE in day-time/solar thermal collection mode, and the other one an RCE in night-time/radiative cooling mode.



Figure 12 – Solar thermal collector plate (left); radiative cooling plate (right)

The temperature in the entrance and exit of each flat plate, the flow rates, and the incoming atmospheric radiation were measured on-site. Also, a nearby weather station measured ambient temperature and solar radiation. Experiments were performed during summer (31/07 to 04/08) in Lleida, and the measured data was used for model validation. The experiments tested the properties and performance of an adaptable cover in real conditions. The model proved accuracy in predicting the thermal behaviour of both operational modes, and the results evidenced the potential for implementing dual functionality: solar thermal collection and radiative cooling.

Once the model was validated, the authors performed a sensitivity analysis to find statistically significant variables, or combinations of variables, of radiative cooling in a

flat plate configuration. The authors presented a complete list of parameters, narrow down the list in some steps (preliminary screening + One-step-at-a-time (OAT) method analysis) and finally performed an Analysis of variance (ANOVA) using a 2^k factorial design.

The performed sensitivity analysis detected five parameters or variables, and four combinations between them, as the most influencing for radiative cooling in a flat plate configuration: air gap thermal conductivity, radiator emissivity and cover transmissivity in the wavelength range of 7-14 μm , water inlet temperature, and water inlet flow; being water inlet temperature the most influencing variable.

In general, and for the studied conditions, higher values of these parameters and variables result in higher cooling generation rates. However, for low values of water inlet temperature ($< 15^\circ\text{C}$, for the studied conditions), low values of air gap thermal conductivity increase cooling energy production. Thus, if low temperatures are to be achieved, vacuum or partial vacuum in the cavity between the cover and the radiator surface may increase the cooling production.

The authors also highlighted the importance of adequately choosing the water inlet temperature because even though higher temperatures increase cooling production values, this temperature should be adequate for cooling purposes. The performance simulation with the optimised parameter values, presented the importance of selecting suitable materials because it may significantly increase the radiative cooling performance.

This model will also allow future exploration of RCE implementation by integrating this model into a complete HVAC or storage system.

6.3. Contribution to the objectives of the PhD thesis

Chapter 6 contributes to accomplishing objectives II, IV and VI, by presenting, in paper 3, a numerical model to simulate an RCE device. This numerical model adapts to the flat-plate configuration and integrates external conditions into the calculations (IV).

Paper 3 also presents a sensitivity analysis performed to detect the most influencing parameters for radiative cooling mode. This detection allowed the optimisation of this operational mode and the extraction of valuable conclusion (VI). Also, by identifying the

most influencing parameters for radiative cooling, the paper studied suitable radiation properties for both technologies (II).

6.4. Journal Paper

Reference:

S. Vall, K. Johannes, D. David, and A. Castell, “A new flat-plate radiative cooling and solar collector numerical model: Evaluation and metamodeling,” *Energy*, vol. 202, art. 117750, 2020. DOI:10.1016/j.energy.2020.117750.



A new flat-plate radiative cooling and solar collector numerical model: Evaluation and metamodeling



Sergi Vall ^a, Kévy Johannes ^b, Damien David ^b, Albert Castell ^{a,*}

^a Department of Computer Science and Industrial Engineering, University of Lleida, Edifici CREA, Pere de Cabrera S/n, 25001, Lleida, Spain
^b Univ Lyon, CNRS, INSA-Lyon, Université Claude Bernard Lyon 1, CETHIL UMR5008, F-69621, Villeurbanne, France

ARTICLE INFO

Article history:
Received 6 September 2019
Received in revised form
27 April 2020
Accepted 29 April 2020
Available online 1 May 2020

Keywords:
Radiative cooling
Solar thermal collector
Numerical modelling
Sensitivity analysis
Renewable energy
Low-grade source

ABSTRACT

Radiative cooling is a renewable technology that can complement or partially replace current cooling technologies. Coupling radiative cooling with another technology, such as solar collection could foster its development and implementation in the market. Therefore, a numerical model capable to simulate the behavior of a coupled radiative cooling and solar collection system is developed and presented in this paper. The model is validated with experimental data for both solar collection and radiative cooling operation, and a sensitivity analysis is performed in order to determine the most influencing parameters. Results show the potential of the device to perform the double functionality: solar thermal collector and radiative cooler. As expected the heating power (17.11 kWh/m^2) is one order of magnitude higher than the cooling one (2.82 kWh/m^2). The sensitivity analysis determined the existence of an important role played by 5 parameters (air gap thermal conductivity, absorptivity/emissivity of the radiator at $7\text{--}14 \mu\text{m}$ wavelength range, transmissivity of the cover material 2 at $7\text{--}14 \mu\text{m}$ wavelength range, water inlet temperature, and water inlet flow) and 4 combinations of these parameters in the radiative cooling mode.

© 2020 Elsevier Ltd. All rights reserved.

1. Introduction

The building sector is a growing sector that accounts for 40% of total energy consumption in the European Union [1], therefore bound to increase its energy consumption in the coming years. Consequently, new environmental and energy policies should be focused on energy efficiency and on increasing the renewable energy production, being these criteria fundamental for the future to come. An important role lies on space conditioning (space heating and cooling) that significantly contributes in the building energy budget (65% [2]) and on domestic hot water (DHW) (13.8% [2]).

When talking about renewable energy sources for space heating and DHW, solar thermal energy comes to mind [3]; however there is no renewable space cooling technology or energy source with the equivalent potential and market implementation like solar collection. In fact, even though there exist a few renewable cooling sources they present significant limitations [4].

Nowadays, compression and absorption heat pumps are the main existing technologies for cooling purposes [5]. Compression

heat pumps are the most common cooling devices. Although compression heat pumps are considered as a renewable source under certain circumstances [6,7], they consume high amounts of electricity. On the other hand, whereas absorption heat pumps may use solar energy as driving heat [8], they present some important disadvantages, such as not being available for residential applications, having low overall efficiencies, requiring high operation temperatures, and needing large cooling towers [9].

Alternatively, radiative cooling is a renewable cooling technology that can complement or partially replace current cooling technologies. Radiative cooling uses the sky as heat sink by taking advantage of its effective temperature lower than ambient temperature [10]. Energy is dissipated to the sky taking advantage of the infrared atmospheric window ($7\text{--}14 \mu\text{m}$) that allows some infrared radiation pass directly to space without intermediate absorption and re-emission [11–13].

The technology readiness level (TRL) of radiative cooling is still low (2–3 over 9, at the step of technology validation/demonstration). A lot of research on radiative cooling has focused on the development of prototypes and numerical models [14], as well as selective materials [15–18]. Zhang et al. [19] developed a numerical model to study the economic viability of a hybrid radiative cooled-

* Corresponding author.
E-mail address: albert.castell@udl.cat (A. Castell).

cold storage cooling system under different climatic conditions. They determined the incremental cost of the system to be viable considering an 8-year payback period. Zhao et al. [20–22] developed a numerical model to simulate a building integrated photovoltaic-radiative cooling system. They concluded that the new concept presents lower electrical efficiency than conventional Building Integrated Photovoltaic (BIPV). However, no commercial device has reached the market due to its low available power density (between 20 and 80 W/m² [23], with peak values of 120 W/m² [24]). Consequently, some improvements are needed in order to make radiative cooling feasible.

A potential solution is to couple radiative cooling with another technology, such as solar collection. The new device would be capable to produce both heat and cold. This combination might reduce the manufacturing and energy production costs that two separate devices would have, thereby improving its market feasibility. Although these two technologies use radiation with different wavelengths and it may seem contradictory to merge both functionalities, this coupling is possible as they are not overlapping technologies in terms of operational time, so there is no interference between them. This concept of combining radiative cooling and solar collection in a single device is mentioned in the present paper as Radiative Collector and Emitter (RCE). From our knowledge, this concept has scarcely been numerically modeled in the literature. Although there exist some TRNSYS types for solar collection (Types 1 and 45), and for PV/T (Types 50, 250 and 560, among others), most of them do not take into account the radiative cooling effect. None of the previous TRNSYS types seems likely to be used for RCE simulation. Solar TRNSYS types that take into account incoming infrared radiation do it by using the sky temperature to imprecisely evaluate it. The same applies for PV/T TRNSYS types. Although in a recent published research, a model combining these two technologies was presented [25], it was not capable to simulate the use of an adaptive cover that can change its optical properties, nor having a movable cover that can change between two materials with different optical properties, as the present model does. No previous research has been conducted into the development of a numerical model coupling solar collection and radiative cooling in the same model having the aforementioned ability. This novelty may entail a big step toward the evaluation of this technology and to further improve its performance. This is the purpose of the present paper.

Moreover, new improvements in the modelling of the radiative cooling are introduced in this paper. The way of treating the incoming radiation in the present paper differs from the numerical modelling of radiative cooling in the literature, where the incoming infrared radiation was considered as a whole value and empirical correlations were used to estimate it [24–32]. The correlations were in general used to calculate the sky temperature [24,27–29] and/or the sky effective emissivity [24,26,28–32] and in some cases the cloudiness effect as well [24,26,28,31,32]. However, some research discussed between the different correlations in the literature [24,31,32], thus proving the lack of consensus on which correlation to use. Alternatively, other research were conducted to take into account the wavelength of the radiation [33,34] by using analytical expressions which led to accurate results but tougher models. In the present research, the radiation is discretized for different wavelength bands to take into account the different optical properties of the materials and also the different amount of incoming radiation from each band. Additionally, measured data of the incoming infrared radiation are used for model validation instead of using empirical correlations.

To summarize, the present work deals with the development of a numerical model capable of evaluating solar collection and radiative cooling in the same device. This numerical model, which

additionally takes into account the radiation at different wavelengths, is implemented in TRNSYS. Finally, a sensitivity analysis is performed to determine the strong parameters of the system for the radiative cooling mode.

2. RCE background

In this paper, the RCE concept is presented as a single device capable of producing heat and cold. Previously, Erell and Etzion 2000 [29] and Matsuta et al., 1987 [35] evaluated the capability of solar collectors to produce radiative cooling. Similarly, Erell and Etzion 1996 [36] evaluated the capability of a radiative cooling device to produce heat. However, the RCE concept is designed from the beginning, to produce both heat and cold. This commitment entails the use of some strategies in its design to allow the generation of such different energy products.

The RCE device was designed to have a similar architecture to a flat plate solar thermal collector, having an absorber/emitter surface and a cover/screen on top of it. The main difference is that it was also designed to be capable of working in two non-simultaneous operating modes: solar collection mode and radiative cooling mode (Fig. 1), producing heat or cold, respectively.

To be able to operate under these different modes, the RCE incorporates a movable cover. This cover is composed of two different sections made of different materials. The section of the cover used for the solar collection mode lets solar radiation pass through and blocks mid and far infrared radiation. On the contrary, the section used for radiative cooling lets thermal radiation pass through. The movable cover consists of a sliding section (material used for solar collection) which slides apart during night.

These general considerations were taken into account when characterizing the numerical model of a novel RCE device.

3. Numerical model

The RCE concept as described above was implemented in a numerical model which is presented here.

3.1. Description of the simulated system

Fig. 2 contains a schematic view of the RCE. The architecture of the RCE is similar to the architecture of a flat plate solar collector. A radiator plate (1) collects or emits energy through radiation. A pipe (2) is welded at the back side of the radiator plate to transfer the heat to/from a fluid. The plate is insulated on the back side with insulation foam (3). On the front, the plate is separated from the external ambient with an air gap (a) and a screen (c).

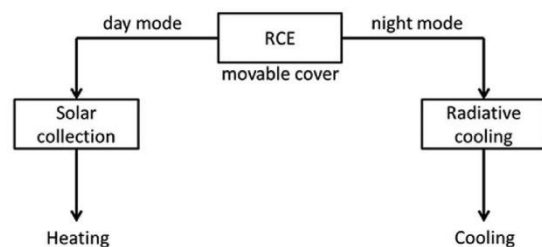


Fig. 1. Block diagram for the operation of the RCE concept.

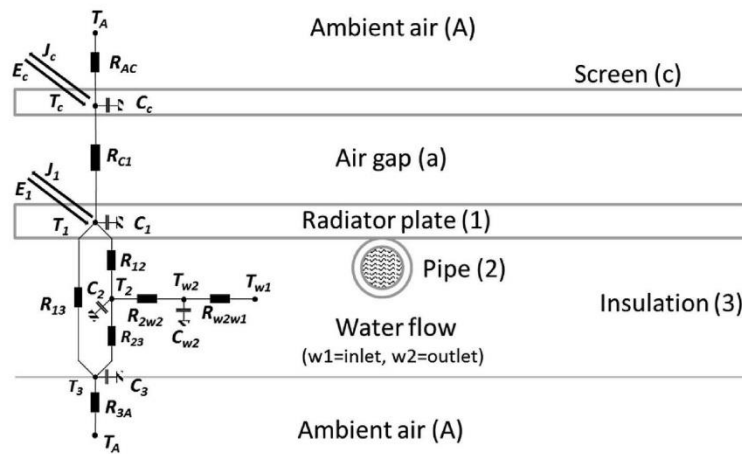


Fig. 2. Sketch of the model and 1D resistance-capacitance thermal model.

3.2. Resistance-capacitance thermal model

3.2.1. Architecture of the model

The system was discretized in several nodes using one dimension (1D) relations based on an electrical analogy to simplify the modelling. Although the use of a two or three-dimension approach may improve the accuracy of the results, the computational time would be much larger and the model implementation on TRNSYS would be much less flexible. Moreover [37], used the 1D discretization method to model a similar system achieving sufficiently accurate results.

The equivalent resistance network of the model is shown in Fig. 2. There is one temperature node for the screen (c), the RCE surface (1), the pipe (2) and its internal (outlet) fluid (w2), and the back insulation (3). The fluid enters the pipe at temperature T_{w1} .

The relations between the nodes are based on basic heat transfer equations. Each node has a thermal capacity (Eq. (1)) and each relation between nodes is represented by a thermal resistance (Eq. (2), Eq. (3)). Eq. (1) and Eq. (2) are presented per unit of length. Eq. (3) represents the thermal resistance between the fluid at the outlet of the pipe (node w2) and a fictitious node (w1) which represents the fluid at the inlet of the pipe. This fictitious node is used to introduce a second dimension required in the model to determine the heat flux between the inlet and the outlet of the pipe. Thus, this node has no capacitance, and can be considered as an input to the model.

$$C_i = \rho_i \cdot C_{p_i} \cdot V_i \left[\frac{J}{m \cdot K} \right] \text{ for } C_c, C_1, C_2, C_3 \text{ and } C_{w2} \quad \text{Eq. 1}$$

$$R_i = \frac{1}{h_i \cdot A_i} \left[\frac{m \cdot K}{W} \right] \text{ for } R_{AC}, R_{C1}, R_{3A} \text{ and } R_{2w2} \quad \text{Eq. 2}$$

$$R_{w2w1} = \frac{1}{\rho \cdot C_p \cdot Q_v} \left[\frac{K}{W} \right] \quad \text{Eq. 3}$$

To determine some of the thermal resistances the convection

heat transfer coefficient is needed. The Nusselt number (Eq. (4)) is obtained from well-known empirical correlations [38]. Four convection phenomena between five surfaces are considered: cover upper surface with ambient air (forced convection: Eq. (5) [39] and Eq. (6) [38], natural convection: Eq. (7) [40,41] and Eq. (8) [42,43], cover lower surface with radiator upper surface (Eq. (9) [44] and Eq. (10) [44]), pipe inner surface with water flow (Eq. (11) [45] and Eq. (12) [46]) and collector lower surface with ambient air (forced convection: Eq. (6) [38], natural convection: Eq. (7) [40,41] and Eq. (8) [42]).

$$\text{Nusselt number : } Nu = \frac{h \cdot L}{k} \quad \text{Eq. 4}$$

For a flat plate with external flow and forced convection Eq. (5) and Eq. (6) are used.

$$\text{Laminar flow : } Nu_L = 0.664 \cdot Re_L^{1/2} \cdot Pr^{1/3} \quad \text{Eq. 5}$$

$$\text{Mixed flow (Turbulent + laminar flow) : } Nu_L = (0.037 \cdot Re_L^{4/5} - 871) \cdot Pr^{1/3} \quad \text{Eq. 6}$$

For a flat plate with natural/free convection Eq. (7) and Eq. (8) are used.

$$\text{Upper surface of Hot Plate/Lower Surface of Cold Plate: } Nu_L = 0.54 \cdot Ra_L^{1/4} \quad \text{Eq. 7}$$

$$\text{Lower Surface of Hot Plate/Upper Surface of Cold Plate: } Nu_L = 0.52 \cdot Ra_L^{1/5} \quad \text{Eq. 8}$$

For inclined rectangular cavities Eq. (9) and Eq. (10) are used.

Heated from below :

$$Nu_L = 1 + 1.44 \cdot \left[1 - \frac{1708 \cdot (\sin 1.8\theta^{1.6})}{Ra_L \cdot \cos \theta} \right] \cdot \left[1 - \frac{1708}{Ra_L \cdot \cos \theta} \right]^+ + \left[\left(\frac{Ra_L \cdot \cos \theta}{5830} \right)^{\frac{1}{4}} - 1 \right]^+ \quad \text{Eq. 9}$$

Heated from above :

$$Nu_L = 1$$

For forced internal flow Eq. (11) and Eq. (12) are used.

$$\text{Laminar : } Nu_D = 3.66 + \frac{0.0668 \cdot Gz}{1 + 0.04 \cdot Gz^{\frac{1}{4}}} \quad \text{Eq. 11}$$

$$\text{Turbulent : } Nu_D = 0.023 \cdot Re_D^{4/5} \cdot Pr^n \quad (n=0.3 \text{ cooling, } n=0.4 \text{ heating})$$

Eq. 12

(16) for different scenarios (Table 3).

$$R_{12} = \frac{T_1 - T_2}{q_{2,upper}} \quad \text{Eq. 14}$$

$$R_{13} = \frac{T_1 - T_3}{q_3 - q_{2,lower}} \quad \text{Eq. 15}$$

$$R_{23} = \frac{T_2 - T_3}{q_{2,lower}} \quad \text{Eq. 16}$$

3.2.2. Conduction thermal resistances

Apart from the equations above, some of the thermal resistances (R_{12} , R_{13} , and R_{23}) were evaluated using a 2D heat transfer model (in COMSOL Multiphysics) to take into account 2D effects in a 1D resistance-capacitance model. Results are presented in section 5.1. This model is based on the heat transfer equation in solids (Eq. (13)).

$$\rho C_p \frac{\partial T}{\partial t} = \nabla \cdot (k \nabla T) + \dot{Q} \quad \text{Eq. 13}$$

The model consists of a radiator plate, a pipe and its union to the radiator, and the insulation (Fig. 3).

The boundary conditions of this model are (Fig. 4): constant and uniform heat flux at the upper surface of the radiator q'_1 , constant and uniform temperature at the inner part of the pipe T_2 , constant and uniform temperature at the lower surface of the radiator T_3 , and adiabatic boundary at the left and right side of the model considering several identical parallel configurations. The model computes the average temperature at the upper radiator surface T_1 , the heat flux at the top and bottom halves of the inner pipe q'_{2upper} and q'_{2lower} , and the heat flux at the bottom side of the insulation q'_3 .

Each resistance was calculated using Eq. (14), Eq. (15) and Eq.

3.2.3. Radiation model

Radiation heat fluxes concern the screen (c), the radiation plate (1), the sky and the Sun (Fig. 5).

These radiation heat fluxes are introduced in the heat balance equations in the form of net radiation heat fluxes \dot{Q}_r . The net radiation heat flux density is the difference between the irradiation E_e and the radiosity J_e (Eq. (17)). The radiosity is the sum of the emitted radiation, the reflected irradiation and the transmitted irradiation (Eq. (18)). The irradiation of a surface is the sum of the irradiations coming from other surfaces (Eq. (19)).

$$\dot{Q}_r = E_e - J_e = \int_0^\infty E_{e,\lambda} \partial \lambda - \int_0^\infty J_{e,\lambda} \partial \lambda \quad \text{Eq. 17}$$

$$J_{e,i} = \varepsilon_i \cdot \sigma \cdot T_i^4 + \rho_i \cdot E_{e,i} + \tau_i \cdot E_{e,i} \quad \text{Eq. 18}$$

$$E_{e,i} = \sum_{j=1}^n F_{ij} \cdot J_{e,j} \quad \text{Eq. 19}$$

The heat fluxes were calculated doing a radiation balance between each surface (subscript 'i') and the rest of surfaces (subscript 'j'), taking into account the incoming radiation (Sun/sky) and the

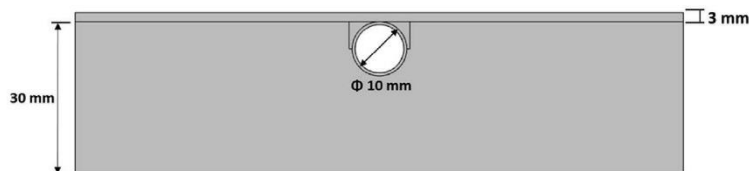


Fig. 3. Model geometry in COMSOL Multiphysics.

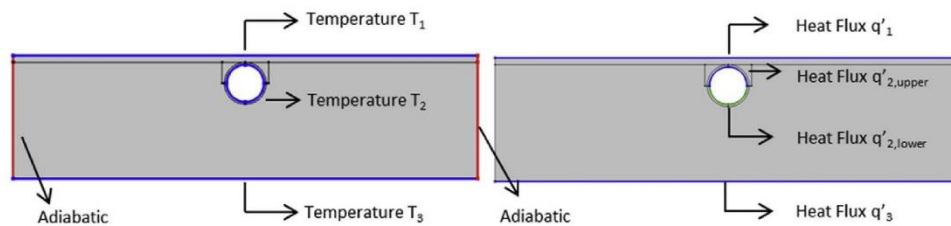


Fig. 4. Important boundary parameters of the model.

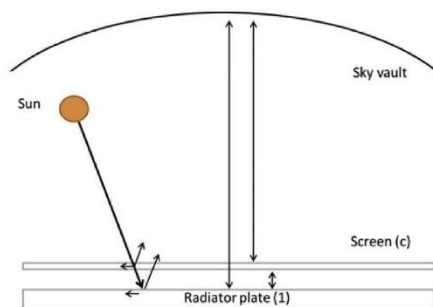


Fig. 5. Radiation model scheme.

outgoing radiation (emitted, reflected, transmitted) (Eq. (17), Eq. (18), Eq. (19) and Fig. 5).

In the model, the radiation balance is done for 4 different wavelength bands (0–4 μm , 4–7 μm , 7–14 μm and >14 μm). Moreover, the model also allows the use of 2 different materials as cover. Thus, the model distinguishes between different wavelength bands, with special care for the infrared atmospheric window (7–14 μm), to fully integrate the double functionality between solar collector and radiative emitter. The model needs data measurements (or data estimations) of solar radiation (<4 μm) and infrared radiation (>4 μm).

3.2.4. Internal procedure

A heat balance equation is built for the 6 nodes of the model. The heat balance equations are first order ordinary differential equations in time. The model solves numerically the differential equations using backward Euler method (or implicit Euler method) providing the agility of a first-order numerical procedure for solving ordinary differential equations and avoiding numerical instability of methods that require small time steps. To solve the systems of equations the Gauss-Seidel iterative method is used.

The coupling of both technologies required the creation of two

operational modes: solar collection mode and radiative cooling mode. In each mode, the cover properties change according to the material assigned to each mode (material 1 for solar collection/material 2 for radiative cooling). Two internal protocols were set to let the user choose between modes or allow the system to do it automatically. By default, the model operates under solar collection mode when there is solar radiation and the collector is heating up the water, and under radiative cooling mode for the rest of situations.

3.3. Experimental setup

In order to experimentally validate the numerical model, an experimental setup consisting of one solar collector (Fig. 6a), one radiative cooler (Fig. 6b), two water tanks, a pump, and the control and data acquisition systems was built. The radiative cooler consisted on a solar collector where the glass screen was replaced by a Polyethylene (PE) film, and the surface of the radiator was painted black in order to adapt it to the required characteristics for radiative cooling.

The solar collector used was 2 m long, 1 m wide and 80 mm high, with transparent 3 mm thick glass and 30 mm glass wool back insulation. The collector also had 8 copper pipes of 8 mm diameter and 0.6 mm thick. The radiative cooler had the same physical properties with a 0.6 mm thick polyethylene film instead of the glass.

For the sake of simplicity, two separate devices were used instead of a single RCE device. This was sufficient to provide accurate data for model validation, which was the main objective of this research.

The experimental setup had four temperature sensors (Pt-100, with an accuracy of 0.045 $^{\circ}\text{C}$) to monitor the inlet and outlet water temperature of the solar collector and the radiative cooling device. The flow rate was measured with two flowmeters; one for the solar collection mode (Badger Meter – Primo Advanced, 0.25% accuracy), and another one for the radiative cooling mode (Schmidt Mess – SDNC 503 GA-20, 4% accuracy). In addition, air temperature and solar radiation data were extracted from a weather station near the installation. The incoming infrared radiation was measured using a



Fig. 6. a) solar collector b) modified solar collector used as radiative cooling device.

Table 1
Parameters and inputs of the RCE model.

Parameters	Standard value	Unit	OAT ^a	
1	Distance between pipes	0.125	m	
2	Pipe length	2	m	
3	Air gap thickness	0.03	m	
4	Radiator thickness	0.003	m	
5	Pipe inner diameter	0.008	m	
6	Pipe wall thickness	0.0006	m	
7	Insulation thickness	0.03	m	
8	Radiator plate thermal conductivity	400	W/m·K	
9	Radiator plate density	8933	kg/m ³	
10	Radiator plate specific heat	385	J/kg·K	
11	Cover thickness material 1	0.0032	m	
12	Cover thermal conductivity material 1	1.3	W/m·K	
13	Cover density material 1	2200	kg/m ³	
14	Cover specific heat material 1	840	J/kg·K	
15	Cover thickness material 2	0.0006	m	
16	Cover thermal conductivity material 2	0.45	W/m·K	
17	Cover density material 2	920	kg/m ³	
18	Cover specific heat material 2	1900	J/kg·K	
19	Air gap thermal conductivity	0.026	W/m·K	X
20	Air thermal conductivity	0.026	W/m·K	
21	Air gap density	1.205	kg/m ³	X
22	Air specific heat	1007	J/kg·K	
23	Air dynamic viscosity	1.821·10 ⁻⁵	N·s/m ²	
24	Air kinematic viscosity	1.511·10 ⁻⁵	m ² /s	
25	Air thermal expansion coefficient	0.00343	1/K	
26	Fluid thermal conductivity	0.58	W/m·K	
27	Fluid density	1000	kg/m ³	
28	Fluid specific heat	4192	J/kg·K	
29	Fluid dynamic viscosity	0.001002	N·s/m ²	
30	Fluid kinematic viscosity	1.006·10 ⁻⁶	m ² /s	
31	Insulation thermal conductivity	0.035	W/m·K	
32	Insulation density	24	kg/m ³	
33	Insulation specific heat	1500	J/kg·K	
34	Radiator solar absorptivity	0.8	—	X
35	Radiator 4–7 μm absorptivity	0.8	—	X
36	Radiator 7–14 μm absorptivity	0.8	—	X
37	Radiator >14 μm absorptivity	0.8	—	X
38	Radiator solar reflectivity	0.2	—	X
39	Radiator 4–7 μm reflectivity	0.2	—	X
40	Radiator 7–14 μm reflectivity	0.2	—	X
41	Radiator >14 μm reflectivity	0.2	—	X
42	Cover solar absorptivity material 1	0.1	—	
43	Cover 4–7 μm absorptivity material 1	0.8	—	
44	Cover 7–14 μm absorptivity material 1	0.8	—	
45	Cover >14 μm absorptivity material 1	0.8	—	
46	Cover solar transmissivity material 1	0.8	—	
47	Cover 4–7 μm transmissivity material 1	0	—	
48	Cover 7–14 μm transmissivity material 1	0	—	
49	Cover >14 μm transmissivity material 1	0	—	
50	Cover solar reflectivity material 1	0.1	—	
51	Cover 4–7 μm reflectivity material 1	0.2	—	
52	Cover 7–14 μm reflectivity material 1	0.2	—	
53	Cover >14 μm reflectivity material 1	0.2	—	
54	Cover solar absorptivity material 2	0.1	—	X
55	Cover 4–7 μm absorptivity material 2	0.1	—	X
56	Cover 7–14 μm absorptivity material 2	0.1	—	X
57	Cover >14 μm absorptivity material 2	0.1	—	X
58	Cover solar transmissivity material 2	0.8	—	X
59	Cover 4–7 μm transmissivity material 2	0.8	—	X
60	Cover 7–14 μm transmissivity material 2	0.8	—	X
61	Cover >14 μm transmissivity material 2	0.8	—	X
62	Cover solar reflectivity material 2	0.1	—	X
63	Cover 4–7 μm reflectivity material 2	0.1	—	X
64	Cover 7–14 μm reflectivity material 2	0.1	—	X
65	Cover >14 μm reflectivity material 2	0.1	—	X
66	Number of parallel pipes	1	—	
Inputs				
1	Water inlet temperature	293	K	X
2	Water inlet flow	1.67·10 ⁻⁵	m ³ /s	X
3	Ambient temperature	—	K	
4	Wind velocity	—	m/s	
5	Global horizontal solar radiation	—	W/m ²	
6	Global horizontal infrared radiation	—	W/m ²	

^a Variables used in the One-step-at-a-time (OAT) analysis.

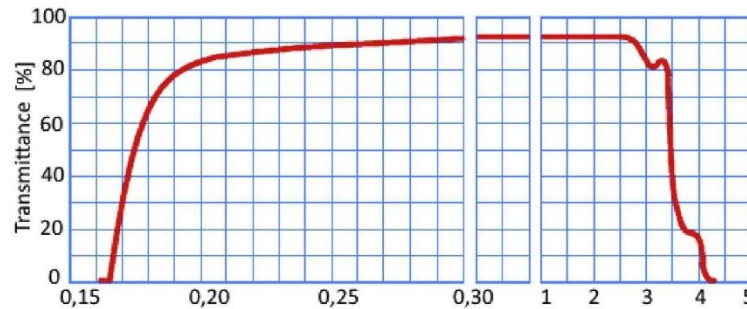


Fig. 7. Quartz glass optical properties [53].

Table 2
Summary of the optical properties for glass and polyethylene (PE) used in the model.

	0–4 μm		4–7 μm		7–14 μm		14 μm <	
	Glass	PE	Glass	PE	Glass	PE	Glass	PE
Transmissivity	0.80	0.80	0	0.80	0	0.80	0	0.80
Emissivity/absorptivity	0.10	0.10	0.80	0.10	0.80	0.10	0.80	0.10
Reflectivity	0.10	0.10	0.20	0.10	0.20	0.10	0.20	0.10

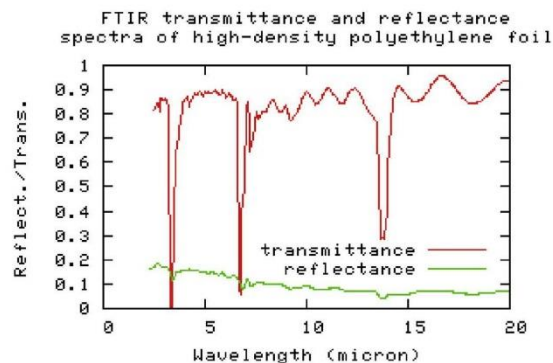


Fig. 8. Polyethylene optical properties [54].

Pyrgometer (LP PIRG 01 – DeltaOhm, 5% accuracy) placed near the experimental setup.

The model was validated for both solar collection mode and radiative cooling mode. Results are presented and discussed in section 5.2. Model validation.

4. Sensitivity analysis

A sensitivity analysis can identify the most influencing inputs and parameters to extract relevant conclusions of the system, such as to determine the robustness of the system, to simplify the model, to find optimal operational parameters values, etc. Additionally, the sensitivity analysis may discover possible interactions or crossed effects between different inputs. In the present research, the sensitivity analysis was used to identify the most influencing parameters, to find the optimal value of some operational parameters and to discover crossed effects between parameters. The sensitivity analysis was only performed for the radiative cooling parameters and inputs, since this type of analysis have already been done for

solar collection [47–51] but not for radiative cooling.

To do so, factorial designs are the most efficient when analyzing the effect of two or more factors or inputs. Among them, the 2^k design is particularly useful because it provides a complete factorial design with the smallest number of simulations [52].

Table 1 presents the different parameters and inputs for the RCE type (66 parameters and 6 inputs).

The optical properties play an important role in the radiation balance; therefore, accurate data is required to characterize the radiator and the cover in the specific ranges. In the reference case, the optical properties used are glass for material 1/solar collection mode (Fig. 7 and summarized in Table 2) and polyethylene (PE) for material 2/radiative cooling mode (Fig. 8 and summarized in Table 2).

The large number of inputs and parameters combined with the duration of each simulation requires strong computational time and resources. For that reason, a strategy to deal with this problem and to perform the sensitivity analysis was used and is presented.

4.1. Preliminary screening

First of all, a preliminary screening was performed to reduce the number of inputs and parameters by discarding the prototype-related parameters (geometry and material properties) and uncontrollable inputs (solar radiation, infrared radiation, ambient temperature and wind speed). This first screening may avoid spending resources inefficiently.

The uncontrollable inputs have an obvious relation with the thermal behavior of the RCE device. For instance, solar radiation is directly related to the heating output of the system as well as the infrared radiation to the cooling output. To some extent, ambient temperature and wind speed also have a relation (a high ambient temperature is better for heating while a low one is better for cooling, the lower wind speed the better for both functions as it is related to the convection losses).

4.2. One-step-at-a-time (OAT)

When required by the still large number of inputs, a One-step-at-a-time (OAT)/Morris method analysis [55,56] was performed to continue with the screening. This method evaluates the effect on the output when changing the value of one input each time. To establish which variables are relevant, the values of the two sensitivity measures were evaluated for each factor. These two measures are the mean of the distribution (μ^*) and the standard deviation (σ). In the present research the output is the cooling production of the RCE device, and values higher than $\mu^* = 0.2$ and

$\sigma = 0.08$ indicate an important overall influence on the output.

This is an easy and simple method to be performed as a basic initial screening. However, this method may miss important information such as the influence and interaction between different inputs.

4.3. 2^k factorial design + analysis of variance (ANOVA)

Finally, a sensitivity analysis was performed using the 2^k factorial design. To analyze the results of the factorial design experiments, an analysis of variance (ANOVA) is performed. With this methodology the inputs or combinations of inputs statistically significant are found.

Moreover, the 2^k factorial design can be used to get the regression model of an experiment or a numerical model. This regression model gives the numerical model output as a function of the input variables and combinations of different variables (as seen in Eq. (20)).

$$y = \beta_0 + \sum_{j=1}^n \beta_j x_j + \sum_{i < j} \sum \beta_{ij} x_i x_j + \varepsilon \quad \text{Eq. 20}$$

This regression model is usually presented only with the main or the relevant parameters or combination of parameters. The regression model accurately represents the model performance when the values of the parameters are within the range for which they were proposed. This regression model can be used to optimize the system performance.

Once the regression model was defined, the output optimization could be performed. The optimization consisted in studying the output variability for each group of related parameters to maximize or minimize the output. This procedure consists on setting the non-interacting parameters at the default value while changing the value of the studied parameter/s. If there is no interaction parameter, the studied parameter is optimized according to the variable coefficient (β_i). Otherwise, the parameters need to be optimized with regard to its interaction parameters. To visually present that optimization, a response surface graph or a contour surface plot may be used. Results on the sensitivity analysis are described in section 5.4. Sensitivity analysis.

Table 3
Parameter values for the different 2D model scenarios.

Scenario	Working as radiative cooling						Working as solar collector		
	1	2	3	4	5	6	7	8	9
Water inlet Temperature [$^{\circ}\text{C}$]	20	15	20	15	20	15	35	50	60
Ambient Temperature [$^{\circ}\text{C}$]	25	25	25	25	25	25	25	25	25
Heat flux [W/m^2]	-50	-25	-100	100	500	1000			

5. Results and discussions

In this section, the results of the 2D heat transfer model, the experimental validation, and the performance of the RCE model are presented, as well as the results of the sensitivity analysis and the optimization of the RCE performance.

5.1. 2D heat transfer model

A 2D model of the radiator plate was developed in order to evaluate the equivalent resistances (Fig. 9) and consider some 2D effects in the 1D model. The results of the resistances are very dependent on the specific design, then, for another configuration (dimension, material, etc.), the equivalent resistances need to be reevaluated.

The equivalent resistances were evaluated using Eq. (14), Eq. (15) and Eq. (16), and the values of the heat flux and the temperature differences were determined from the 2D model. The upper surface heat flux, the pipe inner surface temperature and the bottom surface temperature were the parameters that change according to the different scenarios (see q_1' , T_2 and T_3 in Fig. 4). These scenarios include the device working as solar thermal collector and as radiative cooling by changing the incoming radiation (q_1'), different pipe temperatures (T_2) for cooling and heating, and an outdoor temperature (T_3) to represent all possibilities regarding the heat fluxes (Table 3, see Fig. 10 for reference direction for heat flux).

A mesh independency study was performed in order to reduce the duration of the simulations and reduce the absolute error. The absolute error (evaluated using Eq. (21)) and the total computing time are presented in Table 4.

$$e = |q_1' - q_{2,up}' + q_{2,lower}' - q_3'| \quad \text{Eq. 21}$$

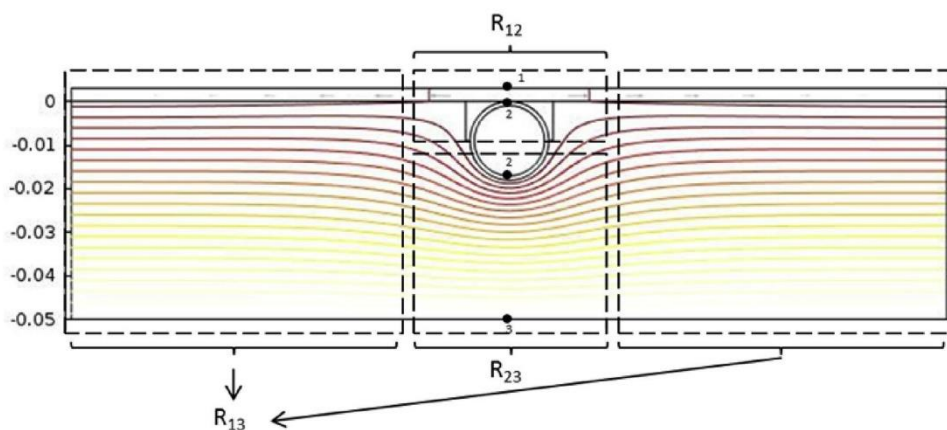


Fig. 9. Isothermal contours of the 2D model (COMSOL Multiphysics) with the equivalent resistances.

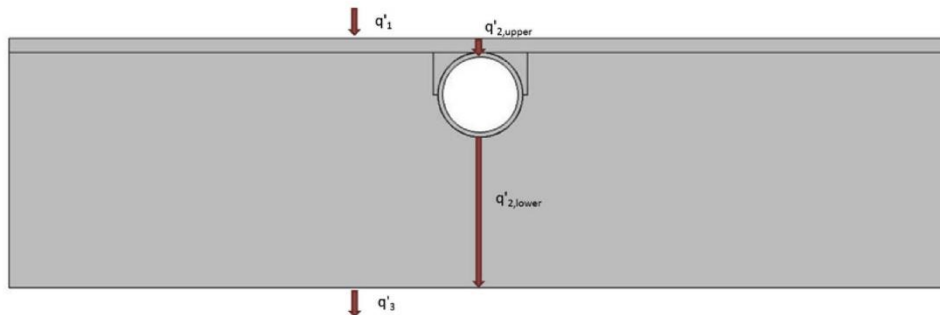


Fig. 10. Heat fluxes reference direction.

Table 4
Absolute error, total computing time and mesh elements for different meshing.

	Extremely coarse	Coarser	Normal	Finer	Extremely Fine
Absolute error [W/m]	0,02643	0,02690	0,02739	0,02776	0,000001
Time [s]	3	4	4	6	6
Mesh elements [-]	591	965	1442	1642	7871

Table 5
Thermal resistances and heat fluxes for the different 2D model scenarios.

Scenario	Working as radiative cooling					Working as solar collector			
	1	2	3	4	5	6	7	8	9
T ₁ [K]	293.10	288.11	293.13	288.13	293.04	288.05	308.25	323.67	339.21
T ₂ [K]	293.15	288.15	293.15	288.15	293.15	288.15	308.15	323.15	338.15
T ₃ [K]	298.15	298.15	298.15	298.15	298.15	298.15	298.15	298.15	298.15
q' ₁ [W/m]	-6.25	-6.25	-3.125	-3.125	-12.5	-12.5	12.5	62.5	125
q' _{2,upper} [W/m]	-5.642	-5.065	-2.525	-1.948	-11.878	-11.301	11.216	59.143	119.592
q' _{2,lower} [W/m]	-0.150	-0.303	-0.154	-0.307	-0.143	-0.296	0.318	0.777	1.212
q' ₃ [W/m]	-0.758	-1.488	-0.754	-1.484	-0.765	-1.495	1.602	4.134	6.620
R ₁₃ [m·K/W]	8.31	8.48	8.36	8.51	8.21	8.43	7.86	7.60	7.59
R ₁₂ [m·K/W]	8.83·10 ⁻³	8.71·10 ⁻³	8.71·10 ⁻³	8.39·10 ⁻³	8.87·10 ⁻³	8.83·10 ⁻³	8.88·10 ⁻³	8.89·10 ⁻³	8.88·10 ⁻³
R ₂₃ [m·K/W]	33.31	33.00	32.55	32.62	34.96	33.79	31.45	32.17	33.00

Table 6
1D equivalent resistances.

R ₁₃ [m·K/W]	R ₁₂ [m·K/W]	R ₂₃ [m·K/W]
8.15	8.77·10 ⁻³	32.98

From the results in Table 4, the resulting mesh consisted in 7800 triangular cells and the simulation absolute error was set to 1·10⁻⁶.

Hereafter, the different cases were simulated (Table 5), and the average values were calculated. Results are presented in Table 6.

Results from Table 6 are consistent to the ideal behavior. On the one hand, there is high thermal resistance between the radiator surface and the bottom as well as between the pipe and the bottom because of the insulation. On the other hand, there is very low resistance between the radiator surface and the pipe because of the high thermal conductivity of metals such as copper or steel. The thermal resistances presented in Table 6 were used in the RCE model.

5.2. Model validation

An experimental validation of the model was done using

empirical data from the experimental setup presented in section 3.3. Experiments were performed from 31–07 to 04–08 in Lleida (ESP). The RCE model was adapted to the prototype and simulations were done using the same boundary conditions. The model was validated comparing the predicted outlet water temperature to the measured one.

Fig. 11 presents the main inputs/outputs of the model with special attention to the water inlet temperature and both the experimental and numerical water outlet temperature. The model results present the same behavior as the experimental ones, therefore validating the model for solar collection and radiative cooling.

Although in the validation experiments two different devices were used (solar collector and radiative cooler), in Fig. 11 the results for both modes are presented together bearing in mind that this would be the behavior of an RCE device. The change in the operation mode is observed at 8 h and 20 h. In order to obtain accurate results, the transition period from one operation mode to the other one was not considered in the evaluation (7–9 h and 19–21 h).

For both modes, the MBD (Mean Bias Difference, Eq. (22)) and the RMSE (Root Mean Square Error, Eq. (23)) between the real outlet temperature and the one predicted by the model were calculated (Table 7).

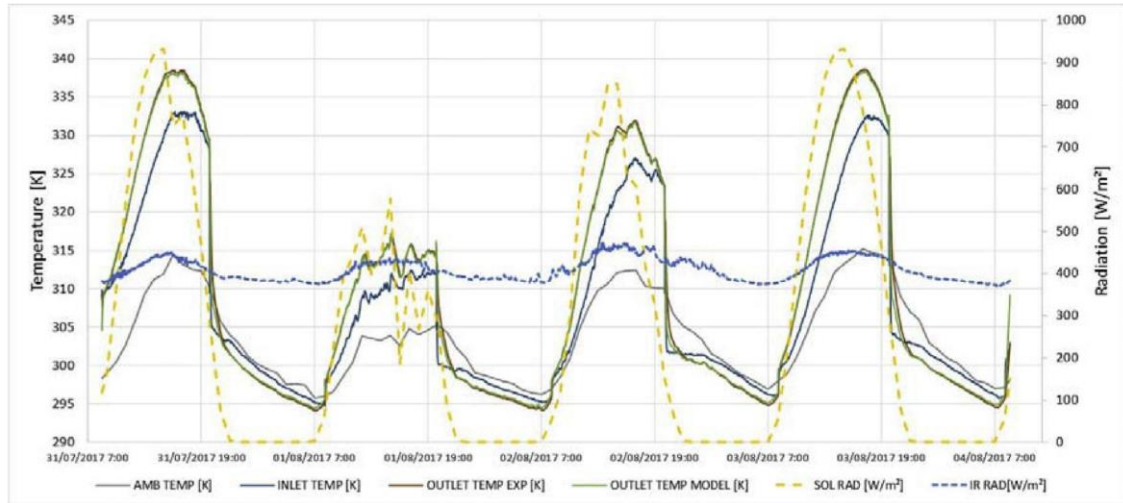


Fig. 11. Input parameters, experimental and numerical outlet temperature.

Table 7
MBD and RMSE for both modes.

	Solar Collection	Radiative Cooling
MBD	-0.19	0.05
RMSE(°)	0.32	0.40

$$RMSE = \sqrt{\frac{1}{n} \sum_{j=1}^n (y_j - \hat{y}_j)^2} \quad \text{Eq. 23}$$

The MBD is -0.19°C for the solar collection mode and 0.05°C for the radiative cooling mode, showing a small dispersion of the results. The RMSE is 0.32°C for the solar collection mode and 0.40°C for the radiative cooling mode, thus validating the model.

$$MBD = \frac{1}{n} \sum_{j=1}^n (y_j - \hat{y}_j) \quad \text{Eq. 22}$$

5.3. Reference case

As for the next sections 5.3 Reference case, 5.4 Sensitivity

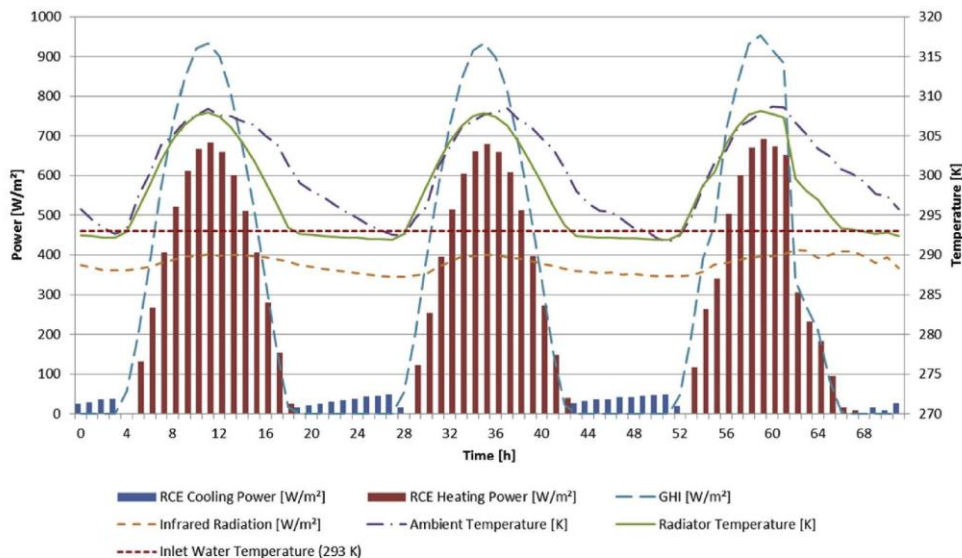


Fig. 12. RCE performance during 3 summer days.

Table 8
Variables used in the OAT method and variables analyzed in ANOVA.

Name	Units	Default Value	Higher value	Lower value	OAT sensitivity measures		ANOVA variables
					μ^a	σ	
Air gap thermal conductivity	W/m·K	0.026	0.05	0.001	4.66	3.62	X
Air gap density	kg/m ³	1.205	2	0.001	-0	-0	
Radiator absorptivity	solar	0.8	0.95	0.7	1.31	0.047	X
	4–7 μm				0.06	0.002	
	7–14 μm				13.23	0.12	X
	>14 μm				0.10	0.005	
Radiator reflectivity ^a	solar	0.2	0.3	0.05	–	–	
	4–7 μm				–	–	
	7–14 μm				–	–	
	>14 μm				–	–	
Cover absorptivity material 2	solar	0.1	0.2	0.05	0.09	0.002	
	4–7 μm				0.01	0.001	
	7–14 μm				0.60	0.206	X
	>14 μm				-0	-0	
Cover transmissivity material 2	solar	0.8	0.9	0.7	0.99	0.553	X
	4–7 μm				0.05	0.026	
	7–14 μm				9.86	5.513	X
	>14 μm				0.08	0.043	
Cover reflectivity ^a material 2	solar	0.1	0.25	0.05	–	–	
	4–7 μm				–	–	
	7–14 μm				–	–	
	>14 μm				–	–	
Water inlet temperature	K	293	310	280	1.72	0.55	X
Water inlet flow	m ³ /s	1.67·10 ⁻⁵	1.67·10 ⁻⁴	1.67·10 ⁻⁶	61960	104483	X

^a Indirectly taken into account by others parameters.

analysis and 5.5 Optimized case, the data used comes from the meteorological station of the Group of Environmental Physics of the University of Girona placed in Girona (Spain, 41.96° N 2.83° E, 110 m a.s.l, Cfa climate). There, the meteorological data required is continuously recorded, and in consequence, longer periods could be analyzed.

Fig. 12 presents the performance of the RCE model during 3 days in summer. Since this paper deals with the RCE model and not with the space conditioning system the water inlet temperature was assumed to be at constant temperature, although in a complete system water would come from the storage tank. The cover material changes automatically between modes (solar collection mode and radiative cooling mode) when no more heat or cold is produced according to the mode. The rest of inputs and parameters are set at default value (Table 8).

Results show the potential of the RCE to perform the double functionality, solar collection and radiative cooling. For the presented period, the solar thermal energy collected is 17.01 kWh/m² and radiative cooling energy is 0.88 kWh/m². As expected, the heating power is one order of magnitude higher than the cooling one; however, while the heating power follows the solar radiation

curve, the cooling power remains almost constant during the whole night.

5.4. Sensitivity analysis

Once the model was defined and validated, a sensitivity analysis was performed by using ANOVA with the results of a 2^k factorial design, and considering the total cooling energy produced as the target variable. The model has a large number of parameters and inputs (Table 1); therefore, to reduce the number of simulations, a first preliminary screening was done, reducing them to 24. After this first screening, an OAT sensitivity analysis was performed concluding that 8 of these 24 input variables were relevant or significant variables according to its two sensitivity measures (Table 8).

Finally, an ANOVA analysis was performed for the remaining 8 variables (Table 9), showing that 5 parameters and 4 combinations of these 5 parameters were important or relevant (p-value < 0.05) to the output: x₁, x₃, x₆, x₇, x₈, x₁x₇, x₃x₇, x₆x₇, x₇x₈. These 5 parameters and 4 combinations represent more than 99% of the model response, having Eq. (24) as regression model of the cooling

Table 9
Variables used in the ANOVA.

$$E_{cooling} = 62.62 - 2567.47 \cdot x_1 - 266.08 \cdot x_3 - 270.01x_6 - 0.24 \cdot x_7 - 503581.9 \cdot x_8 + 8.94 \cdot x_1x_7 + 0.95 \cdot x_3x_7 + 0.97 \cdot x_6x_7 + 1773.92 \cdot x_7x_8$$

Eq. 24

Variable	Name	Unit	Default Value	Higher value	Lower value
x ₁	Air gap thermal conductivity	W/m·K	0.026	0.05	0.001
x ₂	Radiator solar absorptivity	–	0.8	0.95	0.7
x ₃	Radiator 7–14 μm absorptivity	–	0.8	0.95	0.7
x ₄	Cover 7–14 μm absorptivity material 2	–	0.1	0.15	0.05
x ₅	Cover solar transmissivity material 2	–	0.8	0.85	0.7
x ₆	Cover 7–14 μm transmissivity material 2	–	0.8	0.85	0.7
x ₇	Water inlet temperature	K	293	300	285
x ₈	Water inlet flow	m ³ /s	1.6·10 ⁻⁵	1.25·10 ⁻⁴	1.6·10 ⁻⁵

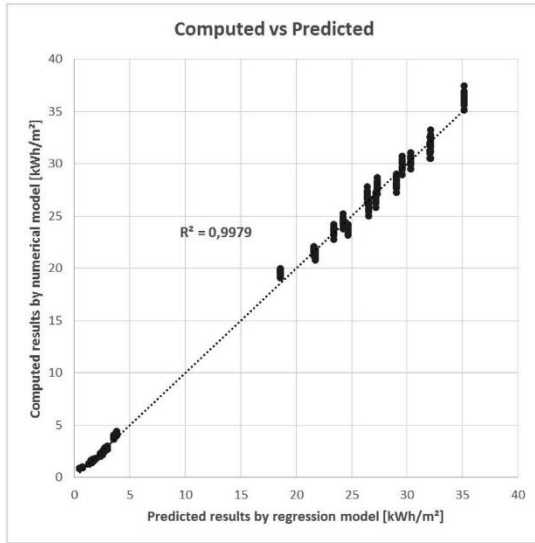


Fig. 13. Comparison between computed and predicted results.

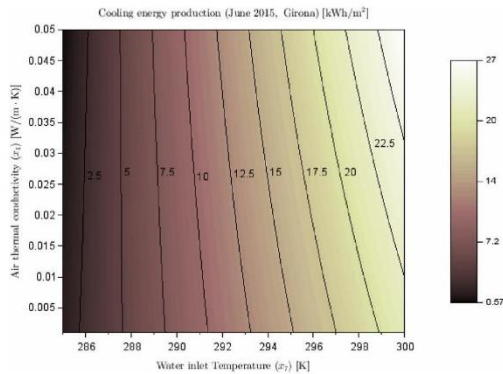


Fig. 14. Contour plot: Air gap thermal conductivity vs. Water inlet temperature ($x_1 - x_7$).

output taking into account the main parameters. The regression model fits the numerical model with high accuracy as can be seen in Fig. 13, presenting $R^2 = 0.9979$ and an average deviation of 6%.

From Eq. (24), the radiative cooling performance can be optimized in order to get the maximum cooling energy production and to discover the operational strategies to do so. Notice that the water inlet temperature (x_7) is an influencing parameter because it appears combined with the rest of parameters in Eq. (24). Each parameter (except x_7) has only one interaction parameter, therefore all parameters except one were optimized in regard to the water inlet temperature while this one was optimized taking into account the other parameters optimizations.

From the regression model (Eq. (24)) one can conclude that:

- 1 The air gap conductivity (x_1) appears as a single parameter and combined with the water inlet temperature (x_7). Analyzing the

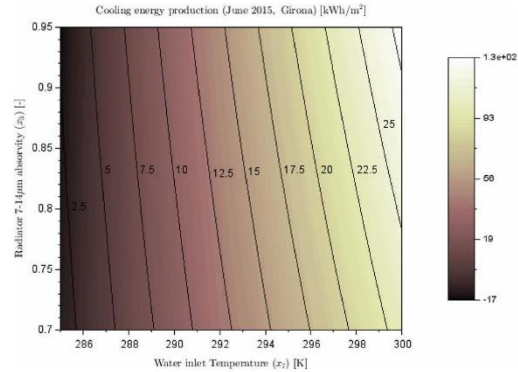


Fig. 15. Contour plot: Radiator 7–14 μm absorptivity vs. Water inlet temperature ($x_3 - x_7$).

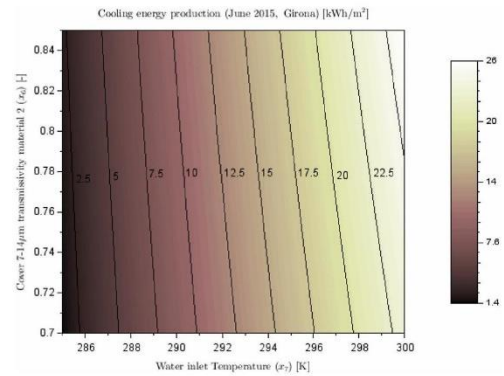


Fig. 16. Contour plot: Cover 7–14 μm transmissivity material 2 vs. Water inlet temperature ($x_6 - x_7$).

tendency of Eq. (24) (Fig. 14) as a function of the air gap conductivity, two different tendencies are observed: (1) when the water inlet temperature is high, the air gap conductivity should be as high as possible to maximize the cooling production, (2) when the water inlet temperature is low, the air gap conductivity should be as low as possible to avoid heat gains from environment. This change of tendency/behavior appears when the water inlet temperature is around 14°C ($\sim 287\text{K}$). This suggests that the use of vacuum between the screen and the radiator plate could improve the RCE behavior if low temperatures are required.

- 2 The radiator absorptivity/emissivity at 7–14 μm (x_3) appears as a single parameter and combined with the water inlet temperature (x_7). Analyzing the tendency of Eq. (24) (Fig. 14) as a function of the radiator absorptivity at 7–14 μm , one can see that the best results are obtained with higher radiator absorptivities at 7–14 μm and water inlet temperatures. This result makes sense because the incoming radiation from sky in that wavelength range is lower than the emitted by a blackbody. This influence decreases at lower temperatures when lower radiation is emitted. From Eq. (24) one can deduce that this tendency changes at around 6°C ($\sim 279\text{K}$), but as this temperature is out of

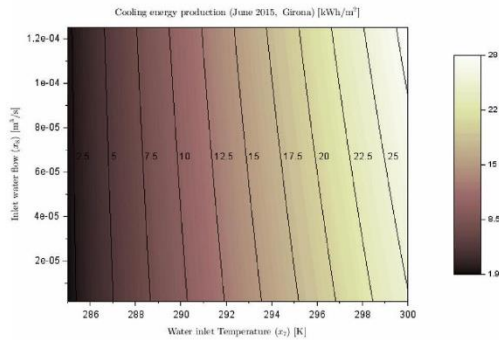


Fig. 17. Contour plot: Water inlet flow rate vs. Water inlet temperature ($x_7 - x_8$).

the valid range for Eq. (24) (285–300K) the authors cannot assure the accuracy of this extrapolation.

- 3 The cover transmissivity at 7–14 μm of material 2 (x_6) appears as a single parameter and combined with the water inlet temperature (x_7). Analyzing the tendency of Eq. (24) (Fig. 16) as a function of the cover transmissivity at 7–14 μm , one can see that the best results are obtained with higher cover transmissivities at 7–14 μm and water inlet temperatures. This result makes sense because increasing the transmissivity in that wavelength range also increases the radiation exchange in that wavelength range. This influence decreases at lower temperatures with low radiation emitted. From Eq. (24) one can deduce that this tendency changes at around 6°C ($\sim 279\text{K}$), but as this temperature is out of the valid range for Eq. (24) (285–300K) the authors cannot assure the accuracy of this extrapolation.
- 4 The water inlet flow rate (x_8) appears as a single parameter and combined with the water inlet temperature (x_7). Analyzing the

tendency of Eq. (24) (Fig. 17) as a function of the water inlet flow rate, one can see that the best results are obtained with higher water inlet flow rates and water inlet temperatures. This result makes sense because for higher flow rates the temperature difference between the inlet and the outlet is reduced, thus emitting more radiation at a higher temperature. From Eq. (24) one can deduce that this tendency changes at around 11°C ($\sim 284\text{K}$), but as this temperature is out of the valid range for Eq. (24) (285–300K) the authors cannot assure the accuracy of this extrapolation.

- 5 Finally, the water inlet temperature (x_7) appears as a single parameter and combined with all the other parameters. This parameter has just one tendency (Figs. 14–17) in the studied range (285–300K), the higher the water inlet temperature, the better. This result makes sense because for higher water inlet temperatures more radiation will be emitted. Thus, water inlet temperature plays an important role.

This parameter analysis allowed determining that for the relevant variables the higher value, the better, except for the air gap thermal conductivity which depends on the water inlet temperature. Therefore, special attention must be paid to the selection of coating materials for the absorber or to the absorber material itself. However, notice that for different absorber materials the 2D resistances may change and thus will the model; therefore, the sensitivity analysis must be recalculated. Finally, these parameters should be accurately measured to ensure accurate results from the numerical model.

5.5. Optimized case

Once the strong parameters were identified and the optimal values found, the same simulations as for the Reference case (section 5.3) were performed using the optimal values to see the improvement in the radiative cooling. These optimal values are within the studied ranges and represent realistic values. The results are presented in Fig. 18.

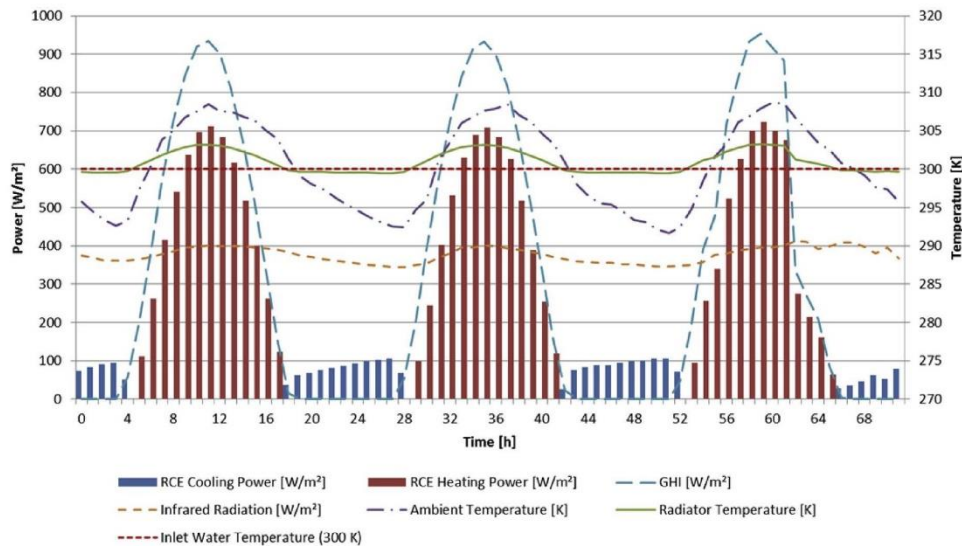


Fig. 18. RCE optimized performance during 3 summer days.

The results show that, in the same period as in Fig. 12, the solar thermal energy collected is 17.11 kWh/m^2 and radiative cooling energy is 2.82 kWh/m^2 . The cooling energy production increases by 300% in regard to the standard values of the RCE performance, showing that important improvements for radiative cooling could be achieved by adjusting the device to the optimal design parameters. On the other hand, the solar collection remains almost constant (reduction around 1.7%).

These results demonstrate the potential of the RCE device to provide heat for Domestic Hot Water and cold for space cooling, being an interesting technology to cover in a renewable way the thermal demands of nearly Zero Energy Buildings.

6. Conclusions

In the present work a numerical model of a Radiative Collector and Emitter (RCE) was presented. RCE is a novel technology combining solar collection and radiative cooling. The numerical model was developed in TRNSYS, becoming this code a new "type" to be used in that software. The model was experimentally validated, and a sensitivity analysis was performed to identify the influencing parameters.

The RCE model proved accurate in representing the thermal behavior of both operational modes of the device. Results showed the potential of the RCE to perform the double functionality: solar thermal collector and radiative cooler. As expected, the heating power is one order of magnitude higher than the cooling one.

From the sensitivity analysis 5 parameters and 4 combinations of these parameters were identified as the most influencing ones for the radiative cooling mode. These parameters are the air gap thermal conductivity, the absorptivity/emissivity of the radiator at $7\text{--}14 \mu\text{m}$ wavelength range, the transmissivity of the cover material at $7\text{--}14 \mu\text{m}$ wavelength range, the water inlet temperature, and the water inlet flow. For the studied range, the best results were obtained with higher values of these parameters. However, when low water inlet temperatures ($< 15^\circ\text{C}$) are required, lower air gap thermal conductivities maximize the cooling energy production. Thus, if low temperatures are to be achieved, vacuum or partial vacuum may help increasing the cooling production ratio. Moreover, the water inlet temperature resulted to be the most influencing parameter and, if possible, this temperature should be as high as possible to increase the cooling ratio. However, although getting good cooling rates, that temperature should be low enough for cooling purposes. The optimal values allow the model to significantly increase the radiative cooling performance; therefore, the materials should be accurately chosen.

The new model will allow exploring the benefits of implementing such technology in a complete system, integrating it with the HVAC and storage devices.

CRedit authorship contribution statement

Sergi Vall: Methodology, Software, Formal analysis, Data curation, Writing - original draft. **Kévy Johanes:** Conceptualization, Methodology, Resources, Supervision, Writing - review & editing. **Damien David:** Methodology, Writing - review & editing. **Albert Castell:** Conceptualization, Supervision, Writing - review & editing, Funding acquisition.

Acknowledgements

Sergi Vall would like to thank the Secretaria d'Universitats i Recerca del Departament d'Economia i Coneixement de la Generalitat de Catalunya for its research fellowship, and La Societat

Econòmica Barcelonesa d'Amics del País for the early research stay fellowship. Sergi Vall and Albert Castell would like to thank the Oficina de Desenvolupament i Cooperació de la Universitat de Lleida for its project grant. The work partially funded by the Spanish government under grant agreement RTI2018-097669-A-I00 (MINISTERIO DE CIENCIA, INNOVACIÓN Y UNIVERSIDADES). The authors would like to thank Generalitat de Catalunya for the project grant given to their research group (2017 SGR 659).

Nomenclature

Symbol Description Equations where appears

A	contact surface per unit of length $\left[\frac{\text{m}^2}{\text{m}}\right]$	2
C	heat capacity at constant pressure per unit of length $\left[\frac{\text{J}}{\text{m}\cdot\text{K}}\right]$	1
C_p	specific heat capacity at constant pressure $\left[\frac{\text{J}}{\text{kg}\cdot\text{K}}\right]$	1, 13
E_e	irradiance or the radiant flux received by a surface per unit of area $\left[\frac{\text{W}}{\text{m}^2}\right]$	17, 18, 19
$E_{e,\lambda}$	spectral irradiance $\left[\frac{\text{W}}{\text{m}^2\cdot\mu\text{m}}\right]$	17
$E_{cooling}$	cooling energy production $\left[\frac{\text{kWh}}{\text{m}^2}\right]$	24
F_{ij}	view factor from surface j to surface i	[–] 19
Gz	Graetz number	[–] 11
h	convection heat transfer coefficient $\left[\frac{\text{W}}{\text{m}^2\cdot\text{K}}\right]$	2, 4
i, j	general species designation/identifier subscript	[–] 18, 22, 23
J_e	radiosity or radiant flux leaving (emitted, reflected, transmitted) a surface per unit of area $\left[\frac{\text{W}}{\text{m}^2}\right]$	17, 18, 19
$J_{e,\lambda}$	spectral radiosity $\left[\frac{\text{W}}{\text{m}^2\cdot\mu\text{m}}\right]$	17
k	thermal conductivity $\left[\frac{\text{W}}{\text{m}\cdot\text{K}}\right]$	4, 13
L	characteristic length for Nusselt number	[m] 4
n	total number of intervals or elements	[–] 19, 20, 22, 23
Nu	Nusselt number	[–] 4
Nu_L	Nusselt number based on characteristic length	[–] 5, 6, 7, 8, 9, 10
Nu_D	Nusselt number based on characteristic diameter	[–] 11, 12
Pr	Prandtl number	[–] 5, 6, 12
q'	heat transfer rate per unit length $\left[\frac{\text{W}}{\text{m}}\right]$	14, 15, 16, 21
\dot{Q}	additional heat sources $\left[\frac{\text{W}}{\text{m}^3}\right]$	13
\dot{Q}_r	radiation balance $\left[\frac{\text{W}}{\text{m}^2}\right]$	17
Q_v	volume flow rate of the fluid $\left[\frac{\text{m}^3}{\text{s}}\right]$	3
R	equivalent resistance $\left[\frac{\text{m}\cdot\text{K}}{\text{W}}\right]$	2
R_{ij}	equivalent resistance between surface i and j $\left[\frac{\text{m}\cdot\text{K}}{\text{W}}\right]$	14, 15, 16

Ra_L	Rayleigh number based on characteristic length [–] 7, 8, 9
Re_D	Reynolds number based on characteristic diameter [–] 12
Re_L	Reynolds number based on characteristic length [–] 5, 6
$R_{w/wj}$	equivalent flux transfer resistance between fluid nodes i and j $\left[\frac{K}{W}\right]$ 3
t	time [s] 13
T	temperature [K] 13, 14, 15, 16, 18
V	volume of the material per unit of length $\left[\frac{m^3}{m}\right]$ 1
x	input variable [–] 20, 24
y	output value [–] 20, 22, 23
β	input variable coefficient [–] 20
e	optical emissivity [–] 18
θ	surface inclination [rad] 9
ϵ	error or residual [–] 20, 21
λ	wavelength [μm] 17
ρ	material mass density $\left[\frac{kg}{m^3}\right]$ or optical reflectivity [–] 1, 3, 13
σ	Stefan-Boltzmann constant: $5.6704 \cdot 10^{-8} \left[\frac{W}{m^2 K^4}\right]$ 18
τ	optical transmissivity [–] 18
∇	gradient operator [–] 13

References

[1] European Parliament. Directive 2010/31/EU of the European parliament and of the council of 19 may 2010 on the energy performance of buildings. *Off J Eur Union* 2010;153:13–35.

[2] ODYSSEE-MURE project. ODYSSEE and MURE database. 2014. www.odyssee-mure.eu. [Accessed 15 March 2017].

[3] Seyboth Kristin, Sverrisson F, Appavou F, Brown A, Epp B, Leidreiter A, et al. *Renewables 2016 global status report*. 2016.

[4] Hughes BR, Chaudhry HN, Ghani SA. A review of sustainable cooling technologies in buildings. *Renew Sustain Energy Rev* 2011;15:3112–20. <https://doi.org/10.1016/j.rser.2011.03.032>.

[5] Ahn H, Rim D, Freihaut JD. Performance assessment of hybrid chiller systems for combined cooling, heating and power production. *Appl Energy* 2018;225:501–12. <https://doi.org/10.1016/j.apenergy.2018.05.045>.

[6] European Commission. Decision of 1 March 2013 (2013/114/EU) establishing the guidelines for Member States on calculating renewable energy from heat pumps from different heat pump technologies pursuant to Article 5 of Directive 2009/28/EC of the European Parliament and of the. *Off J Eur Union* 2013;62:27–35.

[7] European Parliament. Directive 2009/28/EC of the European Parliament and of the Council of 23 April 2009 on the promotion of the use of energy from renewable sources and amending and subsequently repealing Directives 2001/77/EC and 2003/30/EC. *Off J Eur Union* 2009;140:16–62. <https://doi.org/10.3000/17252555.L.2009.140.eng>.

[8] Yin J, Shi L, Zhu MS, Han LZ. Performance analysis of an absorption heat transformer with different working fluid combinations. *Appl Energy* 2000;67:281–92. [https://doi.org/10.1016/S0306-2619\(00\)00024-6](https://doi.org/10.1016/S0306-2619(00)00024-6).

[9] Hassan HZ, Mohamad AA. A review on solar cold production through absorption technology. *Renew Sustain Energy Rev* 2012;16:5331–48. <https://doi.org/10.1016/j.rser.2012.04.049>.

[10] Michell D, Biggs KL. Radiation cooling of buildings at night. *Appl Energy* 1979;5:263–75.

[11] Bell EE, Eisner L, Young J, Oetjen RA. Spectral-Radiance of sky and terrain at wavelengths between 1 and 20 microns. II. Sky measurements. *J Opt Soc Am* 1960;50:1313–20. <https://doi.org/10.1364/JOSA.50.001313>.

[12] Berdahl P, Fromberg R. The thermal radiance of clear skies. *Sol Energy* 1982;29:299–314. [https://doi.org/10.1016/0038-092X\(82\)90245-6](https://doi.org/10.1016/0038-092X(82)90245-6).

[13] Zevenhoven R, Fält M. Radiative cooling through the atmospheric window: a third, less intrusive geoengineering approach. *Energy* 2018;152:27–33. <https://doi.org/10.1016/j.energy.2018.03.084>.

[14] Vall S, Castell A. Radiative cooling as low-grade energy source : a literature review. *Renew Sustain Energy Rev* 2017;77:1–18. <https://doi.org/10.1016/j.rser.2017.04.010>.

[15] Hu M, Zhao B, Ao X, Su Y, Wang Y, Pei G. Comparative analysis of different surfaces for integrated solar heating and radiative cooling: a numerical study. *Energy* 2018;155:360–9. <https://doi.org/10.1016/j.energy.2018.04.152>.

[16] Gao M, Han X, Chen F, Zhou W, Liu P, Shan Y, et al. Approach to fabricating

high-performance cooler with near-ideal emissive spectrum for above-ambient air temperature radiative cooling. *Sol Energy Mater Sol Cells* 2019;200:110013. <https://doi.org/10.1016/j.solmat.2019.110013>.

[17] Liu Q, Wu W, Lin S, Xu H, Lu Y, Song W. Non-tapered metamaterial emitters for radiative cooling to low temperature limit. *Opt Commun* 2019;450:246–51. <https://doi.org/10.1016/j.optcom.2019.05.061>.

[18] Jeong SY, Tso CY, Ha J, Wong YM, Chao CYH, Huang B, et al. Field investigation of a photonic multi-layered TiO2 passive radiative cooler in sub-tropical climate. *Renew Energy* 2020;146:44–55. <https://doi.org/10.1016/j.renene.2019.06.119>.

[19] Zhang K, Zhao D, Yin X, Yang R, Tan G. Energy saving and economic analysis of a new hybrid radiative cooling system for single-family houses in the USA. *Appl Energy* 2018;224:371–81. <https://doi.org/10.1016/j.apenergy.2018.04.115>.

[20] Zhao B, Hu M, Ao X, Pei G. Conceptual development of a building-integrated photovoltaic–radiative cooling system and preliminary performance analysis in Eastern China. *Appl Energy* 2017;205:626–34. <https://doi.org/10.1016/j.apenergy.2017.08.011>.

[21] Zhao B, Hu M, Ao X, Huang X, Ren X, Pei G. Conventional photovoltaic panel for nocturnal radiative cooling and preliminary performance analysis. *Energy* 2019;175:677–86. <https://doi.org/10.1016/j.energy.2019.03.106>.

[22] Hu M, Zhao B, Li J, Wang Y, Pei G. Preliminary thermal analysis of a combined photovoltaic–photothermic–nocturnal radiative cooling system. *Energy* 2017;137:419–30. <https://doi.org/10.1016/j.energy.2017.03.075>.

[23] Cavelius R, Isaksson C, Perednis E, Read GEF. *Passive cooling technologies*. Austrian Energy Agency; 2005.

[24] Eicker U, Dalibard A. Photovoltaic-thermal collectors for night radiative cooling of buildings. *Sol Energy* 2011;85:1322–35. <https://doi.org/10.1016/j.solener.2011.03.015>.

[25] Hu M, Zhao B, Ao X, Su Y, Pei G. Numerical study and experimental validation of a combined diurnal solar heating and nocturnal radiative cooling collector. *Appl Therm Eng* 2018;145:1–13. <https://doi.org/10.1016/j.applthermaleng.2018.08.097>.

[26] Mihalakakou G, Ferrante A, Lewis JO. The cooling potential of a metallic nocturnal radiator. *Energy Build* 1998;28:251–6. [https://doi.org/10.1016/S0378-7788\(98\)00006-1](https://doi.org/10.1016/S0378-7788(98)00006-1).

[27] Heidarinejad G, Farmahini-Farahani M, Delfani S. Investigation of a hybrid system of nocturnal radiative cooling and direct evaporative cooling. *Build Environ* 2010;45:1521–8. <https://doi.org/10.1016/j.buildenv.2010.01.003>.

[28] Zhang S, Niu J. Cooling performance of nocturnal radiative cooling combined with microencapsulated phase change material (MPCM) slurry storage. *Energy Build* 2012;54:122–30. <https://doi.org/10.1016/j.enbuild.2012.07.041>.

[29] Erell E, Etzion Y. Radiative cooling of buildings with flat-plate solar collectors. *Build Environ* 2000;35:297–305. [https://doi.org/10.1016/S0360-1323\(99\)00019-0](https://doi.org/10.1016/S0360-1323(99)00019-0).

[30] Bagiorgas HS, Mihalakakou G. Experimental and theoretical investigation of a nocturnal radiator for space cooling. *Renew Energy* 2008;33:1220–7. <https://doi.org/10.1016/j.renene.2007.04.015>.

[31] Ferrer Tevar JA, Castaño S, Garrido Marijuán A, Heras MR, Pistono J. Modelling and experimental analysis of three radiocooling panels for night cooling. *Energy Build* 2015;107:37–48. <https://doi.org/10.1016/j.enbuild.2015.07.027>.

[32] Sameti M, Kasaean A. Numerical simulation of combined solar passive heating and radiative cooling for a building. *Build Simul* 2015;8:239–53. <https://doi.org/10.1007/s12273-015-0215-x>.

[33] Raman AP, Anoma MA, Zhu L, Rephaeli E, Fan S. Passive radiative cooling below ambient air temperature under direct sunlight. *Nature* 2014;515:540–4. <https://doi.org/10.1038/nature13883>.

[34] Rephaeli E, Raman AP, Fan S. Ultrabroadband photonic structures to achieve high-performance daytime radiative cooling. *Nano Lett* 2013;13. <https://doi.org/10.1021/nl4004283>. A-E.

[35] Matsuda M, Terada S, Ito H. Solar Heating and radiative cooling using a solar collector-sky radiator with a spectrally selective surface. *Sol Energy* 1987;39:183–6.

[36] Erell E, Etzion Y. Heating experiments with a radiative cooling system. *Build Environ* 1996;31:509–17. [https://doi.org/10.1016/0360-1323\(96\)00030-3](https://doi.org/10.1016/0360-1323(96)00030-3).

[37] Plantier C, Fraisse G, Achard G. Development and experimental validation of a detailed flat-plate solar collector model. *ISES Sol. World Congr.* 2003;7. Göteborg, Sweden: 2003.

[38] Bergman TL, Lavine AS, Incropera FP, DeWitt DP. *Fundamentals of heat and mass transfer*. seventh ed. John Wiley & Sons; 2011.

[39] Pohlhausen E. *Der Wärmeaustausch zwischen festen Körpern und Flüssigkeiten mit kleiner reibung und kleiner Wärmeleitung*. ZAMM - Zeitschrift Für Angew Math Und Mech. In: Bergman TL, Lavine AS, Incropera FP, DeWitt DP, editors. *Fundamentals of heat and mass transfer*. seventh ed., vol. 1. John Wiley & Sons; 1921. p. 115–21. <https://doi.org/10.1002/zamm.19210010205>.

[40] Goldstein RJ, Sparrow EM, Jones DC. Natural convection mass transfer adjacent to horizontal plates. *Int J Heat Mass Transf.* In: Bergman TL, Lavine AS, Incropera FP, DeWitt DP, editors. *Fundamentals of heat and mass transfer*. seventh ed., vol. 16. John Wiley & Sons; 1973. p. 1025–35. [https://doi.org/10.1016/0017-9310\(73\)90041-0](https://doi.org/10.1016/0017-9310(73)90041-0).

[41] Lloyd JR, Moran WR. Natural convection adjacent to horizontal surface of various planforms. *J Heat Transfer.* In: Bergman TL, Lavine AS, Incropera FP, DeWitt DP, editors. *Fundamentals of heat and mass transfer*. seventh ed., vol. 96. John Wiley & Sons; 1974. p. 443–7. <https://doi.org/10.1115/1.3450224>.

- 2011.
- [42] Goldstein RJ, Lau K-S. Laminar natural convection from a horizontal plate and the influence of plate-edge extensions. *J Fluid Mech*. In: Bergman TL, Lavine AS, Incropera FP, DeWitt DP, editors. *Fundamentals of heat and mass transfer*, seventh ed., vol. 129. John Wiley & Sons; 1983. p. 55. <https://doi.org/10.1017/S0022112083000646>. 2011.
- [43] Fujii T, Honda H, Morioka I. A theoretical study of natural convection heat transfer from downward-facing horizontal surfaces with uniform heat flux. *Int J Heat Mass Transf*. In: Bergman TL, Lavine AS, Incropera FP, DeWitt DP, editors. *Fundamentals of heat and mass transfer*, seventh ed., vol. 16. John Wiley & Sons; 1973. p. 611–27. [https://doi.org/10.1016/0017-9310\(73\)90227-5](https://doi.org/10.1016/0017-9310(73)90227-5). 2011.
- [44] Hollands KGT, Unny TE, Raithby GD, Konicek L. Free convective heat transfer across inclined air layers. *J Heat Transfer*. In: Bergman TL, Lavine AS, Incropera FP, DeWitt DP, editors. *Fundamentals of heat and mass transfer*, seventh ed., vol. 98. John Wiley & Sons; 1976. p. 189–93. <https://doi.org/10.1115/1.3450517>. 2011.
- [45] Hausen H. Darstellung des Wärmeüberganges in Rohren durch verallgemeinerte Potenzbeziehungen. *Z VDI Beih Verfahrenstechnik*. In: Bergman TL, Lavine AS, Incropera FP, DeWitt DP, editors. *Fundamentals of heat and mass transfer*, seventh ed., vol. 4. John Wiley & Sons; 1943. p. 91. 2011.
- [46] Dittus FW, Boelter LMK. Heat transfer in automobile radiators of the tubular type. *Univ Calif Press Berkeley, Univ Calif Publ Eng*. In: Bergman TL, Lavine AS, Incropera FP, DeWitt DP, editors. *Fundamentals of heat and mass transfer*, seventh ed., vol. 2. John Wiley & Sons; 1930. p. 443–61. 2011.
- [47] Leon MA, Kumar S. Mathematical modeling and thermal performance analysis of unglazed transpired solar collectors. *Sol Energy* 2007;81:62–75. <https://doi.org/10.1016/j.solener.2006.06.017>.
- [48] Liu X, Huang J, Mao Q. Sensitive analysis for the efficiency of a parabolic trough solar collector based on orthogonal experiment. *Int J Photoenergy* 2015;2015:1–7. <https://doi.org/10.1155/2015/151874>.
- [49] Ji J, Lu JP, Chow TT, He W, Pei G. A sensitivity study of a hybrid photovoltaic/thermal water-heating system with natural circulation. *Appl Energy* 2007;84:222–37. <https://doi.org/10.1016/j.apenergy.2006.04.009>.
- [50] Ma F, Gao W, Liu T, Lin W, Li M. An experimental study on the impacts of key parameters of all-glass evacuated tubes on the thermal performances of all-glass evacuated tube solar water heaters. *J Renew Sustain Energy* 2013;5. <https://doi.org/10.1063/1.4803527>.
- [51] Njomo D, Daguinet M. Sensitivity analysis of thermal performances of flat plate solar air heaters. *Heat Mass Transf Und Stoffuebertragung* 2006;42:1065–81. <https://doi.org/10.1007/s00231-005-0063-9>.
- [52] Montgomery DC. Design and analysis of experiments, eighth ed., vol. 2. John Wiley & Sons, Inc.; 2012. <https://doi.org/10.1198/tech.2006.s372>.
- [53] Quartz glass properties n.d. <http://www.continentaltrade.com.pl/quartz-glass-500> (accessed October 28, 2017).
- [54] Polyethylene properties n.d. <https://people.csail.mit.edu/jaffer/FreeSnell/polyethylene.html> (accessed October 28, 2017).
- [55] Morris MD. Factorial sampling plans for preliminary computational experiments. *Technometrics* 1991;33:161–74. <https://doi.org/10.2307/1269043>.
- [56] Campolongo F, Cariboni J, Saltelli A, Schoutens W. Enhancing the Morris method. *Proc 4th Int Conf Sensit Anal Model Output* 2005:369–79.

Chapter 7. Combined Radiative Cooling and Solar Thermal Collection: Experimental Proof of Concept

7.1. Introduction

Although the tremendous radiative cooling research effort made in the literature, there are still some features that limit radiative cooling performance and need to be addressed [22]. Based on the numerical simulation research reviewed from literature, Chapter 4 presented some improvements: the recommendation of cover usage to reduce heat gains, the use of liquid instead of gas as internal fluid heat-carrier to permit control of the system, and the use of heat storage to reach higher cooling power densities. According to the experimental radiative cooling research literature reviewed in Chapter 4, radiative cooling presents applicability for some climates, thus leading up to combine radiative cooling with other technologies for profitability reasons.

The combination of radiative cooling with solar thermal collection in a unique device, here named Radiative Collector and Emitter, is an alternative to make radiative cooling devices profitable and ready to deploy into the new and existing building stock [72]. However, according to the literature reviewed in Chapter 4, there is a lack of a technology capable of producing both solar thermal collection and radiative cooling, caused by some limitations regarding suitable materials for both operation modes.

One major limitation is the undesired convective heat gain from ambient that with the use of a cover can be reduced [73]. However, both technologies use different materials, specially chosen with the desired optical properties.

For solar thermal collection, glass is the usual material because it allows solar radiation to pass through and blocks thermal radiation emitted by the surface of the collector [69]. There are materials with suitable optical properties for radiative cooling, but they are of

difficult availability or mechanically not suitable enough [74]. The extended cover material for radiative cooling is LDPE. The material suitability for both modes is difficult to achieve using a single material with constant optical properties. So, despite the performance benefits of using a cover, some of the existing research used no cover for experimental prototypes [75–77], or used a single material [78], thus limiting the performance of one of the modes.

Chapter 5 introduced and theoretically described a unique feature of RCE: the use of an adaptable cover, which may resolve the problem of finding, or developing, a material suitable for both modes.

Chapter 7 presents a Radiative Collector and Emitter prototype tested under real conditions. The prototype is a first approximation on using an adaptable cover to use two different materials to benefit both operating modes. The data collected and the presented results are to demonstrate the potential of this technology and validate the numerical model presented in Chapter 6.

7.2. Contribution to the state-of-the-art

Paper 4 presents a research on the design, construction and analysis of a Radiative Collector and Emitter (RCE) experimental device. The paper presents the empirical results of an RCE device using an adaptable cover, tested under real conditions to demonstrate its potential energy production and operation. The results proved the device to be capable of heating water during the day-time period and cooling down water below ambient temperature during the night-time period. Moreover, the research aims to discover patterns or behaviours not detected in numerical modelling to improve the technology.

As already explained in Chapter 6, in parallel with numerical modelling, an experimental RCE setup consisting of two flat plates was designed and built (Figure 12). The use of two different devices, one for each operational mode, was to simplify operation and for preliminary concept validation demonstration.

The experimental setup consisted of seven temperature sensors, for temperature measurements in the entrance and exit of each flat plate and storage tank, two flow meters

to evaluate water flow rates, and a Pyrheliometer for incoming atmospheric radiation measurements (Figure 13).

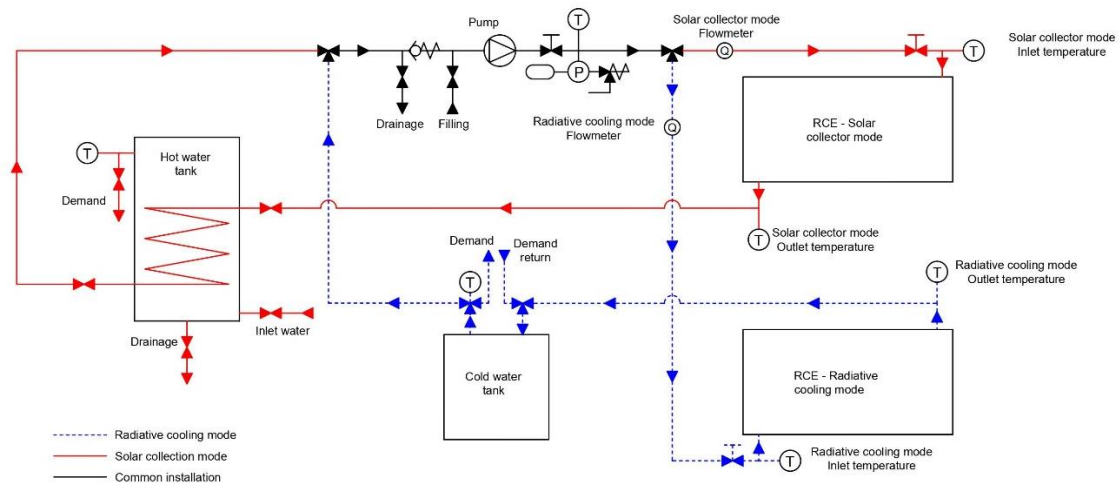


Figure 13 – Experimental setup sketch

A weather station placed close to the experimental setup measured the ambient temperature and the solar radiation. The experimental campaign was carried out during the summer period: from 31/07 to 04/08 in Lleida (Spain).

The experimental campaign allowed the study of the RCE concept under real conditions. The development of an adaptable cover system and the analysis of the transition period from one operation mode to the other were not in this research scope.

The experiments were carried out in summer, and particular interest was posed in radiative cooling. The results proved the ability of the RCE device to heat water during day-time period, with average temperature differences with the ambient of 8-25°C and average heating powers of 120-310 W/m², and to cool down water during night-time period, with average temperatures of 2-3.5°C below ambient and average powers of 22-50 W/m².

Paper 4 also presents two formulas (Eq. 4 and Eq. 5) to evaluate the performance of each operational mode, with particular importance given to the radiative cooling formula:

Solar Collection efficiency:

$$\text{Eq. 4} \quad \eta_{sc} = \frac{\int \dot{q}_{sc} \cdot dt}{A \cdot \int I \cdot dt}$$

Where:

- η_{sc} Solar collection efficiency [-].
- \dot{q}_{sc} Solar Collector (SC) mode device power [W].
- A Collector area [m²].
- I Solar Irradiation, in this case, GHI [W/m²].

Radiative Cooling efficiency:

$$\text{Eq. 5} \quad \eta_{rc} = \frac{\int \dot{q}_{rc} \cdot dt}{A \cdot \int R \cdot dt}$$

Where:

- η_{rc} Radiative cooling efficiency [-].
- \dot{q}_{rc} Radiative Cooling (RC) mode device power [W].
- A Collector area [m²].
- R Effective outgoing infrared Radiation [W/m²] (Eq. 6):

$$\text{Eq. 6} \quad R = R_{\uparrow} - R_{\downarrow} = (\varepsilon \cdot \sigma \cdot T_{rc}^4 - R_{\downarrow})$$

Where:

- R_{\downarrow} Incoming Radiation [W/m²].
- R_{\uparrow} Radiative cooler surface emitted infrared radiation [W/m²].
- ε Radiator emissivity/absorptivity [-].
- σ Stefan-Boltzmann constant, $5.67 \cdot 10^{-8}$ [W/m²/K⁴].
- T_{rc} Radiator temperature (average inlet/outlet) [K].

These formulas (Eq. 4 and Eq. 5) improve another proposed procedure by Hu et al. [44], by using RCE surface temperature instead of ambient temperature, thus becoming a device efficiency formula. This value may help to detect how good the performance is by standardising the results between different devices and allowing the comparison between

them. The prototype achieved average efficiencies up to 49% for solar thermal collection and 32% for radiative cooling.

According to the radiative cooling results, the RCE device cannot provide low-temperature levels (7-12°C) nor good efficiencies (SEER 2-5) as other cooling technologies do. However, this cooling is produced with low energy consumption, and it can be used as a cooling source, thus reducing the use of non-renewable energy. For instance, the cooled water can be used as a direct source, or as an indirect source, used as a heat sink for other technologies, thus improving its efficiency.

During the experiments, dew formation occurred on both sides of the cover, with special care in the inner side. This effect causes emission blockage and may be more problematic in humid climates. Some solutions, such as creating the vacuum in the gap between emitter and windscreen, can eliminate or mitigate the dew formation.

7.3. Contribution to the objectives of the PhD thesis

Chapter 70 contributes to accomplishing objective V by presenting in paper 4 the design, construction and testing of an experimental RCE device tested under real conditions. Paper 4 also evaluates and discusses the results that served to validate the numerical model presented in Chapter 6.

7.4. Journal Paper




Reference:

S. Vall, M. Medrano, C. Solé, and A. Castell, “Combined Radiative Cooling and Solar Thermal Collection: Experimental Proof of Concept,” *Energies*, vol. 13, no. 4, p. 893, 2020. DOI:10.3390/en13040893.



Article

Combined Radiative Cooling and Solar Thermal Collection: Experimental Proof of Concept

Sergi Vall , Marc Medrano , Cristian Solé and Albert Castell * 

Sustainable Energy, Machinery and Buildings (SEMB) Research Group, INSPIRES Research Centre, Universitat de Lleida, Pere de Cabrera s/n, 25001 Lleida, Spain; svall@diei.udl.cat (S.V.); mmedrano@diei.udl.cat (M.M.); csole@diei.udl.cat (C.S.)

* Correspondence: acastell@diei.udl.cat

Received: 29 December 2019; Accepted: 14 February 2020; Published: 18 February 2020



Abstract: Climate change is becoming more important day after day. The main actor to decarbonize the economy is the building stock, especially in the energy used for Domestic Hot Water (DHW), heating and cooling. The use of renewable energy sources to cover space conditioning and DHW demands is growing every year. While solar thermal energy can cover building heating and DHW demands, there is no technology with such potential and development for space cooling. In this paper, a new concept of combining radiative cooling and solar thermal collection, the Radiative Collector and Emitter (RCE), through the idea of an adaptive cover, which uses different material properties for each functionality, is for the first time experimentally tested and proved. The RCE relies on an adaptive cover that uses different material properties for each functionality: high spectral transmittance in the solar radiation band and very low spectral transmittance in the infrared band during solar collection mode, and high spectral transmittance in the atmospheric window wavelength during radiative cooling mode. Experiments were performed during the summer period in Lleida (Dry Mediterranean Continental climate). The concept was proved, demonstrating the potential of the RCE to heat up water during daylight hours and to cool down water during the night. Daily/nightly average efficiencies up to 49% and 32% were achieved for solar collection and radiative cooling, respectively.

Keywords: radiative cooling; solar thermal collection; renewable energy; low-grade energy source; building integration; experimental setup

1. Introduction

The effects of climate change are becoming more dangerous and destructive day after day. This subject is in the public eye and governments are taking actions on this matter. To mitigate or reverse these effects, long-term greenhouse gas emissions goals are being set. One of the main actors to decarbonize the economy is the building stock, responsible for 36% of all CO₂ emissions in the EU. Special consideration must be taken in the energy used for heating and cooling which is up to 50% of the final energy consumption (80% of which in buildings). This is why special efforts are being made in renovating the current building stock by energy efficiency means as well as considering the deployment of renewables [1].

The use of renewable energy sources to cover space conditioning and Domestic Hot Water (DHW) demands seems more likely over the years. While solar thermal energy can cover building heating and DHW demands [2], there is not yet a technology with such potential and development for space cooling. In fact, despite the existence of a few renewable cooling technologies, they present significant limitations [3].

Compression and absorption heat pumps are the main technologies for cooling purposes, compression heat pumps being the most common. These devices consume large amounts of electricity,

although they are considered renewable sources under certain circumstances [4,5]. On the other hand, absorption heat pumps may use solar energy as driving heat, but they present some important disadvantages such as, low efficiency, a need of high temperatures ($>100\text{ }^{\circ}\text{C}$), large equipment sizes and the need for auxiliary equipment such as a cooling tower (which increases the cost of the installation and can result in health problems such as legionella) [6].

Alternatively, radiative cooling is a renewable cooling technology that can complement conventional cooling systems. Radiative cooling uses the sky as a heat sink, benefiting from its effective temperature which is much lower than ambient temperature. Energy can be dissipated to the sky taking advantage of the infrared atmospheric window ($7\text{--}14\text{ }\mu\text{m}$). This window allows infrared radiation to pass directly to outer space without intermediate absorption and re-emission in the atmosphere. Heat dissipation is produced by longwave radiation (thermal radiation) from a surface to the sky. The sky temperature during the night can be lower than $0\text{ }^{\circ}\text{C}$ or even $-10\text{ }^{\circ}\text{C}$ [7], allowing temperatures suitable for cooling. However, this phenomenon is a priori only valid during the night, since during the day solar radiation (shortwave radiation) is higher and the radiation balance results in thermal gains (heating). The sky temperature can be related to the ambient temperature using sky emissivity [8].

Radiative cooling technology attracted a lot of attention in the 1970s, with lots of papers published. However, the lack of suitable materials and solutions in order to reduce the heat gains limited its development. Most of the research done up-to-date has focused in the development of correlations and numerical models to determine the effective temperature of the sky and/or the emissivity of the sky [9–12], in the search of selective materials suitable for the dissipation of radiation at certain wavelengths [13–16] and in the evaluation of some specific radiative cooling devices [17–20].

Etzion and Erell [21] highlighted as one of the limitations for the potential of radiative cooling the effect of ambient air on the radiative surface. The cooling potential of the surface allows reaching temperatures much lower than the ambient ones; however, the heat transfer by convection from the ambient air to the radiative cooler reduces its potential. Although different covers transparent to thermal radiation have been studied, there are still some thermal gains that reduce the potential of radiative cooling.

Bathgate and Bosi [22] determined the potential of a radiative cooling device (based on the optical properties of the materials) for different materials and radiator temperatures. They observed that certain selective materials achieved higher power (even doubling it) than using no selective material (black body).

More recently, significant developments have been achieved in the field of materials capable to produce radiative cooling during both night and daytime. In 2013, Rephaeli et al. were the first ones to develop such a material [23,24]. Later on, other materials were developed with similar properties [25–29]. This demonstrates the huge interest and potential of radiative cooling as a renewable technology.

Even with the great research effort done [30], radiative cooling is not a technology mature enough. No commercial device has reached the market yet. The main drawback is its low available cooling power density (between 20 and 80 W/m^2) [31], with peak values of 120 W/m^2 [32] or even higher with new metamaterials (199 W/m^2 in [33]). Therefore, improvements are needed to make radiative cooling feasible. A potential improvement is the coupling of radiative cooling and solar thermal collection in a single device. This new concept will be able to produce both heat and cold, thus improving its feasibility to reach the market. Despite that these two technologies use different types of radiation (different wavelengths), it is possible to couple them as they are not used at the same time, so there is no interference between them; solar collection works during sunlight hours whereas radiative cooling is more effective at night.

Little research has been done in the combination of both solar collection and radiative cooling in a single device, and most of them only characterized the heat produced by a radiative cooler, but did not intend to design and evaluate a device suitable for both functions. Erell and Etzion identified some

of the main differences between a solar collector and a radiative cooler [18]. They highlighted, apart from the cover material, that the radiative cooler needs a pump to circulate the fluid, while the solar collector can in some cases rely on the thermosiphon effect. On the other hand, the effects of convective heat transfer in a solar collector are always negative, since the fluid is always warmer than the ambient. This is not always the case for the radiative cooler, since the air can be used as a cold source during some moments during the night. Finally, they also highlighted that the geometry pipe-fin of a solar collector is not necessarily the best one for a radiative cooler, as they demonstrated numerically.

Erell and Etzion [34] in 1996 used a radiative cooler to perform some experiments under winter conditions to produce heat. Results showed the capacity of the device to produce heat, considering that the system was designed to produce cold and that it had no cover. The main limitation is that, although radiative cooling devices are very similar in shape as solar collectors, their behavior is completely opposed. While the solar collector operates during the sunlight hours to collect shortwave radiation, the radiative cooler operates during night time emitting longwave radiation. This difference in the radiation wavelength means that conventional covers used in solar collectors are not suitable for radiative cooling (since they do not allow longwave radiation to pass through). This and other limitations found by [34] are nowadays of great interest due to the advances in material development and heat transfer optimization. Similar experiments were done more recently by Hosseinzadeh and Taherian [35] and by Xu et al. [36]. However, in all the studies, no cover was used, dramatically limiting the efficiency of the device.

Vall et al. [37] studied the potential of a new concept consisting of combining solar collection and radiative cooling to partially cover the DHW and cooling demands for different typologies of buildings located in different climates. The new concept showed suitability in some of the studied cities with C (temperate) and D (continental) climates in residential and tertiary buildings.

As stated before, new materials have been recently developed for day-long radiative cooling. However, these materials still present the limitation that they do not allow solar collection at the same time. In 2015, Hu et al. [38] developed a spectral selectivity surface suitable for both solar collection and radiative cooling. The new surface, the TPET, presents high absorptivity/emissivity in both the solar radiation and atmospheric window bands. However, this material will also emit in the atmospheric window band during solar radiation collection, which can diminish the heat collection. Moreover, Hu et al. did not consider the radiative properties of the cover of the solar collector/radiative cooler, using polyethylene as cover, which will reduce the efficiency during solar collection mode due to the high emissivity in the near-infrared wavelength [39].

Thus, a research gap is found in the lack of a technology capable of producing both solar collection heating and radiative cooling (RCE).

In this paper, the new concept of combining radiative cooling and solar thermal collection, which is mentioned as Radiative Collector and Emitter (RCE), is presented and experimentally tested. The new concept relies on an adaptive cover that uses different material properties for each functionality: radiative cooling and solar thermal collection. The adaptive cover will provide high spectral transmittance in the solar radiation band and very low spectral transmittance in the infrared band during the solar collection mode, and high spectral transmittance in the atmospheric window wavelength during radiative cooling mode. This innovation will result in a novel approach, based on the adaptive cover and not the collecting/radiating surface, to combine radiative cooling and solar heating.

The purpose of this research and its main novelty is to prove experimentally, for the first time, the RCE concept through the idea of an adaptive cover, which uses different material properties for each functionality: radiative cooling and solar thermal collection. This will contribute to taking the first step in its potential introduction to the market.

2. Experimental Setup

The experimental setup consisted of a solar collector, a radiative cooler, 2 water tanks, a water pump, 6 temperature sensors, 2 flow meters, a pyrogeometer and the control and data acquisition systems. The acquisition data equipment consisted of a data logger (model DIN DL-01-CPU), connected to the adapter data logger-computer (model AC-250). The computer software to compile the data was STEP TCS-01. The solar collector used was model FUJI-P. It was a $2\text{ m} \times 1\text{ m} \times 80\text{ mm}$ aluminum frame collector, with a transparent 3 mm glass and 30 mm glass-wool back insulation. The collector has 8 copper pipes of 8 mm internal diameter and 0.6 mm thick. In a similar way, radiative cooler is in fact a modified version of the same solar collector (FUJI-P), having replaced the glass screen by a 0.6 mm thick polyethylene (PE) film and having painted the surface of the radiator with black paint in order to adapt it to the required characteristics of radiative cooling mode (Figure 1). They were located one next to the other, on the horizontal plane.

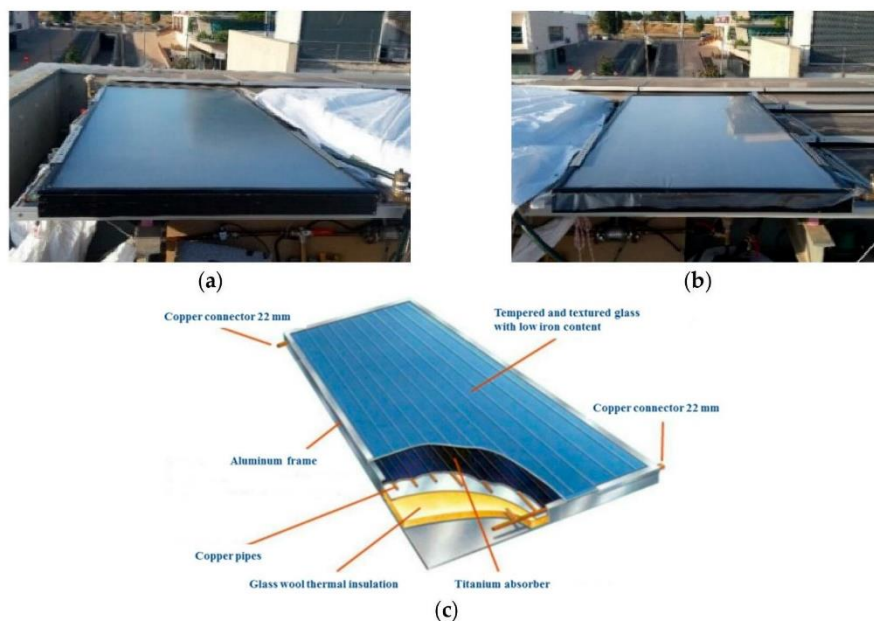


Figure 1. (a) Solar collector; (b) modified solar collector used as a radiative cooling device; (c) Structure of the solar collector FUJI-P (adapted from manufacturer’s technical data [40]).

For the sake of simplification, two separate devices were used instead of a single RCE device. This was sufficient to provide accurate data for concept validation, which was the main objective of this research. Four temperature sensors (Pt-100, with an accuracy of $\pm 0.045\text{ }^{\circ}\text{C}$) were used to monitor the inlet and outlet water temperature of the solar collector and the radiative cooling device. Water flow rates were monitored using a flowmeter for the operation under solar collection mode (Badger Meter-Primo Advanced, 0.25% accuracy), and a flowmeter for the radiative cooling mode (Schmidt Mess-SDNC 503 GA-20, 4% accuracy). Weather data was extracted from a nearby weather station, with the exception of the incoming infrared radiation, which was measured using a pyrogeometer on-site (LP PIRG 01-DeltaOhm, 5% accuracy). All the data from the experiment were registered and recorded at a time-frequency resolution of 1 min. A sketch of the experimental setup is presented in Figure 2.

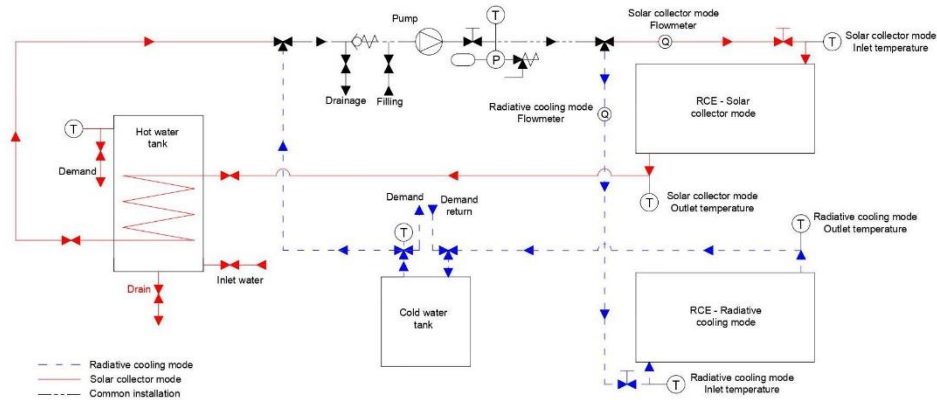


Figure 2. Sketch of the experimental setup.

The film used for the radiative cooler was chosen among different kinds of plastic foils, namely polymethylmethacrylate (PMMA), low-density polyethylene (PELD) and high-density polyethylene (PEHD). Their optical properties were analyzed in the whole spectrum of solar and IR radiations. Three different spectrophotometers were used to cover the UV-vis, the near IR and the far IR spectrum ranges. They were the UV Analytikjena specord 210, the Foss NIR XDS Rapid Content Analyzer and the Jasco FT-IR 6300 series, respectively. PELD film was finally chosen, as it was the most transparent in the infrared band of the electromagnetic radiation. Table 1 shows the resulting mean transmittance in the three measured spectrum ranges for the selected PELD film.

Table 1. Measured mean transmittance for the selected low-density polyethylene (PELD) film.

	UV-Vis	NIR	FT-IR
Range	(0.19–1.1 μm)	(0.4–2.5 μm)	(2.5–15.5 μm)
Mean Transmittance	0.88	0.84	0.98

3. Methodology

3.1. Description of the Experimental Campaign

Experiments were performed for several days combining solar collection mode (from 8.00 to 20.00 h) and radiative cooling mode (from 21.00 to 7.00 h). The experiments were performed during the summer period in Lleida (Dry Mediterranean Continental climate). Specifically, the experimental campaign consisted of two periods; the first one from 26th to 28th July 2017 and the second one from 31st July to 4th August 2017.

The tests were always performed in the same way. Early in the morning, several valves were set to the solar collection mode and the pump was started, so that the water in the secondary circuit, initially in thermal equilibrium with the ambient, could circulate through the RCE and heat up. This water flowed then through the internal heating coil of the hot tank, heating up the water in the tank, which was as well at ambient temperature at the beginning. All the experimental variables were monitored and registered every minute in the data logger. The cloudiness of the sky was observed visually along the day, together with the information about clouds on the online local weather station. After sunset, the set of valves was changed to radiative cooling mode, and then water in the cold tank, initially at ambient temperature, was circulated directly to the RCE, starting the cooling process thanks to the radiative heat transfer to the night sky. As cooling powers are much lower than the heating powers during the day, to prevent heat losses and maximize the cold output, only a primary circuit was used between the cold water tank and the RCE. The water flowrates were kept constant during each test,

although some fluctuations due to the pump operation were observed along the day, with maximum deviations of 25% with respect to the average value (see Table 2). In the second period, the flow rate at night was reduced to about 60% of the daily value to increase the inlet–outlet temperature difference and reduce in that way the uncertainty of the calculated cooling power. The tested range of flow rates was 0.5–1.9 L/min.

Table 2. Operating characteristics of the testing days.

	Date/Hour of Test	Test Label	Clear or Cloudy	Average Volumetric Flow Rate (L/min)
First period	26/07/17 (13:00–20:00)	Day 1.1	Clear	1.36 ± 0.07
	26/07/17 (21:00)–27/07/17 (7:00)	Night 1.1	Clear	1.30 ± 0.02
	27/07/17 (8:00–20:00)	Day 1.2	Clear	1.25 ± 0.2
	27/07/17 (21:00)–28/07/17 (7:00)	Night 1.2	Clear	1.29 ± 0.02
	28/07/17 (8:00–18:00)	Day 1.3	Clear	1.89 ± 0.51
Second period	31/07/17 (8:30–20:00)	Day 2.1	Clear	1.42 ± 0.1
	31/07/17 (21:00)–01/08/17 (7:00)	Night 2.1	Clear	0.63 ± 0.01
	01/08/17 (8:00–20:00)	Day 2.2	Cloudy	1.34 ± 0.14
	01/08/17 (21:00)–02/08/17 (7:00)	Night 2.2	Cloudy	0.56 ± 0.01
	02/08/17 (8:00–20:00)	Day 2.3	Cloudy	1.36 ± 0.09
	02/08/17 (21:00)–03/08/17 (7:00)	Night 2.3	Cloudy	0.57 ± 0.01
	03/08/17 (8:00–20:00)	Day 2.4	Clear	1.34 ± 0.15
	03/08/17 (21:00)–04/08/17 (7:00)	Night 2.4	Clear	0.52 ± 0.02

During the cooling mode, the hot water tank was discharged to ambient temperature using an air–water fin heat exchanger. The same process was used to discharge the cold stored during the night in the cold tank.

The first testing period turned out to be a clear sky period, while the second one combined clear and cloudy days. The details of the testing days, including the operating dates and hours, the day labels and the flow rates used are presented in Table 2.

3.2. Determination of Performance Parameters

To evaluate the performance of the RCE, production rates for both solar collection and radiative cooling were calculated (Equation (1)), as well as efficiencies (Equations (2) and (3)).

$$\dot{q} = v \times \rho \times c_p \times \Delta T \quad (1)$$

where:

\dot{q} is the power of the device (W).

v is the volumetric flow rate (m^3/s).

ρ is the density of the fluid (kg/m^3).

c_p is the heat capacity of the fluid ($\text{J}/\text{kg}\cdot\text{K}$).

ΔT is the temperature difference between inlet flow T_{in} and outlet flow T_{out} (K).

Solar Collection efficiency:

$$\eta_{sc} = \frac{\int \dot{q}_{sc} dt}{A \int I dt} \quad (2)$$

where:

η_{sc} is the solar collection efficiency (-).

\dot{q}_{sc} is the power of the device in Solar Collector (SC) mode (W).

A is the collector area (m^2).

I is the Solar Irradiation; in this case, Global Horizontal Solar Irradiation (W/m^2).

Radiative Cooling efficiency: The efficiency for the radiative cooling mode is based on the one presented in [41] but considering the surface temperature of the RCE device instead of ambient temperature to determine the infrared radiation emitted in the effective outgoing infrared radiation term.

$$\eta_{rc} = \frac{\int \dot{q}_{rc} dt}{A \int R dt} \quad (3)$$

where:

η_{rc} is the radiative cooling efficiency (-).

\dot{q}_{rc} is the power of the device in Radiative Cooling (RC) mode (W).

A is the collector area (m²).

R is the effective outgoing infrared radiation (W/m²).

The value of R is determined as the difference between the infrared radiation emitted by the radiative cooler surface (R_{\uparrow}) and the infrared radiation from the atmosphere (sky) absorbed by this surface (R_{\downarrow}):

$$R = R_{\uparrow} - R_{\downarrow} = (\varepsilon \times \sigma \times T_{rc}^4 - R_{\downarrow}) \quad (4)$$

where:

R_{\downarrow} is the Incoming Radiation (measured on-site) (W/m²).

R_{\uparrow} is the infrared radiation emitted by the radiative cooler surface (W/m²).

ε is the ideal radiator emissivity/absorptivity, in this case 1 (-).

σ is the Stefan–Boltzmann constant, 5.67×10^{-8} (W/m² K⁴).

T_{rc} is the temperature of the radiator (average inlet/outlet) (K).

This radiative cooling net balance of the surface, R , is considered the maximum potential for radiative cooling of the RCE, and should be compared with the actual cooling power that is transferred to the water, \dot{q}_{rc} , to evaluate the radiative cooler efficiency during the night (Equation (3)).

The uncertainty of the above presented experimental parameters (Equations (1)–(3)) have been calculated as a function of the direct measured variables (namely, inlet water temperature T_{in} , outlet water temperature T_{out} , volumetric flow rate v , solar irradiation I and incoming IR radiation R_{\downarrow}) and their associated accuracy. The heat capacity c_p and the density ρ values for water are taken from the literature at the average RCE temperature. Applying the standard method for uncertainty propagation [42], the calculated uncertainty for heating power (day), cooling power (night), solar collector efficiency and radiative cooler efficiency are 3%, 8%, 3% and 20%, respectively. Special care was taken in the selection of instruments with the lowest uncertainties possible, as the low radiative cooling powers at nights made them more critical to finally obtain reasonable uncertainties.

4. Results and Discussion

In the following section direct measurement and calculated parameters for the RCE testing periods are presented and discussed.

4.1. Direct Measurements and Testing Observations

During the first period, the meteorology was stable with all-day clear and sunshine. The outdoor temperature oscillated from 19 to 40 °C, with Global Horizontal Irradiation (GHI) peak values up to 960 W/m², average values of 670 W/m² and Incoming Infrared Radiation average values of 340 W/m². In the second period, the meteorology was stable with some cloudy days and the outdoor temperature oscillated from 23 to 42 °C, with GHI peak values up to 935 W/m², a GHI average value of 539 W/m² and Incoming Infrared Radiation average values of 355 W/m².

In the first testing period, mainly under clear sky conditions, the RCE was capable to produce heat, reaching maximum outlet temperature values of 64 °C (Figure 3), achieving average temperature differences between the outlet water (T_{out}) and the ambient (T_{amb}) around 17–22 °C (Table 2). In the second period, with both cloudy and clear days, the RCE produced heat as well, reaching maximum

outlet temperature values of 67 °C for the two clear days, but lower values the other two days (47–60 °C). The average temperature differences between the outlet water and the ambient in this period were around 8–14 °C (Table 2).

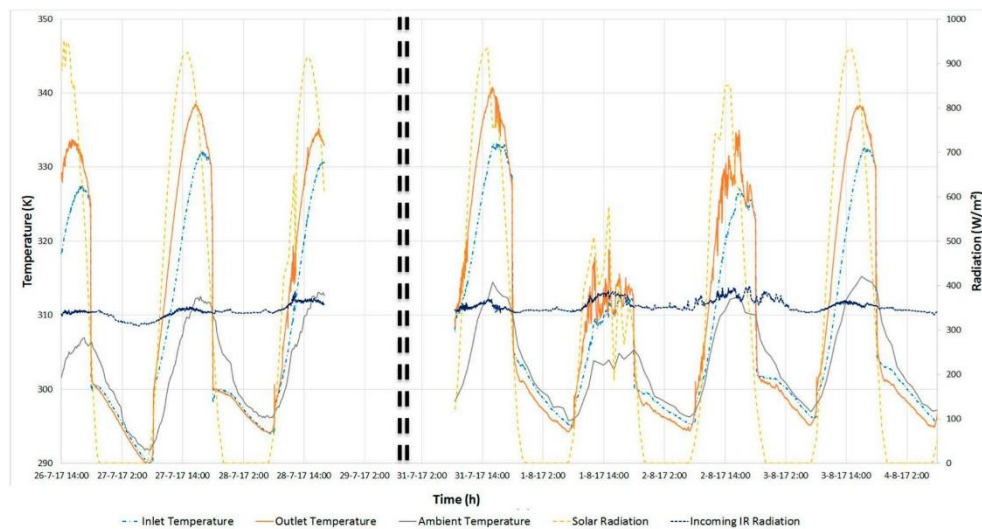


Figure 3. Experimental results of the Radiative Collector and Emitter (RCE) concept.

The measured incoming sky IR radiation remained very stable along the two test periods, in a range 310–400 W/m², with slightly higher values during the days and in cloudy periods, and more oscillations in cloudy periods (Figure 3).

On the other hand, the RCE also showed the capability to produce cold water, reaching minimum outlet water temperatures close to 16 °C in the first period and of 20 °C in the second one (Figure 3), with average temperature differences between the outlet water and ambient around 2–3 °C (Table 2).

Apart from measured data, other empirical details were observed. In some occasions, the radiative emitter presented dew or water moisture attached to the inner part of the plastic foil. This phenomenon was observed during the morning inspection and it was not possible to determine when it occurs as well as the effects on the performance. Despite the effects were not quantified, it reduces the performance of the system because the water film becomes the radiating surface [43]. This effect blocks the direct contact between the surface of the radiator and the sky.

4.2. Heating and Cooling Powers for RCE

Figure 4 shows the calculated heating and cooling power produced by the RCE during the two testing periods (see Equation (1)). Note that for the sake of clarity the cooling power scale (right vertical axis) is one order of magnitude smaller than the heating power scale (left vertical axis) and the absolute value is used for cooling, skipping the negative sign. In the first clear sky period average heating powers of 290–315 W/m² are achieved, with peak values above 500 W/m², whereas in the second period, the average heating powers are smaller (range 120–290 W/m²), with a peak of 539 W/m² in Day 6 (Figure 4 and Table 3). Daily average solar collector efficiencies of 0.43–0.49 are achieved in the first period, while in the second period they are slightly lower, in the range 0.34–0.46 (Table 3). Regarding the cooling power at nights, average values between 13–34 W/m² were achieved, with peak powers above 46 W/m² on Day 4 (Figure 4 and Table 3). Average radiative cooling efficiencies in the range 0.12–0.32 were obtained (Table 3).

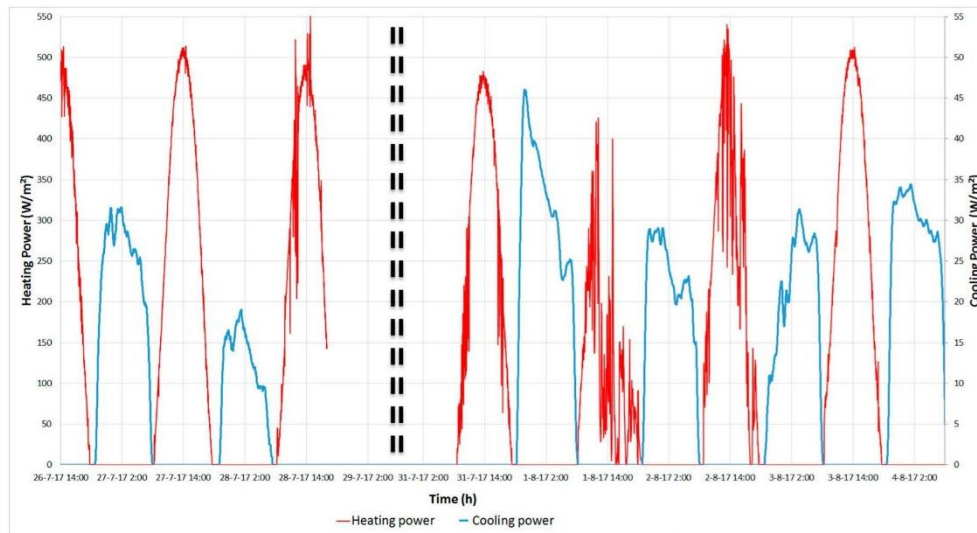


Figure 4. Available heating and cooling power from the RCE concept.

Table 3. Average and peak power produced, average temperature difference and average efficiency by the RCE for both heat and cold production.

Test Period	Heating Power, \dot{q}_{sc} (W/m ²)		Cooling Power, \dot{q}_{rc} (W/m ²)		Average (T _{out} - T _{amb}) (K)		Average Efficiency (%)	
	Average	Peak	Average	Peak	Heating	Cooling	Heating, η_{sc}	Cooling, η_{rc}
Day 1.1	313.3	545.5	-	-	24.98	-	43	-
Night 1.1	-	-	26.04	36.3	-	-2.14	-	24
Day 1.2	293.5	513.8	-	-	19.68	-	46	-
Night 1.2	-	-	12.63	22.5	-	-2.68	-	12
Day 1.3	310.7	583.3	-	-	13.84	-	49	-
Day 2.1	265.7	482.9	-	-	20.65	-	42	-
Night 2.1	-	-	33.35	48.5	-	-2.47	-	32
Day 2.2	122.9	425.7	-	-	8.16	-	34	-
Night 2.2	-	-	23.84	31.6	-	-2.56	-	26
Day 2.3	238.6	538.5	-	-	12.95	-	46	-
Night 2.3	-	-	22.69	33.9	-	-2.62	-	24
Day 2.4	293.0	512.7	-	-	15.71	-	46	-
Night 2.4	-	-	30.64	36.2	-	-3.44	-	28

4.3. Maximum Potential for Cooling

Figure 5 shows the calculated effective IR radiation from the RCE to the sky, which gives the maximum potential for cooling for the RCE. The incoming IR radiation measured by the pyrgeometer and the calculated outgoing IR radiation from the RCE surface (see Equation (4)) are included as well. It is interesting to notice that the potential for cooling increases a lot in the RCE during the day. This is due to the fact that the RCE is working as a solar collector at that time, and the temperature of the absorber/emitter surface is quite high (40–70 °C) and, thus, the capacity to irradiate to the sky increases above 350 W/m² of cooling power. However, the glass cover blocks this potential IR radiation to the sky. The importance of the proposed adaptive cover is highlighted here also for the heating operating mode. If only the PE film was used as cover, this cooling power would be mostly radiated to the sky through the PE film and the solar collector efficiency of the RCE would substantially decrease.

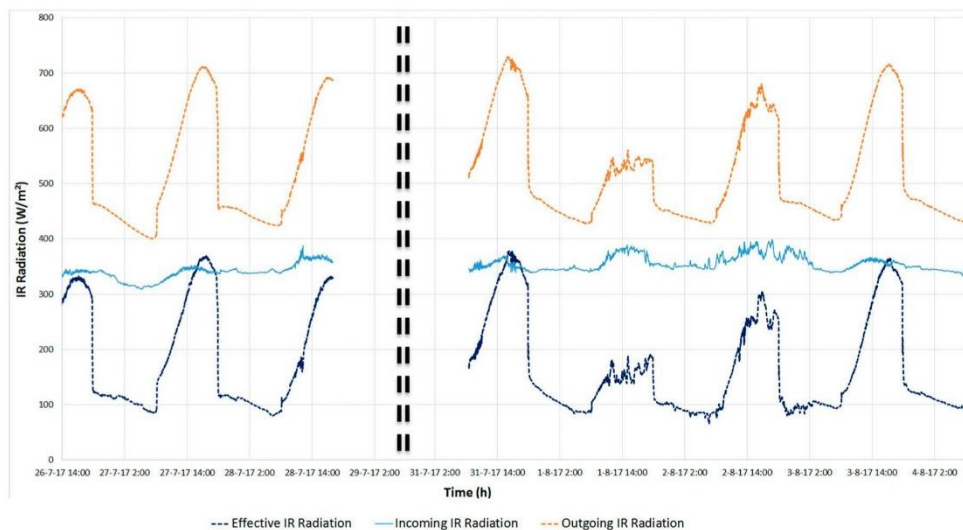


Figure 5. Incoming, outgoing and net effective radiation of the RCE concept.

5. Conclusions

The present research designed, constructed and analyzed experimentally the concept of the combined renewable production of heating and cooling via thermal collection and sky radiative cooling in a single device, the Radiative Collector and Emitter (RCE) device. It proved the concept and showed the potential to be introduced in buildings as an active system for heating and cooling. The results demonstrate the potential of the RCE concept to heat up water during daylight hours and to cool down water during the night.

Along the tested days, the RCE device produced peak heating power values up to 583 W/m^2 during the day, with average efficiencies up to 49%. During the night the RCE achieved peak cooling powers of 33 W/m^2 , with average cooling efficiencies up to 32%. When compared to other cooling technologies such as electrically driven compression water chillers, RCE is not able to provide the same low temperature levels ($7\text{--}12 \text{ }^\circ\text{C}$) or efficiencies (SEER of 2–5). It is important to bear in mind that chillers and other existing cooling technologies consume non-renewable primary energy whereas the RCE is driven by renewable primary energy. When primary energy is considered, RCE average cooling efficiencies are in the same order of magnitude than those of electrically driven compression water chillers (80%–100%, based on a Primary Energy Factor of 2.5 [44]). Thus, the wise decision in a building with both technologies would be to give priority to the RCE, even with a low performance, and then complement the demand and/or temperature level shortcomings with the compression chillers.

Although improvements are required in order to maximize the cold production and reach useful temperature levels, this first RCE prototype has proven the concept of cooling down water below ambient temperature by the use of sky night radiation, while heating up water during the day.

Special attention was put on the radiative cooling mode. Even if it was not the best season for radiative cooling mode, with shorter periods of nighttime, it is in summer when it makes sense to produce cold. The cold produced during the night can be used either as a direct cooling source or as a heat sink for other cooling technologies (such as heat pumps) in order to improve its efficiency, thus reducing the use of non-renewable energies. However, further improvements are required to take full advantage of this new concept.

A negative effect was observed during experimental testing. The formation of dew was on both sides of the cover, but especially in the inner side. The dew on the inner (and outer) side of the cover can be a problem for the performance of the system, especially in humid climates. However, some

solutions such as creating a vacuum between the radiator surface and the cover can eliminate or mitigate its effects.

Future research will address the first prototype of the single RCE device, with a practical solution for an automatically controlled adaptive cover.

Author Contributions: Conceptualization, S.V., A.C. and C.S.; methodology, A.C. and S.V.; formal analysis, S.V. and M.M.; investigation, S.V. and C.S.; data curation, S.V. and M.M.; writing—S.V.; writing—review and editing, M.M., A.C. and C.S.; visualization, S.V. and M.M.; supervision, A.C.; project administration, A.C.; funding acquisition, A.C. All authors have read and agreed to the published version of the manuscript.

Funding: This research was funded by the Oficina de Desenvolupament i Cooperació (ODEC), the Catalan Government (AGAUR–Generalitat de Catalunya) under grant agreement 2017 SGR 659, the Spanish government (Ministerio de Ciencia, Innovación y Universidades) under grant agreement RTI2018-097669-A-I00.

Acknowledgments: The authors would like to thank the Oficina de Desenvolupament i Cooperació de la Universitat de Lleida for the project grant. The authors would like to thank the Catalan Government for the quality accreditation given to their research group (2017 SGR 659). The work was partially funded by the Spanish government under grant agreement RTI2018-097669-A-I00 (Ministerio de Ciencia, Innovación y Universidades). Sergi Vall would like to thank the Secretaria d'Universitats i Recerca del Departament d'Economia i Coneixement de la Generalitat de Catalunya for the research fellowship.

Conflicts of Interest: The authors declare no conflicts of interest. The funders had no role in the design of the study; in the collection, analyses, or interpretation of data; in the writing of the manuscript, or in the decision to publish the results.

References

1. European Parliament. Directive (EU) 2018/844 of the European Parliament and of the Council of 30 May 2018 amending Directive 2010/31/EU on the energy performance of buildings and Directive 2012/27/EU on energy efficiency (Text with EEA relevance). *Off. J. Eur. Union* **2018**, *156*, 75–91. [CrossRef]
2. Kristin, S.; Sverrisson, F.; Appavou, F.; Brown, A.; Epp, B.; Leidreiter, A. *Renewables 2016 Global Status Report; Ren21*: Paris, France, 2016. Available online: https://www.ren21.net/wp-content/uploads/2019/05/REN21_GSR2016_FullReport_en_11.pdf (accessed on 1 June 2018).
3. Hughes, B.R.; Chaudhry, H.N.; Ghani, S.A. A review of sustainable cooling technologies in buildings. *Renew. Sustain. Energy Rev.* **2011**, *15*, 3112–3120. [CrossRef]
4. European Commission. Decision of 1 March 2013 (2013/114/EU) establishing the guidelines for Member States on calculating renewable energy from heat pumps from different heat pump technologies pursuant to Article 5 of Directive 2009/28/EC of the European Parliament and of the. *Off. J. Eur. Union* **2013**, *62*, 27–35.
5. European Parliament. Directive 2009/28/EC of the European Parliament and of the Council of 23 April 2009 on the promotion of the use of energy from renewable sources and amending and subsequently repealing Directives 2001/77/EC and 2003/30/EC. *Off. J. Eur. Union* **2009**, *140*, 16–62. [CrossRef]
6. Hassan, H.Z.; Mohamad, A.A. A review on solar cold production through absorption technology. *Renew. Sustain. Energy Rev.* **2012**, *16*, 5331–5348. [CrossRef]
7. Bell, E.E.; Eisner, L.; Young, J.; Oetjen, R.A. Spectral-Radiance of Sky and Terrain at Wavelengths between 1 and 20 Microns. II. Sky Measurements. *J. Opt. Soc. Am.* **1960**, *50*, 1313–1320. [CrossRef]
8. Zhang, K.; McDowell, T.P.; Kummert, M. Sky Temperature Estimation and Measurement for Longwave Radiation Calculation. In Proceedings of the 15th IBPSA Conf 2017, San Francisco, Ca, USA, 7–9 August 2017. [CrossRef]
9. Swinbank, W.C. Long-wave radiation from clear skies. *Q. J. R. Meteorol. Soc.* **1963**, *89*, 339–348. [CrossRef]
10. Idso, S.B. A Set of Equations for Full Spectrum and 8- to 14 micron and 10.5- to 12.5 micron Thermal Radiation From Cloudless Skies. *Water Resour. Res.* **1981**, *17*, 295–304. [CrossRef]
11. Berdahl, P.; Martin, M. Emissivity of clear skies. *Sol. Energy* **1984**, *32*, 663–664. [CrossRef]
12. Prata, A.J. A new long-wave formula for estimating downward clear-sky radiation at the surface. *Q. J. R. Meteorol. Soc.* **1996**, *122*, 1127–1151. [CrossRef]
13. Catalanotti, S.; Cuomo, V.; Piro, G.; Ruggi, D.; Silvestrini, V.; Troise, G. The radiative cooling of selective surfaces. *Sol. Energy* **1975**, *17*, 83–89. [CrossRef]
14. Granqvist, C.G.; Hjortsberg, A. Radiative cooling to low temperatures: General considerations and application to selectively emitting SiO films. *J. Appl. Phys.* **1981**, *52*, 4205–4220. [CrossRef]

15. Eriksson, T.S.; Lushiku, E.M.; Granqvist, C.G. Materials for radiative cooling to low temperature. *Sol. Energy Mater.* **1984**, *11*, 149–161. [[CrossRef](#)]
16. Tazawa, M.; Jin, P.; Tanemura, S. Thin film used to obtain a constant temperature lower than the ambient. *Thin Solid Films* **1996**, *281–282*, 232–234. [[CrossRef](#)]
17. Mihalakakou, G.; Ferrante, A.; Lewis, J.O. The cooling potential of a metallic nocturnal radiator. *Energy Build.* **1998**, *28*, 251–256. [[CrossRef](#)]
18. Erell, E.; Etzion, Y. Radiative cooling of buildings with flat-plate solar collectors. *Build. Environ.* **2000**, *35*, 297–305. [[CrossRef](#)]
19. Sima, J.; Sikula, O.; Kosutova, K.; Plasek, J. Theoretical Evaluation of Night Sky Cooling in the Czech Republic. *Energy Procedia* **2014**, *48*, 645–653. [[CrossRef](#)]
20. Bagiorgas, H.S.; Mihalakakou, G. Experimental and theoretical investigation of a nocturnal radiator for space cooling. *Renew. Energy* **2008**, *33*, 1220–1227. [[CrossRef](#)]
21. Etzion, Y.; Erell, E. Thermal Storage Mass in Radiative Cooling Systems. *Build. Environ.* **1991**, *26*, 389–394. [[CrossRef](#)]
22. Bathgate, S.N.; Bosi, S.G. A robust convection cover material for selective radiative cooling applications. *Sol. Energy Mater. Sol. Cells* **2011**, *95*, 2778–2785. [[CrossRef](#)]
23. Rephaeli, E.; Raman, A.P.; Fan, S. Ultrabroadband Photonic Structures To Achieve High-Performance Daytime Radiative Cooling. *Nano Lett.* **2013**, *13*, 1457–1461. [[CrossRef](#)] [[PubMed](#)]
24. Raman, A.P.; Anoma, M.A.; Zhu, L.; Rephaeli, E.; Fan, S. Passive radiative cooling below ambient air temperature under direct sunlight. *Nature* **2014**, *515*, 540–544. [[CrossRef](#)] [[PubMed](#)]
25. Huang, Z.; Ruan, X. Nanoparticle embedded double-layer coating for daytime radiative cooling. *Int. J. Heat Mass Transf.* **2017**, *104*, 890–896. [[CrossRef](#)]
26. Huang, Y.; Pu, M.; Zhao, Z.; Li, X.; Ma, X.; Luo, X. Broadband metamaterial as an “invisible” radiative cooling coat. *Opt. Commun.* **2018**, *407*, 204–207. [[CrossRef](#)]
27. Wu, D.; Liu, C.; Xu, Z.; Liu, Y.; Yu, Z.; Yu, L.; Ye, H. The design of ultra-broadband selective near-perfect absorber based on photonic structures to achieve near-ideal daytime radiative cooling. *Mater. Des.* **2018**, *139*, 104–111. [[CrossRef](#)]
28. Yang, P.; Chen, C.; Zhang, Z.M. A dual-layer structure with record-high solar reflectance for daytime radiative cooling. *Sol. Energy* **2018**, *169*, 316–324. [[CrossRef](#)]
29. Wong, R.Y.M.; Tso, C.Y.; Chao, C.Y.H.; Huang, B.; Wan, M.P. Ultra-broadband asymmetric transmission metallic gratings for subtropical passive daytime radiative cooling. *Sol. Energy Mater. Sol. Cells* **2018**, *186*, 330–339. [[CrossRef](#)]
30. Vall, S.; Castell, A. Radiative cooling as low-grade energy source: A literature review. *Renew. Sustain. Energy Rev.* **2017**, *77*, 1–18. [[CrossRef](#)]
31. Cavalius, R.; Isaksson, C.; Perednis, E.; Read, G.E.F. *Passive Cooling Technologies*; Austrian Energy Agency: Vienna, Austria, 2005.
32. Eicker, U.; Dalibard, A. Photovoltaic-thermal collectors for night radiative cooling of buildings. *Sol. Energy* **2011**, *85*, 1322–1335. [[CrossRef](#)]
33. Kong, A.; Cai, B.; Shi, P.; Yuan, X. Ultra-broadband all-dielectric metamaterial thermal emitter for passive radiative cooling. *Opt. Express* **2019**, *27*, 30102–30115. [[CrossRef](#)]
34. Erell, E.; Etzion, Y. Heating experiments with a radiative cooling system. *Build. Environ.* **1996**, *31*, 509–517. [[CrossRef](#)]
35. Hosseinzadeh, E.; Taherian, H. An Experimental and Analytical Study of a Radiative Cooling System with Unglazed Flat Plate Collectors. *Int. J. Green Energy* **2012**, *9*, 766–779. [[CrossRef](#)]
36. Xu, X.; Niu, R.; Feng, G. An Experimental and Analytical Study of a Radiative Cooling System with Flat Plate Collectors. *Procedia Eng.* **2015**, *121*, 1574–1581. [[CrossRef](#)]
37. Vall, S.; Castell, A.; Medrano, M. Energy Savings Potential of a Novel Radiative Cooling and Solar Thermal Collection Concept in Buildings for Various World Climates. *Energy Technol.* **2018**, *6*, 2200–2209. [[CrossRef](#)]
38. Hu, M.; Pei, G.; Li, L.; Zheng, R.; Li, J.; Ji, J. Theoretical and Experimental Study of Spectral Selectivity Surface for Both Solar Heating and Radiative Cooling. *Int. J. Photoenergy* **2015**, *2015*, 807875. [[CrossRef](#)]
39. Hu, M.; Pei, G.; Wang, Q.; Li, J.; Wang, Y.; Ji, J. Field test and preliminary analysis of a combined diurnal solar heating and nocturnal radiative cooling system. *Appl. Energy* **2016**, *179*, 899–908. [[CrossRef](#)]

40. Fujisol S.S.L. Energías Renovables.—N.d. Available online: <https://www.fujisol.com/pdf/ficha-fujip.pdf> (accessed on 22 January 2020).
41. Hu, M.; Zhao, B.; Ao, X.; Zhao, P.; Su, Y.; Pei, G. Field investigation of a hybrid photovoltaic-photothermic-radiative cooling system. *Appl. Energy* **2018**, *231*, 288–300. [[CrossRef](#)]
42. Taylor, B.N.; Kuyatt, C.E. *Guidelines for Evaluating and Expressing the Uncertainty of NIST Measurement Result*; National Institute of Standards and Technology: Gaithersburg, MD, USA, 1994.
43. Erell, E.; Etzion, Y. A Radiative Cooling System Using Water as a Heat Exchange Medium. *Archit. Sci. Rev.* **1992**, *35*, 39–49. [[CrossRef](#)]
44. European Parliament. Directive 2012/27/EU of the European Parliament and of the Council of 25 October 2012 on energy efficiency. *Off. J. Eur. Union Dir.* **2012**, 1–56. [[CrossRef](#)]



© 2020 by the authors. Licensee MDPI, Basel, Switzerland. This article is an open access article distributed under the terms and conditions of the Creative Commons Attribution (CC BY) license (<http://creativecommons.org/licenses/by/4.0/>).

Chapter 8. Conclusions

8.1. Conclusions

The present PhD thesis contributed to increase the technological knowledge of radiative cooling by focusing on the study of radiative cooling technology and on the development and analysis of a combination of radiative cooling with solar thermal collection, named Radiative Collector and Emitter.

The main accomplishments of this PhD are the following:

- The performance of a complete review of radiative cooling literature. The review is structured to help any reader to introduce to the basics of radiative cooling. It then follows to more specific research topics: selective radiative cooling research, numerical and experimental modelling, and recently further extended with new selective day-time radiative cooling and the combination of radiative cooling with other energy generation technologies.
- The development of a theoretical study of the potential integration of a combined radiative cooling and solar thermal collection device into buildings based on the potential energy savings worldwide.
- The performance of a numerical and experimental analysis of the combination of radiative cooling technology with solar thermal collection in the same device. Determination of the most influencing parameters to the radiative cooling production and proof of concept validation.

This PhD thesis presents a complete literature state-of-the-art review of radiative cooling research (Chapter 4), compounded by a review paper (paper 1) and an extension for new disclosed cutting-edge papers reviewed from the continuous research surveillance.

The main conclusions extracted from the literature review are listed below:

- Empirical correlations are simple and of bare precision, because they give an approximate overall value and the physical phenomenon is presented as having a uniform spectrum. Nevertheless, they can be used as a good approach if adapted or chosen for a specific location.
- There is a lack of research on radiative cooling harvesting potential (location, climates, power density, etc.). Radiative cooling technology needs a world climate harvesting analysis to evidence which climates are of interest to be implemented.
- There is scope for selective materials research and development. Even the considerable effort that has been done in developing selective materials suitable for radiative cooling, there is a long way until the development of excellent and affordable selective materials.
- There is a recently rising research interest in developing selective materials for day-time radiative cooling. Day-time radiative cooling is preferred because peak cooling demand occurs during the day-time period.
- The analytical and numerical reviewed research results pointed out the desirability of cover usage, fluid as internal thermal-carrier usage, and heat storage usage.
- There is a need to improve optical properties implementation in numerical modelling to represent better the radiative cooling phenomenon and the optical properties of materials.
- The results from experimental research pointed out the applicability of radiative cooling technology for cold production in some climates. Also, the results lead to provide new functionalities to improve its performance, applicability, and profitability. Recent research trends focus on experimental prototypes combining radiative cooling with other generation technologies. The reason for combining radiative cooling with other technologies is to complement radiative cooling by harvesting other resources, thus making the system more profitable. Combinations with solar photovoltaic or solar thermal collection are the most promising combinations with radiative cooling.
- The comparison between new devices and materials was difficult due to the lack of standardised key performance indicators (KPI), and standard parameters to be analysed.

The conclusions of the state-of-the-art review confirmed the PhD thesis initial idea of combining radiative cooling and solar thermal collection, here named the Radiative Collector and Emitter (RCE). This novel concept was presented in Chapter 5, with some distinguishing features from other research. Moreover, a theoretical study was performed on the integration of this novel RCE concept into buildings worldwide. The main conclusions of the study are listed below:

- The analysis performed presents RCE suitability/preference for climates with warm summers and cool/cold winters. In these climate conditions, RCE presents appropriate coverage ratios of space cooling higher than 25% and DHW higher than 75%.
- The analysis results pointed out that climates with unbalanced demands, either with too high heating demand or too high cooling demand, are not suitable for RCE. Those climates require mainly one technology (solar thermal collection or radiative cooling) with limitations for RCE implantation.
- The results indicate that an appropriate ratio between cooling and DHW demand helps to take full potential of RCE. In particular, buildings with constant heat demands, such as DHW in residential buildings and hotels, and low cooling demands, such as residential buildings in climates with warm summers, are spotted to be more appropriate because they present a better energy demand balance for RCE.
- Further research is required to develop a more detailed numerical model of RCE to improve the accuracy in calculations and the necessity of experimental testing to analyse the RCE technology under real operation conditions.

Based on the conclusions of both the state-of-the-art review and the study of the energy savings potential of the RCE, a new numerical model was developed, experimentally validated, and a sensitivity analysis was performed. The main conclusions from the numerical model simulations (Chapter 6) are listed below:

- The model proved accuracy in predicting the thermal behaviour of both operational modes, and the results evidenced the potential for implementing dual functionality: solar thermal collection and radiative cooling.

- The sensitivity analysis identified five parameters or variables and four combinations between them, as the most influencing for radiative cooling in a flat plate configuration: air gap thermal conductivity, radiator emissivity and cover transmissivity in the wavelength range of 7-14 μm , water inlet temperature, and water inlet flow; being water inlet temperature the most influencing variable.
- For the studied conditions, higher values of these parameters or variables result in higher cooling generation rates. However, for low values of water inlet temperature ($< 15^\circ\text{C}$, for the studied conditions), low values of air gap thermal conductivity increase cooling energy production. Thus, if low temperatures are to be achieved, vacuum or partial vacuum in the cavity between the cover and the radiator surface may increase the cooling production.
- The analysis highlighted the importance of choosing the water inlet temperature adequately. Even though higher temperatures increase cooling production values, this temperature should be adequate for cooling purposes.
- The optimisation process spotted the importance of selecting suitable materials to increase radiative cooling performance significantly.

Based on the conclusions of the state-of-the-art review and the study of the energy savings potential of the RCE, a prototype was experimentally tested. The conclusions from the experimental testing (Chapter 7) are listed below:

- The results proved the RCE prototype capable of heating water during the day-time period and cooling water down below ambient temperature during the night-time period.
- The results show that the RCE prototype did not reach temperature levels as low nor efficiencies as good as other cooling technologies do. However, RCE produces this cooling with low energy consumption.
- During the experiments, dew formation on both sides of the cover was observed, causing emission blockage. A proposed solution is creating the vacuum in the gap between emitter and cover, which can eliminate or mitigate the dew formation.
- The proposed KPI for radiative cooling efficiency can enable the comparison between devices further on.

8.2. Recommendations for future work

The present PhD thesis has opened a new research field, the combination of two different renewable technologies for heat and cold production. Although the accomplishment of all proposed objectives, the research presented in this PhD thesis has a lot more to explore, under the candidate's judgement.

Apart from future work directly connected to present PhD thesis, the candidate finds it appropriate to present general future work for research to come in the field of combining radiative cooling and solar thermal collection:

- Some efforts have to be focused on developing or finding suitable materials for this particular combination; suitable materials for real device application (optical/thermal properties, mechanical properties/durability, manufacturing properties, economical).
- More research focused on the experimental testing of this combination integrated into buildings or other applications to increase available experimental research. There is still a lack of experimental research and the available is still in lab testing or concept proving.

The candidate also presents a list of future work or research that would be of interest according to the results and conclusions presented in this PhD thesis.

8.2.1. Numerical modelling future work

After the development of the numerical model and its validation, the candidate proposes some following steps:

- To integrate the RCE model with an HVAC system covering the demands of a real application to evaluate the energy savings (such as heat pumps).
- To study the phenomenon detected in Chapter 6 regarding the change of tendency for air gap thermal conductivity when the water inlet temperature is at 15°C, since this temperature may depend on the location, weather and season.

- To perform the potential energy-saving study again with the numerical model to improve the previous study accuracy.

8.2.2. Experimental testing future work

The experimental testing was limited to a few specific objectives and conclusions. The candidate proposes some future research:

- To develop and test a mechanical system capable of operating the double cover integrated into an RCE device under real conditions.
- To integrate the device into a testing bench to simulate the energy demands of a building, or to integrate it into a real building.
- To perform a specific analysis of dew formation on the cover.
- To perform experimental testing campaigns for long periods and in different seasons to extend the results and detect possible hidden effects.

Scientific foreign exchange

The PhD candidate did a four months research stay during the realisation of this PhD thesis in the Centre for Energy and Thermal Sciences of Lyon (CETHIL), a joint centre between the National Institute for Applied Sciences of Lyon (INSA Lyon), the French National Scientific Research Centre (CNRS) and the University Claude-Bernard Lyon 1, all under the academic framework of University of Lyon. The research stay was done under the supervision of Dr. Kévy Johanes and Dr Etienne Vergnault. The exchange was possible thanks to the award to promote research in an abroad institution from *Societat Econòmica Barcelonesa d'Amics del País* (SEBAP). In this research stay, the PhD candidate worked on the RCE numerical modelling in TRNSYS and the performance of a sensitivity analysis using ANOVA, which is included in this PhD thesis (Chapter 5, paper 3). This research stay also endorses the ability of the candidate to perform high-level scientific work in an internationally renowned institution, as well as allowing the candidate to claim for the International mention.



References

- [1] European Commission. Climate change consequences. 2020. https://ec.europa.eu/clima/change/consequences_en.
- [2] European Commission. Causes of climate change. 2020. https://ec.europa.eu/clima/change/causes_en.
- [3] IEA. Data and statistics. 2020. <https://www.iea.org/data-and-statistics>.
- [4] United Nations. Framework Convention on Climate Change. Adoption of the Paris Agreement. 21st Conference of the Parties. France, 2015. 2015.
- [5] European Commission. The European Green Deal. 2020. https://ec.europa.eu/info/strategy/priorities-2019-2024/european-green-deal_en.
- [6] Ürge-Vorsatz D, Eyre N, Graham P, Harvey D, Hertwich E, Jiang Y, et al. Chapter 10 - Energy End-Use: Building. *Glob. Energy Assess. - Towar. a Sustain. Futur.*, 2012, p. 649–760.
- [7] Dulac J. Perspectives for a Clean Energy Transition. The Critical Role of Buildings. *Energy Transit Prog Outlook to 2020* 2019:117. doi:10.1017/CBO9781107415324.004.
- [8] OECD/IEA. The Future of Cooling - Opportunities for energy-efficient air conditioning 2018:92.
- [9] Yang L, Yan H, Lam JC. Thermal comfort and building energy consumption implications - A review. *Appl Energy* 2014;115:164–73. doi:10.1016/j.apenergy.2013.10.062.
- [10] Gautam A, Chamoli S, Kumar A, Singh S. A review on technical improvements, economic feasibility and world scenario of solar water heating system. *Renew Sustain Energy Rev* 2017;68:541–62. doi:10.1016/j.rser.2016.09.104.
- [11] Santamouris M, Asimakopoulos DN. *Passive cooling of buildings*. London: James & James; 1996.
- [12] Smale AP, Chuss DT, Chuss DT, Greason MR. *Cosmic Background Explorer* 2008. <http://lambda.gsfc.nasa.gov/product/cobe/>.
- [13] Fernandez N, Wang W, Alvine K, S K. Energy Savings Potential of Radiative Cooling Technologies 2015:72.
- [14] Nasa. Earth's Energy Budget 2017. <https://www.nasa.gov/feature/langley/what-is-earth-s-energy-budget-five-questions-with-a-guy-who-knows/>.
- [15] World Bank Group/ESMAP/ Solargis. Global Horizontal Irradiation (SGI) Map

- and Direct Normal Irradiation (DNI) Map 2019. <https://solargis.com/maps-and-gis-data/download/world>.
- [16] Faninger G. The Potential of Solar Thermal Technologies in a Sustainable Energy Future. IEA Sol Heat Cool Program 2010:1–36.
- [17] Bell EE, Eisner L, Young J, Oetjen RA. Spectral-Radiance of Sky and Terrain at Wavelengths between 1 and 20 Microns. II. Sky Measurements. *J Opt Soc Am* 1960;50:1313–20. doi:10.1364/JOSA.50.001313.
- [18] Bliss RW. Atmospheric radiation near the surface of the ground: A summary for engineers. *Sol Energy* 1961;5:103–20. doi:10.1016/0038-092X(61)90053-6.
- [19] Granqvist CG, Hjortsberg A, Eriksson TS. Radiative Cooling to Low Temperatures with Selectively IR-Emitting Surfaces. *Thin Solid Films* 1982;90:187–90.
- [20] Raman AP, Anoma MA, Zhu L, Rephaeli E, Fan S. Passive radiative cooling below ambient air temperature under direct sunlight. *Nature* 2014;515:540–4. doi:10.1038/nature13883.
- [21] Lu X, Xu P, Wang H, Yang T, Hou J. Cooling potential and applications prospects of passive radiative cooling in buildings: The current state-of-the-art. *Renew Sustain Energy Rev* 2016;65:1079–97. doi:10.1016/j.rser.2016.07.058.
- [22] Vall S, Castell A. Radiative cooling as low-grade energy source : A literature review. *Renew Sustain Energy Rev* 2017;77:803–20. doi:10.1016/j.rser.2017.04.010.
- [23] Goldstein EA, Nasuta D, Li S, Martin C, Raman A, Goldstein E. Free Subcooling with the Sky: Improving the efficiency of air conditioning systems Free Subcooling with the Sky: Improving the efficiency of air conditioning systems. *Int Refrig Air Cond Conf* 2018.
- [24] SkyCoolSystems. SkyCool Systems 2020. <https://www.skycoolsystems.com>.
- [25] Cavelius R, Isaksson C, Perednis E, Read GEF. Passive cooling technologies, Austrian Energy Agency. 2005.
- [26] Chen L, Zhang K, Ma M, Tang S, Li F, Niu X. Sub-ambient radiative cooling and its application in buildings. *Build Simul* 2020;13:1165–89. doi:10.1007/s12273-020-0646-x.
- [27] Li Z, Chen Q, Song Y, Zhu B, Zhu J. Fundamentals, Materials, and Applications for Daytime Radiative Cooling. *Adv Mater Technol* 2020;5:1–19. doi:10.1002/admt.201901007.
- [28] Li W, Li Y, Shah KW. A materials perspective on radiative cooling structures for buildings. *Sol Energy* 2020;207:247–69. doi:10.1016/j.solener.2020.06.095.
- [29] Zhao D, Aili A, Zhai Y, Xu S, Tan G, Yin X, et al. Radiative sky cooling: Fundamental principles, materials, and applications. *Appl Phys Rev* 2019;6. doi:10.1063/1.5087281.
- [30] Kou J, Jurado Z, Chen Z, Fan S, Minnich AJ. Daytime radiative cooling using near-black infrared emitters. *ACS Photonics* 2017:acsphotonics.6b00991.

- doi:10.1021/acsphotonics.6b00991.
- [31] Zhou L, Song H, Liang J, Singer M, Zhou M, Stegenburgs E, et al. A polydimethylsiloxane-coated metal structure for all-day radiative cooling. *Nat Sustain* 2019;2:718–24. doi:10.1038/s41893-019-0348-5.
- [32] Meng S, Long L, Wu Z, Denisuk N, Yang Y, Wang L, et al. Scalable dual-layer film with broadband infrared emission for sub-ambient daytime radiative cooling. *Sol Energy Mater Sol Cells* 2020;208:110393. doi:10.1016/j.solmat.2020.110393.
- [33] Mandal J, Fu Y, Overvig AC, Jia M, Sun K, Shi NN, et al. Hierarchically porous polymer coatings for highly efficient passive daytime radiative cooling. *Science (80-)* 2018;362:315–9. doi:10.1126/science.aat9513.
- [34] Liu J, Zhang D, Jiao S, Zhou Z, Zhang Z, Gao F. Daytime radiative cooling with clear epoxy resin. *Sol Energy Mater Sol Cells* 2020;207:110368. doi:10.1016/j.solmat.2019.110368.
- [35] Zhai Y, Ma Y, David SN, Zhao D, Lou R, Tan G, et al. Scalable-manufactured randomized glass-polymer hybrid metamaterial for daytime radiative cooling. *Science (80-)* 2017;355:1062–6. doi:10.1126/science.aai7899.
- [36] Fan D, Sun H, Li Q. Thermal control properties of radiative cooling foil based on transparent fluorinated polyimide. *Sol Energy Mater Sol Cells* 2019;195:250–7. doi:10.1016/j.solmat.2019.03.019.
- [37] Zhao B, Hu M, Ao X, Pei G. Performance evaluation of daytime radiative cooling under different clear sky conditions. *Appl Therm Eng* 2019;155:660–6. doi:10.1016/j.applthermaleng.2019.04.028.
- [38] Lee GJ, Kim YJ, Kim HM, Yoo YJ, Song YM. Colored, Daytime Radiative Coolers with Thin-Film Resonators for Aesthetic Purposes. *Adv Opt Mater* 2018;6:1–8. doi:10.1002/adom.201800707.
- [39] Zhu Y, Wang D, Fang C, He P, Ye YH. A multilayer emitter close to ideal solar reflectance for efficient daytime radiative cooling. *Polymers (Basel)* 2019;11:1–10. doi:10.3390/polym11071203.
- [40] Ao X, Hu M, Zhao B, Chen N, Pei G, Zou C. Preliminary experimental study of a specular and a diffuse surface for daytime radiative cooling. *Sol Energy Mater Sol Cells* 2019;191:290–6. doi:10.1016/j.solmat.2018.11.032.
- [41] Jeong SY, Tso CY, Ha J, Wong YM, Chao CYH, Huang B, et al. Field investigation of a photonic multi-layered TiO₂ passive radiative cooler in sub-tropical climate. *Renew Energy* 2020;146:44–55. doi:10.1016/j.renene.2019.06.119.
- [42] Huang X, Li N, Wang J, Liu D, Xu J, Zhang Z, et al. Single Nanoporous MgHPO₄·1.2H₂O for Daytime Radiative Cooling. *ACS Appl Mater Interfaces* 2020;12:2252–8. doi:10.1021/acsami.9b14615.
- [43] Jeong SY, Tso CY, Wong YM, Chao CYH, Huang B. Daytime passive radiative cooling by ultra emissive bio-inspired polymeric surface. *Sol Energy Mater Sol Cells* 2020;206:110296. doi:10.1016/j.solmat.2019.110296.

- [44] Li N, Wang J, Liu D, Huang X, Xu Z, Zhang C, et al. Selective spectral optical properties and structure of aluminum phosphate for daytime passive radiative cooling application. *Sol Energy Mater Sol Cells* 2019;194:103–10. doi:10.1016/j.solmat.2019.01.036.
- [45] Yang Y, Long L, Meng S, Denisuk N, Chen G, Wang L, et al. Bulk material based selective infrared emitter for sub-ambient daytime radiative cooling. *Sol Energy Mater Sol Cells* 2020;211:110548. doi:10.1016/j.solmat.2020.110548.
- [46] Li T, Zhai Y, He S, Gan W, Wei Z, Heidarinejad M, et al. A radiative cooling structural material. *Science* 2019;364:760–3. doi:10.1126/science.aau9101.
- [47] Torgerson E, Hellhake J. Polymer solar filter for enabling direct daytime radiative cooling. *Sol Energy Mater Sol Cells* 2020;206:110319. doi:10.1016/j.solmat.2019.110319.
- [48] Ziming C, Fuqiang W, Dayang G, Huaxu L, Yong S. Low-cost radiative cooling blade coating with ultrahigh visible light transmittance and emission within an “atmospheric window.” *Sol Energy Mater Sol Cells* 2020;213:110563. doi:10.1016/j.solmat.2020.110563.
- [49] Bhatia B, Leroy A, Shen Y, Zhao L, Gianello M, Li D, et al. Passive directional sub-ambient daytime radiative cooling. *Nat Commun* 2018;9:1–8. doi:10.1038/s41467-018-07293-9.
- [50] Hu M, Zhao B, Ao X, Ren X, Cao J, Wang Q, et al. Performance assessment of a trifunctional system integrating solar PV, solar thermal, and radiative sky cooling. *Appl Energy* 2020;260:17. doi:10.1016/j.apenergy.2019.114167.
- [51] Hu M, Zhao B, Ao X, Zhao P, Su Y, Pei G. Field investigation of a hybrid photovoltaic-photothermic-radiative cooling system. *Appl Energy* 2018;231:288–300. doi:10.1016/j.apenergy.2018.09.137.
- [52] Zhao D, Aili A, Zhai Y, Lu J, Kidd D, Tan G, et al. Subambient Cooling of Water: Toward Real-World Applications of Daytime Radiative Cooling. *Joule* 2019;3:111–23. doi:10.1016/j.joule.2018.10.006.
- [53] Goldstein EA, Raman AP, Fan S. Sub-ambient non-evaporative fluid cooling with the sky. *Nat Energy* 2017;2:1–7. doi:10.1038/nenergy.2017.143.
- [54] Aili A, Zhao D, Lu J, Zhai Y, Yin X, Tan G, et al. A kW-scale, 24-hour continuously operational, radiative sky cooling system: Experimental demonstration and predictive modeling. *Energy Convers Manag* 2019;186:586–96. doi:10.1016/j.enconman.2019.03.006.
- [55] Yuan J, Yin H, Cao P, Yuan D, Xu S. Daytime radiative cooling of enclosed water using spectral selective metamaterial based cooling surfaces. *Energy Sustain Dev* 2020;57:22–31. doi:10.1016/j.esd.2020.04.008.
- [56] Hu M, Zhao B, Ao X, Feng J, Cao J, Su Y, et al. Experimental study on a hybrid photo-thermal and radiative cooling collector using black acrylic paint as the panel coating. *Renew Energy* 2019;139:1217–26. doi:10.1016/j.renene.2019.03.013.
- [57] Chen Z, Zhu L, Li W, Fan S. Simultaneously and Synergistically Harvest Energy from the Sun and Outer Space. *Joule* 2019;3:101–10.

- doi:10.1016/j.joule.2018.10.009.
- [58] Chen Z, Zhu L, Raman A, Fan S. Radiative cooling to deep sub-freezing temperatures through a 24-h day-night cycle. *Nat Commun* 2016;7:1–5. doi:10.1038/ncomms13729.
- [59] Zhao B, Hu M, Ao X, Chen N, Xuan Q, Jiao D, et al. Performance analysis of a hybrid system combining photovoltaic and nighttime radiative cooling. *Appl Energy* 2019;252:113432. doi:10.1016/j.apenergy.2019.113432.
- [60] Hu M, Zhao B, Ao X, Chen N, Cao J, Wang Q, et al. Feasibility research on a double-covered hybrid photo-thermal and radiative sky cooling module. *Sol Energy* 2020;197:332–43. doi:10.1016/j.solener.2020.01.022.
- [61] Liu J, Zhou Z, Zhang D, Jiao S, Zhang J, Gao F, et al. Research on the performance of radiative cooling and solar heating coupling module to direct control indoor temperature. *Energy Convers Manag* 2020;205:112395. doi:10.1016/j.enconman.2019.112395.
- [62] Michell D, Biggs KL. Radiation cooling of buildings at night. *Appl Energy* 1979;5:263–75.
- [63] Eicker U, Dalibard A. Photovoltaic-thermal collectors for night radiative cooling of buildings. *Sol Energy* 2011;85:1322–35. doi:10.1016/j.solener.2011.03.015.
- [64] Berdahl P, Fromberg R. The thermal radiance of clear skies. *Sol Energy* 1982;29:299–314. doi:10.1016/0038-092X(82)90245-6.
- [65] Berdahl P, Martin M. Emissivity of clear skies. *Sol Energy* 1984;32:663–4. doi:10.1016/0038-092X(84)90144-0.
- [66] Tang R, Etzion Y, Meir IA. Estimates of clear night sky emissivity in the Negev Highlands, Israel. *Energy Convers Manag* 2004;45:1831–43. doi:10.1016/j.enconman.2003.09.033.
- [67] Crawford TM, Duchon CE. An Improved Parameterization for Estimating Effective Atmospheric Emissivity for Use in Calculating Daytime Downwelling Longwave Radiation. *J Appl Meteorol* 1999;38:474–80. doi:10.1175/1520-0450(1999)038<0474:AIPFEE>2.0.CO;2.
- [68] ur Rehman N, Uzair M, Siddiqui MA, Khamooshi M. Regression Models and Sensitivity Analysis for the Thermal Performance of Solar Flat-Plate Collectors. *Arab J Sci Eng* 2019;44:1119–27. doi:10.1007/s13369-018-3432-7.
- [69] Duffie JA, Beckman WA. *Solar Engineering of Thermal Processes*. Hoboken, NJ, USA: John Wiley & Sons, Inc.; 2013. doi:10.1002/9781118671603.
- [70] Calise F, Figaj RD, Vanoli L. Experimental and numerical analyses of a flat plate photovoltaic/thermal solar collector. *Energies* 2017;10. doi:10.3390/en10040491.
- [71] Njomo D, Daguene M. Sensitivity analysis of thermal performances of flat plate solar air heaters. *Heat Mass Transf Und Stoffuebertragung* 2006;42:1065–81. doi:10.1007/s00231-005-0063-9.
- [72] Vall S, Castell A, Medrano M. Energy Savings Potential of a Novel Radiative Cooling and Solar Thermal Collection Concept in Buildings for Various World

- Climates. *Energy Technol* 2018;6:2200–9. doi:10.1002/ente.201800164.
- [73] Erell E, Etzion Y. Radiative cooling of buildings with flat-plate solar collectors. *Build Environ* 2000;35:297–305. doi:10.1016/S0360-1323(99)00019-0.
- [74] Bathgate SN, Bosi SG. A robust convection cover material for selective radiative cooling applications. *Sol Energy Mater Sol Cells* 2011;95:2778–85. doi:10.1016/j.solmat.2011.05.027.
- [75] Erell E, Etzion Y. Heating experiments with a radiative cooling system. *Build Environ* 1996;31:509–17. doi:10.1016/0360-1323(96)00030-3.
- [76] Hosseinzadeh E, Taherian H. An Experimental and Analytical Study of a Radiative Cooling System with Unglazed Flat Plate Collectors. *Int J Green Energy* 2012;9:766–79. doi:10.1080/15435075.2011.641189.
- [77] Xu X, Niu R, Feng G. An Experimental and Analytical Study of a Radiative Cooling System with Flat Plate Collectors. *Procedia Eng* 2015;121:1574–81. doi:10.1016/j.proeng.2015.09.180.
- [78] Hu M, Pei G, Li L, Zheng R, Li J, Ji J. Theoretical and Experimental Study of Spectral Selectivity Surface for Both Solar Heating and Radiative Cooling. *Int J Photoenergy* 2015;2015:1–9. doi:10.1155/2015/807875.
- [79] Gentle AR, Smith GB. A Subambient Open Roof Surface under the Mid-Summer Sun. *Adv Sci* 2015;2:2–5. doi:10.1002/advs.201500119.